23 December 2005

Science

Vol. 310 No. 5756
Pages 1853–2000 $10

Breakthrough of the Year

Evolution
IN ACTION

125 YEARS OF GLOBAL Science

AAAS

Mx3005P™ System
Most Flexible

Mx3000P® System
Most Affordable

Performance runs in the family.

Choose the personal QPCR system that's right for you.

Stratagene now offers two affordable, fully-featured quantitative PCR (QPCR) systems. The new five-color Mx3005P™ QPCR System includes expanded features to support a wider range of real-time QPCR applications, such as simultaneous five-target detection and alternative QPCR probe chemistries. The Mx3000P® QPCR System is still the most affordably priced four-color 96-well system available.

- **A four- or five-color instrument, with user-selected filters**
- **Advanced optical system design for true multiplexing capability, and wider application support**
- **QPCR Software with enhanced data analysis and export functionality**

Need More Information? Give Us A Call:

Stratagene USA and Canada
Order: (800) 424-5444 x3
Technical Services: (800) 894-1304 x2

Stratagene Europe
Order: 00800-7000-7000
Technical Services: 00800-7400-7400

Stratagene Japan K.K.
Order: 03-5159-2060
Technical Services: 03-5159-2070

www.stratagene.com

STRATAGENE®

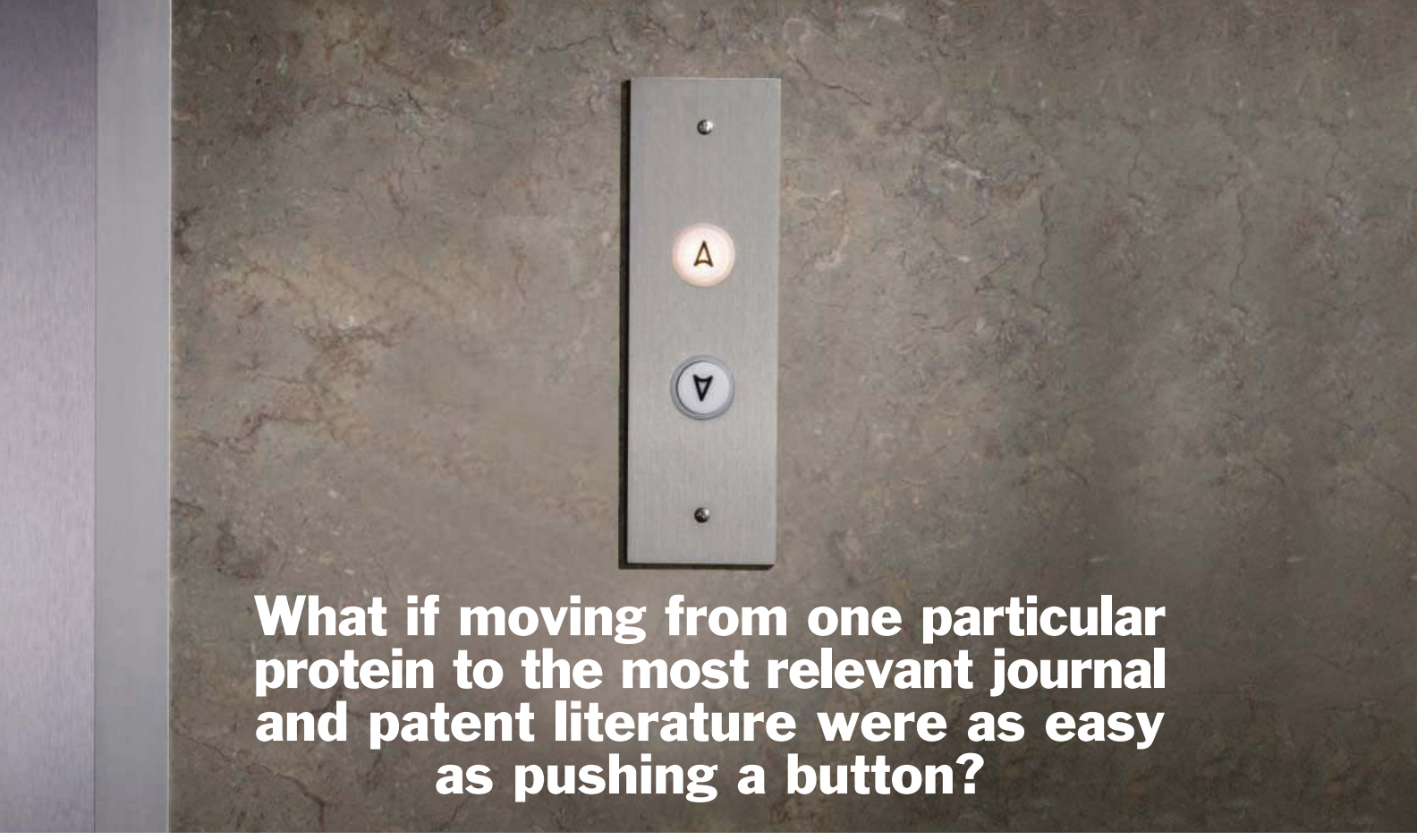

What if moving from one particular protein to the most relevant journal and patent literature were as easy as pushing a button?

It is.

Not only does SciFinder provide access to more proteins and nucleic acids than any publicly available source, but they're a single click away from their referencing patents and original research.

Coverage includes everything from the U.S. National Library of Medicine's (NLM) MEDLINE® and much more. In fact, SciFinder is the only single source of patents and journals worldwide.

Once you've found relevant literature, you can use SciFinder's powerful refinement tools to focus on a specific research area, for example: biological studies such as target organisms or diseases; expression microarrays; or analytical studies such as immunoassays, fluorescence, or PCR analysis. From each reference, you can link to the electronic full text of the original paper or patent, plus use citation tools to track how the research has evolved and been applied.

Visualization tools help you understand results at a glance. You can categorize topics and substances, identify relationships between areas of study, and see areas that haven't been explored at all.

Comprehensive, intuitive, seamless—SciFinder directs you. It's part of the process. To find out more, call us at 1-800-753-4227 (North America) or 1-614-447-3700 (worldwide) or visit www.cas.org/SCIFINDER.

SciFinder®

Part of the process.℠

HisTrap FF crude

Take an xpress run with HisTrap FF crude

The new ÄKTAxpress™ TWIN has chromatography knowledge built in. It automatically purifies eight samples delivering >95% pure tagged protein. ÄKTAxpress can extend from two to twelve modules, and has been designed to adapt to your future purification needs. By combining ÄKTAxpress with HisTrap™ FF Crude prepacked columns, you can now apply sonicated unclarified samples without the centrifugation/filtration steps. Getting more histidine-tagged protein with less effort just takes a little pure imagination.

Visit www.amershambiosciences.com/aktaxpress

ÄKTAxpress TWIN

imagination at work

GE14-05

Science

Volume 310
23 December 2005
Number 5756

SPECIAL ISSUE

BREAKTHROUGH OF THE YEAR

The cover image symbolizes the host of genetic studies and field observations that have shed light on the mechanisms that drive Darwinian evolution. A model DNA molecule is emblazoned with species representing key advances of 2005, including a stickleback fish; the influenza virus; a European blackcap; a chimpanzee; a fruit fly; and three members of *Homo sapiens*, including Charles Darwin himself. [Photo illustration: Chris Bickel and Kelly Buckheit; images: C. Goldsmith/CDC; W. A. Cresko; David Scharf/Peter Arnold; Andy Bright; Jupiter Images]

DEPARTMENTS

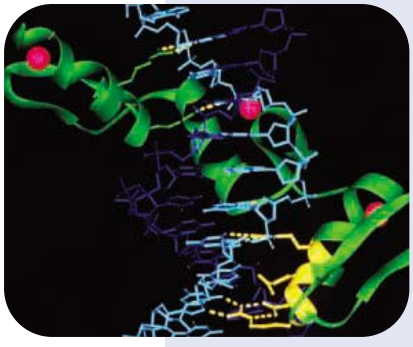

1894

NEWS OF THE WEEK

1896

NEWS FOCUS

LETTERS

BOOKS *ET AL.*

POLICY FORUM

Contents continued

HUMAN FRONTIER SCIENCE PROGRAM (HFSP)

12 quai St. Jean, 67080 STRASBOURG Cedex, FRANCE

E-mail:grant@hfsp.org
Web site: http://www.hfsp.org

OPPORTUNITIES FOR INTERDISCIPLINARY RESEARCH

The Human Frontier Science Program (HFSP) supports **international** collaborations in basic research with emphasis placed on *novel*, **innovative** and **interdisciplinary** approaches to fundamental investigations in the life sciences. Applications are invited for grants to support projects on **complex mechanisms of living organisms**.

CALL FOR LETTERS OF INTENT FOR RESEARCH GRANTS: AWARD YEAR 2007

The HFSP research grant program aims to stimulate novel, daring ideas by supporting collaborative research involving biologists together with scientists from other disciplines such as chemistry, physics, mathematics, computer science and engineering. Recent developments in the biological and physical sciences and emerging disciplines such as computational biology and nanoscience open up new approaches to understanding the complex mechanisms underlying biological functions in living organisms. Preliminary results are not required in research grant applications. Applicants are expected to develop new lines of research through the collaboration; projects must be distinct from applicants' other research funded by other sources. HFSP supports only international, collaborative teams, with an emphasis on encouraging scientists early in their careers.

International teams of scientists interested in submitting applications for support must first submit a letter of intent online via the HFSP web site. The guidelines for potential applicants and further instructions are available on the HFSP web site (www.hfsp.org).

Research grants provide 3 years support for teams with 2 – 4 members, with not more than one member from any one country, unless more members are absolutely necessary for the interdisciplinary nature of the project, which is an essential selection criterion. Applicants may also establish a local **interdisciplinary** collaboration as a component of an international team but will be considered as 1.5 team members for budgetary purposes (see below). The principal applicant must be located in one of the member countries* but co-investigators may be from any other country. Clear preference is given to **intercontinental** teams.

TWO TYPES OF GRANT ARE AVAILABLE

Young Investigators' Grants are for teams of scientists who are all within 5 years of establishing an independent laboratory and within 10 years of obtaining their PhDs.

Program Grants are for independent scientists at all stages of their careers, although the participation of younger scientists is especially encouraged.

Awards are dependent upon team size and successful teams will receive up to $450,000 per year for the whole team.

Important Deadlines:
Compulsory pre-registration for password: **20 MARCH 2006**
Submission of Letters of Intent: **30 MARCH 2006**

**Members are Australia, Canada, the European Union, France, Germany, Italy, Japan, the Republic of Korea, Switzerland, the United Kingdom and the United States.*

Science

Perspectives

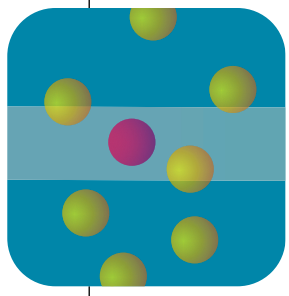

1913 & 1938

Review

Science Express www.sciencexpress.org

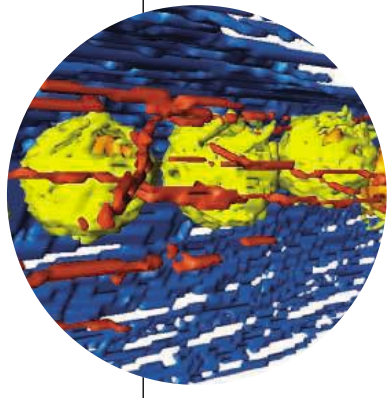

Brevia

Research Articles

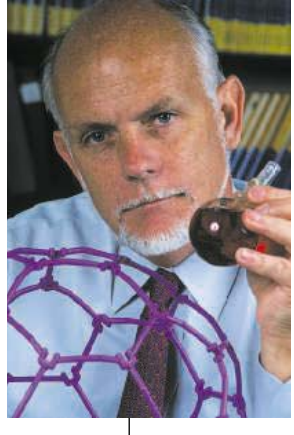

1916

Contents continued

Now The Right Side Knows What The Left Side Is Doing.

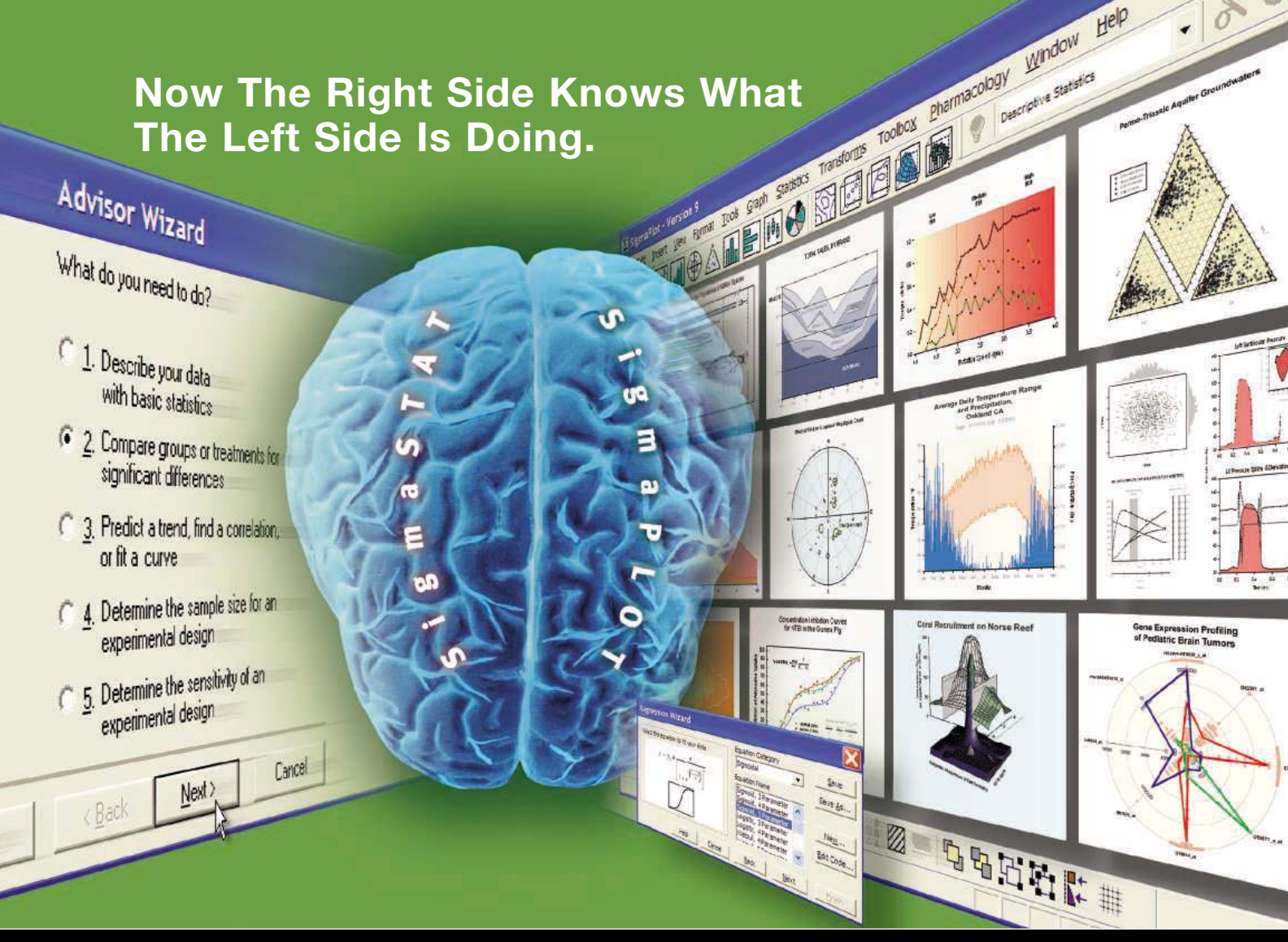

Combine the Powerful Statistical Output of SigmaStat with the Publication-quality Graph Creation of SigmaPlot

SigmaPlot is the award-winning technical graphing and data analysis software package used by more than 100,000 researchers worldwide who need to produce defensible research and create compelling graphs that clearly present their results for technical publications, presentations or the web. SigmaStat 3.1 now seamlessly integrates with SigmaPlot 9.0 for deeper statistical analysis within SigmaPlot's statistics menu.

SigmaPlot allows you to:

> Create graphs easily and publish your work anywhere
> Import, analyze & manage data quickly and easily
> Choose over 80 different 2-D and 3-D graph types
> Customize every element of your graphs
> Instantly access SigmaPlot from Microsoft® Excel
> Streamline your work by automating repetitive tasks

SIGMAPLOT
Exact Graphs for Exact Science

Add SigmaStat 3.1 to get easy-to-use, expert statistical analysis within SigmaPlot!

SigmaStat guides you through your analysis:

> Suggests the appropriate statistical test
> Checks assumptions in the data to avoid statistical error
> If your data violates any of those assumptions, the Advisor Wizard suggests another test
> Generates an intelligent report that explains your results in plain English – not statistical jargon
> Even handles messy data with missing values

SIGMASTAT
Advisory Statistics for Scientists

With SigmaStat you'll have the expertise of a professional statistical consultant at your fingertips!

FREE ONLINE TUTORIALS & 30-DAY TRIAL SOFTWARE AVAILABLE AT WWW.SYSTAT.COM

SigmaScan® — *Automated Image Analysis*
TableCurve 2D — *Automated Curve Fitting Analysis*
TableCurve 3D — *Automated Surface Fitting Analysis*
PeakFit — *Automated Peak Separation Analysis*
SYSTAT — *Comprehensive Statistical Analysis*

adsci

Reports continued

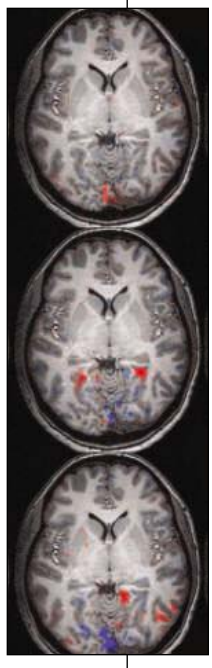

1963

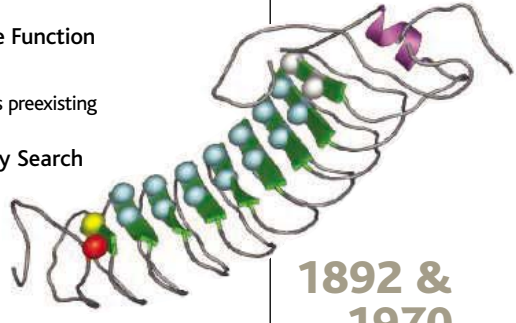

1892 & 1970

AAAS
ADVANCING SCIENCE, SERVING SOCIETY

SCIENCE (ISSN 0036-8075) is published weekly on Friday, except the last week in December, by the American Association for the Advancement of Science, 1200 New York Avenue, NW, Washington, DC 20005. Periodicals Mail postage (publication No. 484460) paid at Washington, DC, and additional mailing offices.

Domestic individual membership and subscription (51 issues): $135 ($74 allocated to subscription). Domestic institutional subscription (51 issues): $550; Foreign postage extra: Mexico, Caribbean (surface mail) $55; other countries (air assist delivery) $85. First class, airmail, student, and emeritus rates on request. Canadian rates with GST available upon request, GST #1254 88122. Publications Mail Agreement Number 1069624. **Printed in the U.S.A.**

Change of address: allow 4 weeks, giving old and new addresses and 8-digit account number. **Postmaster:** Send change of address to *Science*, P.O. Box 1811, Danbury, CT 06813–1811. **Single copy sales:** $10.00 per issue prepaid includes surface postage; bulk rates on request. **Authorization to photocopy** material for internal or personal use under circumstances not falling within the fair use provisions of the Copyright Act is granted by AAAS to libraries and other users registered with the Copyright Clearance Center (CCC) Transactional Reporting Service, provided that $15.00 per article is paid directly to CCC, 222 Rosewood Drive, Danvers, MA 01923. The identification code for *Science* is 0036-8075/83 $15.00. *Science* is indexed in the *Reader's Guide to Periodical Literature* and in several specialized indexes.

Contents continued ▶

"I think the dosage needs adjusting. I'm not nearly as happy as the people in the ads."

It's time for genetics.

What if you could use DNA to identify patients who respond well to your drug? You might use that knowledge to reach more patients and expand your market, or to get a drug to market faster. Either way – patients win. Perlegen is helping drug companies do just that – today.

Working with you, we can comprehensively analyze the DNA from hundreds of patients taking your drug. Out of the millions of genetic variations between patients, we help you identify the ones that are associated with strong efficacy, poor efficacy, or side effects. Perlegen's unparalleled coverage of the genome and experienced team of analysts mean you get clinically relevant answers, not just data, in a matter of months.

We partner with the top pharmaceutical companies around the world. We also license late-stage drugs. If you have a drug that can benefit from our approach, please contact us.

Patients are waiting.

genetics@perlegen.com
Mountain View, California • 650-625-4500
Tokyo, Japan • +81 (0)3 3444-6080
www.perlegen.com

Targeting today's drugs. Discovering tomorrow's.™

PERLEGEN SCIENCES®

sciencenow www.sciencenow.org Daily News Coverage

Worth Waiting For?
The longer it takes a woman to get pregnant, the more likely she is to have a son.

Beating the Diagnostic Clock
Chips speed synthesis of radioactive tracers for biomedical imaging.

Kill a Badger, Save a Cow?
U.K. government to examine strategy for preventing epidemic of bovine TB.

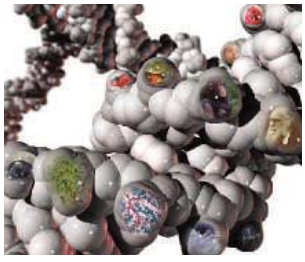

Evolutionary scientists emerging.

ScienceCareers.org www.sciencecareers.org Career Resources for Scientists

Related Breakthough of the Year section page 1878; Editorial page 1869

Global: Evolution—Getting in on the Action *J. Austin*
NextWave talks to some of the scientists working in *Science*'s 2005 breakthrough field.

US: The Evolution of Butterfly Vision *R. Arnette*
Adriana Briscoe studies the evolution of vision in butterflies, moths, and skippers.

Europe/Finland: Evolutionary Ecology, Locally and Globally *A. Forde*
Finland's Hanna Kokko talks about her life and her career as an evolutionary ecologist.

Europe/Spain: Diversity in Evolutionary Genetics *E. Pain*
Young Spanish scientists show us that there are many paths into evolution research.

Canada: The Natural Evolution of Careers *A. Fazekas*
In Canada, evolutionary science has had several good decades, but the good times may be ending.

science's sage ke www.sageke.org Science of Aging Knowledge Environment

Review: Harnessing Hormonal Signaling for Cardioprotection *V. L. Ballard and J. M. Edelberg*
The jury is still out when it comes to a beneficial role for estrogen on the heart.

News Focus: Loose Chromosomes Sink Cells *M. Leslie*
Gene-silencing mechanism falters in patients with premature aging disorder.

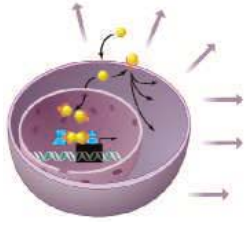

The actions of estrogens.

My STKE: A virtual signaling toolbox.

science's stke www.stke.org Signal Transduction Knowledge Environment

My Folders
Create your own electronic filing cabinet to organize STKE information that is important for your research.

My Display Settings
Customize your search results to get the information you need faster.

My Saved Searches
Save your favorite searches to execute on demand.

Separate individual or institutional subscriptions to these products may be required for full-text access.

“My research focuses on identifying functional and molecular differences between (…)”

(…) individual dopaminergic midbrain neurons, involved in disease patterns such as drug addiction, Schizophrenia and Parkinson’s disease. Single-cell gene expression analysis techniques including the Leica Microdissection system are crucial for our research.”

Prof. Dr. Birgit Liss, Department of Normal and Pathological Physiology, Institute of Molecular Neurobiology, Philipps University Marburg, Germany

www.leica-microsystems.com

Leica
MICROSYSTEMS

The Zircon's Tale

Earth's oldest preserved continental crust dates to about 4 billion years ago, much after Earth's formation (4.55 billion years ago); a major question has been how much continental crust had formed previously and been recycled back into the mantle. Some early rocks in Australia contain relic crystals of zircon, recycled from earlier rocks. Zircon harbors uranium, and these have been dated to up to 4.4 billion years ago. **Harrison *et al.*** (p. 1947, see Perspective by **Amelin**) have analyzed lutetium and hafnium isotopes in a large number of these early zircons. This isotopic system provides information on the differentiation of major silicate reservoirs on the Earth. The data imply that significant continental crust must have formed on Earth early on, perhaps by nearly 4.5 billion years ago.

Seeing the Forest for the Trees

Tree plantations are a potentially valuable tool for slowing the increase of carbon dioxide concentrations in the atmosphere, but they also can affect the water and soil resources on which they depend. **Jackson *et al.*** (p. 1944) analyze these often-neglected effects, using a combination of field research, regional economic and climate modeling, and more than 600 already-published observations, to show that afforestation can dramatically reduce water availability, as well as salinize and acidify the surrounding soil. They find that tree plantations caused nearby streams to dry up in more than one-tenth of the cases studied, and that stream flow was reduced by half, on average. These findings should help illuminate the costs of carbon sequestration by afforestation, rather than only their benefits.

Mars, Above and Below

The Mars Express satellite carries an instrument called MARSIS (Mars Advanced Radar for Subsurface and Ionospheric Sounding), which has been imaging Mars with radar waves. The radar waves penetrate the surface, including the kilometer-thick polar ice caps, to reveal subsurface features. As described by **Picardi *et al.*** (p. 1925, published online 30 November), the data reveal the base of icy deposits near the martian north pole, showing that the crust there is rigid, and a buried circular crater, 250 km in diameter, in the Chryse Planitia lowlands. The radar echoes also reveal information about the martian ionosphere. **Gurnett *et al.*** (p. 1929, published online 30 November) show that reflections occur where there are sharp changes or gradients in electron density, and with characteristic frequency signatures. In many scans of the ionosphere, Gurnett *et al*. record a range of echo types, including oblique signals in regions where the relic magnetic field preserved in Mars' crust is strong.

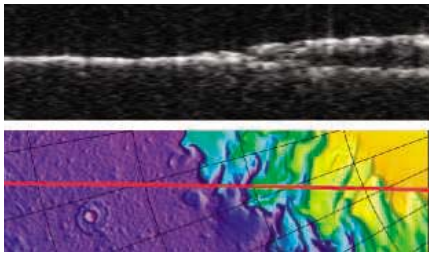

CREDITS (TOP TO BOTTOM): PORNILLOS *ET AL.*; ASI/NASA/ESA/UNIV. OF ROME/JPL

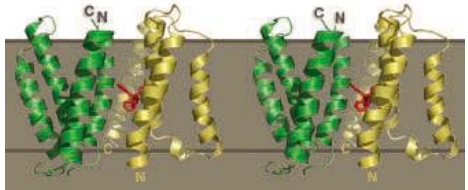

Multidrug Transporter Caught in the Act

Multidrug transporters are integral membrane proteins found in bacteria, which can expel a wide range of drugs and thereby complicate the treatment of a variety of bacterial infections. One such protein, EmrE is a proton-dependent transporter that confers resistance to positively charged hydrophobic antibiotics, including tetracycline. **Pornillos *et al.*** (p. 1950) now report the structure of EmrE in complex with a translocation substrate, tetraphenylphosphonium, at 3.7 angstrom resolution. Two EmrE polypeptides form an asymmetric, antiparallel dimer with substrate bound at the dimerization interface. The structure suggests a mechanism in which an asymmetric translocation pathway confers unidirectional transport.

Controlled Conversion

In the absence of a magnetic field, the two nuclear spin states of an isolated hydrogen atom are completely equivalent. However, in molecules with more than one hydrogen atom, the spins interact with one another, and the total energy changes slightly with their relative orientations. In low-pressure conditions, such as interstellar space, interconversion of such isomers is poorly understood. **Sun *et al.*** (p. 1938; see the Perspective by **Hougen and Oka**) have used the differential absorption of infrared light by the four nuclear spin isomers of ethylene (C_2H_4) to produce a nonequilibrium population, depleted in one isomer. By monitoring the evolution of this gaseous sample, they find that the isomers of similar inversion symmetry can interconvert efficiently, but do not transform to isomers of opposite symmetry.

MicroRNAs and the Aging Worm

MicroRNAs are present in diverse organisms, including humans, and control processes such as cell division and cell death. **Boehm and Slack** (p. 1954) now extend that repertoire of functions to include aging. In the nematode *Caenorhabditis elegans*, *lin-4*, a microRNA that is a key regulator of the stage-specific timing of cell division patterns during the larval stage, also influences the life span and the pace of aging in the adult. The microRNA and its target, *lin-14*, act in insulin/insulin-like growth factor–1 signaling pathway to influence life span and the pace of aging. Loss of *lin-4* shortens worm life span. A common mechanism thus serves to control the timing of two processes—development and aging.

Maintaining the Amino Acid Supply Chain

The efficiency and fidelity of protein synthesis is a key factor in cellular survival under a variety of growth conditions. Now **Vabulas and Hartl** (p. 1960) show that, under conditions of acute restriction in amino acid supply, continued protein biogenesis in mammalian cells is maintained by proteasomal degradation of preexisting proteins. Amino acid deficiency leads to severe depletion of the intracellular amino acid pool within minutes of proteasome inhibition and, concomitantly, protein translation is

CONTINUED ON PAGE 1867

impaired. Both nascent and newly synthesized polypeptides remain protected from proteasomal degradation. At most, only a few percent of polypeptides are immediately degraded upon synthesis, indicating that, in contrast to previous estimates, protein biogenesis is a highly efficient process.

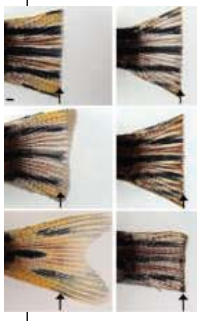

CREDIT: WHITEHEAD *ET AL.*

Prospects for Limb Regeneration

Salamanders are able to regenerate a lost limb, a feature of ongoing development sadly lost to humans. **Brockes and Kumar** (p. 1919) review what is known about amphibian limb regeneration and speculate on how these observations could inform application of stem cell and regenerative medicine to mammalian cases. Zebrafish as well can regenerate their fins. Regeneration occurs through initial formation of a clump of undifferentiated cells, the blastema, which through growth and differentiation elaborates a replacement fin. **Whitehead *et al.*** (p. 1957; see the Perspective by **Antebi**) have now identified one of the signaling factors critical to formation of the blastema. In zebrafish the *dob* (*devoid of blastema*) mutation affects a gene that encodes signaling factor Fgf20, which seems to be used specifically for regeneration rather than for normal embryonic development.

Observing the Formation and Recollection of Memories

Recent advances in analyzing the large data sets collected during functional brain imaging studies have revealed patterns of neuronal activity that can be associated reliably with the recall of remembered stimuli. After seeing pictures or listening to sounds, subjects are able, when prompted, to retrieve or reactivate their memories of these items, and brain scans taken during the retrieval period are similar to those taken when the same items were studied directly. **Polyn *et al.*** (p. 1963) now show that reactivation of such stored representations occurs prior to a verbal report of recollection in a free recall paradigm, where subjects were not prompted to remember specific items, but were reporting which of these items "resurfaced" in their memory and when. These results provide support for the theoretical framework of shifting brain states in dynamic cognition.

Challenging Immune Diversity Dogma

The adaptive immune system has been thought to be confined to the realm of jawed vertebrates, where somatic mechanisms of genetic variation have evolved to generate immune receptors in great diversity that are clonally dispersed among its lymphocytes. However, recently jawless fish have been shown to be able to generate diversity among immune-like receptors, and indeed some invertebrates produce diverse immunoglobulin-like molecules. Extending their original discovery of variable lymphocyte receptors (VLRs) in the sea lamprey, **Alder *et al.*** (p. 1970) now provide information on the form, function, and potential extent of somatic genetic diversity in this system. Leucine-rich repeats (LRRs) are randomly selected from a large bank of LRR modules by a sequential mechanism of rearrangement so that an estimated diversity of VLRs rivaling that of immune receptors in mammals is possible. Furthermore serial immunization of lampreys was found to elicit the responses expected in a developing adaptive immune response to an antigen.

Rapid Radiation of Animals

Despite many years of effort, the relationships within and between major groups of metazoa remain uncertain and controversial. Using substantial quantities of sequence data from several key animal taxa, **Rokas *et al.*** (p. 1933; see the Perspective by **Jermiin *et al.***) find a contrast between the history of the metazoan and fungal kingdoms—two groups that originated at a similar time in life's history. In particular, for animals, the lack of resolution of ancient clades is a signature of closely spaced series of clade-generating events. This explicit molecular support for the rapid radiation of animals is in agreement with previous inferences from the fossil record.

Genetic Engineering that is Right on Target!

The TargeTron™ Gene Knockout System is a revolutionary method for rapid and specific disruption of genes in prokaryotic organisms. Utility of the technology has been demonstrated for prokaryotic genetic engineering, systems biology and functional genomics approaches.

The method exploits the retrohoming ability of group II introns and utilizes a simple PCR step to "re-target" the TargeTron group II intron for specific insertion into the host genome. Gene knockout using the TargeTron system has been validated in a broad range of bacterial strains such as *Escherichia coli*, *Staphylococcus aureus*, *Lactococcus lactis*, *Clostridium perfringens*, *Shigella flexneri* and *Salmonella typhimurium*.

- Targeted and permanent gene disruption
- Simple, streamlined protocol; Knockouts in 3 days or less
- Minimal screening to isolate mutants.
- No cell conjugation or specific host factor requirements
- >90% successful targeted insertion

Product	Description	Unit
TA0100A	TargeTron™ Gene Knockout System	3EA 10EA

For additional details and product availability, please visit www.sigma-aldrich.com/s1target

Breakthrough of the Year

Well, here we are again: Breakthrough time. You might wonder what could possibly top last year's selection of the Mars exploration; indeed it's hard to forget that, since the rovers are still chugging along, having outlasted their 90-day warranties by more than a year! But the Breakthrough for 2005 should not disappoint: Evolution in Action.

Wait a minute, I hear you cry. Hasn't it been a trying year for evolution, considering the debates about teaching evolutionary theory in science classes in the United States and the headlines about Intelligent Design? On the contrary; in the research community, it's been a great year for understanding how evolution works, through both experiment and theory.* No single discovery makes the case by itself; after all, the challenge of understanding evolution makes multiple demands: How can we integrate genetics with patterns of inherited change? How do new species arise in nature? What can the new science of comparative genomics tell us about change over time? We have to put the pieces together, and it could not be a more important challenge: As the evolutionary geneticist Theodosius Dobzhansky once said, "Nothing in biology makes sense except in the light of evolution."

Our scientist/journalist teams have compiled a splendid case for this exploding science. One of my favorites is the European blackcap, a species of warbler that spends the winter in two separate places but then reunites to breed, with birds selecting mates from those who shared the same wintering ground. Assortative mating of this kind can produce a gradual differentiation of the two populations. Biologists have shown that new species can arise because of geographic barriers that separate subpopulations, but the divergent evolution shown in this case could result in new species arising within a single range.

A favorite, if unlikely, subject for evolutionary studies is the small fish called the stickleback. Repeatedly, sticklebacks have moved from the sea into fresh water. When that happens, the fish shed the rather heavy armor plates that protect them from marine predators, freeing themselves to enjoy *la dolce vita fresca*. New species have been generated in each invasion, always in the same way: by rapid evolutionary selection of the same rare and ancient gene.

The exciting thing about evolution is not that our understanding is perfect or complete but that it is the foundation stone for the rest of biology. As such, researchers are eager to explore issues that have been seen as problems. Genes that are now known to exert complex effects on body form at the macro level answer the commonly stated objection that complex structures could not have evolved from simpler precursors. And so it goes: Scientific challenges are raised, inviting answers.

Last year's crystal ball of things to watch for wasn't perfectly clear. For example, nothing seems to be working very well in the area of obesity drugs. And the haplotype map of the human genome isn't quite ready to provide us with well-hyped individual genetic barcodes that we can take into the doctor's office to predict our risk of developing complex diseases such as cancer, diabetes, and mental illness.

There were some hot runners-up this time around, as well. New insights about brain disorders came from studies showing that Tourette syndrome and dyslexia are associated with genes tied to normal neural development. It was also a year of triumph for robotic missions sent to probe the solar system: the Cassini-Huygens mission explored the saturnian system, including Titan;Voyager crossed the heliopause to reach the outer limit of the solar system; Deep Impact speared a comet; and Japan's Hayabusa visited a distant asteroid.

An especially significant runner-up was climate change. 650,000-year-old ice cores from Antarctica give a continuous record of correlations between atmospheric carbon dioxide and methane and the temperature changes imposed by glacial cycles. New information put to rest the idea, popular with those skeptical about global warming, that satellite measurements, in contrast to ground measurements, showed cooling. One by one, holes in the global warming case are being filled. Government actions should follow; of that, I'll say more in the first *Science* issue of the new year.

Donald Kennedy
Editor-in-Chief

*AAAS is collaborating with leading scientific organizations at the AAAS Annual Meeting (16 to 20 February 2006, St. Louis, MO) to give teachers a voice on the evolution issue and a way to tell the scientific community how best to support them.

10.1126/science.1123757

Advancing RNAi Technology.

Dharmacon...the world's most trusted siRNA resource

- The largest and most referenced siRNA supplier
- Target any unique human, mouse or rat gene
- Highest level of guaranteed silencing available
- Innovative technologies to enhance specificity
- Breakthrough siRNA transfection reagents
- Expert technical support

Leading RNAi researchers count on Dharmacon's state-of-the-art *SMART*selection™ and *SMART*pool® technologies for potent and specific gene silencing. Four individual siRNAs and a *SMART*pool siRNA reagent are available for over 66,000 unique human, mouse, and rat genes - each with the industry's best performance guarantee and backed by our expert technical support. Simply use our on-line si*GENOME*™ search tool to identify the siRNA reagents for your target gene.

No wonder Dharmacon is the most frequently referenced siRNA supplier in peer-reviewed journals!

Want to know more about RNAi? Visit our website to request your FREE copy of the RNAi Technical Reference & Application Guide today.

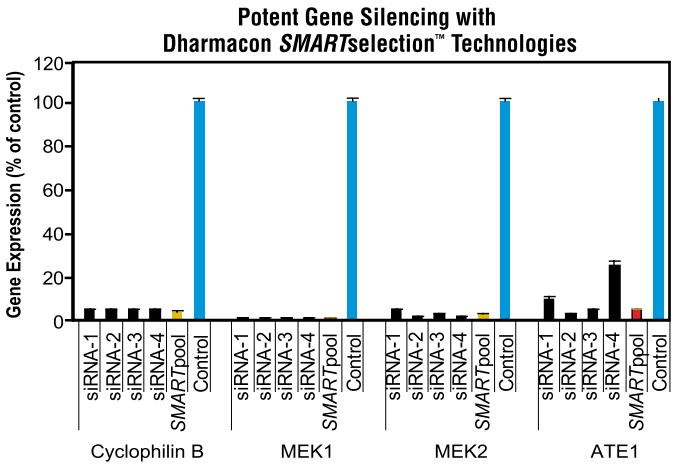

DHARMACON
RNA TECHNOLOGIES

www.dharmacon.com
Tel: 303-604-9499 or 800-235-9880 • Fax: 303-604-9680

For European offices and distributors, please visit www.perbio.com
PERBIO

EDITORS' CHOICE

edited by Stella Hurtley

IMMUNOLOGY

Not So Spineless

Sea urchins are sophisticated invertebrates whose biology holds many clues to the evolution of the vertebrates. These organisms very effectively remove any invading bacterial pathogens and other foreign material from within their coeloms by means of a range of macrophage-like cells. It seems that sea urchins have a simplified version of the complement system that can mediate opsonization of pathogens. Nair *et al.* have been investigating the immune responses of sea urchins by analysis of expressed sequence tags generated from coelomocytes and discovered that a wide range of genes are up-regulated in response to bacterial lipopolysaccharide. What was particularly interesting was a previously unknown gene family that represented 60% of the ESTs and could undergo alternative splicing to yield around 15 translatable elements. The evidence suggested that these were immune response proteins under positive selection for diversification, and revealed a greater level of complexity of putative responses than anticipated for an invertebrate group. — CA

Physiol. Genomics **22**, 33 (2005)

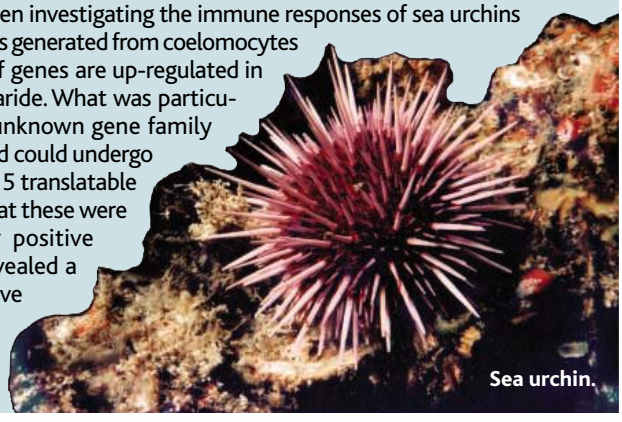

Sea urchin.

CHEMISTRY

A Well-Fitted Coating

Most heterogenous metal catalysts consist of metal nanoparticles on a ceramic oxide support, but for systems that exhibit strong metal-support interactions (such as noble metals with cerium oxide), the maximum interaction might involve completely coating a metal nanoparticle with oxide. Yeung *et al.* have used a modified microencapsulation method, previously demonstrated for silica, for encapsulating platinum nanoparticles with ceria. Increasing the Pt loading from 1 to 5% created particles with larger Pt cores and thinner coatings of ceria. The thinnest coating (1.7 nm) increased the band transition for ceria from 3.18 to 3.33 electron volts, and increased the water-gas shift (WGS) activity ($H_2O + CO \rightarrow H_2 + CO_2$) from negligible CO conversion for pure ceria to 63%. Unlike most other noble metal–ceria catalysts, these nanoparticles, which expose few noble metal sites, exhibit no activity for the competing reactions of methanation and higher hydrocarbon formation. — PDS

J. Am. Chem. Soc. 10.1021/ja056102c (2005).

MATERIALS SCIENCE

Electrostatic Stitching

Supported lipid bilayers are often used as model systems for studying surface phenomena because of their well-defined planar geometry. One interesting phenomenon relates to the "fluid-to-gel" phase transition that occurs when the mobile liquid-crystalline ordering crystallizes as the temperature is lowered. However, it is difficult to study this phase transition in simple single-component bilayers, such as those composed of zwitterionic phospholipids, because of a high density of defects that form in the gel phase. The defects are most likely caused by shrinkage of the area occupied by a lipid molecule as the tilt angle of the headgroup changes on cooling. Zhang *et al.* tested this hypothesis by studying the effects of adding cationic or anionic lipids to a bilayer composed of a zwitterionic phosphatidylcholine. With the addition of the cationic lipid, defects no longer formed on gelation. Measurements of the headgroup orientation showed that the cationic lipid increased the tilt angle in the fluid phase, but that it no longer changed on cooling. The cationic lipid is expected to be well dispersed because of electrostatic repulsions, and they may act to stitch together the bilayer, thus giving it stability through the phase transition. The addition of anionic lipids, which is expected to be unfavorable, led to defects in the gel phase, supporting the stitching hypothesis. — MSL

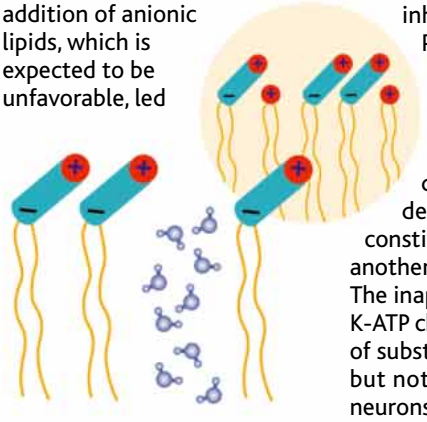

Schematics of gel-phase morphologies without (main) and with (inset) cationic lipid.

J. Phys. Chem. B, 10.1021/jp055995s (2005).

NEUROSCIENCE

Parkinson's and Potassium Channels

Parkinson's disease (PD) results from the selective loss of dopaminergic neurons in the substantia nigra of the brain. However, dopaminergic neurons in nearby parts of the brain are not affected, even though the genes implicated in familial inherited PD, as well as toxins that can induce symptoms of PD, are not restricted in their effects. Why then is this small region targeted for destruction in PD? There are hints that substantia nigra neurons show disruptions in mitochondrial respiratory function. Diminished cellular metabolism, as well as oxidative stress, can in turn cause the potassium (K)–ATP channels of dopaminergic neurons to open. Liss *et al.* investigated the interaction between these channels, the signals that control their function, and the degeneration of neurons. The K-ATP channel mediates dopaminergic neuron degeneration in response to mitochondrial complex 1 inhibition, in response to PD-inducing treatment of susceptible mice, and also in the mutant *weaver* mouse, in which dopaminergic neuron degeneration is due to constitutive activation of another potassium channel. The inappropriate function of K-ATP channels is characteristic of substantia nigra neurons, but not of dopaminergic neurons in other nearby brain areas, in which the channels

CONTINUED ON PAGE 1873

PNAS *Legacy*

90 years *of scientific research*

more than 390,000 pages

and over 80,000 articles

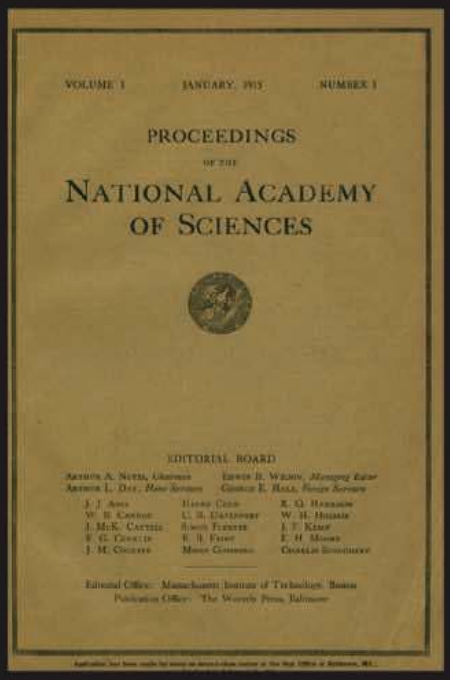
VOLUME 1 JANUARY, 1915 NUMBER 1

PROCEEDINGS

OF THE

NATIONAL ACADEMY

OF SCIENCES

EDITORIAL BOARD

The Proceedings of the National Academy of Sciences (PNAS) is pleased to announce that its legacy content dating back to the 1915 inaugural issue is now digitally archived, searchable, and freely available on the PNAS web site at **www.pnas.org**

PNAS

Proceedings of the National Academy of Sciences of the United States of America

seem to be connected to cellular metabolism through different signaling networks. — PJH

Nat. Neuro **8**, 1742 (2005).

ASTRONOMY

Kuiper Belt Curiosity

Pluto is only one of several large bodies in the outer solar system's Kuiper belt. Brown *et al.* describe the discovery of the largest object in orbit beyond Neptune, 2003 UB313, whose brightness suggests that it exceeds the size of Pluto. By tracing the object's motion in archival images, they show that it follows a highly eccentric orbit inclined 44° from the ecliptic plane, which contains most of the objects that are orbiting the Sun. Such an extreme orbit may have arisen if the body formed closer to the Sun and was scattered outward by gravitational interactions. Frozen methane is detected on the surface in infrared spectra, with characteristics very similar to Pluto. However, 2003 UB313 is not as red as Pluto, suggesting that the distribution of methane and other hydrocarbons on its surface is different and may even change with temperature as it swings closer to the Sun. — JB

Astrophys. J. **635**, L97 (2005).

CELL BIOLOGY

Organization Without an Organizer

Within cells, the tracks provided by microtubules are important for a whole variety of cellular processes, not least when microtubules form into a spindle in order to promote the separation of chromosomes during mitosis. Such microtubule arrays are arranged around organizing centers known as the centrosomes. However, within the cell there also exist well-organized arrays of microtubules that form without the aid of centrosomes. Reilein *et al.* describe the organizing principles involved in producing acentrosomal microtubule networks found in the basal cortex of epithelial cells. Microtubules are formed from tubulin monomers, and microtubule networks in a steady state contain growing and shrinking microtubules. Typically, in order to grow, microtubules need to be anchored somehow. By imaging microtubule dynamics in cytoplasts derived from the base of epithelial cells, the authors showed that networks of microtubules form based on microtubule-microtubule interactions and microtubule-cortex interactions. Each type of interaction increased microtubule stability. By modeling the parameters involved, in particular by including stabilizing interactions, the authors could replicate in silico the type of stable arrays observed within cells. — SMH

Microtubule networks (green, top) forming over 20 min. in situ (top and middle) and in silico (bottom); original microtubules are yellow (middle and bottom).

CREDIT: REILEIN *ET AL.*, *J. CELL BIOL.* **171**, 845 (2005)

J. Cell Biol. **171**, 845 (2005).

HIGHLIGHTED IN *SCIENCE*'S SIGNAL TRANSDUCTION KNOWLEDGE ENVIRONMENT

Science's STKE www.stke.org

β-Arrestin Regulates Notch Abundance

β-Arrestin, well known for its role in G protein–coupled receptor regulation, is also being recognized for its roles in regulating other types of receptors. Mukherjee *et al.* report that *Drosophila* β-arrestin, Kurtz (Krz), is involved in controlling the abundance of the receptor Notch. Notch is a single transmembrane receptor that is cleaved in response to ligand binding, releasing a fragment that translocates to the nucleus to regulate transcription. Krz was found in two different screens for proteins that interacted with the Notch regulator and with putative E3 ubiquitin ligase Deltex (Dx). In flies, loss of Krz function led to increased Notch abundance. Overexpression of both Krz and Dx produced Notch loss-of-function phenotypes and reduced Notch protein abundance. In transfected *Drosophila* S2 cells, Krz and Dx together promoted ubiquitination of Notch. Notch signaling is highly sensitive to gene dosage effects, and β-arrestin appears to be one component that contributes to this sensitivity. — NG

Nat. Cell Biol. **7**, 1191 (2005).

www.sciencemag.org

Science

1200 New York Avenue, NW
Washington, DC 20005
Editorial: 202-326-6550, FAX 202-289-7562
News: 202-326-6500, FAX 202-371-9227

Bateman House, 82-88 Hills Road
Cambridge, UK CB2 1LQ
+44 (0) 1223 326500, FAX +44 (0) 1223 326501

Subscription Services For change of address, missing issues, new orders and renewals, and payment questions: 800-731-4939 or 202-326-6417, FAX 202-842-1065. Mailing addresses: AAAS, P.O. Box 1811, Danbury, CT 06813 or AAAS Member Services, 1200 New York Avenue, NW, Washington, DC 20005

Institutional Site Licences please call 202-326-6755 for any questions or information

Reprints: Author Inquiries 800-635-7181
Commercial Inquiries 803-359-4578
Corrections 202-326-6501

Permissions 202-326-7074, FAX 202-682-0816

Member Benefits Bookstore: AAAS/BarnesandNoble.com bookstore www.aaas.org/bn; Car purchase discount: Subaru VIP Program 202-326-6417; Credit Card: MBNA 800-847-7378; Car Rentals: Hertz 800-654-2200 CDP#343457, Dollar 800-800-4000 #AA1115; AAAS Travels: Betchart Expeditions 800-252-4910; Life Insurance: Seabury & Smith 800-424-9883; Other Benefits: AAAS Member Services 202-326-6417 or www.aaasmember.org.

science_editors@aaas.org (for general editorial queries)
science_letters@aaas.org (for queries about letters)
science_reviews@aaas.org (for returning manuscript reviews)
science_bookrevs@aaas.org (for book review queries)

Published by the **American Association for the Advancement of Science (AAAS)**, *Science* serves its readers as a forum for the presentation and discussion of important issues related to the advancement of science, including the presentation of minority or conflicting points of view, rather than by publishing only material on which a consensus has been reached. Accordingly, all articles published in *Science*—including editorials, news and comment, and book reviews—are signed and reflect the individual views of the authors and not official points of view adopted by the AAAS or the institutions with which the authors are affiliated.

AAAS was founded in 1848 and incorporated in 1874. Its mission is to advance science and innovation throughout the world for the benefit of all people. The goals of the association are to: foster communication among scientists, engineers and the public; enhance international cooperation in science and its applications; promote the responsible conduct and use of science and technology; foster education in science and technology for everyone; enhance the science and technology workforce and infrastructure; increase public understanding and appreciation of science and technology; and strengthen support for the science and technology enterprise.

Information for Contributors

See pages 135 and 136 of the 7 January 2005 issue or access www.sciencemag.org/feature/contribinfo/home.shtml

EDITOR-IN-CHIEF **Donald Kennedy**
EXECUTIVE EDITOR **Monica M. Bradford**
DEPUTY EDITORS **R. Brooks Hanson, Katrina L. Kelner**
NEWS EDITOR **Colin Norman**

Editorial SUPERVISORY SENIOR EDITORS Barbara Jasny, Phillip D. Szuromi; SENIOR EDITOR/PERSPECTIVES Lisa D. Chong; SENIOR EDITORS Gilbert J. Chin, Pamela J. Hines, Paula A. Kiberstis (Boston), Beverly A. Purnell, L. Bryan Ray, Guy Riddihough (Manila), H. Jesse Smith, Valda Vinson, David Voss; ASSOCIATE EDITORS Marc S. Lavine (Toronto), Jake S. Yeston; ONLINE EDITOR Stewart Wills; CONTRIBUTING EDITOR Ivan Amato; ASSOCIATE ONLINE EDITOR Tara S. Marathe; BOOK REVIEW EDITOR Sherman J. Suter; ASSOCIATE LETTERS EDITOR Etta Kavanagh; INFORMATION SPECIALIST Janet Kegg; EDITORIAL MANAGER Cara Tate; SENIOR COPY EDITORS Jeffrey E. Cook, Harry Jach, Barbara P. Ordway; COPY EDITORS Cynthia Howe, Alexis Wynne Mogul, Jennifer Sills, Trista Wagoner; EDITORIAL COORDINATORS Carolyn Kyle, Beverly Shields; PUBLICATION ASSISTANTS Ramatoulaye Diop, Chris Filiatreau, Joi S. Granger, Jeffrey Hearn, Lisa Johnson, Scott Miller, Jerry Richardson, Brian White, Anita Wynn; EDITORIAL ASSISTANTS E. Annie Hall, Lauren Kmec, Patricia M. Moore, Brendan Nardozzi, Michael Rodewald; EXECUTIVE ASSISTANT Sylvia S. Kihara; ADMINISTRATIVE SUPPORT Patricia F. Fisher

News SENIOR CORRESPONDENT Jean Marx; DEPUTY NEWS EDITORS Robert Coontz, Jeffrey Mervis, Leslie Roberts, John Travis; CONTRIBUTING EDITORS Elizabeth Culotta, Polly Shulman; NEWS WRITERS Yudhijit Bhattacharjee, Adrian Cho, Jennifer Couzin, David Grimm, Constance Holden, Jocelyn Kaiser, Richard A. Kerr, Eli Kintisch, Andrew Lawler (New England), Greg Miller, Elizabeth Pennisi, Robert F. Service (Pacific NW), Erik Stokstad; Carolyn Gramling (intern); CONTRIBUTING CORRESPONDENTS Marcia Barinaga (Berkeley, CA), Barry A. Cipra, Jon Cohen (San Diego, CA), Daniel Ferber, Ann Gibbons, Robert Irion, Mitch Leslie (NetWatch), Charles C. Mann, Evelyn Strauss, Gary Taubes, Ingrid Wickelgren; COPY EDITORS Linda B. Felaco, Rachel Curran, Sean Richardson; ADMINISTRATIVE SUPPORT Scherraine Mack, Fannie Groom BUREAUS: Berkeley, CA: 510-652-0302, FAX 510-652-1867, New England: 207-549-7755, San Diego, CA: 760-942-3252, FAX 760-942-4979, Pacific Northwest: 503-963-1940

Production DIRECTOR James Landry; SENIOR MANAGER Wendy K. Shank; ASSISTANT MANAGER Rebecca Doshi; SENIOR SPECIALISTS Jay Covert, Chris Redwood **Preflight** DIRECTOR David M. Tompkins; MANAGER Marcus Spiegler; SPECIALIST Jessie Mudjitaba

Art DIRECTOR Joshua Moglia; ASSOCIATE ART DIRECTOR Kelly Buckheit; ILLUSTRATORS Chris Bickel, Katharine Sutliff; SENIOR ART ASSOCIATES Holly Bishop, Laura Creveling, Preston Huey; ASSOCIATE Nayomi Kevitiyagala; PHOTO RESEARCHER Leslie Blizard

***Science* International**

Europe (science@science-int.co.uk) EDITORIAL: INTERNATIONAL MANAGING EDITOR Andrew M. Sugden; SENIOR EDITOR/PERSPECTIVES Julia Fahrenkamp-Uppenbrink; SENIOR EDITORS Caroline Ash (Geneva: +41 (0) 222 346 3106), Stella M. Hurtley, Ian S. Osborne, Stephen J. Simpson, Peter Stern; ASSOCIATE EDITOR Joanne Baker EDITORIAL SUPPORT Alice Whaley; Deborah Dennison ADMINISTRATIVE SUPPORT Janet Clements, Phil Marlow, Jill White; NEWS: INTERNATIONAL NEWS EDITOR Eliot Marshall DEPUTY NEWS EDITOR Daniel Clery; CORRESPONDENT Gretchen Vogel (Berlin: +49 (0) 30 2809 3902, FAX +49 (0) 30 2809 8365); CONTRIBUTING CORRESPONDENTS Michael Balter (Paris), Martin Enserink (Amsterdam and Paris); INTERN Michael Schirber

Asia Japan Office: Asca Corporation, Eiko Ishioka, Fusako Tamura, 1-8-13, Hirano-cho, Chuo-ku, Osaka-shi, Osaka, 541-0046 Japan; +81 (0) 6 6202 6272, FAX +81 (0) 6 6202 6271; asca@os.gulf.or.jp JAPAN NEWS BUREAU: Dennis Normile (contributing correspondent, +81 (0) 3 3391 0630, FAX 81 (0) 3 5936 3531; dnormile@gol.com); CHINA REPRESENTATIVE Hao Xin, + 86 (0) 10 6307 4439 or 6307 3676, FAX +86 (0) 10 6307 4358; haoxin@earthlink.net; SOUTH ASIA Pallava Bagla (contributing correspondent +91 (0) 11 2271 2896; pbagla@vsnl.com); ASIA Richard Stone +66 2 662 5818 (rstone@aaas.org)

EXECUTIVE PUBLISHER **Alan I. Leshner**
PUBLISHER **Beth Rosner**

Fulfillment & Membership Services (membership@aaas.org) DIRECTOR Marlene Zendell; MANAGER Waylon Butler; SYSTEMS SPECIALIST Andrew Vargo; SPECIALISTS Pat Butler, Laurie Baker, Tamara Alfson, Karena Smith, Vicki Linton; CIRCULATION ASSOCIATE Christopher Refice

Business Operations and Administration DIRECTOR Deborah Rivera-Wienhold; BUSINESS MANAGER Randy Yi; SENIOR BUSINESS ANALYST Lisa Donovan; BUSINESS ANALYST Jessica Tierney; FINANCIAL ANALYST Michael LoBue, Farida Yeasmin; RIGHTS AND PERMISSIONS: ADMINISTRATOR Emilie David; ASSOCIATE Elizabeth Sandler; MARKETING: DIRECTOR John Meyers; MARKETING MANAGERS Darryl Walter, Allison Pritchard; MARKETING ASSOCIATES Julianne Wielga, Mary Ellen Crowley, Catherine Featherston; DIRECTOR OF INTERNATIONAL MARKETING AND RECRUITMENT ADVERTISING Deborah Harris; INTERNATIONAL MARKETING MANAGER Wendy Sturley; MARKETING/MEMBER SERVICES EXECUTIVE: Linda Rusk; JAPAN SALES Jason Hannaford; SITE LICENSE SALES: DIRECTOR Tom Ryan; SALES AND CUSTOMER SERVICE Mehan Dossani, Kiki Forsythe, Catherine Holland, Wendy Wise; ELECTRONIC MEDIA: MANAGER Lizabeth Harman; PRODUCTION ASSOCIATES Sheila Mackall, Amanda K. Skelton, Lisa Stanford, Nichele Johnston; APPLICATIONS DEVELOPER Carl Saffell

Advertising DIRECTOR WORLDWIDE AD SALES Bill Moran

Product (science_advertising@aaas.org); MIDWEST Rick Bongiovanni: 330-405-7080, FAX 330-405-7081 • WEST COAST/W. CANADA B. Neil Boylan (Associate Director): 650-964-2266, FAX 650-964-2267 • EAST COAST/E. CANADA Christopher Breslin: 443-512-0330, FAX 443-512-0331 • UK/EUROPE/ASIA Tracey Peers (Associate Director): +44 (0) 1782 752530, FAX +44 (0) 1782 752531 JAPAN Mashy Yoshikawa: +81 (0) 33235 5961, FAX +81 (0) 33235 5852 ISRAEL Jessica Nachlas +9723 5449123 • TRAFFIC MANAGER Carol Maddox; SALES COORDINATOR Deiandra Simms

Classified (advertise@sciencecareers.org); U.S.: SALES DIRECTOR Gabrielle Boguslawski: 718-491-1607, FAX 202-289-6742; INSIDE SALES MANAGER Daryl Anderson: 202-326-6543; WEST COAST/MIDWEST Kristine von Zedlitz: 415-956-2531; EAST COAST Jill Downing: 631-580-2445; CANADA, MEETINGS AND ANNOUNCEMENTS Kathleen Clark: 510-271-8349; LINE AD SALES Emnet Tesfaye: 202-326-6740; SALES COORDINATORS Erika Bryant; Rohan Edmonson Christopher Normile, Joyce Scott, Shirley Young; INTERNATIONAL: SALES MANAGER Tracy Holmes: +44 (0) 1223 326525, FAX +44 (0) 1223 326532; SALES Christina Harrison, Svitlana Barnes; SALES ASSISTANT Helen Moroney; JAPAN: Jason Hannaford: +81 (0) 52 789 1860, FAX +81 (0) 52 789 1861; PRODUCTION: MANAGER Jennifer Rankin; ASSISTANT MANAGER Deborah Tompkins; ASSOCIATES Christine Hall; Amy Hardcastle; PUBLICATIONS ASSISTANTS Robert Buck; Natasha Pinol

AAAS Board of Directors RETIRING PRESIDENT, CHAIR Shirley Ann Jackson; PRESIDENT Gilbert S. Omenn; PRESIDENT-ELECT John P. Holdren; TREASURER David E. Shaw; CHIEF EXECUTIVE OFFICER Alan I. Leshner; BOARD Rosina M. Bierbaum; John E. Burris; John E. Dowling; Lynn W. Enquist; Susan M. Fitzpatrick; Richard A. Meserve; Norine E. Noonan; Peter J. Stang; Kathryn D. Sullivan

AAAS
ADVANCING SCIENCE, SERVING SOCIETY

AstraZeneca Pharmaceuticals *proudly announces the* 21st Annual Excellence in Chemistry Award Winners

Pictured from left are Dean Toste, David Nugiel (Committee Chairperson), Scott Denmark, and Phil Baran.

Awardees:

Professor Dean Toste
University of California, Berkeley

Professor Phil Baran
Scripps Research Institute

Distinguished Lecturer:

Professor Scott Denmark
University of Illinois

AstraZeneca Excellence in Chemistry Award 2005

At AstraZeneca, we recognize that advances in medicine rely on innovations in chemistry. As a commitment to future advances, each year we award talented academic researchers who, early in their careers, have made outstanding contributions to synthetic, mechanistic, or bioorganic chemistry. In selecting these awardees, our senior scientists consult a world-leading chemist, who also serves as the distinguished lecturer. This year marks the 21st year of the AstraZeneca Excellence in Chemistry Award.

With best wishes for continued innovation and excellence in chemical research, AstraZeneca congratulates this year's award winners.

AstraZeneca
life inspiring ideas

www.astrazeneca-us.com

Science's 2005 Breakthrough of the Year video

Evolutionary Biology

Watch the Breakthrough of the Year video at
www.sciencemag.org/sciext/btoy2005

Get the insider's perspective on the editorial featured in this issue of *Science*...interviews with researchers on their extraordinary findings on how evolution proceeds and an insightful commentary by Donald Kennedy—*Science*'s Editor-in-Chief.

FREE ACCESS to this issue until 31 March 2006

Produced by Biocompare and *Science*

biocompare®
The Buyer's Guide for Life Scientists.™

Science
AAAS

NetWatch

edited by Mitch Leslie

EDUCATION

Information Eruption

If lava flows or ash spews somewhere on Earth, the crew at Volcano World takes note. Hosted by the University of North Dakota in Grand Forks, the site posts weekly updates that describe current eruptions and lets you zoom in on the location using the mapping program Google Earth. You can also peruse a catalog that supplies charts, photos, and records of past activity for volcanoes such as Rabaul in the South Pacific (above). The ash plume from its 1994 eruption ascended more than 18 kilometers. To learn more about volcanism, flip through the FAQ section. Volcano World's experts answer more than 1000 reader queries on everything from the relation between lava color and temperature (yellow is hotter than red) to the effect of Krakatau's 1883 explosion on global climate. (The ash it ejected caused a one-quarter-degree cooling that lasted up to 2 years.) Or for a little lava tourism, follow the Volcano of the Week feature to an interesting peak.

volcano.und.nodak.edu

EXHIBITS

Victorian Plant Man

The British botanist Joseph Dalton Hooker (1817–1911) served as Darwin's advocate, confidante, and sounding board. But he was an influential researcher in his own right, as readers can learn at this site from science historian Jim Endersby of Cambridge University in the United Kingdom. Hooker's taxonomic studies helped untangle the species pouring in from Britain's sprawling empire in the mid- and late-1800s. He also ran the Royal Botanic Gardens at Kew for 20 years and pushed to transform botany from a genteel hobby into a profession. The site's biography touches on Hooker's early collecting expeditions, which took him from New Zealand to the Himalayas, and his struggle to find a permanent job. He didn't land a secure position until his father hired him to be assistant director at Kew in 1855. Visitors can also browse a selection of Hooker's writings, including his description of Darwin's botanical specimens from the Galápagos Islands.

www.jdhooker.org.uk

WEB TEXT

Before the Double Helix

Science historians and others interested in James Watson's work prior to the discovery of DNA's structure will find a nugget here: Watson's 1950 Ph.D. dissertation from Indiana University, Bloomington. Visitors can leaf through all 92 pages of *The Biological Properties of X-ray Inactivated Bacteriophage* at the university's digital library.

webapp1.dlib.indiana.edu/metsnav/general/navigate.do?oid=VAA2040

FUN

Spinning Spiders

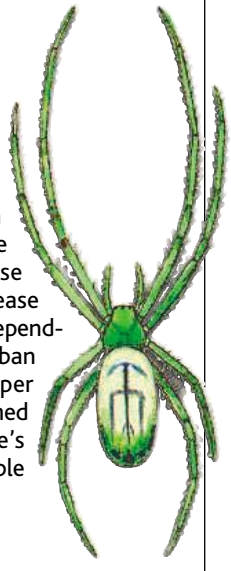

Like snakes and other scary critters, spiders have inspired more than their share of superstitions and tall tales. At The Spider Myths Site, curator Rod Crawford of the Burke Museum in Seattle, Washington, squashes more than 50 common errors about the misunderstood arachnids. Take those well-meaning folks who "liberate" house spiders outside. The animals often die after release because many species that lurk indoors are as dependent on our homes as we are. Then there's the urban legend that we each swallow four live spiders per year during our sleep. In fact, there are no confirmed instances of spiders climbing into someone's mouth, Crawford says, and it's virtually impossible to swallow them unwittingly.

www.washington.edu/burkemuseum/spidermyth

TOOLS

Scourge of a Continent

HIV is hammering Africa, with infection rates of more than 30% in countries such as Botswana. Researchers will find tools for analyzing HIV molecular data and information on the main African strain at BioAfrica, created by virologists at Oxford University and the University of Pretoria in South Africa. BioAfrica complements other HIV sites, such as the sequence bank at Los Alamos National Lab in New Mexico (NetWatch, 23 August 2002, p. 1243), by spotlighting HIV's subtype C, the viral variant that predominates in the southern part of the continent. Users can download free software for determining a virus's subtype or visit a new proteomics section that probes the sequences and structures of HIV's 19 proteins. The site also includes plenty of background on subtype C, including charts that follow its spread starting in the early 1980s. Above, an AIDS patient in Zambia.

www.bioafrica.net

Send site suggestions to netwatch@aaas.org. Archive: www.sciencemag.org/netwatch

CREDITS (TOP TO BOTTOM): IMAGE SCIENCE AND ANALYSIS LABORATORY/NASA JOHNSON SPACE CENTER; REUTERS

Breakthrough of the Year

Equipped with genome data and field observations of organisms from microbes to mammals, biologists made huge strides toward understanding the mechanisms by which living creatures evolve

Evolution in Action

The *big* breakthrough, of course, was the one Charles Darwin made a century and a half ago. By recognizing how natural selection shapes the diversity of life, he transformed how biologists view the world. But like all pivotal discoveries, Darwin's was a beginning. In the years since the 1859 publication of *The Origin of Species*, thousands of researchers have sketched life's transitions and explored aspects of evolution Darwin never knew.

BREAKTHROUGH ONLINE
For an expanded version of this section, with references and links, see www.sciencemag.org/sciext/btoy2005

Today evolution is the foundation of all biology, so basic and all-pervasive that scientists sometimes take its importance for granted. At some level every discovery in biology and medicine rests on it, in much the same way that all terrestrial vertebrates can trace their ancestry back to the first bold fishes to explore land. Each year, researchers worldwide discover enough extraordinary findings tied to evolutionary thinking to fill a book many times as thick as all of Darwin's works put together. This year's volume might start with a proposed rearrangement of the microbes at the base of the tree of life and end with the discovery of 190-million-year-old dinosaur embryos.

Amid this outpouring of results, 2005 stands out as a banner year for uncovering the intricacies of how evolution actually proceeds. Concrete genome data allowed researchers to start pinning down the molecular modifications that drive evolutionary change in organisms from viruses to primates. Painstaking field observations shed new light on how populations diverge to form new species—the mystery of mysteries that baffled Darwin himself. Ironically, also this year some segments of American society fought to dilute the teaching of even the basic facts of evolution. With all this in mind, *Science* has decided to put Darwin in the spotlight by saluting several dramatic discoveries, each of which reveals the laws of evolution in action.

All in the family

One of the most dramatic results came in September, when an international team published the genome of our closest relative, the chimpanzee. With the human genome already in hand, researchers could begin to line up chimp and human DNA and examine, one by one, the 40 million evolutionary events that separate them from us.

The genome data confirm our close kinship with chimps: We differ by only about 1% in the nucleotide bases that can be aligned between our two species, and the average protein differs by less than two amino acids. But a surprisingly large chunk of noncoding material is either inserted or deleted in the chimp as compared to the human, bringing the total difference in DNA between our two species to about 4%.

Chimp champ. Clint, the chimpanzee whose genome sequence researchers published this year.

Somewhere in this catalog of difference lies the genetic blueprint for the traits that make us human: sparse body hair, upright gait, the big and creative brain. We're a long way from pinpointing the genetic underpinnings of such traits, but researchers are already zeroing in on a few genes that may affect brain and behavior. This year, several groups published evidence that natural selection has recently favored a handful of uniquely human genes expressed in the brain, including those for endorphins and a sialic acid receptor, and genes involved in microcephaly.

The hunt for human genes favored by natural selection will be sped by newly published databases from both private and public teams, which catalog the genetic variability among living people. For example, this year an international team cataloged and arranged more than a million single-nucleotide polymorphisms from four populations into the human haplotype map, or HapMap. These genetic variations are the raw material of evolution and will help reveal recent human evolutionary history.

Probing how species split

2005 was also a standout year for researchers studying the emergence of new species, or speciation. A new species can form when populations of an existing species begin to adapt in different ways and eventually stop interbreeding. It's easy to see how that can happen when populations wind up on opposite sides of oceans or mountain ranges, for

CREDITS: (DNA) C. BICKEL/*SCIENCE*; (CHIMPANZEE) YERKES NATIONAL PRIMATE RESEARCH CENTER

example. But sometimes a single, contiguous population splits into two.

Evolutionary theory predicts that this splitting begins when some individuals in a population stop mating with others, but empirical evidence has been scanty. This year field biologists recorded compelling examples of that process, some of which featured surprisingly rapid evolution in organisms' shape and behavior.

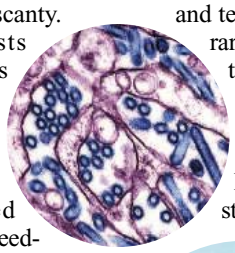

For example, birds called European blackcaps sharing breeding grounds in southern Germany and Austria are going their own ways—literally and figuratively. Sightings over the decades have shown that ever more of these warblers migrate to northerly grounds in the winter rather than heading south. Isotopic data revealed that northerly migrants reach the common breeding ground earlier and mate with one another before southerly migrants arrive. This difference in timing may one day drive the two populations to become two species.

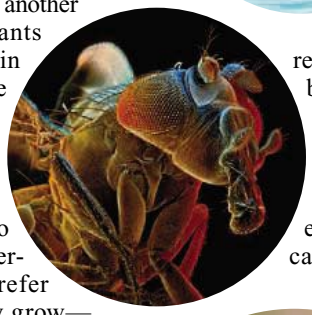

Two races of European corn borers sharing the same field may also be splitting up. The caterpillars have come to prefer different plants as they grow—one sticks to corn, and the other eats hops and mugwort—and they emit different pheromones, ensuring that they attract only their own kind.

Biologists have also predicted that these kinds of behavioral traits may keep incipient species separate even when geographically isolated populations somehow wind up back in the same place. Again, examples have been few. But this year, researchers found that simple differences in male wing color, plus rapid changes in the numbers of chromosomes, were enough to maintain separate identities in reunited species of butterflies, and that Hawaiian crickets needed only unique songs to stay separate. In each case, the number of species observed today suggests that these traits have also led to rapid speciation, at a rate previously seen only in African cichlids.

Other researchers have looked within animals' genomes to analyze adaptation at the genetic level. In various places in the Northern Hemisphere, for example, marine stickleback fish were scattered among landlocked lakes as the last Ice Age ended. Today, their descendants have evolved into dozens of different species, but each has independently lost the armor plates needed for protection from marine predators. Researchers expected that the gene responsible would vary from lake to lake. Instead, they found that each group of stranded sticklebacks had lost its armor by the same mechanism: a rare DNA defect affecting a signaling molecule involved in the development of dermal bones and teeth. That single preexisting variant—rare in the open ocean—allowed the fish to adapt rapidly to a new environment.

Biologists have often focused on coding genes and protein changes, but more evidence of the importance of DNA outside genes came in 2005. A study of two species of fruit flies found that 40% to 70% of noncoding DNA evolves more slowly than the genes themselves. That implies that these regions are so important for the organism that their DNA sequences are maintained by positive selection. These noncoding bases, which include regulatory regions, were static within a species but varied between the two species, suggesting that noncoding regions can be key to speciation.

That conclusion was bolstered by several other studies this year. One experimental paper examined a gene called *yellow*, which causes a dark, likely sexually attractive, spot in one fruit fly species. A separate species has the same *yellow* gene but no spot. Researchers swapped the noncoding, regulatory region of the spotted species' *yellow* gene into the other species and produced dark spots, perhaps retracing the evolutionary events that separated the two. Such a genetic experiment might have astonished and delighted Darwin, who lamented in *The Origin* that "The laws governing inheritance are quite unknown." Not any longer.

To your health

Such evolutionary breakthroughs are not just ivory-tower exercises; they hold huge promise for improving human well-being. Take the chimpanzee genome. Humans are highly susceptible to AIDS, coronary heart disease, chronic viral hepatitis, and malignant malarial infections; chimps aren't. Studying the differences between our species will help pin down the genetic aspects of many such diseases. As for the HapMap, its aims are explicitly biomedical: to speed the search for genes involved in complex diseases such as diabetes. Researchers have already used it to home in on a gene for age-related macular degeneration.

And in 2005, researchers stepped up to help defend against one of the world's most urgent biomedical threats: avian influenza. In October, molecular biologists used tissue from a body that had been frozen in the Alaskan permafrost for almost a century to sequence the three unknown genes from the 1918 flu virus—the cause of the epidemic that killed 20 million to 50 million people. Most deadly flu strains emerge when an animal virus combines with an existing human virus. After studying the genetic data, however, virologists concluded that the 1918 virus started out as a pure avian strain. A handful of mutations had enabled it to easily infect human hosts. The possible evolution of such an infectious ability in the bird flu now winging its way around the world is why officials worry about a pandemic today.

A second group reconstructed the complete 1918 virus based on the genome sequence information and studied its behavior. They found that the 1918 strain had lost its dependence on trypsin, an enzyme that viruses typically borrow from their hosts as they infect cells. Instead, the 1918 strain depended on an in-house enzyme. As a result, the reconstructed bug was able to reach exceptionally high concentrations in the lung tissue of mice tested, helping explain its virulence in humans. The finding could point to new ways to prevent similar deadly infections in the future.

Darwin focused on the existence of evolution by natural selection; the mechanisms that drive the process were a complete mystery to him. But today his intellectual descendants include all the biologists—whether they study morphology, behavior, or genetics—whose research is helping reveal how evolution works.

–ELIZABETH CULOTTA AND ELIZABETH PENNISI

CREDITS: C. GOLDSMITH/CDC (AVIAN FLU); W. A. CRESKO *ET AL.*, *PNAS* **101**, 6050 (2004) (STICKLEBACK); DAVID SCHARF/PETER ARNOLD (*DROSOPHILA*); ANDY BRIGHT (EUROPEAN BLACKCAP)

The Runners-Up >>

2 Planetary Blitz

Scientists and engineers outdid themselves in 2005 in mounting exploratory expeditions beyond Earth. They had spacecraft at or on the way to the moon, Mercury, Venus, Mars, a comet, an asteroid, Saturn, and the very edge of the solar system. At the Red Planet, three orbiters and two rovers beamed back terabytes of data. The high point of a banner year, however, came on Saturn's haze-shrouded moon Titan. In January, the European spacecraft Huygens drifted down to a familiar-looking but fundamentally weird world.

The first landing on another planet's moon revealed a world where infrequent but drenching rains of liquid methane wash low hills, cutting networks of steep-sided valleys and flushing icy debris and dark organic crud out into shallow lakes. The lakes then evaporate away, although the lander apparently settled into ground still soaked with methane. The discovery of a sort of hydrologic cycle shaping another world is a first.

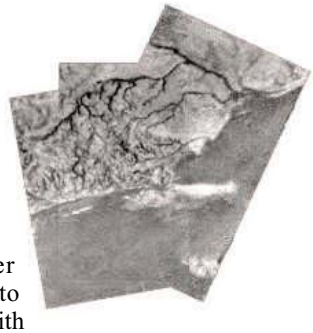

Drenched. Huygens found a familiar-looking world washed by methane rains.

A fleet of other explorers joined Huygens this year. The aging Voyager 1 reported approaching the "edge" of the solar system, where the solar wind slows abruptly. The

Scorecard 2004

Slam-dunks and near-fizzles gave our editors a mixed record for prophecy this year.

Recycling pays. New results confirmed that autophagy is much more than just a way for nutrient-starved cells to recycle membrane components and cytoplasmic molecules. Studies indicated that autophagy helps the immune response to bacteria and viruses and that some microbes have developed ways to counter or even exploit the cellular process. Researchers also began to detail how autophagy is connected to both neurodegeneration and cancer.

Obesity drugs. No new drugs for obesity were approved in 2005, but rimonabant continues to show promise in clinical trials, and Sanofi-Aventis may receive U.S. Food and Drug Administration approval for it in 2006.

HapMapping along. The International HapMap Project delivered on schedule, publishing its first version this past October. (A finer resolution copy will come out in 2006.) A California company, Perlegen Sciences, published its own map last February. The $138 million map also helped lead scientists to a macular degeneration gene and a gene for skin color; how much it will help next year, and how widely it will be used, remain open questions.

Cassini-Huygens at Saturn. So far the joint U.S., European, and Italian mission to the ringed planet has been a blazing success. Amid the smallest of glitches, the Huygens lander drifted down to Titan's surface, revealing an icy landscape carved by rains of liquid methane. Elsewhere in the system, Enceladus proved energetic for such a little moon, spewing ice and water from its south pole to form the nebulous E ring. The bizarre F ring sported a spiral-necklace companion ring. And another 55 orbits of Saturn are still on Cassini's agenda.

Paper tigers. North Korea says it will give up its nuclear weapons program, but the devil is in the details, none of which have been worked out. Meanwhile, Iran's new hard-line government insists that uranium enrichment is an inalienable right, leaving little hope that negotiations will prevent Iran from acquiring the means and know-how to develop a nuclear arsenal.

European Research Council. The ERC, an agency that would fund top basic research across Europe, has morphed in just a few years from a scrappy grassroots movement to the darling of politicians. In April, the European Commission made the ERC the centerpiece of its bid to double the E.U.'s research funding. And in July the commission appointed 22 high-profile scientists to the ERC's scientific council, which will divvy up the first grants. But political wrangling over the E.U.'s overall budget has left the ERC in limbo. By December, the proposed doubling for research was off the table, and scientists feared that the ERC could be left with only token funding—and disappointed applicants.

Regulating nano. Governments worldwide are working hard to develop standards for nanomaterials, come up with programs to test their safety, and regulate their use.

CREDITS (TOP, LEFT TO RIGHT): JPL/NASA; ESA/NASA/JPL/UNIVERSITY OF ARIZONA; (CRYSTAL BALLS) TERRY SMITH

Deep Impact spacecraft plowed into comet Tempel 1 to reveal a fluffy subsurface. Cassini repeatedly swung by Saturn's rings, Titan, and other moons. SMART-1 arrived at the moon on its ion-drive engine. Hayabusa got up-close and personal with asteroid Itokawa. Stardust headed home with bits of comet Wild 2. And all the while, MESSENGER cruised toward Mercury, and the Mars Reconnaissance Orbiter and Venus Express spiraled toward their targets. Planetary scientists, for the time being at least, are in their second golden age of solar system exploration.

3 Blooming Marvelous

Several key molecular cues behind spring's burst of color came to light in 2005. In August, for example, three groups of plant molecular biologists finally pinned down the identity of florigen, a signal that initiates the seasonal development of flowers. The signal is the messenger RNA of a gene called *FT*. When days get long enough, this RNA moves from leaves to the growth tip, where the FT protein interacts with a growth tip–specific transcription factor, FD. The molecular double whammy ensures that blossoms appear in the right place on the plant at the right time of year.

Researchers also gained new insights into the workings of a gene called *LEAFY* that is involved in stimulating flowering. Comparisons of *LEAFY* in moss, ferns, and cress suggest that over the past 400 million years, just a few base changes have converted the gene from a broad-spectrum growth stimulator—as it still is in moss—to one that seems to fire up only for flowering in more recently evolved plants.

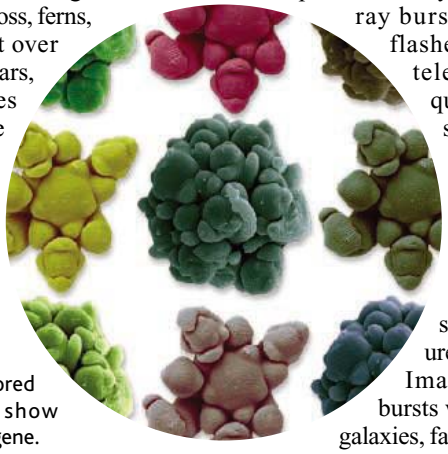

Microbouquet. False-colored nascent cress flowers show effects of mutant *LEAFY* gene.

The plant hormone gibberellin helps control the later stages of flower development, as well as other aspects of cell growth involved in cellular expansion. In 2005, researchers identified the receptor for this hormone in rice, a valuable step in improving crops. Plant biologists also pinpointed another key receptor, for the essential plant growth hormone auxin. This receptor is part of the cell's protein-degradation machinery that destroys the proteins that keep auxin activity in check.

Finally, the plant gene *HOTHEAD*—important for putting the finishing touches on flower design—proved to be quite a head-scratcher. Alleles of this gene, found in one generation of the self-fertilizing weed *Arabidopsis* but missing in the next, showed up again in the third generation. The discovery suggests that, surprisingly, cells may have a cache of RNA from which to reconstruct the missing allele.

4 Neutron Stars Gone Wild

Astrophysicists adore neutron stars, the city-sized corpses of stars that pack matter into its most extreme state. This year, new instruments yielded vivid insights into the most violent behaviors of these objects.

The fireworks started on 27 December 2004, when a 0.2-second pulse of radiation from near the center of the Milky Way seared detectors on more than a dozen spacecraft. Despite its distance, the blast was brighter in x-rays and gamma rays than any solar eruption. Weeks of analysis showed that the probable source was a nearly global starquake on a "magnetar," an unstable young neutron star encased by the strongest magnetic fields known. Such flares had happened before, but this one was 100 times more potent.

Astrophysicists proposed that giant magnetar flares in nearby galaxies solved part of the mystery of short gamma ray bursts (GRBs)—random flashes in the heavens that telescopes had not been quick enough to see. But starting in May, NASA high-energy satellites caught several short GRBs at much greater distances. Ground-based telescopes, many of them new robotic systems, swung to measure the fading aftermaths. Images revealed that the bursts were in the outskirts of galaxies, far from nurseries of massive stars that create young neutron stars. Moreover, the telescopes found no traces of supernova explosions, thought to produce longer GRBs.

The evidence matched a favored scenario for short GRBs: a rapid, cataclysmic merger of two ancient neutron stars or a neutron star and a black hole. Researchers can't yet discriminate between the two types of collisions. But that should change as the Swift satellite and other instruments expose more of the fleeting bursts. On the ground, space-rippling gravitational waves from merging neutron stars could trigger the Laser Interferometer Gravitational-Wave Observatory for the first time.

Flash points. Collisions between neutron stars (*top*) or a neutron star and a black hole appear to spark most short bursts of gamma rays.

5 Miswiring the Brain

Although dozens of genes have been linked to brain disorders in recent years, connecting the dots between genetics and abnormal behavior has been anything but child's play. This year, however, researchers gained clues about the mechanisms of diverse disorders including schizophrenia, Tourette syndrome, and dyslexia. A common theme seems to be emerging: Many of the genes involved appear to play a role in brain development.

In November, two reports put meat on the bones of previous claims that variants of a gene called *DISC1* increase the risk of schizophrenia. One research team found that inhibiting *DISC1* activity in mice alters brain development, causing subtle abnormalities in the animals' cerebral cortices similar to those seen in postmortem brains from schizophrenia patients. Another team linked *DISC1* to molecular signaling pathways important in brain development and in regulating neurotransmitter levels, which are often out of whack in psychiatric patients.

In October, researchers described a rare genetic defect that appears to cause Tourette syndrome. The mutation likely causes only a tiny fraction of Tourette cases, but its discovery may be an important lead. One gene that's disrupted, *SLITRK1*, influences branch

CREDITS (TOP TO BOTTOM): NASA/SONOMA STATE UNIVERSITY/AURORE SIMONNET; DANA BERRY/NASA; A. MAIZEL AND J. BERGER

Breakdown of the Year: U.S. Particle Physics

Particle physicists in the United States would probably like to forget 2005. Budget woes forced the cancellation of two major experiments just as researchers were about to start construction. That leaves none in the works to replace those currently studying particles called quarks—the sorts of experiments that have long been the heart of the field. At the same time, the U.S. Department of Energy (DOE) asked physicists to consider which of two existing particle colliders they would rather shut down early to save money.

Researchers around the globe fear that if U.S. particle physics withers, so will the entire field. "We all need a vitally active U.S. community," says Brian Foster of Oxford University in the U.K. "That's what's driven particle physics in the past, and hopefully that's what will drive it in the future."

Physicists got a shock in February, when DOE nixed BTeV, a $140 million experiment that would have run at the Fermi National Accelerator Laboratory (Fermilab) in Batavia, Illinois (*Science*, 11 February, p. 832). Using beams from Fermilab's Tevatron collider, BTeV would have studied bottom quarks, heavier, unstable cousins of the down quarks found in protons and neutrons. BTeV researchers were expecting to get the final go-ahead for construction.

Early end? Either SLAC's PEP-II collider (*above*) or Fermilab's Tevatron could shut down ahead of schedule.

Less surprisingly, in August the National Science Foundation pulled the plug on the Rare Symmetry Violating Processes (RSVP) experiment at DOE's Brookhaven National Laboratory in Upton, New York (*Science*, 19 August, p. 1163). RSVP would have looked for new physics in the decays of particles called muons and K^0 mesons. But its construction costs had ballooned from $145 million to $282 million, and its lifetime operating costs had tripled to $250 million.

In May, DOE's Office of Science requested a study, due early next year, of the relative merits of shutting down either the Tevatron or the PEP-II collider at the Stanford Linear Accelerator Center in Menlo Park, California (*Science*, 27 May, p. 1241). The Tevatron smashes protons into antiprotons at the highest energies achieved to make top quarks and other particles; PEP-II collides electrons and positrons and cranks out bottom quarks. Researchers plan to turn off PEP-II in 2008 and the Tevatron in 2009, but decommissioning one of them earlier might free up money for future projects.

Meanwhile, researchers in Europe are assembling the Large Hadron Collider at CERN, the particle physics laboratory near Geneva, Switzerland. Scheduled to start up in 2007, the $7.7 billion machine might produce the long-sought Higgs boson, the particle thought to give others their mass. At the same time, physicists in Japan have their KEK-B collider producing bottom quarks and are studying wispy particles called neutrinos. (Fermilab is also pursuing neutrino physics.)

But particle physicists from Europe and Asia aren't celebrating the passing of the torch from the United States. They say a strong U.S. program is essential for the survival of the field, especially if they hope to build the proposed International Linear Collider (ILC), a multibillion-dollar global facility that most see as the future of particle physics. "It is very clear that without the participation of the U.S. it is impossible" to build the ILC, says Akira Masaike of the Japan Society for the Promotion of Science in Washington, D.C.

On that front, at least, 2005 brought some reasons for optimism, says Fred Gilman of Carnegie Mellon University in Pittsburgh, Pennsylvania. Physicists from the United States, Europe, and Asia united in their commitment to the ILC as never before. "Before, the international effort was the sum of three parts," Gilman says. "Now there is central leadership." And officials in DOE's Office of Science remain enthusiastic about the ILC, Gilman says. Physicists plan to have a preliminary design—and a price tag—for that dream machine by the end of 2006.

–ADRIAN CHO

Flawed circuits? Many brain disorders are linked to genes affecting development.

formation by neurons and is active during development in brain regions thought to be altered in Tourette syndrome and other conditions, including obsessive compulsive disorder. New research also links developmental genes to dyslexia, identifying three genes—*KIAA0319*, *DCDC2*, and *ROBO1*—that may cause faulty wiring in neural circuits involved in reading.

Much of the new work suggests that genetic miscues, rather than causing neuropsychiatric disorders outright, alter brain biology in the womb in a way that predisposes us to problems later in life. A better understanding of how this happens may help reduce the risks.

6 Geochemical Turmoil

When researchers announced in June that they had detected isotopic differences between earthly and extraterrestrial rocks, geochemists had to scrap their long-standing view of how Earth formed and evolved. They no longer believe that thoroughly mixed dust and ice agglomerated 4.5 billion years ago to form an Earth that has remained more or less mixed ever since. Something more interesting must have happened.

Key to the cosmochemical revolution was new technology. In the early 1980s, researchers

Complicated. Young Earth had a more interesting history than scientists believed.

CREDITS (TOP TO BOTTOM): C. PRICE/TAXI/GETTY IMAGES; STANFORD LINEAR ACCELERATOR CENTER; WILLIAM K. HARTMANN/PLANETARY SCIENCE INSTITUTE

measured the ratio of neodymium isotopes both in the chondritic meteorites thought to represent the solar system's starting material and in rocks derived from Earth's interior. The neodymium ratios were the same, within analytical error, implying that chondritic meteorites and accessible parts of Earth still resemble the solar system's starting material. But advances in mass-spectrometer technology have whittled away at the error bars. When researchers measured the same sort of rocks this year, they found a 20-part-per-million difference that had been undetectable in the earlier scatter.

The minute isotopic difference has opened a yawning chasm between cosmochemists. One camp simply assumes that Earth got its makings from a part of the nascent solar system that happened to have a distinctive, nonchondritic composition. Others believe that the presolar nebula was compositionally uniform, not lumpy, but that shortly after Earth's formation, while its rock was still roiling in a "magma ocean," a portion enriched in heat-generating elements separated out and sank beyond geochemists' ken. Today, it may still lie between molten core and rocky mantle, its heat helping generate the core's magnetic field and sending plumes of hot rock toward the surface.

7 Protein Portrait

This year, researchers got their best look yet at the molecular structure of a voltage-gated potassium channel, a protein as essential to nerve and muscle as transistors are to computers. Sitting in the cell membrane, these tiny gatekeepers open and close in response to voltage changes, controlling the flow of potassium ions. The new atomic-scale portrait should be extremely useful for biophysicists seeking to understand the workings of these crucial proteins. It may also represent a step toward reconciling a recent debate that has rankled the usually calm community of ion channel researchers. Or maybe not.

It all started in May 2003, when Roderick MacKinnon of Rockefeller University in New York City and colleagues published the first-ever structure of a voltage-gated potassium channel and proposed a model to explain how it worked. Everyone agreed that the snapshot was a technological feat. But many researchers suspected that the channel, called KvAP, had been distorted by the preparations for imaging, and critics complained that MacKinnon's proposed mechanism contradicted decades of experiments. A flurry of angry e-mails ensued. Unpleasant things were said.

This August, MacKinnon (who subsequently won the 2003 chemistry Nobel)

CREDIT: DISASTER RESEARCH CENTER/UNIVERSITY OF DELAWARE

Disasters: Searching for Lessons From a Bad Year

No doubt about it, the 12 months since the last Breakthrough of the Year issue have been an *annus horribilis*. Three major natural disasters—the 2004 "Christmas tsunami" in the Indian Ocean, Hurricane Katrina on the U.S. Gulf Coast, and the Pakistan earthquake—left nearly 300,000 dead and millions homeless. In Pakistan, the disaster is still unfolding as winter engulfs the devastated communities.

Insurance companies classify such events as "acts of God": misfortunes for which no one is at fault. But in their aftermath, many scientists are pointing out that natural disasters are anything but natural: Societies can mitigate their impacts by making the right decisions about where and how people live, how information is shared, and what kind of research to invest in. And some are pushing new ideas to make that happen.

For example, Aromar Revi, a New Delhi–based disaster mitigation consultant to the Indian government, envisions "a public database like Google Earth" that would allow researchers around the world to map the "risk landscape down to the ZIP-code level." Such a system would enable nations with a shared risk to build better warning networks. But there are serious hurdles to going global. For example, India refused to share data for an international tsunami warning system because it could also reveal their nuclear tests (*Science*, 9 December, p. 1604). Nor will such a network come cheap, but Revi says governments will soon realize that it "is worth every cent of the many hundreds of millions of dollars it would cost to build and maintain."

A disaster warning system is only as good as the science behind it. For some events, such as hurricanes and volcanoes, science has vastly improved forecasts. But for others, such as earthquakes, decades of research may have illuminated how and where they are likely to strike, but not when.

Don't blame God. Better planning could make natural disasters much less disastrous, experts say.

Even with greatly enhanced warning systems and infrastructure, natural disasters will continue to wreak enormous damages. Who will pay for it? After the past year's $200 billion in damages from weather-related disasters alone—three times higher than for any previous year—some economists are calling for a radical rethink of disaster relief. Rather than relying on the fickle charity of the international community, countries should invest in a new kind of disaster insurance that transfers the risk to financial markets, says Reinhard Mechler, an economist at the International Institute for Applied Systems Analysis in Laxenburg, Austria. Such a plan relies on scientists to create a finer-grained map of the probability of various disasters and the range of their impacts (*Science*, 12 August, p. 1044).

Science funding could soon feel the effects of the past year of disasters. Two months before Hurricane Katrina struck, the U.S. president's National Science and Technology Council capped a 10-year study by publishing a report called Grand Challenges for Disaster Reduction. The report singled out social sciences as an area deserving a boost, citing the need for strategies to get emergency information to populations that often distrust the authorities. More interdisciplinary science is also needed, says one of the report's co-authors, Priscilla Nelson, a civil engineer at the New Jersey Institute of Technology in Newark. Because the causes and impacts of disasters are so broad, she says, we need teams of geophysicists who can talk fluently with epidemiologists, and engineers with psychologists.

One thing is all but certain: Even worse years lie ahead. Vulnerable urban populations of the developing world are set to double by 2030, as are coastal populations everywhere. Meanwhile, changing climate threatens to bring more hurricanes due to warming and chronic coastal flooding due to rising sea levels, among other worrying possibilities. Looking back over 2005, says Nelson, these disasters should be taken as "opportunities to learn."

—JOHN BOHANNON

John Bohannon is a writer in Berlin, Germany.

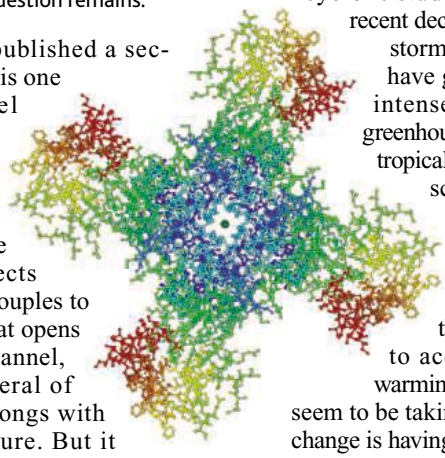

New model. Biochemists described the cell's K^+ channel, but a big question remains.

and colleagues published a second structure—this one of a rat channel called Kv1.2. The new portrait provides an unprecedented look at how the part of the channel that detects voltage changes couples to the mechanism that opens and closes the channel, and it rights several of the perceived wrongs with the KvAP structure. But it doesn't seem to resolve the most contentious issue: how the voltage sensor works. Only time—and more data—will tell.

8 A Change in Climate

The crescendo of evidence indicting humans for global warming produced a breakthrough this year. Some U.S. politicians began talking and occasionally acting as if they will have to do something sooner or later about the growing emissions of greenhouse gases.

The new science was much like that of the past decade, just more insistent and more ominous. In January, climate modelers announced even higher confidence in earlier assertions that the oceans—down to great depths—have warmed in recent decades just as models said they would. Each of two tropical cyclone studies found that over recent decades more and more storms around the world have grown to the most intense levels as rising greenhouse gases have warmed tropical waters. At higher latitudes, scientists announced, Arctic Ocean ice cover had hit another record low, this time with the added warning that the feedbacks expected to accelerate high-latitude warming—and presumably ice loss—seem to be taking hold. And all this climate change is having an effect. It's altering everything from bird migration patterns in Australia to microbial compositions in sea-floor muck.

Whether as a direct result of the mounting scientific evidence or not, the mood in the United States showed signs of shifting. The U.S. Senate passed a resolution declaring that the threat warrants mandatory controls on greenhouse emissions if costs to the country are not significant. In the Northeast, nine states have agreed to limit emissions from power plants there. The governors of California, Oregon, and Washington have agreed to jointly encourage energy efficiency. And California Governor Arnold Schwarzenegger called for his state to cut greenhouse gas emissions dramatically over the next 45 years. Show biz or not, the talk is heating up.

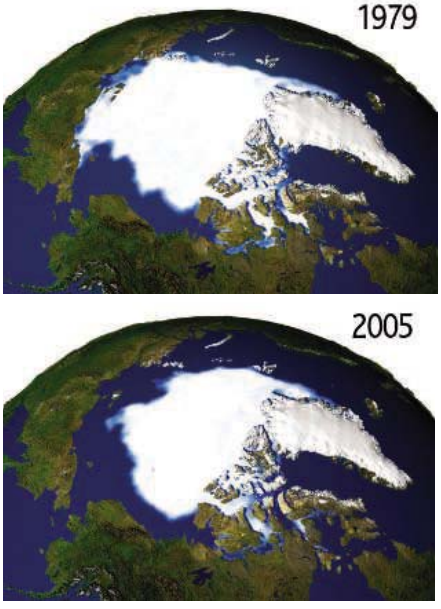

Less is less. Arctic ice cover hit a new low in 2005 as the world warmed.

9 Systems Biology Signals Its Arrival

Make room in the lab, molecular biologists; the engineers have arrived. Engineers have long excelled at understanding complex systems such as power grids and the Internet by tracking how information moves through a network. This year, that approach took off among systems biologists working to understand how cells respond to the myriad chemical and environmental signals bombarding them from all sides.

Molecular biologists have spent decades teasing apart individual cell signaling pathways, in the process building up ever more complex networks. But a static picture of those networks doesn't do justice to the webs of feedback loops and other complex interactions that produce a given output, such as the release of a particular intracellular messenger. To reveal these dynamics, systems biologists are now tracking multiple inputs and outputs of these networks simultaneously.

This year, for example, researchers in the United States used the approach to create a model of nearly 8000 chemical signals involved in a network leading to apoptosis, or programmed cell death. Along the way, they discovered new apoptosis signaling routes. Another U.S. team used gene-expression data to identify 40 genes that help trigger obesity, three of which had never been identified before. Other like-minded teams gained novel insights into signaling networks that control immune cells known as T cells and CA1 neurons in the hippocampus.

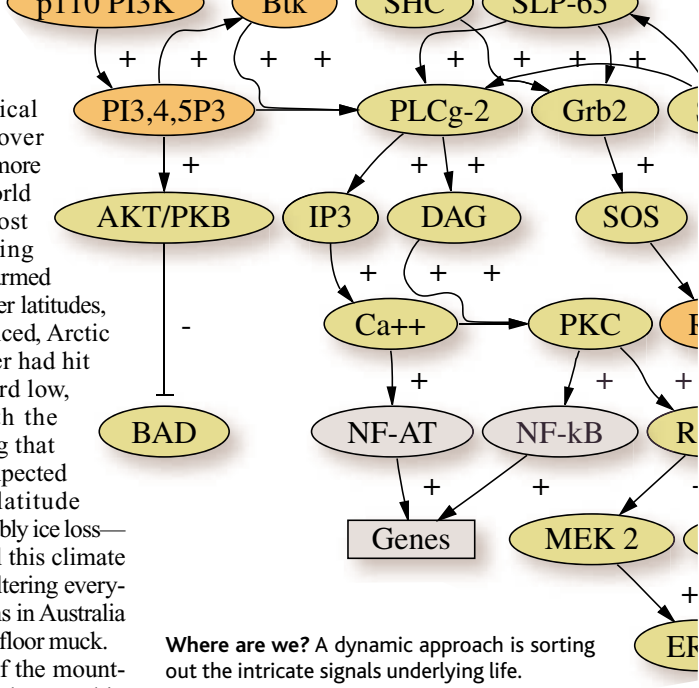

Where are we? A dynamic approach is sorting out the intricate signals underlying life.

It's still early days for systems biology. But proponents anticipate that the emerging dynamic view of cell signaling networks will lead to a better understanding of complex diseases such as cancer and diabetes and to new treatments as well.

10 Bienvenu, ITER

After 18 months of often bitter wrangling, the $12 billion International Thermonuclear Experimental Reactor (ITER) has a home at last. In June, international negotiators broke a diplomatic deadlock over whether to build ITER at Cadarache in southern France or in Rokkasho, Japan. The winner: Cadarache.

The basic concept behind ITER—using superconducting electromagnets to hold a plasma of hydrogen isotopes at a temperature and pressure high enough to achieve nuclear fusion—was born in the 1980s. But the design effort, split among centers in Europe, Japan, and the United States, didn't always go smoothly. In the late 1990s, after the engineering design was complete, governments balked at the price and asked the designers to cut the construction cost by half. The United States withdrew from the

CREDITS (CLOCKWISE FROM TOP LEFT): S. B. LONG *ET AL.*, *SCIENCE* **309**, 833 (2005); STKE; NASA

Areas to Watch in 2006

Avian flu. Whether or not a pandemic kicks off in 2006, research on flu vaccines and drugs will expand—as will debates on who should get them first should a pandemic occur. Also look for a wealth of data on the molecular biology, evolution, epidemiology, and even the history of influenza. And keep your fingers crossed.

Gravity rules. After years of refinements, the first phase of the Laser Interferometer Gravitational-Wave Observatory (LIGO) has reached its promised sensitivity. LIGO's laser chambers in Louisiana and Washington state will monitor the sky during most of 2006—with a smaller facility in Germany, called GEO-600, joining the network later in the year. If two neutron stars merge within 50 million light-years or so, the devices could detect the death spiral. It's a long shot, but we're betting they will.

RNAi-based treatments. They're moving into human patients with startling speed, and 2006 should offer the first hints of how well the highly touted technique works. Company-funded trials in macular degeneration and the pediatric illness respiratory syncytial virus are under way; another targeting hepatitis C is supposed to launch soon, with some therapies for neurological diseases to follow. Oh, and another treatment that's coming down the pike: RNAi for permanent hair removal.

Catching rays. The speediest atomic nuclei in the universe, called ultrahigh-energy cosmic rays, may open a new frontier of physics. The sprawling Pierre Auger Observatory in Argentina will near completion in 2006, offering the best chance to explore those limits. Already, Auger's powerful combination of ultraviolet telescopes and water-tank detectors is measuring different aspects of the particle showers sparked by incoming rays. Early results affirm a theorized energy threshold, imposed by interactions in space, that cosmic rays rarely cross.

Small worlds. With ever-better methods of pulling DNA from environments such as soils and the human gut, researchers are documenting the incredible microbial diversity on this planet. In 2006, expect a flurry of papers detailing the evolution and molecular bases of microbial communities and the relationships, both beneficial and pathogenic, between microbes and their partners; more examples of lateral transfer of genes between species; and—just possibly—consensus about a microbial family tree and a much sharper picture of how eukaryotic cells arose.

Seconding supersolidity. Two years ago, physicists reported that solidified helium appears to flow like a liquid without any viscosity. Theorists debate whether such "superflow" is possible in a well-ordered crystal, and no one has reproduced the result yet. Look for someone to confirm the observation—or shoot it down.

Homing in on high-T_c. In 1986, physicists discovered that certain compounds laden with copper and oxygen carry electricity without resistance, some now at temperatures as high as 138 kelvin. Twenty years later, researchers still aren't sure precisely how high-T_c superconductors work. But a variety of exquisitely sensitive experimental techniques should cull the vast herd of possible explanations.

Now you see it? A fleeting glimpse captured on video raised hopes that the ivory-billed woodpecker might not be extinct after all.

Bird to watch for. Early in 2005, a blurry video and new sightings of the ivory-billed woodpecker, considered extinct for the past 60 years, wowed conservationists and birders alike. Some skeptics remained unconvinced by the 1.2-second footage, but many later were swayed by audio tapes of the woodpecker's call and distinctive "tap, tap." Biologists are scouring the Arkansas bayou, where there have now been more than a dozen sightings, for more evidence that they are not seeing a ghost of a bird past. We're betting this "ghost" proves to be the real thing.

project in 1999, only to rejoin in 2003. By late 2003, only one hurdle remained: choosing the site. Government ministers from the by-then six members—China, the European Union (E.U.), Japan, South Korea, Russia, and the United States—gathered in Washington, D.C., for a gala signing ceremony. But when the time came to vote, they split down the middle.

More technical studies of the two sites were carried out, but both sides dug in their heels. Rumors of political skullduggery abounded: Europeans suspected that the United States refused to support the French site to punish France for opposing the war in Iraq, while other whispers suggested that the United States had backed the Japanese site in exchange for Japan's support for the war. In the end, Japan and the E.U. hammered out a deal between themselves. In June this year, after months of delicate diplomacy, Japan withdrew Rokkasho in exchange for a bigger share of construction contracts and a hefty European contribution to a fusion research facility in Japan.

Now ITER researchers can look forward to a few decades working under the warm Mediterranean sun. And who knows? The world may get a working fusion reactor at last.

–THE NEWS STAFF

Closing the circle. After 20 years of research, fusion scientists are ready to start building the ITER reactor.

CREDITS (TOP TO BOTTOM): J. W. FITZPATRICK *ET AL.*, *SCIENCE* **308**, 1460 (2005); ITER

This Week

PAGE 1887
Mammoth sequence

1890
Early adaptive immunity

STEM CELLS

Cloning Researcher Says Work Is Flawed but Claims Results Stand

Acknowledging that his team made "various serious errors and shortfalls," cloning researcher Woo Suk Hwang has asked *Science* to retract his celebrated paper reporting the creation of embryonic stem (ES) cells from 11 patients suffering from diabetes, an immune system disease, and spinal cord injury. But as *Science* went to press, Hwang was insisting that, contrary to the claims of a collaborator, his team succeeded in creating these patient-specific stem cells and that they intend to replicate their results.

Pressure on Hwang and his group has been growing as scientists and the press have raised questions about the evidence presented in the paper, first published online in May this year (*Science*, 17 June, p. 1777). In another paper in 2004, Hwang and colleagues reported the first ever production of embryonic stem cells from a cloned human blastocyst. In the 2005 paper, another group led by Hwang reported that they had established 11 ES cell lines from embryos cloned from patients, a step toward someday making genetically matched replacement tissue. No lab has replicated their results.

But in early December on a Korean Web site, an anonymous writer, who claims to be a life scientist, pointed out duplications in some of the photographs of ES cells published in the 2005 paper. According to a *Science* statement, a few hours later Hwang notified *Science*'s editorial offices of what he called "an unintentional error" that led to "about 4 pictures being used redundantly." More questions arose after critics questioned DNA traces used to demonstrate that the cell lines were a genetic match with the skin cells donated by the 11 patients to create cloned embryos (*Science,* 16 December, p. 1748). On 15 December, coauthor Sung Il Roh, a fertility expert at MizMedi Hospital in Seoul who collected oocytes from donors for Hwang's work, told Korean media that Hwang had confessed to falsifying evidence for 9 of the reported 11 cell lines.

The next day, at a packed press conference at Seoul National University (SNU), a defiant Hwang told reporters that he was "surprised and taken aback" by Roh's assertion, although he acknowledged that he had talked with Roh. Reading a prepared statement, Hwang said, "I want to make it really clear that our research team produced patient-specific (stem cells)." He acknowledged, however, that the team had problems with their cell lines. He said that last January, contamination with yeast had destroyed at least six of the lines the team had created. Based on Hwang's statement, it's not clear whether any of these original six lines were alive at the time the *Science* paper was submitted in March. The group was "lax in our management and committed many mistakes," said Hwang. He said they would thaw the five remaining cell lines to try to demonstrate that they match their donors, a process that Hwang said could take about 10 days.

Serious errors. Cloning researcher Woo Suk Hwang has said he will withdraw a landmark paper published in *Science* earlier this year because of errors but says the conclusions are valid.

CREDIT: KIM KYUNG-HOON/REUTERS

Hwang also said that MizMedi might be responsible for mixing up cell lines from its own research with those used in the experiments that produced the *Science* paper, and he called for an investigation. Roh held an emotional press conference shortly thereafter in which he reportedly reiterated his claims and accused Hwang of lying.

At a 16 December press briefing in Washington, D.C., *Science* Editor-in-Chief Donald Kennedy said that Hwang and Gerald Schatten of the University of Pittsburgh, who was corresponding author on the paper, had told *Science* editors in a phone call the previous day that several aspects of the data "could not be trusted" and asked that the paper be retracted, pending the agreement of the 23 other authors. Kennedy said the scope of the paper's flaws is still unclear. Kennedy added, however, that although the paper contains errors that were known at the time of submission, there is not at present evidence to conclude scientific misconduct.

When questions were first raised about duplicated images, editors at *Science* said that it appeared the duplications occurred after the paper was accepted and when new, higher-resolution images were substituted for publication. But Katrina Kelner, *Science*'s deputy editor for life sciences, says it now appears there were problems in the original submission as well. Although the four duplications that Hwang pointed out to editors were not in the original submission, she says, the original figure had at least one apparent duplication that also appeared in the final version. Figure S1 shows 68 cell photographs, which purport to show evidence of 10 of the 11 cell lines expressing up to 6 different protein markers typical of ES cells. But one image labeled as cell line number 8, expressing a marker called SSEA-4, shows the same colony of cells, though slightly shifted, as an image labeled cell line 7, marker SSEA-3. Kelner says that editors have asked the researchers to explain the images, "but we haven't gotten answers."

It also seems that questions raised during the review process may have unwittingly helped undo the paper. In their original submission, Kelner says, the authors provided fingerprints from only some of the cell ▶

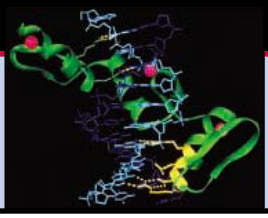

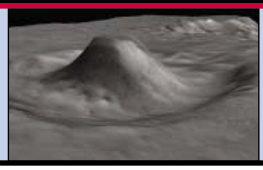

lines. Reviewers asked for fingerprinting data from the remaining lines. It is not clear if the questionable fingerprints were in the first submission or in the additional data the reviewers requested. Editors declined to specify which lines were missing in the original submission.

The controversy has focused attention on the peer review process used by *Science* and most other scientific journals. Kelner says that even before the problems with the Hwang paper came to light, the journal had planned to institute a policy early next year to systematically examine papers for "inappropriate manipulation of images" by computer programs that leave telltale traces. But she says such techniques can only do so much. "I don't think that would have picked up these problems. You had to be looking for duplications."

Science editors acknowledge that the paper was reviewed and published in 2 months, about half the average time from submission to publication. But other researchers say that even with a longer review period, the peer review process is not designed to detect outright falsification. "I'm convinced by looking at the *Science* paper that it was publishable on the basis of data presented," says Irving Weissman, a stem cell scientist at Stanford University.

Even if Hwang's team produces convincing data that it created patient specific lines, observers have called into question other papers by Hwang and various collaborators. Postings on the same Korean Internet message board claim there is similar evidence of tampering in the supplementary data for the 2004 paper. Others are raising questions about a report in *Nature* this year describing the first cloned dog (*Science*, 5 August, p. 862). Critics say that the brief report leaves open the possibility that the two look-alike dogs resulted from embryo splitting—that they are essentially identical twins. To prove the case, the researchers should have demonstrated that that the puppy and cloned adult carry different mitochondrial DNA, but the paper includes no such evidence.

Some answers may come from investigations now under way at Seoul National University and the University of Pittsburgh. The SNU committee comprises seven SNU professors, including chair Myung Hee Chung, and two scientists from other Korean institutions. In contrast to some calls from the scientific community, there are no non-Korean members. In the initial phase of the probe, the committee intends to check lab notes, examine existing data, including micrographs of cells and DNA fingerprint traces, and interview researchers. A second phase is expected to involve testing, including new DNA fingerprinting of the five frozen cell lines Hwang claims will vindicate him. The committee may also check cell lines held at MizMedi.

The committee has clamped restrictions on the lab. Computer storage drives have been seized. Researchers will not be allowed to have access to any related data and must receive prior permission for limited research, which will be under surveillance. A video camera has been set up at the culturing lab to catch any unauthorized comings and goings.

The committee got to work on 18 December, summoning 24 members of Hwang's research team to the school for individual questioning. The committee reportedly intends to issue an interim report by 24 December.

Korean scientists are dismayed at the spectacle but split over Hwang's culpability. "I've known Dr. Hwang for 10 years, and I just cannot believe [the accusations against him]; maybe I don't want to believe them," says an SNU colleague who did not want to be identified. A harsher view comes from a senior scientist who has no connection to Hwang or SNU: "I don't think it makes sense that he continues his research after losing his credibility and integrity."

Sun Min Lee, a spokesperson for the People's Foundation for the Donation of Ova for Research and Therapeutic Purposes, which was set up to support stem cell research efforts when Hwang's work came under fire, says they still have hundreds of women volunteering to donate eggs.

At least three groups have announced plans to make their own patient specific cells, a key step in validating the approach Hwang reported. Alison Murdoch and her colleagues at the University of Newcastle in the United Kingdom announced to the press in May that they had produced cloned early embryos but no ES cells. Ian Wilmut of the University of Edinburgh also has received government and ethical approval to begin work. A group at Harvard University is poised to start as soon as it receives ethical approval from all institutions involved.

George Daley, a member of the Harvard group, says it is too early to tell how flawed the 2005 report is. "Hwang's group was skilled enough to be capable of doing what they claimed," he says. "We'll see how much of the Hwang methodology proves useful when we and others attempt to incorporate it into our own work."

Wilmut agrees. "I very much hope that Hwang and his group can be given time to collect their thoughts," he says. "I am sure that they did make good steps forward and derive cell lines. I hope that they can assemble their data and present it in full because it will help the rest of us to know what can be achieved."

–DENNIS NORMILE, GRETCHEN VOGEL, AND CONSTANCE HOLDEN

With reporting by Ji-soo Kim, Mark Russell, and Yvette Wohn in Seoul.

Pushing forward. Hwang told a press conference that his team would produce new evidence that they had made stem cells from cloned human embryos.

CREDIT: KIM KYUNG-HOON/REUTERS

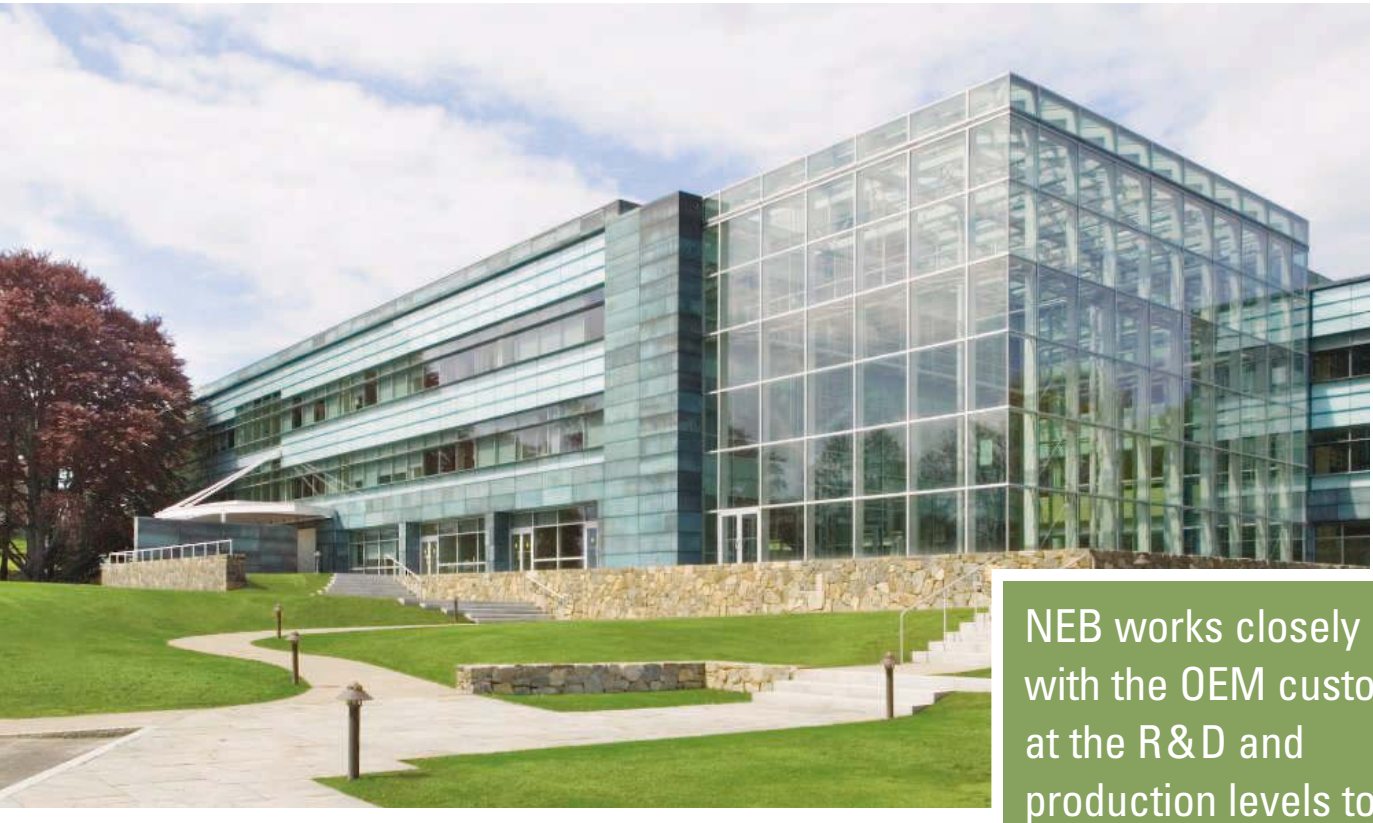

NEB's new state-of-the-art 140,000 sq. ft. research and production laboratory

NEB works closely with the OEM customer at the R&D and production levels to optimize reagent integration...

NEB your first choice for **OEM**

PRODUCING REAGENTS TO DRIVE HIGH THROUGHPUT GENOME TECHNOLOGIES

Choose New England Biolabs as your OEM partner and gain access to the world's largest selection of recombinant and native enzymes for genomic research – all produced in large scale with stringent specifications that ensure success for your high throughput technologies.

Housed in a new state-of-the-art facility, NEB's USA headquarters includes a modern fermentation center and fully equipped laboratories for production, quality control, product development and basic research. At New England Biolabs, science has always been a priority and through this approach, NEB's reagents have gained a world-wide reputation for setting the highest of standards for quality and value.

Access an array of reagents that offer OEM customers the highest purity, remarkable consistency and value. Discover what many of today's leading innovators in technology development already know – NEB is your first choice for OEM.

SELECTION OF RECOMBINANT ENZYMES (R) FROM NEB DRIVING HIGH THROUGHPUT GENOME TECHNOLOGIES

- *Bst* DNA Polymerase
- Deep Vent DNA Polymerase
- *Taq* DNA Polymerase
- Therminator DNA Polymerase
- DNA Polymerase I, Large (Klenow) Fragment
- Klenow (3'→ 5' exo$^-$)
- T4 DNA Polymerase
- Exonuclease I (E. coli)
- Exonuclease III (E. coli)
- Lambda Exonuclease
- Antarctic Phosphatase
- *Taq* DNA Ligase
- T4 DNA Ligase
- T4 Polynucleotide Kinase

All of these reagents are purified from a recombinant source. Look for the recombinant symbol (R) for quality you can trust.

FOR PRODUCTS THAT MEET YOUR STRINGENT SPECIFICATIONS, CONTACT:

oem@neb.com

- **New England Biolabs Inc.** 240 County Road, Ipswich, MA 01938 USA 1-800-NEB-LABS Tel. (978) 927-5054 Fax (978) 921-1350 www.neb.com
- **Canada** Tel. (800) 387-1095 info@ca.neb.com
- **Germany** Tel. 0800/246 5227 info@de.neb.com
- **UK** Tel. (0800) 318486 info@uk.neb.com
- **China** Tel. 010-82378266 beijing@neb-china.com

NEW ENGLAND BioLabs® Inc.

the leader in enzyme technology

Mammoth achievement. Researchers managed to sequence a large chunk of DNA from a Siberian mammoth.

CREDIT: GIANNI DAGLI ORTI/CORBIS

ANCIENT DNA

New Methods Yield Mammoth Samples

Ancient DNA has always held the promise of a visit to a long-vanished world of extinct animals, plants, and even humans. But although researchers have sequenced short bits of ancient DNA from organisms including potatoes, cave bears, and even Neandertals, most samples have been too damaged or contaminated for meaningful results.

Now in a paper published online by *Science* this week*, an international team reports using new technology to sequence a staggering 13 million basepairs of both nuclear and mitochondrial DNA from a 27,000-year-old Siberian mammoth. Also this week, a *Nature* paper reports using a souped-up version of more conventional methods to sequence a mammoth's entire mitochondrial genome.

Besides helping reveal the origins of mammoths, the new nuclear data serve as a dramatic demonstration of the power of the new technique to reliably sequence large amounts of ancient DNA, other researchers say. "The 'next generation' sequencer that was used [in the *Science* paper] will revolutionize the field of ancient DNA," predicts evolutionary biologist Blair Hedges of Pennsylvania State University in University Park. Ancient DNA pioneer Svante Pääbo of the Max Planck Institute for Evolutionary Anthropology in Leipzig, Germany, who co-led the independent mitochondrial study, calls the nuclear DNA work "really great—the way forward in ancient DNA is to go for the nuclear genome with technologies like this."

To get mammoth samples for the new method, molecular evolutionary geneticist Hendrik Poinar of McMaster University in Hamilton, Canada, took bone cores from woolly mammoths found in permafrost and stored in a frigid Siberian ice cave. When Poinar returned the samples to his lab, he was surprised by the amount of DNA that emerged, particularly from one mammoth jawbone. This specimen had been recovered from the shore of Lake Taimyr, where very cold winters and short, cool, and dry summers turned out to be ideal conditions for preserving DNA.

Poinar sent the DNA-rich sample to genomicist Stephan C. Schuster at Pennsylvania State University, University Park, who is working with a new genome sequencer developed by a team at Stanford University and 454 Life Sciences Corp. of Branford, Connecticut (*Nature*, 15 September, p. 376). This rapid, large-scale sequencing technology sidesteps the need to insert DNA into bacteria before amplifying and sequencing it. Instead, scientists break DNA into small fragments, each attached to a tiny bead and encapsulated by a lipid bubble where the DNA is multiplied into many copies for sequencing. Because each fragment is isolated before copying, the method avoids bias from copying large amounts of contaminant DNA from bacteria or humans.

The researchers were stunned by how well the method worked on ancient DNA, which is notoriously difficult to extract and sequence: "I would have been happy if we got 10,000 bases of mammoth DNA," said Poinar. Instead, they got 28 million basepairs, 13 million from the mammoth itself. Their preliminary analysis shows that the mammoth was a female who shared 98.55% of her DNA with modern African elephants. But mammoths were apparently closest kin to Asian elephants, as shown by Pääbo's mitochondrial study, which retrieved about 17,000 basepairs.

Poinar's team also found sequences from bacteria, fungi, viruses, soil micro-organisms, and plants, which the researchers say will help reconstruct the mammoth's ancient world. The technique was so productive that the authors predict it will be used soon to sequence entire genomes of extinct animals. —ANN GIBBONS

With reporting by Michael Balter.

*www.sciencmag/org/cgi/content/abstract/1123360

ScienceScope

Peach State Sticker Shock

Georgia scientists are worried that a U.S. federal appeals panel might side with Cobb County school officials after the panel heard oral arguments last week on the content of antievolution stickers placed in textbooks.

Georgia Citizens for Integrity in Science Education say that a three-judge panel in Atlanta received "erroneous" information at its 15 December hearing. The court was reviewing a lower court ruling that the stickers, which call evolution "a theory, not a fact," unconstitutionally advance a religious view. The court failed to acknowledge scientific errors in the sticker, the education group laments, and wrongly assumed that the school board acted before fundamentalist parents complained, thus mooting the argument that the stickers were a response to religious influences. The school board disavows any religious motive, saying that the stickers encourage "critical thinking."

—CONSTANCE HOLDEN

Flu Preparedness Dealt Blows

PARIS—Efforts to wield two key weapons against a future H5N1 influenza pandemic have suffered setbacks. Last week, French vaccine maker Sanofi Pasteur announced that a prototype H5N1 vaccine containing aluminum as an "adjuvant," or immune booster, appears to offer protection only when two doses of 30 micrograms of antigen each were given.

Sanofi calls the study "progress," but many researchers are disappointed that the booster didn't allow smaller doses to protect. Because the world's flu vaccine manufacturing capacity is limited, they had hoped that the addition of aluminum might bring the dose needed all the way down to 2 micrograms or less, enabling vaccine makers to make billions of doses. "[A] much better adjuvant is needed," says Albert Osterhaus of Erasmus Medical Center in Rotterdam, the Netherlands.

Meanwhile, in this week's *New England Journal of Medicine*, researchers report having isolated from two Vietnamese patients H5N1 strains that are highly resistant to the drug oseltamivir, stockpiled by rich countries. Before that, only one partially resistant H5N1 strain had been found. An accompanying commentary says the "frightening" results mean that oseltamivir must be used wisely and urges measures to prevent people from hoarding the drug.

—MARTIN ENSERINK

DRUG TESTING

Massive Trial of Celebrex Seeks to Settle Safety Concerns

Since the COX-2 inhibitor Vioxx was yanked off the market more than a year ago, the remaining anti-inflammatory painkillers have been under a cloud of suspicion. Which are the safest, the least likely to contribute to heart attacks and strokes? And which are the most dangerous?

Pfizer, maker of the COX-2 inhibitors Celebrex and Bextra (which was pulled in April), is placing a $100 million bet on a 20,000-person, international trial led by the Cleveland Clinic in Ohio. But some experts are concerned that the design of the trial, announced last week, could load the dice in Celebrex's favor and put patients at risk. European Union (E.U.) countries have declined to participate because of their concerns about Celebrex's safety.

Three-way race. Pfizer is putting up at least $100 million for Celebrex to take on naproxen (*above*, *right*) and ibuprofen.

The clinical trial is unusual for focusing on patients with heart disease, including those who recently underwent bypass surgery and those at risk of cardiac problems. The approach is meant to mirror conditions in the real world. "If you have arthritis and you have heart disease, we can't ask you to tolerate the pain. So what do I give you?" says Steven Nissen of the Cleveland Clinic, who's leading the trial. "In the absence of knowledge, we're just guessing." Nissen has criticized Vioxx and other COX-2 drugs, although at a U.S. Food and Drug Administration (FDA) meeting last February, he voted to keep Bextra on the market.

Patients in the Celebrex trial will be randomly and blindly assigned to receive either Celebrex or one of two older anti-inflammatory drugs—ibuprofen or naproxen. The trial will end after 715 "events"—heart attacks, strokes, or deaths—have occurred, says Nissen. That's expected to take roughly 4 years.

But some scientists wonder whether the study will really resolve questions about the drug's safety. "The important thing in science is to make sure you've controlled all your variables," says Alastair Wood, a drug-safety expert and associate dean of Vanderbilt University School of Medicine in Nashville, Tennessee. "Here, there's another variable in the room that potentially could affect some of the outcomes."

That variable is aspirin, used by heart disease and at-risk patients to reduce clotting. Previous trials have often excluded those on aspirin, which will be given in low doses to all the volunteers in the Pfizer trial because they're at higher risk.

The catch, says Garret FitzGerald, a pharmacologist and cardiologist at the University of Pennsylvania, is that aspirin reduces clotting by acting on COX-1. That's one of the molecules targeted by ibuprofen and naproxen, but mostly ignored by Celebrex. Previous studies in animals and humans have suggested that both ibuprofen and naproxen, but not COX-2 inhibitors, "can interfere to undermine the cardiovascular protection of aspirin," says FitzGerald. If so, a finding that heart attacks and strokes are the same in all three drug groups might actually mean that Celebrex is less safe, because the cardiovascular benefits of aspirin may be decreased for those taking ibuprofen or naproxen but not for those in the Celebrex group.

The solution, say both FitzGerald and Wood, is to banish aspirin from the study and give patients clopidagrel, or Plavix, a more expensive drug made by Bristol-Myers Squibb that has cardiovascular benefits similar to aspirin but doesn't work through COX molecules. Nissen disputed that approach in an e-mail, noting that clinically, chronic clopidagrel use isn't indicated for heart disease patients, and its effects are not known. He also said the interaction between aspirin and ibuprofen remains speculative.

The ethics of the new trial are also getting mixed reviews. Although some clinical trials are faulted for relying on the healthiest patients, this one has garnered criticism for planning to enroll the sickest. "Why take the highest-risk people?" asks Curt Furberg, an epidemiologist at Wake Forest University School of Medicine in Winston-Salem, North Carolina, who suggests instead tracking them through health databases of hun- ▶

DEEP-SEA DRILLING

Scientific Drill Ship to Be Reborn

SAN FRANCISCO, CALIFORNIA—The *JOIDES Resolution* ends its 20-year career as the world's lone deep-sea scientific drilling ship next week. But the National Science Foundation (NSF) hopes that $115 million will bring her back into the water, better than ever.

An NSF-funded group has contracted with the ship's owner to rebuild and upgrade the *Resolution*, beginning next fall. When the work has been completed, it would join the Japanese behemoth *Chikyu* late in 2007, ending an 18-month drilling hiatus and beginning the most ambitious ocean drilling ever attempted.

The renamed ship will be more capable and comfortable, NSF's Assistant Director for Geosciences Margaret Leinen told an audience last week at the American Geophysical Union meeting here. The ship, representing the U.S. contribution to the International Ocean Drilling Program, will have 50% more shipboard laboratory space, an enhanced drilling system, and a greater variety of analytical instrumentation. But the biggest applause greeted her description of the improved creature comforts: No more four-person staterooms or eight-person bathrooms, Leinen promised, and there will be a sauna. To stay on schedule, however, NSF needs $42 million from Congress in its next budget to complement what it has received in the past 2 years.

The half-billion-dollar *Chikyu*, which during a shakedown cruise this month retrieved its first sediment core, will become fully operational in September 2007. Its first challenge will be a series of holes working up to a superdeep hole into the fault that generates great earthquakes off the coast of Japan. But more work lies beyond that 6-year project, Y. Tatsumi of the Japan Drilling Earth Science Consortium reminded the audience. He urged the community to begin planning other ambitious projects, including drilling through the ocean's rocky crust. An ill-fated attempt to pierce the ocean crust (*Science*, 18 April 2003, p. 410) 40 years ago gave rise to modern scientific drilling. **–RICHARD A. KERR**

dreds of thousands of patients like the one kept by Kaiser Permanente. The E.U. will not participate because its drug regulatory agency contraindicates Celebrex for heart disease patients.

Still, "the trouble in the real world is that people have multiple illnesses," says oncologist Richard Goldberg of the University of North Carolina, Chapel Hill, whose ongoing trial of whether Celebrex could prevent colon polyps ground to a halt earlier this year after Vioxx was pulled for lack of new recruits. It "wouldn't surprise me" if this latest study faces the same problem, he says.

But Nissen's Cleveland Clinic colleague Eric Topol, who is not involved in the study, isn't worried. "It'll recruit very quickly," he predicts. "It's not like you're doing a trial to hurt anybody." –JENNIFER COUZIN

U.S. SCIENCE POLICY

Bill Seeks Billions to Bolster Research

Saying that academic research is the key to a strong economy, a bipartisan group of U.S. senators has assigned the National Science Foundation (NSF) a central role in a multibillion-dollar proposal to boost U.S. competitiveness. And they're hoping that, for NSF, the second time around will be a charm.

The legislation, introduced last week and dubbed the National Innovation Act of 2005, would nearly double the NSF budget, now $5.5 billion, by 2011. It would create hundreds of new graduate fellowships, encourage all federal agencies to invest in high-risk research, and revise the tax code to promote more industrial spending on research. It recommends federal investment in advanced manufacturing, regional economic development, health care, and defense technologies. It would also create an interagency Council on Innovation to evaluate all relevant legislative initiatives.

Innovation trio. From left, Senators Joseph Lieberman, George Allen, and John Ensign unveil competitiveness legislation.

CREDIT: KERRY ARNOT

"Whenever I meet with industry, they tell me that supporting university-based research is the single most important thing that we could do to bolster U.S. competitiveness," said Senator Joseph Lieberman (D–CT), co-sponsor of the proposal with Senator John Ensign (R–NV), at a press briefing. "It's the raw material from which they innovate." Fourteen senators have signed on as co-sponsors of the bill, S.2109, which closely tracks recommendations made 1 year ago by a blue-ribbon panel of business and academic leaders assembled by the Council on Competitiveness (www.compete.org).

Even as the press briefing was taking place in the Capitol, three of the bill's co-sponsors were meeting at the White House with President George W. Bush to discuss a similar piece of legislation to bolster U.S. scientific prowess being prepared by Senator Lamar Alexander (R–TN). That bill is expected to conform to an October report by the National Academies' National Research Council (*Science*, 21 October, p. 423).

Science lobbyists are thrilled by the bill's underlying message. The legislation "reflects a consensus among the nation's business and academic communities concerning actions we must take to ensure our future global competitiveness and our national security," says the Association of American Universities, which represents 62 research-intensive universities. ASTRA, a consortium that lobbies for increased spending in the physical sciences and engineering, calls the bill its number-one legislative priority in 2006.

All that support will go for naught, however, unless Congress loosens the purse strings. Despite a 2002 law calling for a 5-year doubling of NSF's budget, Congress actually cut the agency's budget last year and gave it only a small increase this year. Lieberman says he expects things to be different this time around: "There's a new sense of urgency and a new level of understanding about the importance of university-based research. I think we can do it." –JEFFREY MERVIS

ScienceScope

Lawmakers Zap NASA Head

NASA chief Mike Griffin wants to refocus all space station research on crewed spaceward voyages. But Congress last week agreed on an authorization bill which demands NASA spend at least 15% of its station funds on microgravity research not related to exploration. Griffin, meanwhile, told a meeting of the American Geophysical Union earlier this month that NASA faces "some daunting fiscal issues" amidst visions for robot miners on Mars and a census of extrasolar planets. –ANDREW LAWLER

Cambridge to Clamp Patent Rights

The University of Cambridge, U.K., is tightening the reins on academic patents after faculty and staff overwhelmingly backed a plan to centralize intellectual property under a group called Cambridge Enterprise. Dissenters wanted to preserve rules that gave researchers more control over their patents (*Science*, 9 December, p. 1597). Cambridge computer scientist Ross Anderson now aims to spark a debate on what he calls the university's "abuse" of authority during the debate. –ELIOT MARSHALL

Researcher Freed in Iraq

German archaeologist Susanne Osthoff, abducted by insurgents in Iraq on 25 November, was freed this week. Osthoff had tried to protect archaeological sites from looting after the U.S.-led invasion and was involved with a conservation project in Mosul earlier this year. Her liberation is "fantastic news," says archaeology writer Roger Atwood, who visited looted sites with her in 2003. –MICHAEL BALTER

E.U. Research Budget Set

BERLIN—The dream of a doubling in European Union research funding is dead. In a compromise worked out last week, the leaders of the 25 E.U. member countries agreed on a budget for 2007–2013 that is about 16% smaller than the one proposed in April (*Science*, 15 April, p. 342). Instead of receiving €10 billion per year, research funding would rise from €5 billion to €8.75 billion in 2013. The smaller boost "is clearly not what we wanted," said E.U. research commissioner Janez Potočnik, but "it reflects today's political reality." He said it was not clear how much the squeeze would affect funding for the new European Research Council. –GRETCHEN VOGEL

CONDENSED-MATTER PHYSICS

Mismatched Cold Atoms Hint at a Stellar New Superfluid

A puff of ultracold atoms may help physicists decipher the weird nuclear matter in the hearts of neutron stars. Two groups report online in *Science* this week that when they tweaked such frigid atoms to mimic superdense nuclear matter, the atoms continued to pair up and flow without resistance, just as electrons do in a superconductor. One group even claims evidence of a new type of resistance-free flow, or superfluidity.

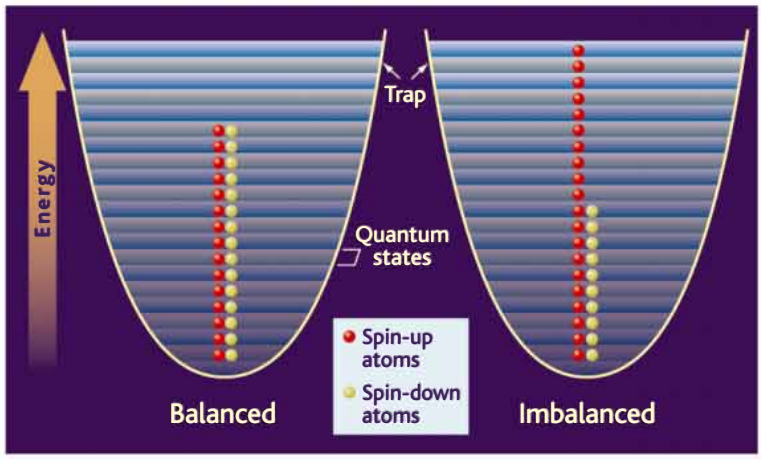

Find a partner. When atoms spinning one way outnumber those spinning the other, they still can pair and flow freely—perhaps like matter in a neutron star.

Theorists have predicted that new forms of superfluidity might exist in neutron stars, and an atomic analog may enable them to test those ideas directly. "To have that become something you can study in the laboratory is like a gift from heaven," says theorist Frank Wilczek of the Massachusetts Institute of Technology (MIT) in Cambridge.

In each experiment, a gas of the isotope lithium-6 is trapped in a laser beam and chilled to less than a millionth of a kelvin. Quantum mechanics dictates that no two identical lithium-6 atoms can fill the same energy "state," so the trapped atoms stack into the energy ladder of quantum states two at a time—one spinning one way and the other spinning the opposite way. Researchers then apply a magnetic field to make the atoms attract or repel one another.

When equal numbers spin each way while the atoms repel, opposite-spinning atoms form loose "Cooper pairs" whose connection depends on the motion of the other atoms (*Science*, 6 February 2004, p. 741). These pairs flow through one another without resistance, as Martin Zwierlein, Wolfgang Ketterle, and colleagues at MIT proved in June, when they tried to rotate the cloud of atoms (*Science*, 24 June, p. 1848). Instead of turning as a whole, it sprouted tiny whirlpools called vortices—hallmarks of superfluidity.

Now, the MIT experimenters report online (www.sciencemag.org/cgi/content/abstract/1122318) that superfluidity persists when atoms spinning one way outnumber potential partners by as much as 70%. The imbalanced gas mimics the dense soup of subatomic "quarks" at the center of a neutron star, as there some types of quarks outnumber others.

Whether the particles are atoms or quarks, standard theory forbids superfluidity when one type of them stacks to higher energy than the other, Ketterle says. But, he says, the results jibe with the notion that extra members of the majority are squeezed to sides of the laser trap, leveling the energy stacks in the middle.

More speculatively, Guthrie Partridge, Randall Hulet, and colleagues at Rice University in Houston, Texas, claim online (www.sciencemag.org/cgi/content/abstract/1122876) that the lithium superfluid remains mixed at small imbalances. Atoms spinning in opposite directions absorb light of different colors. By measuring the absorption of the colors in various parts of the cloud, the researchers showed that the extra atoms migrated to the edges only when the imbalance exceeded 9%.

No one has ever detected an imbalanced superfluid before, although Wilczek and others have devised scenarios in which one could exist. "On the face of it, [Hulet's result] is consistent with the kind of superfluid we've been predicting," Wilczek says, "but it's by no means proof."

The Rice researchers haven't shown that their gas is ever superfluid, Ketterle says. Hulet agrees, but he says that previous experiments show the gas is superfluid when the imbalance is zero, and the easiest explanation is that his team is seeing a transition from one superfluid to another. "Anything else, while not ruled out, would have to be even more exotic," Hulet says.

Future experiments will put the purported superfluid to the test. Regardless of the outcome, however, ultracold atoms have begun to live up to their potential as a portal into new and exotic physics. **–ADRIAN CHO**

IMMUNOLOGY

Jawless Fish Have Form of Adaptive Immunity

Evolution doesn't like to do things just once. It came up with flight three times, for example—in insects, birds, and bats. Now it appears that evolutionarily distinct immune systems have exploited a similar genetic trick to battle microbes. New research on page 1970 reveals that the immune defenses of jawless fish such as lampreys generate as much diversity as the immune system that organisms from sharks onward in evolution use. And both employ a similar technique: rearranging DNA.

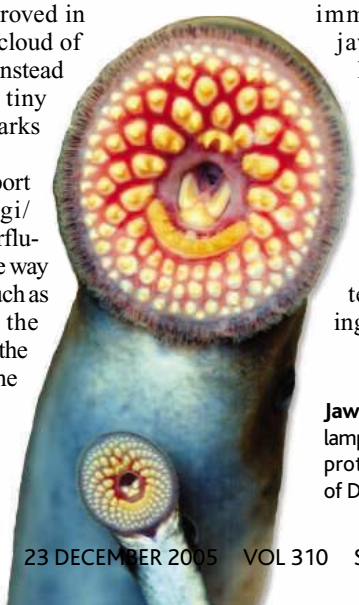

Jaw-dropping find. These lampreys make key immune proteins by shuffling bits of DNA.

CREDIT (BOTTOM): DAVE BRENNER/MICHIGAN SEA GRANT ARCHIVES

Researchers don't yet know whether the lamprey's immune system arose before our own or if it spun off from its own evolutionary tangent, but they're impressed by its sophistication. "It's just fascinating that there's another adaptive immune system," says David Davies of the National Institute of Diabetes and Digestive and Kidney Diseases in Bethesda, Maryland, who studies Toll-like receptors, other immune proteins that recognize pathogens.

The immune system in sharks, mammals, and other jawed vertebrates generates antibodies—proteins that recognize very specific molecular features of invading pathogens—by rearranging DNA segments and inducing random mutations to give rise to a hundred million million different possible proteins. This allows the immune system to adapt to each new infectious agent by boosting production of antibodies specific for the attacking microbe.

Comparative immunologist Zeev Pancer of the Center of Marine Biotechnology Institute in Baltimore, clinical ▶

immunologist Max Cooper, a Howard Hughes Medical Institute investigator at the University of Alabama, Birmingham, and colleagues knew that lampreys responded to invading microbes by generating their own diverse set of proteins called variable lymphocyte receptors (VLRs). These proteins contain varying numbers of different leucine-rich segments, which are often involved in binding to other molecules.

But just how diverse are VLRs? In one experiment, the team identified hundreds of unique VLRs by immunizing lampreys with anthrax spores and collecting the fish's immune cells. Other experiments and a close look at the predicted protein sequence for each identified VLR allowed the researchers to estimate all the possible sequences for a VLR. They calculated that lampreys can make as many as 10^{14} different immune proteins.

Yet there's only a single *VLR* gene in the germline of lampreys, for example, and two in hagfish. So, "we hypothesized that the genes rearrange" in each immune cell to create distinct VLRs, Pancer says.

They then looked at the actual *VLR* gene in dozens of lamprey immune cells and found that each was unique, having been formed by shuffling around nearby DNA sequences, each of which encode short leucine-rich segments.

Finally, the team looked closely at the types of VLRs in blood after the fish were immunized. The amount of VLR protein that could bind the anthrax rose over 8 weeks, but these same proteins did not attach to spores from another bacterium. This indicated that the lamprey could tailor its production of VLRs to a particular microbe, the hallmark of an adaptive immune response.

Whether vertebrates started out with a VLR system and later gave it up for the antibody-based immunity is anybody's bet. The study authors are looking both in invertebrates—squid and octopus—and in bony fish for remnants of such a system. "It may well be that this exists in us because nature very rarely throws things away," says Davies. But immunologist Gary Litman of All Children's Hospital in St. Petersburg, Florida, is skeptical that VLRs represent a forerunner to antibody-based immunity in vertebrates. "The jawless fish are not a simple step from jawed vertebrates," he says. "There's a huge transition, and the jawless fish are highly derived and specialized."

In any event, the lamprey work "deserves a lot of attention," says Litman. "It seems to be that the [adaptive] immune system has been reinvented by any number of mechanisms."

–MARY BECKMAN

Mary Beckman is a writer in southeastern Idaho.

CREDIT: J. HUART/ESA

SATELLITE NAVIGATION

Europe's Answer to GPS Could Be a Boon for Research

CAMBRIDGE, UNITED KINGDOM—On 26 December, a European satellite is set to lift off from Baikonur cosmodrome in Kazakhstan and, once in orbit 23,000 kilometers above Earth's surface, start transmitting time signals. Although small—roughly the size of a freezer—the satellite GIOVE-A is the start of something big.

The craft is the first test bed for Europe's answer to the U.S. Global Positioning System (GPS) satellites. Dubbed Galileo, the European system, like GPS, will consist of a constellation of satellites carrying atomic clocks. A receiver can use their signals to calculate its position to an accuracy of a few meters. Combining Galileo with GPS will double the number of transmitters, and with Galileo's updated technology, researchers expect it to bring a sharp improvement in quality and reliability, which in turn will enable new studies of the atmosphere and oceans. The system might even provide a way of watching for tsunamis.

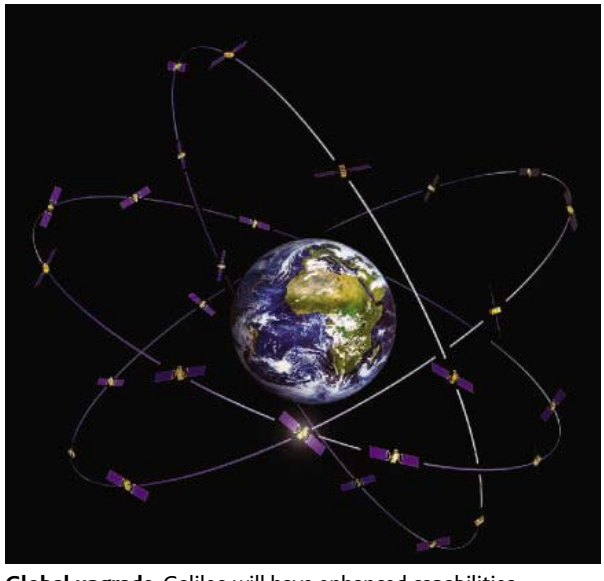

Global upgrade. Galileo will have enhanced capabilities.

Satellite navigation is simple in principle: The spacecraft (24 for GPS, 27 for Galileo when it is fully operational around 2010) transmit regular signals that give each craft's identity and the precise time of transmission. A receiver which can pick up signals from four different craft is able to calculate its position in three dimensions.

GPS receivers have become so cheap that they're widely used by hikers and drivers. But GPS remains a military system, and the Pentagon can degrade or even turn off the signal in times of crisis. Galileo, in contrast, has been designed with business in mind. "Guarantee of service is the basic difference," says Dominique Detain of the European Space Agency, which is developing Galileo jointly with the European Union.

GPS receivers have already become a common research tool, providing position data points in survey work and monitoring movement of tectonic fault lines. In the late 1980s, atmospheric researchers realized they could use GPS signals to probe Earth's atmosphere. A GPS signal that passes through the atmosphere as it travels from a GPS satellite to a satellite equipped with a receiver will be refracted. This refraction gives a detailed vertical profile of the atmosphere between the two craft, revealing temperature and pressure.

This information is "really very valuable for climate benchmarking," says physicist James Zumberge of NASA's Jet Propulsion Laboratory in Pasadena, California, which has pioneered the technique. It would be highly valued by weather forecasters, too, except that they need continuous and global coverage. A single receiver in low Earth orbit is only in the right configuration to pick up a signal passing through the atmosphere a few times per day. Galileo, however, will double the number of signal sources, and a joint U.S./Taiwanese project called Cosmic, which will launch next spring, will add six GPS-receiving satellites.

Researchers are also excited about a technique that detects satellite navigation signals bounced off the ocean surface. A team from the University of Surrey in Guildford, U.K., demonstrated the technique earlier this year, deriving sea surface roughness from reflected GPS signals. But the Galileo signal has extra features that may also allow researchers to measure wave height and the height of the ocean surface. Radar satellites can already make such measurements, but they are large, expensive, and narrowly focused. A satellite with a navigation receiver, in contrast, could weigh just 10 kilograms. "You could put up a whole load of them and get global coverage at low cost," says Martin Unwin of the Surrey team. Such a constellation could even provide an efficient tsunami early warning system. "People are looking into it," says Zumberge.

–DANIEL CLERY

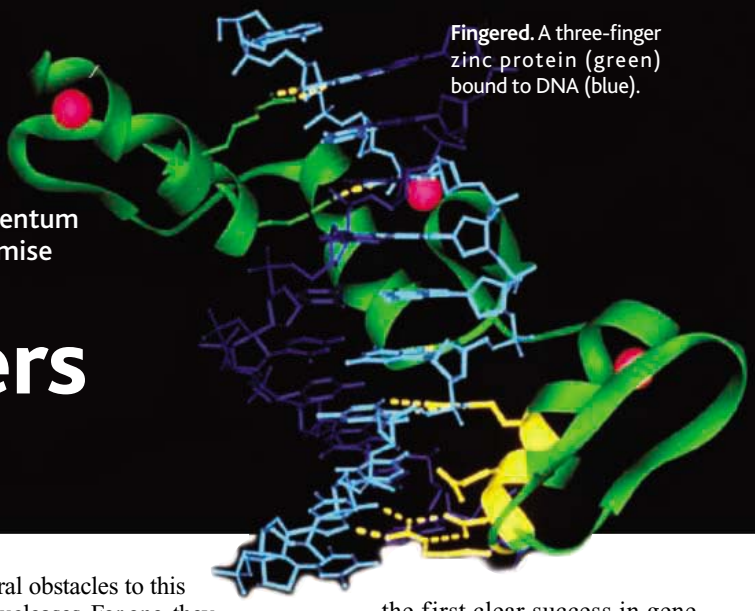

Fingered. A three-finger zinc protein (green) bound to DNA (blue).

The struggling field of gene therapy could regain its momentum if proteins called zinc finger nucleases live up to their promise of efficiently and safely repairing mutations

Putting the Fingers On Gene Repair

Imagine one of your car's headlights winks out, but instead of simply replacing the bulb, you attach a third headlight. That's typically how genetic engineering works today. When molecular biologists want to boost a plant's drought resistance, for example, or repair the cells of a patient with an inherited disease, they paste a new gene into a random spot on a chromosome and hope it does the job. Nobody has yet figured out a good way to directly repair a cell's defective genes.

Now a technology is emerging that could enable scientists to much more readily repair or alter a cell's existing genes. The key is an engineered protein called a zinc finger nuclease that latches onto a specific gene and snips its DNA. The cell then heals the broken strand using copies of a replacement gene that researchers also supply—in the case of gene therapy, the copies would lack the disease-causing mutation in the original.

In the past 3 years, researchers have shown that zinc finger nucleases can successfully modify existing genes in fruit flies and plants. They've even fixed, in a lab dish at least, human cells bearing a mutation that causes a deadly inherited immune disease. Although no disease gene has yet been repaired in a mammal, much less in a person, researchers are hopeful that the work will lead to clinical applications. The ability to routinely edit genes in lab-grown cells, animals, and plants would also be a boon for basic scientists exploring gene function. "This would be a phenomenal research tool. It could change the way we do science," says molecular biologist Matthew Porteus of the University of Texas Southwestern Medical Center in Dallas.

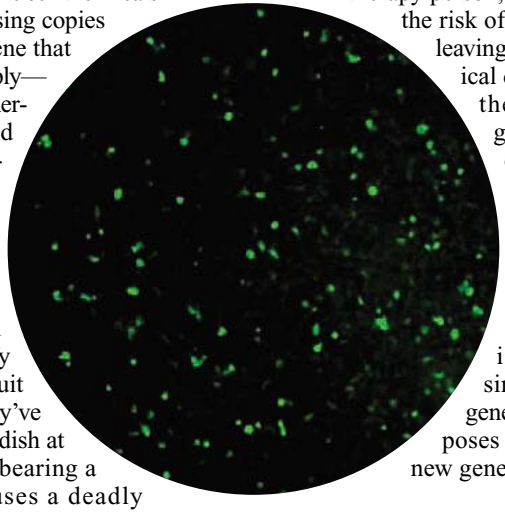

Glowing success. Human cells began to shine after zinc finger nucleases repaired a gene for green fluorescent protein.

There remain several obstacles to this vision for zinc finger nucleases. For one, they must be tailored for each target gene, which only a few labs can do at the moment. Several of these groups are gearing up to make the customized proteins more widely available, hoping to get around the fact that one company owns the broadest collection of zinc finger nucleases as well as sweeping patents on their use. Some biologists are concerned that this firm will stifle the field's progress.

Finally, like other gene-therapy strategies, the use of zinc finger nucleases poses serious safety questions. "It's a very exciting approach," says Richard Mulligan of Harvard University. But he cautions, "As an old gene-therapy person, my view is this runs the risk of moving too quickly, leaving out too many biological details, and suffering the same fate as the gene-therapy field overall."

Product placement

Gene therapists and other biologists would like to be able to modify a cell's existing genes because simply inserting a new gene into a cell's genome poses problems. First, that new gene may not function in the same way as the one it's meant to replace. The introduced gene usually lands in a random location, far from the promoters and other noncoding regions that control the natural gene. That often means the cell makes too much or too little of the added gene's protein product.

Moreover, the random nature of the gene insertion has led to serious side effects. In the first clear success in gene therapy, scientists in the past 6 years have apparently cured nearly two dozen children with severe combined immunodeficiency disease (SCID) by stitching a corrective gene into patients' blood cells. But three patients with X-linked SCID developed leukemia, seemingly because the retrovirus carrying the corrective gene inserted its package of DNA near an oncogene. In theory, says Mulligan, repairing the endogenous gene that causes X-SCID should be much safer.

Scientists have tried to exploit one of the cell's natural repair mechanisms to edit genes, but with limited success. When a chromosome is damaged, cellular enzymes can restore it using a corresponding strand of DNA as a template, usually from the cell's other copy of the chromosome—a process called homologous recombination. Scientists can piggyback on this natural repair system by tricking the cell into performing homologous recombination using added DNA as the template instead. Although this strategy works well enough in yeast and is routinely used to make "knockout," or transgenic, mice, the rate of repair—one in a million cells—is too low to be useful in other species. Another gene-repair technique, chimeraplasty, has not proven to be easily reproduced, if it works at all (*Science*, 13 December 2002, p. 2116).

More recently, researchers seeking a way to make gene repair via homologous recombination work better turned to zinc fingers, discovered by Aaron Klug's group at the Laboratory of Molecular Biology in Cambridge, U.K., in 1986. Molecular structures containing about 30 amino acids and held together by a zinc ion, they're key components of many proteins involved in transcription, the process by which a gene's information is converted from DNA into RNA. Indeed, zinc fingers determine where so-called transcription factors bind. Each

CREDITS (TOP TO BOTTOM): SANGAMO BIOSCIENCES INC.; *NATURE* **435**, 646 (2005)

finger nestles into the DNA helix at a specific set of three bases (such as GCG), allowing a transcription factor to turn on a specific gene. Klug's lab and others next showed that they can mix and match different zinc fingers to latch onto specific sequences of DNA—there are 64 possible three-base combinations.

Researchers then began exploiting zinc fingers to ferry molecules to a unique position along a chromosome—for example, fusing them to proteins that turn genes on or off so that such proteins would regulate a specific gene. And that inspired the idea of zinc finger nucleases as a way to spur homologous recombination. The strategy is to attach zinc fingers to enzymes called endonucleases that make double strand breaks in DNA. When these enzymes are added to a cell, the usual rate of homologous recombination—1 in a million cells—rises to at least 1 in 1000. In 1996, Srinivasan Chandrasegaran's group at Johns Hopkins University in Baltimore, Maryland, reported that by attaching three different zinc fingers to these DNA-snipping enzymes, they could cut a piece of a free-floating DNA at a precise location. (The researchers add two nucleases that first land on each side of the point they wish to cut and then combine to snip the DNA.) With Dana Carroll's group at the University of Utah, Salt Lake City, they later showed that when new DNA was inserted into frog eggs and cleaved by a zinc finger nuclease, the cells then fixed the break.

The next step was to see whether zinc finger nucleases could alter specific genes in a cell's chromosomes. In 2002, Carroll's group showed in fruit fly larvae that the nucleases could mutate a gene that controls the insect's color. Some of the resulting flies had patches of yellow where they would normally be dark.

That work didn't attempt to replace the cleaved portion of the color gene, but Carroll's team reported doing that in 2003 in *Science* (2 May 2003, p. 764). In addition to the zinc finger nucleases, they added copies of a different version of the color gene into the fly larvae and showed that the larvae incorporated that variant via homologous recombination. In the same issue, Porteus and David Baltimore of the California Institute of Technology in Pasadena reported a similar success. They showed for the first time in human cells that zinc finger nucleases could be used to repair a mutation in the gene, albeit a nonhuman reporter gene inserted into the cells.

The first proof of principle that zinc finger nucleases can correct a human disease gene came this spring. In the April online edition of *Nature*, Porteus and scientists at Sangamo BioSciences Inc. in Richmond, California, showed that such nucleases could make a one-base change in a functional copy of *IL2Rγ*, the gene that causes X-SCID, in human cells. The zinc finger nucleases worked with relatively high efficiency—18% in primary blood cells and 5% in T cells, the cells that would need to be targeted in X-SCID patients.

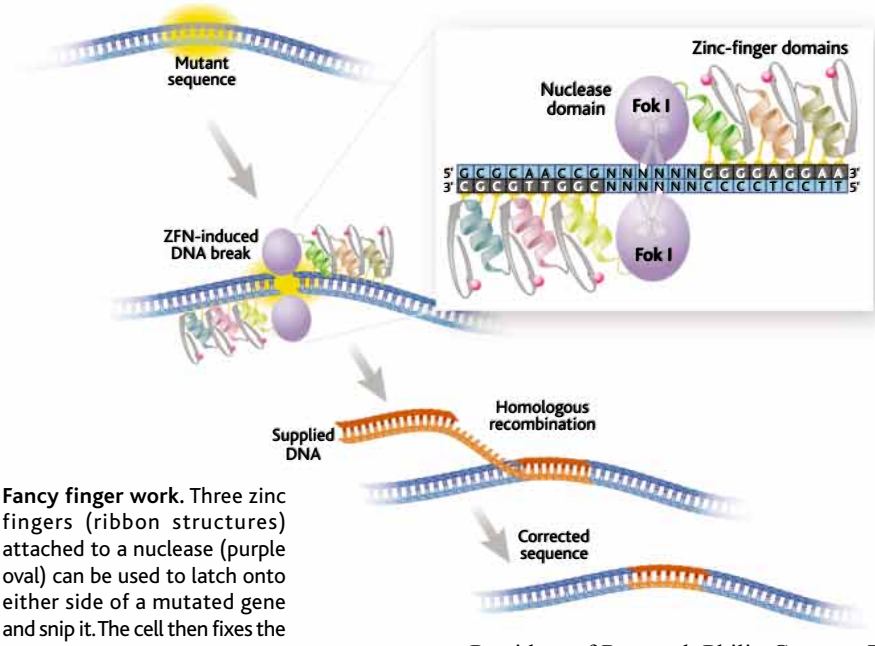

Fancy finger work. Three zinc fingers (ribbon structures) attached to a nuclease (purple oval) can be used to latch onto either side of a mutated gene and snip it. The cell then fixes the break with supplied DNA.

Sangamo also intends to use zinc finger nucleases to correct mutations in other blood diseases, such as hemophilia. The general strategy is to isolate bone marrow or other blood-forming stem cells from a patient, correct the mutation in the cells in lab dishes, and put the stem cells back.

And in a twist on repairing disease genes, Sangamo is also testing whether zinc finger nucleases can treat HIV patients by disabling the gene for a protein, called CCR5, that the HIV virus uses to enter cells. In 2006, Sangamo and collaborators hope to begin clinical trials in which a person's HIV-susceptible immune cells would be replaced with bone marrow cells that have had their *CCR5* genes knocked out.

Delivery problems

Whereas Sangamo may be optimistic that zinc finger nucleases will soon enter the clinic, others say the technology needs to be mature. "It's certainly not going to be a slam dunk. There's a huge number of things standing in the way," says Michael Blaese of the Institute for Inherited Disease Research in Newton, Pennsylvania.

One of the first hurdles is to get enough zinc finger nucleases into the right kinds of cells. Scientists don't just add the proteins to cells. Instead, DNA encoding an engineered nuclease is coaxed into cells with a jolt of electricity. But the immature T cells that researchers would like to target in X-SCID patients are too fragile for such electroshock. The company is now working on ferrying DNA encoding the zinc finger nucleases into cells using disabled lentiviruses. "It's perfect for our technology," says Sangamo Vice President of Research Philip Gregory. The team hopes to show they can this way repair the *IL2Rγ* gene in cells extracted from an X-SCID patient by next summer.

Yet safety issues remain. Zinc finger nucleases can create double strand breaks at DNA sequences other than the target gene, which in theory could lead to cancer. Sangamo says it has greatly reduced that risk by using very specific nucleases, ones with an extra zinc finger. They're also using nucleases that cannot pair up in wrong combinations. "It's a very neat solution," says Carroll, who collaborates with Sangamo. With this technique, the company sees only a minimal increase over the background rate of double strand breaks, says Gregory. Mulligan, who has tested many zinc finger nucleases for off-target effects, is skeptical that this solves all the problems, however.

Despite such safety issues, the flurry of successful experiments with zinc finger nucleases has created a demand for the proteins among many other groups. "People are lining up," says Daniel Voytas, a plant biologist at Iowa State University in Ames. Plant scientists, for example, are keenly interested because some critics of engineered foods containing foreign genes may be more willing to accept crops made by tweaking an existing gene. Voytas's group reported in a November issue of *The Plant Journal* the first demonstration of gene modification using zinc finger nucleases in plants.

CREDIT: K. SUTLIFF/*SCIENCE*

Still, the problem, says Porteus, is that the work is so challenging that you have to be an experienced zinc finger biologist to craft nucleases that work well. The simplest way to create a nuclease that targets enough DNA sequence to hit a specific gene is a "modular design" approach, favored by Carlos Barbas of The Scripps Research Institute in San Diego, California, that yokes together three different zinc fingers and a nuclease to home in on a nine-nucleotide sequence of DNA. But there is debate about whether these nucleases will work in all cases. If a nuclease isn't specific enough, many cells die from off-target breaks, and efficiency is low; only a tiny fraction of cells receive the desired change. Others optimize their nucleases—that is, they try out many design variations to identify the best one. Harvard's J. Keith Joung, for example, generates libraries of zinc finger combinations that vary slightly and then tests them in cells.

Sangamo, which has published some of the zinc fingers it uses to make nucleases and maintains a huge proprietary library of other zinc fingers generated by a company Klug founded, also optimizes the proteins but declines to publicly reveal exactly how. Selecting a zinc finger nuclease "is the beginning of the design problem, not the end," Gregory says. The company's *Nature* paper shows the benefits of the tweaking, he says—the nuclease used became five times more efficient after optimization. "That process is not easy," Gregory says, defending the company's decision to keep its technology confidential. Klug, whose institution licensed his work to Sangamo and could receive royalties, agrees, adding that the company is still refining zinc fingers. "I wouldn't release the technology until it's fully developed," he says.

Sangamo CEO Ed Lanphier also points out that the company collaborates with dozens of academic labs and has no objections to independent efforts to develop the technology. "If they want to go out and work hard in this area, that's great," he says.

But some say Sangamo is hindering progress. For instance, last year, Voytas attempted to license one of Sangamo's zinc finger nuclease patents in order to launch his own plant biotech firm, but the two sides failed to reach an agreement. Barbas, too, contends that Sangamo is "inhibit[ing] the technology from proliferating." He says that the company recently called Scripps to question a Web site he created where biologists can type in a gene's DNA sequence and learn how to create zinc fingers to target it (www.scripps.edu/mb/barbas/zfdesign/zfdesignhome.php). (Sangamo's Lanphier said he could not comment on the matter.)

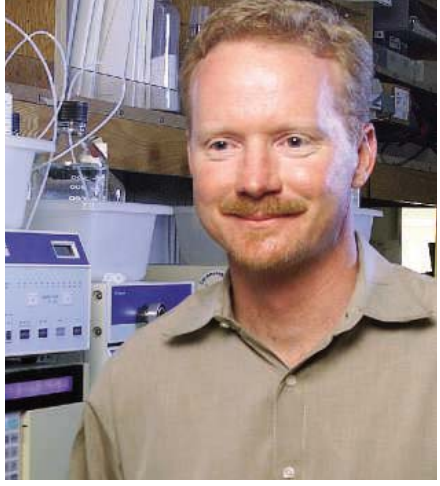

Spreading the word. Scripps's Carlos Barbas launched a Web site to share zinc-finger technology with the academic community.

Other researchers agree that without more involvement from academic researchers, the technology will never mature. Chandrasegaran at Johns Hopkins is seeking funding for a multi-institution collaboration that would design zinc finger nucleases to target 30 disease genes. Meanwhile, Joung, Voytas, Porteus, and Andrea Cristani of Imperial College London have formed a consortium to publicly share zinc finger nuclease technology. The group has posted a Web site (www.zincfingers.org), and it expects, by next year, to disburse at a nominal cost materials that will allow others to make and test the nucleases.

The consortium will also seek to answer questions such as whether using more zinc fingers—six on each nuclease rather than the usual three or four, for example—improves specificity. "My interest is not to circumvent Sangamo's patents. I just want to make the technology available, easy to use, efficient, and robust," Joung says. If that happens, gene therapists trying to repair disease genes may have finally found the tool they've sought.

–JOCELYN KAISER

Tree Growth

The Sky Is Not the Limit

Trees can live thousands of years but can't grow hundreds of meters. Tree biologists are discovering why

Transplanted to New York City, the tallest tree in the world would shade the Brooklyn Bridge. Moved to Pisa, it would be twice the height of the Leaning Tower. At 113 meters, this record California redwood begs a question: Why do some trees grow so tall? Scientists, of course, see the question from a different perspective: Why don't trees grow even taller? "This is one of the big mysteries in plant growth," says Brian Enquist, a functional ecologist at the University of Arizona, Tucson.

Genetics clearly has something to do with tree height variations: You don't see many towering dogwoods, and conifers tend to top hardwoods. The environment also plays a key role; that redwood wouldn't be so giant in scrubland. But neither genetics nor environment can fully explain why, no matter the species, as a tree gets taller, its growth rate slows, sometimes dramatically. In Australia, mountain ash (*Eucalyptus regnans*) saplings can sprout more than 2 meters per year. By age 90, the tree is inching up just 50 centimeters per year, and by age 150, upward growth has ceased. And the gradual stalling of tree growth is not just an academic issue. Foresters care because maximum tree height is a good predictor of a stand's productivity, and environmentalists want to know the role of tree height and forest growth in the regulation of climate changes.

The obvious answer to why trees stop growing is that they simply get old and "feeble." But new evidence seems to discount this cause, at least to some degree. Now, researchers—some of whom have been hoisted to canopies with construction cranes to take a look at what happens at the tops of trees—are focusing on water transport and photosynthesis. Newly published and unpublished results suggest that the function of water-conducting cells declines as a tree pushes ever higher. "Thanks to this work, the state of the field is changing rapidly," says Karl Niklas, a plant biophysicist at Cornell University.

Size matters

Maurizio Mencuccini, a forest ecologist at the University of Edinburgh, U.K., has been retrieving the growing tips of old trees to test whether age-related genetic changes are at the root of maximum tree heights. He and his colleagues have just finished a study of ash, sycamore, Scots pine, and poplar trees to tease apart the effects of a tree's age and size on growth, as the two are intimately connected.

Mencuccini hypothesized that if age is the primary reason growth slows, an elderly

CREDIT: COURTESY OF C. BARBAS

tall tree's growth tips should still grow slowly when grafted onto young rootstock. Leaves and needles should look "old" as well. However, if tree size itself is the key to the changes seen in "aged" trees, then an old graft on young roots should resume growing fast and have the leaves of a much younger tree. As Mencuccini's group reported in the November *Ecology Letters*, growth tips from old trees resumed normal growth when grafted onto the rootstock. "Basically, it's size that matters, not absolute age," says Mencuccini. But "we still don't fully grasp why size is so important in affecting tree physiology," he adds.

Other tree researchers have been reevaluating a proposal dating back 50 years that looks to photosynthesis as the arbiter of tree height. At that time, the rationale was that extensive root or wood growth and respiration would eventually outpace the leaves' ability to produce enough energy to sustain those tissues. If that were the case, growth would become so slow and incremental that the tree couldn't keep up with natural losses such as die-back of the crown and would get stuck at a particular height. In the past decade, however, experiments have shown these energy-deficit explanations to be flawed. Neither roots nor woody growth hogged as much energy as researchers had thought.

In the 1990s, Michael Ryan, a forest ecologist now at the U.S. Department of Agriculture (USDA) Forest Service in Fort Collins, Colorado, and his colleagues found that leaves on smaller, younger trees are much more photosynthetically productive than leaves at the tops of taller trees. The reason, they surmised, might be that the higher leaves lack sufficient water, so he and Barbara Bond, a forest ecologist at Oregon State University, Corvallis, proposed what they called the hydraulic limitation hypothesis. "As a tree grows taller, it gets harder to pull water to the top," and that shortfall curtails photosynthesis, summarizes Bond. Friction is the problem, she adds: The farther the water has to travel, the more resistance it encounters.

To check out their hypothesis, Ryan and Bond focused on stomata, tiny pores on the leaf's surface that can close to slow water loss that comes about as evaporation sucks water up the tree and into the air, leaving the leaves high and dry. But stomata also take in the carbon dioxide necessary for photosynthesis, and Ryan and Bond found that the stomata on the uppermost leaves close frequently, presumably because the top of the tree isn't getting sufficient water and needs to limit further loss through evaporation. This curtails needed carbon dioxide intake. As a result, "trees stop growing when their ability to transport water to their leaves becomes insufficient [for photosynthesis]," explains Roland Ennos, a biomechanicist at the University of Manchester, U.K.

Less water at the top of a tall tree also means lower hydrostatic pressure, or turgor, within cells, which is necessary for plant cells to expand. At some point, water pressure inside cells at the tops of trees may drop enough to stop cell growth directly. Bond, as well as Frederick Meinzer and David Woodruff, plant ecophysiologists at the USDA Forest Service in Corvallis, were among the first to show that this decrease in pressure might affect tree growth. And the role of hydrostatic pressure was borne out in 2004—at least in the world's tallest trees. George Koch, a tree biologist at Northern Arizona State University in Flagstaff, and his colleagues reported that redwoods need hundreds of kilograms of water a day to keep their cells thriving, and turgor in 110-meter-high needles was half that in 55-meter-high needles. Based on this trend, his team calculated that redwoods could not exceed 130 meters in height.

Others are finding that connections between water-conducting cells may affect the ultimate height of trees. Unpublished data by Jean-Christophe Domec and his colleagues at Oregon State University, Corvallis, indicate that pores in these connections shrink to cope with the increased water tension. If the pores get too small, tree growth stalls. But, as Jarmila Pittermann and colleagues at the University in Utah, Salt Lake City, report on page 1924, the height at which resistance reaches this tipping point differs between conifers and hardwoods. The relatively larger pores in these connections in conifers allow for more water flow, potentially giving conifers a chance to tower over other types of trees.

CREDIT: *NATIONAL GEOGRAPHIC*/GETTY IMAGES

Green giant. At 113 meters, this northern California redwood is the world's tallest known tree.

But water-transport problems can't be the whole story. Ryan and his colleagues tracked photosynthesis, water flow, growth, and other parameters of eucalyptus seedlings in Hawaii for almost 7 years. The older, 25-meter trees grew much more slowly than the younger ones, Ryan and his colleagues reported last year. The work did demonstrate that photosynthesis slowed, but water was too plentiful to be the cause. "Our simple idea that getting water to the tree top limits height growth is not correct for all trees," says Ryan.

Although it's clear from all these studies, says Ryan, "that taller trees are different physiologically from shorter, younger trees," he and his colleagues still don't know how these differences stop tree growth. Solving that mystery remains a tall order.

–ELIZABETH PENNISI

San Andreas Drillers Find a Strangely Weak Fault

SAN FRANCISCO, CALIFORNIA—Almost 12,000 earth and planetary scientists (a new record) of every stripe met here 5 to 9 December to discuss topics as varied as the inner workings of the San Andreas fault and ancient muck on Mars.

Drillers have punched kilometers down through the San Andreas fault for the first time. A first glance at this "natural earthquake machine" reveals that the fault is relatively weak but not what weakened it, researchers reported at the meeting. In their quest to understand how quakes get started and why almost all fizzle out, investigators will drill straight through the heart of San Andreas quakes as they build the San Andreas Fault Observatory at Depth (SAFOD).

The SAFOD drill bit broke through the fault zone in central California last summer, just north of last year's moderate Parkfield earthquake. Drillers were extending the hole begun west of the fault by bending the hole toward the east and through the fault at a depth of almost 3 kilometers, close to a 100-meter patch on the fault that was breaking every 2 years in magnitude-2 quakes.

Before they divert drilling toward their ultimate target, the quake patch, SAFOD workers are looking around a bit, reported geophysicist Mark Zoback of Stanford University in California. He is a co–principal investigator of the SAFOD component of the EarthScope project (*Science*, 26 November 1999, p. 1655) funded by the U.S. National Science Foundation. Zoback and his colleagues are particularly curious about the stress that builds along a fault and eventually drives fault rupture.

Deep reach. Scientific drilling into the San Andreas found a weak fault and retrieved altered and deformed fault rock (*inset*).

SAFOD workers had two ways to get at fault stress. In one, they gauged the stress response of surrounding rock by sending sonic signals out from the hole. The changing orientation of the stress across the fault matched the pattern theorists had predicted for a weak fault—one that slips under relatively slight stress. When Colin Williams of the U.S. Geological Survey in Menlo Park, California, and USGS colleagues measured temperature and thermal conductivity down the hole, they found that the fault is not a source of heat. That's another sign of a weak fault. (Because of their high friction, strong faults generate lots of heat when they slip.) Other researchers had suggested that the San Andreas is weak (*Science*, 6 March 1992, p. 1210).

Why the weakness? So far, no one knows. Many geoscientists suspect that pressurized fluids—most likely salty water trapped within the fault zone—pry apart the opposite sides of the fault, reducing the amount of stress needed to make it slip. But "right now we see no evidence of overpressurization," Zoback says. The SAFOD researchers did not detect any pressure surge when they hit the fault zone, and seismic waves passing along the fault to the drill hole showed none of the expected effects of overpressurization, he said.

To get to the bottom of how a weak, normally pressurized fault generates earthquakes, in 2007, SAFOD will drill short spurs off the main hole, targeting the fault patch that slips in small quakes. Researchers hope to learn how it does that and perhaps whether big quakes work the same way. The view from inside even a small earthquake machine, they say, is proving far more informative than the view from outside looking in.

An Early, Muddy Mars Just Right for Life

When the Opportunity rover found the salty sedimentary remains of standing water on Mars, the prospects for early life on another planet brightened considerably. Although acid-laden, those early waters were nothing that martian life couldn't have adapted to. It's harder to imagine life originating under such conditions, however. Now, by analyzing the infrared "colors" of the martian surface, planetary scientists have identified clayey rocks that mark an even earlier warm and wet era, one more persistently wet and blessedly less acidic. The origin of martian life now looks brighter too.

Key to refining the water history of Mars was the powerful OMEGA spectrometer aboard the orbiting Mars Express spacecraft. OMEGA can probe the ground in enough detail and in the right range of infrared wavelengths to identify the distinctive absorption peaks of clays and sulfate salts (*Science*, 6 August 2004, p. 770).

Since announcing the first firm detection of martian clay last March, OMEGA team members have formed a clearer picture of how clays fit in the geologic history of Mars, reported OMEGA team leader Jean-Pierre Bibring of the University of Paris South in Orsay. Clays and the sulfate salts that mark the Opportunity deposits do not generally occur together, they found. And clays seem to have formed in a time before martian acid was corroding rock to produce the sulfate salts. In the Nili Fossae region, for example, clays appear beneath—and therefore were deposited earlier than—fresh, unweathered rock rich in olivine. They may even have formed before the early giant Isidis impact of some 4 billion years ago. All in all, clays appear to have formed within hundreds of millions of years after the planet did, and before the sulfates formed, said Bibring, about the time life could have been appearing on Earth.

CREDITS: M. ZOBACK/STANFORD UNIVERSITY; STEPHEN HICKMAN/USGS (INSET)

That timing—first clay, then sulfate—boosts the prospects for life on Mars by providing it with a possible birthplace other than the later acid bath. "The kind of chemical reactions we think were important to giving rise to life on Earth simply could not have happened" under the conditions Opportunity found, says paleontologist Andrew Knoll of Harvard University, a rover team member. The pH 1 sulfuric acid that leached rock to produce Opportunity's sulfates would have worked against the evolution of increasingly complex organic compounds that could lead to life. And it wasn't even always wet. The Opportunity landing site wasn't a "shallow sea," as initially assumed, but a salty sand sea with intermittent puddles between the dunes, team members write in a set of papers in the 30 November issue of *Earth and Planetary Science Letters*.

Clay, on the other hand, connotes a more hospitable environment, Bibring noted. The earlier clay era was "probably most favorable to have hosted the emergence of life," he said, "and could still host biorelics." On Earth, the smectite clays identified by OMEGA form under the mild, more continuously wet, and far less acidic conditions of the midlatitudes. OMEGA data are "pretty good evidence" of "more Earthlike conditions" on earliest Mars, agrees planetary geologist James Head of Brown University. Now planetary scientists must decide where to send their next, far more capable rover: to the well-characterized and safe Opportunity site, one of the newly enticing but poorly understood clay sites, or somewhere else found by the upcoming Mars Reconnaissance Orbiter?

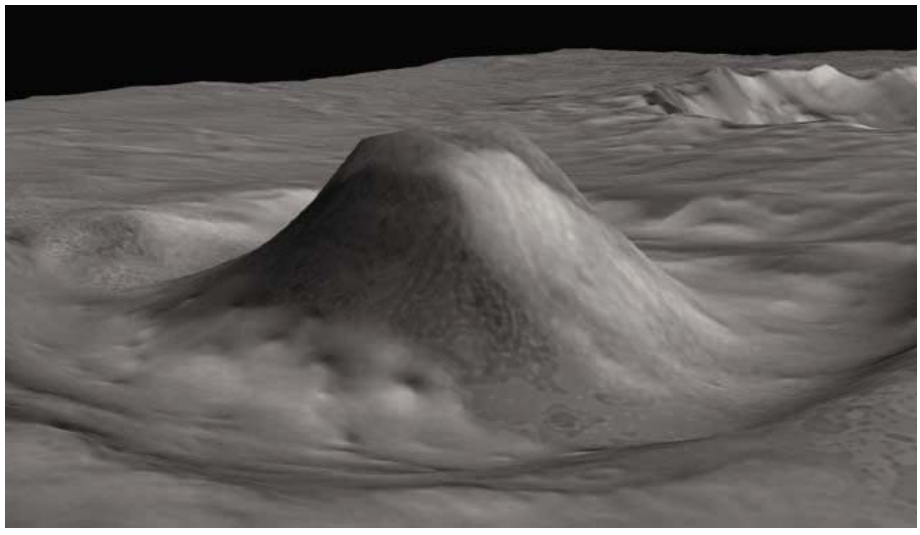

Towering remains. This 1-kilometer-tall pile of sediment (digitally stretched vertically) is taller than the surrounding crater rim, suggesting that sediment once covered the entire crater.

CREDIT: M. MALIN

Mars Saucer Mystery Baffles the Experts

Planetary geologist Michael Malin brought a long-standing, almost personal, problem to a joint planetary sciences/hydrology meeting session. Despite years of contemplating images returned by his camera now orbiting on Mars Global Surveyor, Malin can't for the life of him figure out how hundreds of impact craters on Mars were filled with some sort of sediment, some to overflowing, and then partially emptied of kilometers' worth of fill. Perhaps the terrestrial geologists in the audience could help?

Malin's prime example was 160-kilometer Henry Crater near the equator in the ancient highlands of Arabia Terra. A broad mound now covers much of the impact crater's floor and rises nearly as high as the crater's rim. The mound shows flat-lying layers, often monotonously uniform in thickness, which match layers in material still adhering to the crater wall.

To a geologist, it looks as if Henry was once filled to the top with sediment—40,000 cubic kilometers of it—and then was largely emptied. Some other craters were buried well above their rims, to judge by the height of lingering sediment piles. "We're pretty confident it happened," said Malin, of Malin Space Science Systems Inc. in San Diego, California. "We don't know how it happened." There is no obvious high ground that could have eroded to produce the sediment and no apparent gaps or channels through which running water might have carried sediment into or out of the crater. In fact, there's no sign of what erosive agent was at work. And there is no clue to where the kilometers of missing sediment have gone.

Malin has some ideas, of course. Rhythmic climatic variations—perhaps paced by the nodding of Mars's rotational axis over the millennia—probably turned sedimentation on and off to produce the layering. With no clear signs of wind-deposited layers, the sediments might initially have been laid down in seas, says Malin, although no one else has suggested seas up to several kilometers deep in the highlands. And wind is the leading candidate to whisk dust-size sediment particles from craters, but today's wispy atmosphere hardly seems up to the task. "It's hard to wrap your imagination around it," says planetary scientist Robert Sullivan of Cornell University, "whether it was all water, all wind, or a combination. I remain as puzzled as Mike."

The audience could offer no immediate solutions either, forcing Malin to fall back on the next probe to Mars. The Mars Reconnaissance Orbiter arrives in March, bringing far sharper eyes to bear on the cryptic half-full saucers of Mars. **–RICHARD A. KERR**

Snapshots From the Meeting

Double whammy. Folklore has it that "earthquake weather" in California is sultry, but in Taiwan it really is blustery, according to seismologists Selwyn Sacks and Alan Linde of the Carnegie Institution's Department of Terrestrial Magnetism. While they were monitoring the strain within boreholes in eastern Taiwan during the second half of 2004, nine typhoons passed over, they reported. During five of them, so-called slow earthquakes swept unfelt across the deep, inclined fault below. Sacks and Linde reason that the low atmospheric pressure at the heart of typhoons can relieve some of the pressure squeezing the fault and keeping it from slipping. Under the reduced pressure, the fault slips, helping rapidly push up Taiwan's coastal mountains several centimeters per year.

Not so hot. Earlier this year, some climate researchers warned that the climate system could be so sensitive to rising greenhouse gases that the next century would see truly scorching heat (*Science*, 28 January, p. 497). At the meeting, climate modeler Reto Knutti of the National Center for Atmospheric Research in Boulder, Colorado, and colleagues reported that such extreme warming is "very unlikely." In simulations with extremely high sensitivities, they found unrealistically large temperature swings between winter and summer region by region. The best agreement with the seasonal cycle came at climate sensitivities that would warm the world by 3°C to 3.5°C when carbon dioxide doubles, the sort of moderately large sensitivity many researchers had been coming to favor. **–R.A.K.**

Random Samples

Edited by Constance Holden

The First Americans

An analysis of ancient Brazilian skulls has lent new weight to the controversial theory that not one but two distinct populations from Asia colonized the Americas.

Scientists have long believed that starting about 12,000 years ago, the ancestors of present-day American Indians migrated from northeast Asia across the Bering land bridge. But in recent years, Walter Neves of the University of São Paolo in Brazil has argued that these immigrants were preceded by people from Southeast Asia who came from the same stock that settled Australia and Melanesia.

Last week, Neves and his colleague Mark Hubbe claimed new support for this idea from an analysis of 81 skulls, ranging in age from 7500 to 11,500 years, found in the Lagoa Santa region of southeast Brazil. Detailed comparisons revealed that the skulls did not resemble people from northeast Asia, who tend to have short, wide skulls with relatively flat faces, but rather took after present-day people from Australia and Melanesia, whose skulls tend to be long and narrow with projecting faces. Because other, similar ancient skulls have been found in North and South America, Neves and Hubbe concluded in a paper published online in the *Proceedings of the National Academy of Sciences* that two distinct populations probably colonized the New World.

Physical anthropologist Clark Larsen of Ohio State University in Columbus cautions that changes in diet over time can modify the jaw muscles in ways that also alter skull shape, without major genetic changes. Nonetheless, says archaeologist Tom Dillehay of Vanderbilt University in Nashville, Tennessee, "Neves is building a more solid case."

What's in a Tooth?

The male narwhal has long fascinated whale researchers, who have puzzled over the function of the 2.5-meter-long spiral tusk that juts out from its upper jaw, like the horn of the mythical unicorn. Now dentist Martin Nweeia, who teaches at Harvard School of Dental Medicine in Boston, has revealed that the tooth is not an icebreaker or a weapon as some have thought, but a sensor.

At the 16th Biennial Conference on the Biology of Marine Mammals in San Diego, California, last week, Nweeia reported from lab studies and narwhal observations in the Canadian Arctic that the tooth has an extremely sensitive surface with millions of tiny nerve endings. It can detect changes in water temperature and pressure, and chemicals that enable the whales to gauge salinity—an indication of ice formation—and find fish to eat.

Nweeia now plans to put water-filled plastic gaskets around 45-cm lengths of teeth on Arctic narwhals and monitor—via brain and muscle electrodes as well as hydrophones—the whales' responses to different salinity levels.

Ice Ages as History

"Anthropogenic climate change will basically produce another planet. ... Earth won't have another ice age until humans go extinct."

—James Hansen of NASA Goddard Institute for Space Studies in New York City on 6 December at the meeting of the American Geophysical Union in San Francisco

Signs Support Chomsky

A study of several deaf people who improvised a form of sign language to communicate with their families lends weight to what linguist Noam Chomsky first argued in the 1950s: that grammar is innate rather than learned.

The study, by cognitive scientists Marie Coppola and Elissa Newport of the University of Rochester in New York, focused on three young deaf adults, each raised in an isolated area of Nicaragua with no contact with anyone who knew formal sign language.

To see if the three so-called home signers employed the grammatical concept of "subject," Coppola showed them 66 videotaped events in which subjects were either active (such as "John") or inanimate (such as a door). The signers were then asked to describe to a family member what had happened. The signers nearly always began their description with the subject—an indication to Coppola and Newport that they had incorporated this grammatical concept.

To make sure, the researchers did a second study in which they showed vignettes depicting events in which characters changed from being active agents to being the "topic" of an action (for example, a woman arranges some flowers, then a man kisses her.) Again, the signers always put the subject at the beginning, the researchers reported online last week in the *Proceedings of the National Academy of Sciences*.

"Home signers could get their message across" without using grammatical concepts, says psychologist Ann Senghas of Barnard College in New York City. But this study shows that even when people make up their own sign language, "language-learning and language-processing mechanisms kick in."

Mayan Masterpiece

This detail is from what archaeologists say is the earliest known Maya painting, a large mural dated from 100 B.C.E. The January issue of *National Geographic* will describe its discovery at the site of San Bartolo in Guatemala.

CREDITS (TOP TO BOTTOM): GLENN WILLIAMS; INSET: MARTIN NWEEIA; KENNETH GARRETT/*NATIONAL GEOGRAPHIC*

Edited by Yudhijit Bhattacharjee

SIDELINES

Brain of the month. 2003 physics Nobel Prize–winner Anthony Leggett—and his brain—appear as Mr. January in a new calendar produced by the Beckman Institute for Advanced Science and Technology at the University of Illinois, Urbana-Champaign. "Big Brains on Campus" features a dozen staff members to showcase the institute's magnetic resonance imaging resources. The image of Leggett's brain highlights his cerebral cortex, a potential well-spring of his ingenuity. A scan of women's basketball coach Theresa Grentz, Ms. March, zooms in on her limbic system, a possible source of her passion for the game. See www.beckman.uiuc.edu/bigbrains.html

CREDITS (TOP TO BOTTOM): JON CHASE/HARVARD UNIVERSITY NEWS OFFICE; BECKMAN INSTITUTE FOR ADVANCED SCIENCE & TECHNOLOGY; JUSTIN IDE/HARVARD UNIVERSITY NEWS OFFICE; SAM OGDEN

PIONEERS

Amazing racer. What a year it has been for William Tan. The 48-year-old neuroscientist took time off from his research to compete in wheelchair races around the globe, including a grueling marathon spanning all seven continents. In the process, he raised $1.5 million to establish a professorship in pediatric oncology at his alma mater, the National University of Singapore (NUS).

Stricken with polio at age 2 and paralyzed from the waist down, Tan has been a marathoner since 1980 and has raised more than $14 million for charitable causes around the world, including children with disabilities, needy patients requiring dialysis treatments or prosthetics, and victims of the 11 September 2001 terrorist attacks. The seven-continent challenge—which Tan completed in 10 weeks—included a harrowing ride across Antarctica's alternately steep, rocky, and slushy terrain. "At one point, I sank 2 feet into the … slush and had to be pulled out by five runners," he says. Still, he finished the 42-kilometer race. Tan's tenacity and energy are "incredibly inspiring," says NUS president Shih Choon Fong.

With his marathon year drawing to an end, Tan will return to St George Hospital in Sydney, Australia, as a resident in internal medicine. He also plans to continue neuroscience research.

THREE Q'S

David Page has spent his entire career at the Whitehead Institute for Biomedical Research in Cambridge, Massachusetts, which shares faculty with the Massachusetts Institute of Technology (MIT) but is run by its own board. This month, the 49-year-old geneticist was named its fourth director.

Q: An "artist colony extraordinaire" is how you describe Whitehead. Are you serious?

A: Absolutely. We live by the credo of academic freedom. We hire people, invest in their careers, and let the faculty chart their own paths. We identify the most creative people and let 'em loose.

Q: There are rumors that MIT might try to absorb Whitehead. Would you back such a move?

A: That's news to me! I do not report to the president of MIT; we have our own board of directors. In terms of day-to-day academic life, we are joined at the hip with MIT. That relationship is a tremendous benefit, since we can turn on a dime. No, I wouldn't change that.

Q: Whitehead is now quite literally in the shadow of Novartis, the MIT McGovern Institute, and the new Broad Institute founded by former Whitehead researcher Eric Lander. Does that leave you feeling anxious?

A: I'm amused by a lot of the conversation about biomedical research models, since the premise is that there surely is one right model. I'd suggest that we want to see a diverse portfolio and different business plans. And our business plan is to maintain the best artist colony we can.

IN BRIEF

• John O'Keefe of University College London and Lynn Nadel of the University of Arizona in Tucson are the joint winners of the $200,000 Grawemeyer psychology award, given by the University of Louisville in Kentucky. They receive the honor for their work on the brain's mapping system.

• Darrell Kirch has been chosen to be the next president of the Association of American Medical Colleges (AAMC). Currently senior vice president for health affairs at Pennsylvania State University, University Park, Kirch will assume the post when current AAMC president Jordan Cohen steps down in June 2006.

MONEY MATTERS

Out of state. Political opposition to human embryonic stem (ES) cell research in Missouri has produced a windfall for Harvard University developmental biologist Kevin Eggan. It comes as a 5-year, $6 million grant from Jim and Virginia Stowers, founders of the Stowers Institute for Medical Research (SIMR) in Kansas City, that will be channeled through the newly incorporated Stowers Medical Institute in Cambridge, Massachusetts.

Eggan is the first university researcher to receive funding from the Stowers, whose previous gift of $2 billion has been used only at SIMR. Some Missouri legislators want to outlaw research on ES cells and somatic cell nuclear transfer, and SIMR officials hope that Eggan's grant will help persuade Missouri residents to support a constitutional amendment to protect such research. Eggan says the money will go toward his work on human ES cells, including efforts to create new cell lines using nuclear transfer.

Retraction

WE WISH TO RETRACT OUR REPORT "REQUIREment of voltage-gated calcium channel β_4 subunit for T lymphocyte functions" (*1*). The conclusions of our paper were based in part on electrophysiological data. We now believe that the data in Fig. 4B (prepared by S.B.) are erroneous, and that the conclusions of the electrophysiological results cannot be relied upon. In the interests of scientific integrity and the scientific literature, we believe the appropriate response is to retract this paper in its entirety.

RICHARD A. FLAVELL,[1] LEONARD K. KACZMAREK,[2,3] ABDALLAH BADOU,[1] EMILE L. BOULPAEP,[2] ROOMA DESAI,[3] SRISAILA BASAVAPPA,[2,4] DIDI MATZA,[1] YOU-QING PENG,[4] WAJAHAT Z. MEHAL[1]
[1]Section of Immunobiology, Howard Hughes Medical Institute, [2]Department of Cellular and Molecular Physiology, [3]Department of Pharmacology, Yale University School of Medicine, New Haven, CT 06520, USA. [4]Digestive Diseases Unit, Department of Medicine, Pharmacology and Physiology, University of Rochester School of Medicine, Rochester, NY 14642, USA.

Reference
1. A. Badou *et al.*, *Science* **307**, 117 (2005).

Human Embryonic Stem Cells

THE RECENT TRIAL IN THE PRESS OF THE ETHICS and scientific validity of publications on human somatic cell nuclear transfer ("Evidence of a pluripotent human embryonic stem cell line derived from a cloned blastocyst," W. S. Hwang *et al.*, 12 Mar. 2004, p. 1669; "Patient-specific embryonic stem cells derived from human SCNT blastocysts," W. S. Hwang *et al.*, 17 June 2005, p. 1777) highlights the hopes people place in this emerging area of science to meet therapeutic needs and the high standards the scientific community must bring to the field.

Accusations made in the press about the validity of the experiments published in South Korea are, in our opinion, best resolved within the scientific community. In 1998, following the publication of success in producing a cloned mammal using somatic cell nuclear transfer (*1*), there were accusations that it was a scientific fraud. In response to these charges, Sir Alec Jeffreys of the University of Leicester offered to independently verify that the animal was indeed a clone by directly obtaining source tissue from the Hannah Research Institute and blood from Dolly. Sir Alec's laboratory then performed DNA fingerprinting and microsatellite analysis confirming that Dolly's DNA, that of the cells banked at the Institute, and the original adult tissue were one and the same.

It may not come as a surprise that, in a similar vein, charges of fraud would be levied against Hwang's laboratory. We welcome the facts that Hwang has called for an assessment of the work in his laboratory and that the National University has started to make the arrangements. As we (I.W. and K.C.) confirmed the validity of our work by cooperating with an independent study, we encourage Hwang's laboratory to cooperate with us to perform an independent test of his cell lines to determine their nuclear and mitochondrial genotype in comparison with the donors of the original cells.

> **"Accusations made in the press about the validity of the experiments published in South Korea are ... best resolved within the scientific community."**
>
> –WILMUT ET AL.

Many patients and family members of patients with degenerative diseases place great hopes in regenerative medicine. This trust and the monies that many public agencies are investing in the science underscore the sobriety the scientific community should bring to the publications of scientific results. In addition to a willingness to facilitate the independent verification of published results, it may be helpful to institute an Internet database to publish the DNA fingerprinting and microsatellite data on new lines to ensure against the cross-contamination of cell cultures or scientific misconduct.

IAN WILMUT,[1] MICHAEL D. WEST,[2] ROBERT P. LANZA,[2] JOHN D. GEARHART,[3] AUSTIN SMITH,[4] ALAN COLMAN,[5] ALAN O. TROUNSON,[6] KEITH H. CAMPBELL[7]
[1]Centre for Reproductive Biology, The Queen's Medical Research Institute, University of Edinburgh, 47 Little France Crescent, Edinburgh EH16 4TJ, UK. [2]Advanced Cell Technology, One Innovation Drive, Worcester, MA 01605, USA. [3]Institute for Cell Engineering, Johns Hopkins University School of Medicine, 733 North Broadway, Baltimore, MD 21205, USA. [4]The Institute for Stem Cell Research, University of Edinburgh, Edinburgh EH9 3JQ, Scotland, UK, and the Institute for Stem Cell Biology, University of Cambridge, Cambridge CB2 1QT, UK. [5]ES Cell International, 11 Biopolis Way, # 05-06 Helios, Singapore 138667. [6]Monash Immunology and Stem Cell Laboratories, Monash University, Wellington Road, Clayton, Melbourne, Victoria 3800, Australia. [7]Division of Biological Sciences, University of Nottingham, Loughborough, Leicestershire LE12 5RD, UK.

Reference
1. I. Wilmut *et al.*, *Nature* **385**, 810 (1997).

Editor's Note: As we went to press, Hwang had stated his intention to retract the 17 June 2005 paper.

Inka Accounting Practices

WE ARE DELIGHTED THAT G. URTON AND C. J. Brezine have discovered concrete examples of khipus indicating the existence of an accounting hierarchy similar to those previously postulated ("Khipu accounting in ancient Peru," Reports, 12 Aug., p. 1065). Nevertheless, we would like to amplify various points raised by their Report.

We were surprised that the authors recounted the theory of the Inka administration's decimal structure without mentioning works that express serious doubts about the concrete application of this kind of administration at the regional level (*1*–*4*). It appears that the system was rarely exact even when a decimal vocabulary was used (*5*–*7*). The population of the Inka province of Huayla, for example, consisted of 12 guaranga (the Quechua term for a group of 1000), which were split into 4 units of 3 guaranga. Yet, on the eve of Spanish conquest, two of the guaranga in a known unit had approximately 750 taxpayers and one had 950 (*5*).

Urton's and Brezine's discovery of identical khipus accords well with previous accounts of exact copies of khipus shown to Spanish administrators and judges in the 16th century (*8*, *9*). Nevertheless, Spanish transcriptions and translations of khipus do not support Urton and Brezine's hypothesis that the khipu system was flexible, tolerating inexact counts and matches. Colonial testimonies argue unanimously for the exactitude of the system (*10*).

We have demonstrated previously that when khipus were read, every now and then ±1 errors occurred on whichever decimal level (*10*). Nevertheless, we consider it unlikely that almost half of the summation numbers would have been encoded erroneously, as proposed for khipu UR068. There may be various explanations other

than that of Urton and Brezine for the closeness of the summation numbers. In early colonial khipus, this kind of variation can be found, for example, in the annual fulfillment of earlier taxation requirements known as the Spanish tasa (*10*).

Finally, Urton and Brezine argue that the khipus of the upper hierarchy include place identifiers. Indeed, toponyms and personal names have previously been treated as part of khipu texts (*2*, *11*). We also have argued that the main towns of the Inka State had specific numeric values that were encoded in khipus, and furthermore, that more complicated systems seem to have been used to encode the names of minor villages and the many personal names that appear in various decoded khipu texts in Spanish historical records (*5*, *10*). To us, it seems that Urton and Brezine have applied our hypothesis to their specific case. Unfortunately, they do not manage to prove anything and the statement continues to be an unproven hypothesis.

MARTTI PÄRSSINEN AND JUKKA KIVIHARJU
Latin American Studies, Ibero-American Center (Renvall Institute), University of Helsinki, Post Office Box 59, Helsinki FI-00014, Finland.

References and Notes

1. Å. Wedin, *El sistema decimal en el imperio incaico: Estudio sobre estructura política, división territorial y población* (Insula, Madrid, 1965).
2. J. V. Murra, *Formaciones económicas y políticas del mundo andino* (Instituto de Estudios Peruanos, Lima, 1975).
3. F. Salomon, *Native Lords of Quito in the Age of the Incas* (Cambridge Univ. Press, Cambridge, 1986).
4. C. Julien (*9*), however, has argued that in the Lupaca province, in the South, the Aymara population was grouped into guaranga. Whether her interpretation is correct or not, the actual size of a supposed guaranga oscillated in that province between 866 and 1804 adult men, according to the transcription of an Inka khipu (*8*).
5. M. Pärssinen, *Tawantinsuyu. The Inca State and Its Political Organization* (Societas Historica Finlandiae, Helsinki, 1992).
6. M. Rostworowski, *Señoríos indígenas de Lima y Canta* (Instituto de Estudios Peruanos, Lima, 1978).
7. M. A. Cornejo Guerrero, *Arqueológicas* **24**, 149 (2000).
8. G. Díez de San Miguel, *Visita hecha a la provincia de Chucuito (1567)* (Casa de la Cultura, Lima, 1964).
9. C. J. Julien, *Ethnohistory* **35**, 257 (1988).
10. M. Pärssinen, J. Kiviharju, *Textos Andinos: Corpus de textos khipu incaicos y coloniales, Tomo I* (Instituto Iberoamericano de Finlandia and Universidad Complutense de Madrid, Madrid, 2004).
11. J. H. Rowe, *Histórica* **9**, 193 (1985).

Response

PÄRSSINEN AND KIVIHARJU'S COMMENTS and references point out a number of important issues we were unable to cover in our Report because of space constraints.

It is our understanding that both precise decimal administration and variations on this concept existed in the Inka empire. Colonial informants, especially those in the former capital Cusco (*1*–*4*), presented decimal administration as a complete, ideal system, although it is clear that the reality in the provinces was quite different from that ideal. Pärssinen and Kiviharju question the inaccuracy of the Puruchuco khipu; it is our belief that such inaccuracy is precisely the sort of variance from ideal decimal values that may have characterized Inka decimal administration at the provincial or local level. The principal task in interpreting pre-Hispanic and colonial record keeping in the Andes remains one of attempting to understand the causes and the significance of differences between colonial informants' testimony about Inka administration in comparison to the information actually recorded (often from khipu transcriptions) in colonial censuses and other statistical records. While we were not surprised that the decimal ideal was not reflected in the numbers and sums recorded in the Puruchuco khipu, we still believe that describing the ideal is essential to gaining a full picture of Inka administrative practices.

Although much of the material discussed in our Report is based on analysis of numerical values on the khipu, we were led to that analysis through other structural similarities within this group of artifacts: pendant cord spacing, color repetitions, and relative position of numerical magnitudes within their pendant groups. Therefore, our hypothesis of an accounting hierarchy is not based solely on the numbers, which indeed do not represent exact summations between levels I and II.

We regret that we did not specifically mention work on the referencing of toponyms and personal names in the khipu (*5*, *6*), and we appreciate the inclusion of additional references in their Letter.

Finally, we take this opportunity to remind readers that complete data on all of the khipu discussed in our Report are available on our Web site, http://khipukamayuq.fas.harvard.edu/.

GARY URTON AND CARRIE J. BREZINE
Department of Anthropology, Peabody Museum, Harvard University, 11 Divinity Avenue, Cambridge, MA 02138, USA.

References and Notes

1. B. Cobo, *History of the Inca Empire* [1653] (Univ. of Texas Press, Austin, TX, 1979) (see especially pp. 198–202).
2. Polo de Ondegardo, in *Colección de Libros y Documentos Referentes a la Historia del Perú*, vol. 4, H. H. Urteago, Ed. (Imprenta y Libreria Sanmarti y Ca, Lima, Peru, 1917), pp. 45–94 (see especially p. 51).
3. C. J. Julien, in *The Inca and Aztec States, 1400–1800*, G. A. Collier, R. I. Rosaldo, J. D. Wirth, Eds. (Academic Press, New York, 1982), pp. 119–151.
4. M. Rostworowski, C. Morris, in *The Cambridge History of the Native Peoples of the Americas*, vol. III, *South America*, part I, F. Salomon, S. B. Schwartz, Eds. (Cambridge Univ. Press, Cambridge, 1999), pp. 769–863 (see especially pp. 811–812).
5. M. Pärssinen, *Tawantinsuyu. The Inca State and Its Political Organization* (Societas Historica Finlandiae, Helsinki, 1992).
6. M. Pärssinen, J. Kiviharju, *Textos Andinos: Corpus de textos khipu incaicos y coloniales* (Instituto Iberoamericano de Finlandia and Universidad Complutense de Madrid, Madrid, 2004).

Letters to the Editor

Letters (~300 words) discuss material published in *Science* in the previous 6 months or issues of general interest. They can be submitted through the Web (www.submit2science.org) or by regular mail (1200 New York Ave., NW, Washington, DC 20005, USA). Letters are not acknowledged upon receipt, nor are authors generally consulted before publication. Whether published in full or in part, letters are subject to editing for clarity and space.

Highlighting the STAR Collaboration

THE MEMBERS OF THE STAR COLLABORATION at the Relativistic Heavy Ion Collider (RHIC) were disappointed by the article "Dueling experiments close in on source of proton's spin" (A. Cho, News of the Week, 4 Nov., p. 757). The article provides a description of the recent results from the PHENIX and COMPASS experiments on the contribution that gluons make to the spin of the proton but does not mention that the STAR experiment has yielded important, complementary new results that bear directly on this question as well.

STAR, like PHENIX, measures asymmetries in high-energy polarized proton collisions. The STAR results, like the PHENIX and COMPASS results, argue against the extreme model that the gluons in the proton are fully polarized.

In the language of perturbative quantum chromodynamics (pQCD), the STAR and PHENIX measurements involve the same initial states—a mixture of quark+quark, quark+gluon, and gluon+gluon collisions—but different final states. Interpreting jet asymmetries such as those measured by STAR introduces less theoretical uncertainty regarding final-state effects. Furthermore, the STAR results extend to considerably higher transverse momentum, where the applicability of pQCD for interpreting the observed spin asymmetries is believed to be quite reliable. In contrast, the reported PHENIX and COMPASS measurements that provide the greatest discriminating power among competing models of the proton involve rather low transverse momentum pions and quite low momentum transfer di-hadrons, respectively, where questions still remain regarding the reliability of the corresponding pQCD calculations that have been performed to date.

All three experiments are complementary. Each involves a unique mix of theoretical uncertainties, so the fact that they lead to a consistent conclusion is far more convincing than is the case for any subset of them.

TIMOTHY HALLMAN*
Department of Physics, Brookhaven National Laboratory, Upton, NY 11973, USA.
*Spokesperson of STAR

BEHAVIOR

Hormones in the Middle

Ellen D. Ketterson

I first became interested in hormones and social behavior while conducting an experiment on birds in the field. My colleagues and I were studying the evolution of male parental care by comparing the reproductive success of two groups of female dark-eyed juncos (*Junco hyemalis*), those rearing young with the assistance of a male and those forced to rear young alone because we had captured their mates. We reasoned that any difference between the two groups could be attributed to the male's help, giving us a quantitative measure in numbers of offspring of what that help was worth. As it turned out, however, our experiment was not so simple. Removing males led to the appearance of "replacements" whose presence had not been anticipated but whose behavior proved fascinating. Some replacement males fed the female's offspring, while others chased and courted the females but ignored the offspring (*1*). I had to know what underlay these different male behaviors. Did an individual's experience of having been a parent in the past, or of having copulated with a particular female, make him more or less likely to care for his neighbor's young? If there were selective advantages to adopting, why did only some of the males adopt? Was parental behavior latent in all male birds owing to its early origin within the clade? And what was the role of hormones such as testosterone and prolactin?

Hormones and Animal Social Behavior
by Elizabeth Adkins-Regan

Princeton University Press, Princeton, NJ, 2005. 429 pp. $79.50, £51.95. ISBN 0-691-09246-X. Paper, $45, £29.95. ISBN 0-691-09247-8. Monographs in Behavior and Ecology.

In *Hormones and Animal Social Behavior*, Elizabeth Adkins-Regan addresses the roles played by hormones in the social life of animals. The author, a behavioral endocrinologist at Cornell University, aims her book at researchers who seek a greater understanding of behaviors whose profitability to the actor depends on how other animals respond. Social behavior includes fighting, mating, signaling, pair bonding, and parenting. Adkins-Regan explores how hormones connect variation in these behaviors to variation in fitness, life history, alternative phenotypes, sex, and evolution. In so doing, she takes the reader sledding from brain to behavior and from hormones to gene expression, up and down through levels of analysis that often change within a single sentence.

Adkins-Regan's approach to hormones and behavior is one part common sense and one part rigor. The common sense is expressed in an informal writing style that sometimes makes you smile. For example, when she describes the ability of one individual's behavior to alter gene expression in another, she refers to the power of animals to "tickle each others' genomes." And when she summarizes the role of hormones in the development of insect castes in which an individual's caste develops not as dictated by its genes but by its nutritional and social environment, she writes that "queens are made, not laid." The author couples her conversational style with insistence on the most rigorous standards for knowing. She frequently points out how confined our knowledge is by the small number of species studied and hammers home the point that it is not safe to assume that what is true for one species is true for another.

One of Adkins-Regan's many accomplishments in the book is her successful integration of Niko Tinbergen's celebrated four questions. Tinbergen was awarded a Nobel Prize for his seminal contributions to ethology, the most lasting of which may be the roadmap he provided for the study of animal behavior. According to Tinbergen (*2*), a full understanding of any behavior requires that we know how it develops, how it is mediated by underlying mechanisms, how it contributes to fitness, and how it evolved. Many have cited the importance of this approach, but to my mind Adkins-Regan is the first to have achieved a true synthesis, and she has done so by putting hormones front and, importantly, center. To oversimplify, the environment acts on the animal from the outside to stimulate hormone release, while genes work from the inside to produce the enzymes that synthesize hormones and the receptor proteins that respond to them in target tissues. The hormone in the center stimulates or represses behaviors that influence fitness, causing the hormonal mechanisms that mediate behavior to evolve as social behavior evolves.

Deep understanding of the role of hormones in the expression and evolution of behavior is nevertheless challenging. In the relatively easy cases (for example, aggressive behavior in male chickens), you castrate and the behavior goes away; you provide hormone replacement, and the behavior comes back. More often, however, in the strictest sense hormones cannot be said to cause behavior, because the organism can produce the behavior in the absence of the hormone. That is, the behavior is "there" in the animal, and the hormone's role is to facilitate, mediate, coordinate, suppress, and otherwise alter the likelihood of the behavior's expression. Consequently, hormones often rise in the circulation after a behavior is expressed, as a response to the cues from the environment that elicited the behavior. Hormones may thus function to prepare the organism for future encounters with these same cues. Relying on an expected correlation between past and future can spare the animal drawbacks of expressing a behavior like aggression when it is not called for. The immune system and the development of acquired immunity provide a good analogy.

Mating under the influence. In the rough-skinned newt (*Taricha granulosa*), the interactions of peptides and steroids lead males to mate in response to female stimuli except when a predator threatens.

CREDIT: FRANK MOORE/OREGON STATE UNIVERSITY

The evanescence of hormones and their loose connection with behavior can be frustrating to ecological and evolutionary biologists who were drawn to hormones because of their association with fundamental questions in sexual selection: sex differences,

The reviewer is in the Department of Biology, Indiana University, 1001 East Third Street, Bloomington, IN 47405, USA. E-mail: ketterso@indiana.edu

exaggerated displays and ornaments, female choice, male-male aggression, and male parental care. Wattles and plumes are evidence that sexual selection has occurred and measuring them is a straightforward affair, but the hormonal systems that promote their development are less a fixed property on which selection can act. More often these systems are plastic or flexible attributes of an individual that respond to changes in the environment; to obtain meaningful results, the attributes must be measured in relation to those of other individuals with which the organism interacts.

Is there potential for selection on this kind of hormonally mediated trait? Certainly. Individuals vary in hormonal response to cues from the environment and in sensitivity to the hormones they produce. This nexus of sensitivity and response can be acted on by selection, giving rise to differences in aggression, bonding, and fighting. But as Adkins-Regan so clearly explains, we are just beginning to understand how. For example, we know very little about how different traits come to be regulated by the same hormone and even less about how they might escape such control. In well-studied cases like the links among testosterone, aggression, and parental behavior, the hormone is known to facilitate the coexpression of adaptive characters to form suites or syndromes. Such hormonal pleiotropy can help to explain genetic correlations that cause characters to respond to selection in a coordinated way. But what happens when one or a few of these co-occurring correlated characters are no longer beneficial? How, in a mechanistic sense, are correlations broken and short-term constraints overcome? Answers are currently elusive, but the guideposts Adkins-Regan provides to young researchers should make them more attainable.

At least two practical applications of the perspective provided by the book broaden its appeal. First, it offers insight regarding how animals are likely to respond to climate change. Many seasonal organisms employ hormones to coordinate their breeding to the time when conditions in the environment are appropriate. The cues that trigger hormone secretion and behavioral and physiological response differ by species and sex, but in general they have proven to be reliable predictors over time. Alternative cues that are better predictors of the new realities brought by climate change will surely be available, and over time selection will favor those individuals that adjust the timing of their breeding. But the unit of selection may be the coordinated hormonal responses of males and females, and such adjustments may take some time, whereas the rate of environmental change may be rather rapid. A second practical application concerns endocrine-disrupting chemicals in the environment, and here organisms may have less opportunity to adjust. Some of these chemicals hijack ancient and fundamental mechanisms that cannot be readily revamped. Although understanding hormonal mechanisms can again enhance predictions regarding outcomes, the ability of selection to fix the situation may be far more limited.

My only criticisms of Adkins-Regan's book are really requests for more. More illustrations would have been useful throughout, more extensive treatment of invertebrates and plants would have been welcome, and certain passages would have benefited from more citations. My overriding conclusion, however, is that *Hormones and Animal Social Behavior* is a highly illuminating book that is also a pleasure to read.

References

1. L. Wolf, E. D. Ketterson, V. Nolan Jr., *Anim. Behav.* **36**, 1601 (1988).
2. N. Tinbergen, *Z. Tierpsychol.* **20**, 410 (1963).

10.1126/science.1119728

ECONOMICS

Taxation with Representation

Thomas Piketty

Growing Public is an ambitious attempt to disentangle the complex interaction between social spending and economic growth in the developed countries since the 18th century. There is no doubt that Peter Lindert's book will have a long-lasting impact in the social sciences, both for its substantive conclusions and for its methodological contributions.

Over the past 30 years, Lindert (an economist and economic historian at the University of California, Davis) has published articles and reference books on long-running trends in income and wealth distribution in the United States and the United Kingdom and on the quantitative history of social spending. Drawing on his past work as well as an impressive array of archival material and new research, the author offers a fresh look at two old questions: Why did the uses of taxes for social programs evolve the way they did in Western Europe and North America over the past three centuries? And what was the impact of such social spending on economic growth and development?

The author's key conclusion can be summarized as follows: modern welfare states are the fruit of democracy, not of bureaucracy, and democratic markets are basically efficient. According to Lindert, and contrary to a view commonly held (especially in the United States), this explains why the rise of social spending—from less than 1% of the gross domestic product (GDP) in the United Kingdom and the Netherlands in 1750 to over 30% of GDP in Nordic countries in 2000—has had no long-term negative impact on economic growth in these countries. Instead, the effect might even have been a positive one. In particular, Lindert persuasively demonstrates that countries with large welfare states have always been careful enough to finance their social spending using a distortion-minimizing tax mix. For instance, tax progressivity (the increase in average tax rates with increasing income) has typically been more modest in the Nordic countries than in the low-spending Anglo-American world. More generally, countries with large welfare states have created substantial tax exemptions to encourage savings and capital accumulation. These countries have also relied extensively on proportional taxes on labor income (payroll taxes and social contributions) and consumption (especially of goods that are addictive, used in leisure activities, or threaten health or the environment, such as tobacco, alcohol, and gasoline). In addition, the structure of spending in the large welfare states has been designed to minimize negative effects on productivity—for example, through an emphasis on public health and education or on pro-women and anti–old-age labor supply policies.

Lindert argues that this careful fine-tuning of the structure of taxes and spending in modern welfare states is not accidental. It is instead largely due to functional democracy: democratic political markets provide checks and balances that allow control of the costs of social spending. Lindert's emphasis

Growing Public: Social Spending and Economic Growth Since the Eighteenth Century
by Peter H. Lindert

Volume 1, The Story
Cambridge University Press, Cambridge, 2004. 396 pp. $65, £42.50. ISBN 0-521-82174-6. Paper, $24.99, £17.99. ISBN 0-521-52916-6.

Volume 2, Further Evidence
240 pp. $75, £50. ISBN 0-521-82175-4.

The reviewer is at the Ecole Normale Supérieure–Ecole des Hautes Etudes en Sciences Sociales, 48 Boulevard Jourdan, 75014 Paris, France. E-mail: piketty@ehess.fr

on the workings of democracy is what makes his book much more than yet another liberal attempt to convince conservatives that social expenditures are useful. Lindert turns the standard free-market argument on its head and shows that modern welfare states actually go hand in hand with income growth and well-functioning political markets. Drawing lessons for the developing world from his historical tour of Western democracies, Lindert aptly concludes: "The safe prediction…is that by 2050 most countries cutting the share of GDP spent on social transfers and public education will be troubled countries. The way to keep social spending from rising over the first half of the twenty-first century would be to have no growth in average real income, no gain in life expectancy, and no shift toward democracy." In the same vein, reviewing the empirical evidence on the causal relationship between taxes and growth, the author shows that cross-country regressions that conclude social spending has a negative impact on growth are largely driven by the inclusion of Third World, high-spending nondemocracies such as Robert Mugabe's (current) Zimbabwe or Joseph Désiré Mobutu's (former) Zaire: "The fact that such kleptocracies were bad for economic growth tells us nothing about Europe's welfare states."

As part of his political perspective, Lindert analyzes the intricate relation between the structure of democracy and the evolution of social spending during the 18th and 19th centuries. For instance, he attributes the United Kingdom's early leadership in income transfers (to aid the lower classes) to the influence of the landed elite and its interest in keeping the rural labor force in the countryside. He views the fall of U.K. poor relief after the 1830s as a consequence of the ascent of the urban elite following electoral reform and political centralization. Conversely, Lindert sees German and U.S. leadership in public education expenditures over most of the 19th century as a result of the opportunities that political decentralization offered to local, progressive communities. (In Germany and the United States, the rise of universal suffrage and centralization came after a national consensus on public education had emerged). Equally illuminating are Lindert's careful data collection and comparisons of private giving between the time of church charities (less than 0.2% of GDP during the 18th and 19th centuries) and in the modern period (over 2% in GDP in 2000).

The author's arguments are basically sound and convincing. Some readers might look for extra material on the nondemocratic historical genesis of the distortion-maximizing tax mix used by Europe's high-spending countries. (War shocks played a major role in the development of capital exemptions, and tax competition has done so in the recent past.) Others might wish to find more on the virtues of tax progressivity per se. (With purely proportional taxes funding large-scale social spending, and no tax progressivity at all, excessive concentration of wealth might reappear in the long run). But given that the book already includes such an impressive set of quantitative and qualitative evidence covering three centuries of social spending and political processes, such complaints would be misplaced.

Most of the book's critics will probably choose to focus on methodological issues. As one might expect, it is hard to address grandiose historical questions of the kind Lindert raises while at the same time maintaining a rigorous approach to issues of causality. The author's methodological approach does not fall into any particular existing category but can be described as "pragmatic quantitative history." After exhaustively gathering available evidence on a given issue, country, or time period (with an emphasis on quantitative data whenever possible), he runs regressions and computes correlations in all possible directions. (The second volume of the work, intended for specialists in social science, provides detailed descriptions of his analyses and the data. And Linder has made his major underlying data sets available at www.econ.ucdavis.edu/faculty/fzlinder.) He supplements his statistical analyses with historical accounts and well-chosen anecdotes in order to derive strong (and generally plausible) conclusions. The book appears at a time when most economists and a growing share of social scientists are converging toward fairly stringent criteria for how causality relations should be established in the social sciences (especially in the area of policy evaluation). That methodological consensus emphasizes identification issues, natural and controlled experiments, and a limited set of well-defined policy issues that can be addressed properly. It is, to a considerable extent, the opposite of Lindert's approach, which proceeds through "reverse engineering from the historical facts back to a set of model predictions and only then to the assumptions of the model." Many economists will probably be worried about this; at the very least, they would prefer to see more detailed and rigorous empirical testing of a number of specific hypotheses raised in the various chapters. The key question is whether Lindert's pragmatic methodology is sufficiently constrained so as to be reproducible. To put it bluntly: Lindert can carry it out, but can my doctoral students do so?

Such questions are legitimate, but at the end of the day they are probably misplaced. *Growing Public* has an incomparable merit. At a time when many social scientists focus on narrow and local issues (those for which causality relationships can be rigorously established), Lindert reminds us that they can (and should) also offer clever thinking on big questions.

10.1126/science.1101319

CREDIT: BRIAN HAYES

BROWSINGS

Infrastructure. A Field Guide to the Industrial Landscape. *Brian Hayes.* Norton, New York, 2005. 542 pp. $49.95, C$73. ISBN 0-393-05997-9.

Although it doesn't fit in a hip pocket, this guide will help any technotourist to identify structures commonly encountered (if often overlooked) in outdoors urban habitats and industrial landscapes. Through his striking photographs and informative text, Hayes explains what the manufactured objects are called and what they do. He covers hardware of mining, waterworks, agriculture, energy, communication, transportation, and waste disposal—such as oil-filled switches (left), used at substations to quench the arc that forms when a large electric current is interrupted.

COMMUNICATION

Social Values and the Governance of Science

George Gaskell,[1]* Edna Einsiedel,[2] William Hallman,[3] Susanna Hornig Priest,[4] Jonathan Jackson,[1] Johannus Olsthoorn[5]

In recognition of the tensions between science and society (*1*), and as research increasingly enters value-laden areas, proposals have been made for scientists to engage with other communities on the ethical, legal, and social implications of science and technology (*2*) and for the "public voice" to be brought into the formative stages of decision-making (*3*). Such measures, it is argued, should result in socially viable paths for scientific innovation.

Enhanced online at www.sciencemag.org/cgi/content/full/310/5756/1908

As a contribution to this debate, we present findings from representative and comparable social surveys (*4*) in the United States (n = 1200), Canada (n = 2000), and the European Union (n = 25,000) on who the public thinks should make decisions on science policy and what criteria should guide such decisions. We then investigate how positions on science policy relate to people's opinions about the utility and regulation of technological innovation.

Survey respondents were asked two forced-choice questions (*4*). First, should decisions about technology be left to the experts or based on the views of the public? Second, should decisions be made on the basis of scientific evidence or on moral and ethical considerations? Clearly, forcing a choice between the pairs of options precluded a middle way. But we wanted to find out in whom and in what type of evidence the public had most confidence. The responses to these questions allowed us to divide the public into four "groups" reflecting different principles of governance: scientific elitists opted for decisions taken on expert advice based on scientific evidence; moral elitists opted for decisions taken on expert advice based on moral and ethical criteria; scientific populists opted for decisions based on average citizen's views of the scientific evidence; and, moral populists opted for decisions based on the average citizen's views of the moral and ethical issues.

The distribution of people in the United States, Canada, and Europe who opted for each principle of governance is shown in the table (p. 1909). The scientific elitists were the largest group in the United States, Canada, and Europe (54, 49, and 52% respectively). Overall, two-thirds opted for a scientific basis to decision-making and just under three-quarters wanted experts to be in the driving seat. This can be read as a vote of confidence in "sound science." But is it a ringing endorsement? Just over a third of respondents valued moral and ethical considerations over scientific evidence; one-quarter of respondents preferred the public over experts in decision-making.

Were these different positions on the governance of science related to people's views about the utility of science? Survey respondents were asked whether they were optimistic or pessimistic about the prospects for society of three technologies—computers and information technology, biotechnology, and nanotechnology (see chart, this page).

For each technology, the scientific elitists were more optimistic than the other groups, with the exception of the Canadian moral elitists on nanotechnology. The moral elitists were generally more optimistic than the scientific populists about nanotechnology and biotechnology. Finally, the moral populists were always the least optimistic of the four groups.

Furthermore, there were marked differences in optimism both between the scientific elitists and the moral populists, and among the United States, Canada, and Europe. The mean difference between scientific elitists and moral populists (across the United States, Canada, and Europe) was 13% for computers and IT, 18% for nanotechnology, and 26% for biotechnology. Thus, although the utility of computers and IT was relatively consensual, judgments about the societal contribution of biotechnology (and to a lesser extent nanotechnology) were more strongly associated with views on the governance of science.

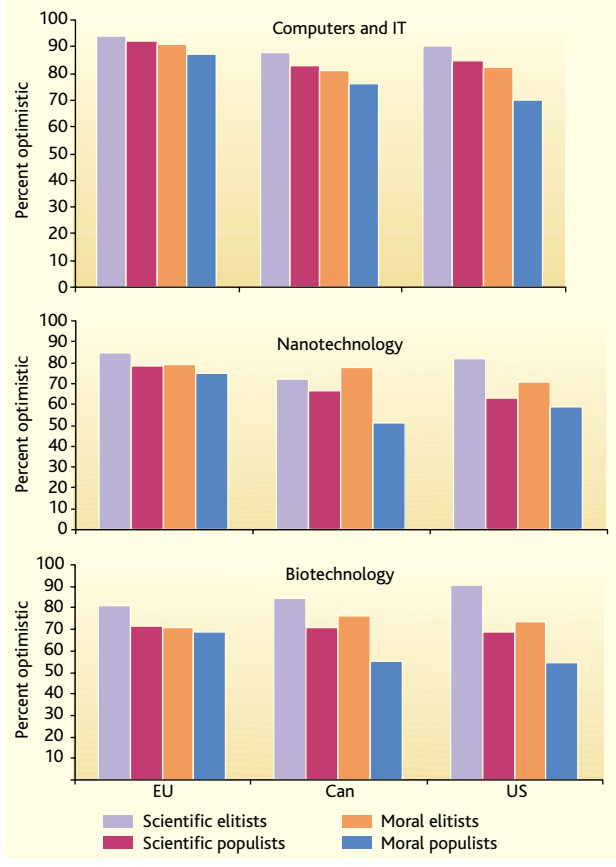

A transatlantic divide was also apparent. The mean difference in optimism between scientific elitists and moral populists for the three technologies was greater for the United States (26%) and Canada (20%) than for Europe (9%). By implication, disagreements about the value implications of these technologies were stronger in North America than in Europe.

But is this plausible given the continued political conflict in Europe over the introduction of genetically modified (GM) crops and

[1]Methodology Institute, London School of Economics and Political Science, London WC2A 2AE, UK. [2]Faculty of Communication and Culture, University of Calgary, Calgary, AB T2N 1N4, Canada. [3]Food Policy Institute, Rutgers University, New Brunswick, NJ 08901, USA. [4]College of Mass Communications and Information Studies, University of South Carolina, Columbia, SC 29208, USA. [5]Canadian Biotechnology Secretariat, Ottawa, K1A 0H5 Canada.

*Author for correspondence. E-mail: g.gaskell@lse.ac.uk

food? We think so, and have argued as such elsewhere (*5*). The survey question asked about "biotechnology" not GM. Since the de facto moratorium on GM crops was introduced in Europe in 1999, media coverage across Europe on the issue has declined (*6*) and the continued discussions in Brussels (including an unofficial lifting of the moratorium in 2004) have gone largely unnoticed by the public. Europeans have become more positive about biotechnology (*4*), seemingly associating it with the human genome project and medical applications, rather than agriculture and food biotechnologies.

PERCENTAGES APPROVING STEM CELL RESEARCH AND GM FOOD WITH TIGHT CONTROL AND REGULATION

	Scientific elitists	Scientific populists	Moral elitists	Moral populists	Controversy index*
Stem cell approval (%)					
EU	62	56	51	43	1.44
Canada	91	75	91	61	1.49
US	90	53	85	38	2.37
GM food approval (%)					
EU	48	41	36	37	1.30
Canada	62	44	51	45	1.38
US	76	54	57	40	1.90

*The ratio of the percentages of scientific elitists and moral populists

What are the implications of the principles of governance for people's views on regulation? Both GM food and stem cell research have stoked controversies about risks and benefits, moral and ethical issues, public consultation, and regulation. To determine how the different groups viewed the regulation of these technologies, respondents were given a brief description of stem cell research and GM food, and asked to choose one of the following alternatives: approve, approve with tight control and regulation, approve only in special cases, and not approve in any circumstances (*4*). For this analysis, we combined the first two of these response alternatives, because few chose unqualified approval, and the first two approximated current regulations.

Among the United States, Canada, and Europe, we found a relatively consistent pattern of response for stem cell research and GM food when comparing the scientific elitists and the moral populists (see table). The former were more likely to approve the applications than the latter. But even given tight regulation and control, Europe's scientific elitists were less likely to support the two applications than the same groups in the United States or Canada.

In the last column of the table, we show a "controversy index," which is the ratio of approval offered by the scientific elitists and the moral populists. As this index increases, it is more probable that the technology is controversial or likely to be so. On this criterion, stem cell research was more controversial than GM food, and for both technologies, the United States had the highest score.

For stem cell research, in both the United States and Canada, it seems that being critical of the reliance on scientific evidence (moral elitists) reduced the extent of support far less than being critical of the reliance on experts (scientific populists). For GM food, being critical of either scientific evidence or of experts appeared to have a similar impact in terms of declining support. By contrast, in Europe, moral elitism was associated with a greater decline in approval than scientific populism for both stem cell research and GM food. The perceived absence of moral and ethical considerations in decision-making seems to be a greater concern in Europe than the absence of public participation. In summary, among the critics of sound science, it appears that in the United States and Canada, it is who decides rather than on what basis that is most important, while in Europe, it is the reverse—the grounds are more important than who makes the decision.

Finally, we explored the characteristics of people who opted for the different principles of governance. Common to the surveys were indicators of education, religiosity, age, gender, and a measure of institutional trust based on trust in politics and trust in the media. These characteristics were used as predictors of the groups using multinomial logistic regression. Here, one group—the scientific elitists—was used as the reference category, and we determined whether each of the three other groups differed significantly on any given characteristic, holding the other factors constant (*4*).

By comparison with the scientific elitists, the other three groups had lower institutional trust. Furthermore, with the exception of Canada, these three groups have lower educational achievement. Of particular note was the contrast between the United States on the one hand, and Canada and Europe on the other. In the United States, religious beliefs were strongly related to critical attitudes to science and technology. For both the scientific and moral populists in the United States, it was the combination of strong religious beliefs, lower educational achievement, and lower generalized trust that most clearly distinguished them from the scientific elitists. Although Miller (*7*) showed that in the past the U.S. public consistently reconciled conflicts between science and faith in favor of science, is this still true?

In summary, we found a majority in favor of current science policy, with this group seeing more utility in technology and more likely to approve technologies within current regulations. We also found a minority in favor of ethically informed decision-making and public engagement in science, with less positive views about technology, in particular emerging and controversial technologies.

What are the implications for science policy? Some might argue that because current policy achieved majority support, the status quo should prevail. But such an approach might be shortsighted for the following reasons.

First, there is the risk of alienating the more moderate sections of the minority, whose position finds support in influential journals, including *Science* (*2*). A positive response to their desire for greater involvement and more consideration of the moral and ethical issues may make a significant contribution to building trust in science policy.

Second, people ask: "What sort of society do we want, and how can new technology help in achieving it?" These are questions about ethics and social values; science alone cannot answer them. The public expect and want science and technology to solve problems, but they also want a say in deciding which problems are worth solving. This is not a matter of attracting public support for an agenda already established by science and scientists, but rather of seeing the public as participants in science policy with whom a shared vision of socially viable science and technological innovation can be achieved.

References and Notes

1. G. Gaskell, M. W. Bauer, Eds., *Biotechnology 1996–2000: The Years of Controversy* (Science Museum Publications, London, 2001)
2. A. I. Leshner, *Science* **307**, 815 (2005).
3. "Going public," *Nature* **431**, 883 (2004).
4. Details can be found on *Science* Online.
5. G. Gaskell, N. Allum, S. Stares, "Europeans and Biotechnology in 2002: Eurobarometer 58.0" (European Commission, Brussels, 2003); (europa.eu.int/comm/public_opinion/archives/eb/ebs_177_en.pdf).
6. M. W. Bauer, S. Howard, "Biotechnology and the Public: Europe, North America, and Japan, 1973–2002" (Tech. rep., London School of Economics, London, 2004).
7. J. D. Miller, *Public Underst. Sci.* **13**, 273 (2004).

8. Support for this project is acknowledged from Genome Canada, the Canadian Biotechnology Strategy Fund of the Government of Canada, and the Directorate General for Research, European Commission.

0.1126/science.1119444

Supporting Online Material
www.sciencemag.org/cgi/content/full/310/5756/1908/DC1

EVOLUTION

Is the "Big Bang" in Animal Evolution Real?

Lars S. Jermiin, Leon Poladian, Michael A. Charleston

The origin and evolution of animals have remained hotly debated issues ever since Darwin drew attention to the relative paucity of fossils from the Precambrian, which ended 543 million years ago (Mya) (*1*). On the one hand, a growing collection of exquisitely preserved fossils of soft-bodied animals from the Cambrian has highlighted the existence of Cambrian representatives of most of the living animal phyla (*2*). This has given rise to the "Cambrian Explosion" hypothesis (*3*) that most animal phyla arose ~543 Mya within a short period (see the figure). On the other hand, studies of increasingly large molecular data sets suggest that many of the same phyla arose in the Precambrian (*4*–*6*), leading to considerable and occasionally intemperate debate on the timing of divergence of animal phyla. The article by Rokas *et al*. (*7*) on page 1933 in this issue presents a new aspect to this controversy.

Motivated by the desire to resolve the early evolution of animals, while accounting for insufficient data from some taxa, Rokas *et al*. used an alignment of 12,060 amino acids, encoded by 50 genes, to infer the phylogeny of 16 representatives from nine animal phyla. Eleven of these were from Porifera, Cnidaria, Platyhelminthes, Mollusca, Annelida, and Priapulida. These six phyla have not been adequately represented in recent molecular studies of early animal evolution (*4*–*6*). Given the aligned data, Rokas *et al*. inferred a phylogeny with several distinct speciation events that were consistently supported by the data, but with a conspicuous polytomy (multiple, concurrent divergence events) involving the protostome phyla, and another involving the bilaterate, cnidarian, and poriferan lineages. Recognizing that a polytomy may be due to rapid speciation, or to poor or insufficient data, Rokas *et al*. then explored whether convergence, "rogue" sequences, compositional heterogeneity, missing or inadequate data, or mutational saturation could have affected the phylogenetic estimate, and found that none of these were likely. In the absence of other explanations, they concluded that their data support rapid speciation during the early evolution of animals.

This conclusion is significant because it is consistent with the Cambrian Explosion hypothesis. Whereas previous molecular studies have concluded that the divergence of animal phyla occurred gradually over a period stretching hundreds of millions of years into the Precambrian (*4*–*6*), the present study suggests that two episodes of multiple divergence events occurred, each over just a few million years. This conclusion is consistent with a phylogeny based on fossil data (see the figure), thus reconciling a key difference in opinion between evolutionary biologists and paleontologists. However, Rokas *et al*. did not date these episodes, so corroboration of the Cambrian Explosion hypothesis is conditional on future estimates of the

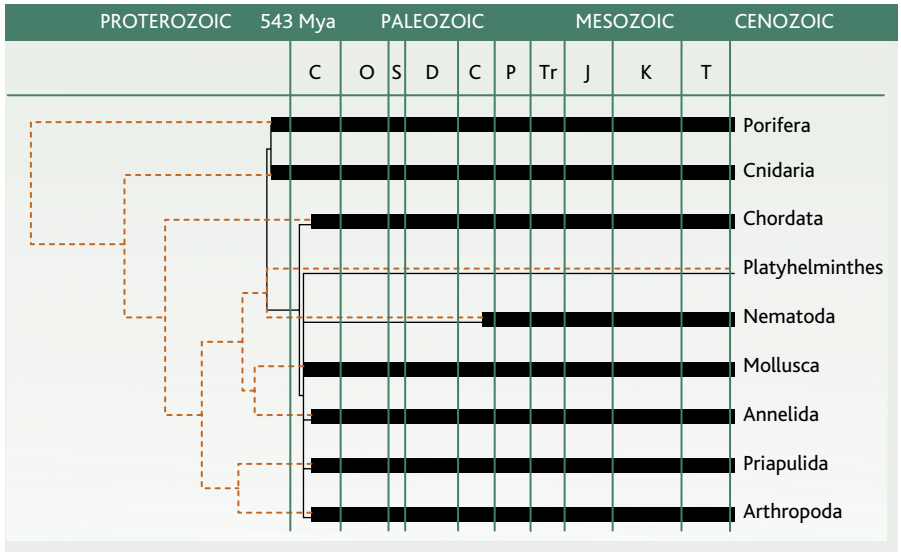

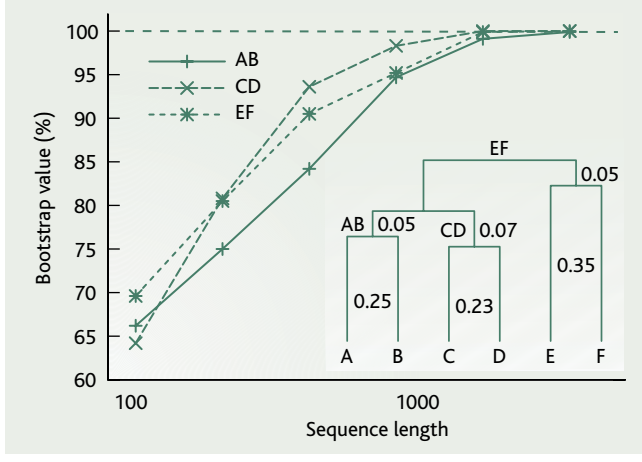

The debate on early evolution of animals. (**Top**) The fossil record and evolution of 9 of the 35 currently recognized metazoan phyla suggest that most animal phyla diverged/arose at the beginning of the Cambrian (C) period. The thick lines represent the known ranges of fossils from their first appearance in the fossil record (*16*). Thin lines represent the inferred metazoan phylogeny based on fossil data. Dashed lines represent an amalgam of three conservative estimates of the inferred metazoan phylogeny (*4*–*6*). (**Bottom**) Demonstration of the increase in bootstrap values when longer sequences are used. The phylogenetic tree shown (**inset**) is that used to generate six nucleotide sequences labeled A to F, each of length 100; these were duplicated to a length of 200, 400, 800, 1600, and 3200 bases. The internal branches are labeled AB, CD, and EF; the numbers at each branch are proportional to time. The data were generated under a Markov model that allows two classes of substitutions, using Seq-Gen (*17*); bootstrap values were estimated with PAUP* (*18*).

L. S. Jermiin is at the School of Biological Sciences, L. Poladian is at the School of Mathematics and Statistics, and M. A. Charleston is at the School of Information Technology, University of Sydney, NSW 2006, Australia. E-mail: lars.jermiin@usyd.edu.au All authors are members of the Sydney University Biological Informatics and Technology Centre (SUBIT), University of Sydney, NSW 2006, Australia.

divergence dates not falling well within the Precambrian.

Is the conclusion drawn by Rokas *et al*. sound? At first glance, it appears so, but can their conclusion stand up to closer scrutiny? Accepting that the genes analyzed by the authors evolved without gene duplication and that the amino acids are aligned correctly, most phylogenetic methods assume that the evolutionary dynamics of the 12,060 amino acid sites are independently and identically distributed, and that they evolved under the same stationary, reversible, and homogeneous conditions (*8*). The assumptions arise from the need to render phylogenetic methods tractable and easy to use, and they are unlikely to be realistic. To account for the observation that the sites in a gene may evolve at different rates, some phylogenetic methods are able to model rate heterogeneity across sites using a Γ distribution (*9*). Rokas *et al*. used this approach for the whole alignment but did not consider that different parts of the alignment may require different Γ distributions. Nor did they consider that some sites may vary nonindependently (*10*) and that the distribution of variable sites may vary across lineages and through time, an issue that is notoriously difficult to resolve (*11*). A logical extension to the work would be to partition the alignment and estimate the evolutionary rates for different genes separately.

Violation of the assumed stationary, reversible, and homogeneous conditions may lead to compositional differences in the aligned amino acid sequences and hence to errors in phylogenetic estimates (*12*). Rokas *et al*. recognized this potential source of error but used a test that is known to be flawed, even though better tests are known (*13*). Furthermore, they chose a phylogenetic method that, while it accounts for compositional variation in the sequence alignment, is unsuitable: It assumes that the sites are independently and identically distributed, which they have already shown not to be the case. Moreover, they used a single Markov (probabilistic) model to analyze the alignment of amino acids, in effect using a "one size fits all" approach, where it would have been better to use several Markov models to capture gene-specific differences in the evolutionary processes (*14*).

Rokas *et al*. used nonparametric bootstrap and posterior probabilities to gauge support for the pattern and order of speciation events (branches in their phylogenetic tree). The former is widely recognized to be statistically unwise. Bootstrap values are estimates of the expected frequency with which speciation events (internal branches) occur in the optimal tree, using data constructed from the original alignment by sampling sites with replacement (*15*). It is not a measure of accuracy or confidence, but of data consistency. Further, the increase in bootstrap value when more genes are included may be misleading, because longer sequences naturally tend to have higher bootstrap values (see the figure). The posterior probabilities of speciation events being correctly identified are also prone to error when the phylogenetic assumptions are violated in the sense described above.

In light of these concerns, are the conclusions of Rokas *et al*. justified? Should we ignore their study? Most certainly not, because they have produced a wealth of data and have shown that it might just be possible that the fossil record can be reconciled with molecular data. This, in itself, should be cause for celebration and an incentive to acquire sequence data from the remaining 26 animal phyla. Likewise, it should encourage development of methods that assess when data violate phylogenetic assumptions, and that cope with such data. To achieve these goals, we need to know more about the structure and function of gene products before we can develop models that appropriately address the early evolution of animals.

References

1. C. Darwin, *The Origin of Species by Means of Natural Selection.* (John Murray, London, ed. 6, 1888), p. 313.
2. D. E. G. Briggs, R. A. Fortey, *Paleobiology* **32**, S94 (2005).
3. S. J. Gould, *Wonderful Life: The Burgess Shale and the Nature of History* (Hutchinson Radius, London, 1989).
4. E. J. Douzery, E. A. Snell, E. Bapteste, F. Delsuc, H. Philippe, *Proc. Natl. Acad. Sci. U.S.A.* **101**, 15386 (2004).
5. K. J. Peterson *et al.*, *Proc. Natl. Acad. Sci. U.S.A.* **101**, 6536 (2004).
6. K. J. Peterson, N. J. Butterfield, *Proc. Natl. Acad. Sci. U.S.A.* **102**, 9547 (2005).
7. A. Rokas, D. Krüger, S. B. Carroll, *Science* **310**, 1933 (2005).
8. V. Jayaswal, L. S. Jermiin, J. Robinson, *Evol. Bioinformatics Online* **1**, 62 (2005).
9. Z. Yang, *Trends Ecol. Evol.* **11**, 367 (1996).
10. D. Penny, B. J. McComish, M. A. Charleston, M. D. Hendy, *J. Mol. Evol.* **53**, 711 (2001).
11. P. J. Lockhart *et al.*, *Mol. Biol. Evol.* **23**, 40 (2006).
12. S. Y. W. Ho, L. S. Jermiin, *Syst. Biol.* **53**, 623 (2004).
13. L. S. Jermiin, S. Y. W. Ho, F. Ababneh, J. Robinson, A. D. W. Larkum, *Syst. Biol.* **53**, 638 (2004).
14. M. Pagel, A. Meade, *Syst. Biol.* **53**, 571 (2004).
15. J. Felsenstein, *Evolution* **39**, 783 (1985).
16. J. W. Valentine, D. Jablonski, D. H. Erwin, *Development* **126**, 851 (1999).
17. A. Rambaut, N. C. Grassly, *Comp. Appl. Biosci.* **13**, 235 (1997).
18. D. L. Swofford, *Phylogenetic Analysis Using Parsimony (*and Other Methods), 4.0 Beta* (Sinauer, Sunderland, MA, 2002).

10.1126/science.1122440

PHYSIOLOGY

The Tick-Tock of Aging?

Adam Antebi

The relationship between organismal development and aging has long been a matter of intense debate. It seems natural to posit that developmental timing mechanisms that culminate in reproductive maturity continue to affect post-reproductive biology, with consequences for total organism life span. On the other hand, evolutionary theories of aging discount regulated aging per se, because the force of selection declines with age and drops precipitously after reproductive potential ends. In other words, a program that actively ages the organism is unlikely to be selected for in evolution. Instead, aging is thought to entail the passive stochastic accumulation of damage to molecules, cells, and organs, leading to loss of fertility and organismal demise. Therefore, the notion that regulated intrinsic biological timers control aging seems superficially untenable.

Just this possibility, however, has been raised by Boehm and Slack on page 1954 of this issue (*1*). The have found that components of a nematode's (*Caenorhabditis elegans*) heterochronic circuit—namely the *lin-4* microRNA and its target, the nuclear protein encoded by *lin-14*—not only perturb developmental timing but also influence organismal life span. They do so by regulating insulin/IGF-1 (insulin-like growth factor–1) signaling, a cellular regulatory pathway whose modest decrease in activity leads to increased longevity across taxa (*2*).

Just as each cell in a developing organism has a positional identity that is determined by gradients of morphogens and hierarchies of transcription factor activity, cells also have a temporal identity dictated by regulatory signaling cascades. Pioneering work in *C. elegans* led to the discovery of the heterochronic loci (*3*), which constitute a regulatory circuit that confers temporal identity to the various tissues. These genes determine cellular programs of division, migration, and differentiation that are appropriate for a specific developmental stage. In addition, the interactions among these heterochronic loci ensure the proper succession of larval temporal fates. Normally, *C. elegans* develops to adulthood through four larval stages, L1 to L4. Worms with mutations in the heterochronic loci inappropriately express cel-

The author is at the Huffington Center on Aging, Department of Molecular and Cellular Biology, Baylor College of Medicine, Houston, TX 77030, USA. E-mail: aantebi@bcm.tmc.edu

lular programs at the wrong stage that could result, for example, in the expression of adult features in the juvenile or conversely, juvenile features in the adult. A molecular analysis has revealed that most heterochronic loci are evolutionarily conserved. Perhaps most striking are the examples of *lin-4* and *let-7* microRNAs, short 21- to 24-nucleotide RNAs that post-transcriptionally regulate gene expression (*4*–*6*). First discovered in the worm, orthologs are found conserved across species, including human (*7*). This spawned the discovery of large families of similar molecules whose diverse functions are only just beginning to be explored. As part of an early larval timer, a rise in *lin-4* microRNA expression triggers larval stage L2 and later developmental programs by decreasing the expression of a molecular target, *lin-14*. It does so by binding with imperfect complementarity to sequences in the 3′-untranslated region of the messenger RNA (mRNA) that encodes *lin-14*, inhibiting translation and mRNA stability (*4*, *5*). A decrease in the expression of *lin-14* mRNA and protein is seen in the developing worm, but expression persists in some tissues in the adult.

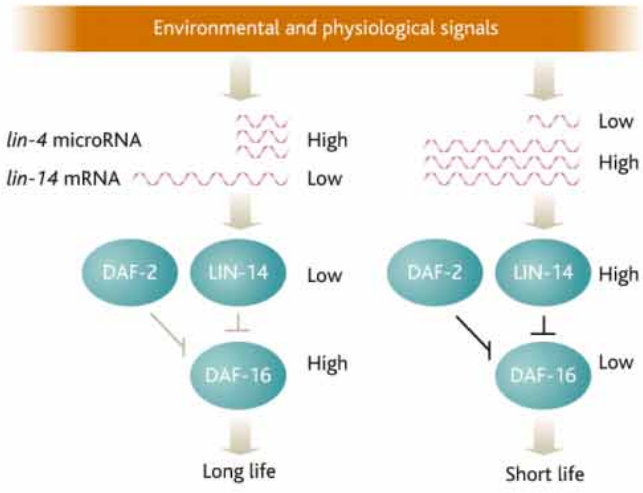

Regulation of adult life span by the *lin-4* microRNA. (Left) When *lin-4* microRNA activity is high, expression of *lin-14* mRNA and protein are low. Hence, the DAF-16 transcription factor is active and promotes long life. **(Right)** When *lin-4* activity is low, *lin-14* activity is high, and DAF-16 is inhibited, resulting in short life. *lin-4* and *lin-14* gene products may work downstream of, or in parallel to, DAF-2 (the insulin-like receptor) to modulate DAF-16. Proteins are depicted as oval shapes.

However, the role of *lin-14* and other heterochronic loci in the adult worm has been little explored, largely because cells of the adult are postmitotic (except for germline cells) and therefore do not display any overt stage-specific cellular programs. Clearly, though, adult animals undergo germline maturation, growth, homeostasis, and metabolic changes, as well as seemingly coordinated shifts in gene expression (*8*). Conceivably, such changes could arise from intrinsic timing mechanisms at work in the adult. Hence, Boehm and Slack sought to test the hypothesis that the heterochronic loci influence adult longevity.

Remarkably, they found that overexpression of *lin-4* microRNA results in a modest increase in adult life span (by 15%), and conversely, that loss of a functional *lin-4* gene shortens life (by 53%). These adult phenotypes, as in larvae, depend on *lin-14*. Worms lacking a functional *lin-14* gene (loss-of-function mutants) were long-lived (by 28%), whereas those that overexpress *lin-14* (gain-of-function mutants) were short-lived (by 63%). In worms lacking both *lin-4* and *lin-14*, the long-lived *lin-14* phenotype largely prevailed (a life span 14% longer than wild type), suggesting that *lin-4* works at least in part through *lin-14*. Similarly, the developmental phenotypes of *lin-14* mutants (precocious) prevail over *lin-4* (delayed) in the *lin-4 lin-14* double mutant worms. The fact that the same epistatic relations hold for *lin-4* and *lin-14* in both the developing larva and aging adult supports the idea that a similar regulatory pathway is at work.

The question then arises as to whether longevity is determined by developmental events or adult events. To address this, Boehm and Slack took advantage of conditional manipulation of *lin-14* expression. By using a temperature-sensitive allele, they bypassed developmental defects and performed shifts to the nonpermissive temperature that caused a decrease in *lin-14* expression in the adult. Interestingly, post-developmental temperature shifts still caused extended life span. Accordingly, decreasing *lin-14* expression by RNA interference in adults also extends life, which suggests a function independent of development and specific for adults. As correlates of longevity, *lin-14* loss-of-function mutants were found to be more resistant to heat stress and slower to accumulate lipofuscin, a marker of aged tissues.

Molecular genetic studies first identified insulin/IGF-1 signaling as a key modulator of nematode life span (*9*, *10*). Remarkably, the same was later shown to be true for flies and mice (*2*). Specifically, decreased insulin/IGF-1 signaling results in the nuclear translocation of a transcription factor called DAF-16/FOXO. This transcription factor turns on genes for stress resistance, DNA repair, innate immunity, and heat shock, and, as a consequence, the worm's life span is doubled.

Given the central role of insulin/IGF-1 signaling in aging, Boehm and Slack asked whether *lin-4* and *lin-14* impinged on this pathway. Indeed, they found that worms with a mutation in *daf-16* as well as in *hsf-1*, a longevity gene encoding a transcription factor for turning on heat shock proteins, abolished longevity mediated by *lin-14*. Moreover, longevity of a worm with a mutation in *daf-2*, the gene encoding the insulin-like receptor, was not further increased by a loss-of-function mutation in *lin-14*. Finally, a short-lived *lin-4* mutation largely suppressed the longevity of the *daf-2*/insulin-like receptor mutant, placing *lin-4* activity downstream or parallel to that of the receptor. These genetic studies argue that *lin-4* and *lin-14* could somehow regulate *daf-16* via insulin/IGF-1 signal transduction or a parallel signaling pathway (see the figure).

The union of signaling pathways that control developmental timing and life span is not without precedent, because the worm nuclear hormone receptor DAF-12 operates in both (*11*). However, if a conserved microRNA and its target converge on DAF-16/FOXO to influence adult longevity, this raises the intriguing notion that intrinsic developmental clocks can modulate aging. Alternatively, *lin-4* and *lin-14* may have undescribed metabolic outputs somewhat independent of a timer. Notably, the heterochronic circuit is initialized by food cues, with nutrient inputs at distinct points of L1 and L3 diapause, periods of arrested development entered under conditions of starvation. In particular, both *lin-4* and *daf-16* are required for entry into the L3 dauer diapause, which is a long-lived stress-resistant stage.

In either scenario, the results of Boehm and Slack raise a myriad of questions. How do *lin-4* and *lin-14* converge on *daf-16*? What tissues are involved? Is this a mechanism of regulation observed in the wild-type worms under some conditions? What other signaling pathway components are involved? Do microRNAs regulate longevity in higher animals? If so, what are they and what are their targets?

Finally, how might the paradox of intrinsic timers and "regulated" aging be reconciled with the evolutionary theories of aging? One possibility is that the tempo of reproductive development needs to be coordinated between the tissues, as well as with nutrient availability and the environment. Under conditions of adversity, regulatory

signaling pathways that delay reproduction and increase somatic endurance could adaptively retard organismal decline. When exercised in the adult, such mechanisms could secondarily extend life. Another notion is that developmental timing mechanisms that determine a species' life plan may somehow influence the life span. Perhaps the great natural variation in animal life spans is determined by such global temporal regulators.

References

1. M. Boehm, F. Slack, *Science* **310**, 1954 (2005).
2. C. Kenyon, *Cell* **120**, 449 (2005).
3. V. Ambros, H. R. Horvitz, *Science* **226**, 409 (1984).
4. R. C. Lee, R. L. Feinbaum, V. Ambros, *Cell* **75**, 843 (1993).
5. B. Wightman, I. Ha, G. Ruvkun, *Cell* **75**, 855 (1993).
6. B. J. Reinhart *et al.*, *Nature* **403**, 901 (2000).
7. A. E. Pasquinelli *et al.*, *Nature* **408**, 86 (2000).
8. S. A. McCarroll *et al.*, *Nat. Genet.* **36**, 197 (2004).
9. C. Kenyon, J. Chang, E. Gensch, A. Rudner, R. Tabtiang, *Nature* **366**, 461 (1993).
10. K. D. Kimura, H. A. Tissenbaum, Y. Liu, G. Ruvkun, *Science* **277**, 942 (1997).
11. B. Gerisch, C. Weitzel, C. Kober-Eisermann, V. Rottiers, A. Antebi, *Dev. Cell* **1**, 841 (2001).

10.1126/science.1122816

CHEMISTRY

Nuclear Spin Conversion in Molecules

Jon T. Hougen and Takeshi Oka

Molecules with identical nuclei having nonzero spin can exist in different states called nuclear spin modifications by most researchers and nuclear spin isomers by some. Once prepared in a particular state, the arrangement of spins can in principle convert to another arrangement. The concept of nuclear spin modifications in molecules (*1*) is intriguing to chemists because interconversion between different spin states is often slow enough to be considered negligible for many purposes. This in turn allows one to treat different spin modifications as though they were different molecules both in terms of spectroscopy and collision dynamics. In addition, these spin modifications are associated one-to-one with different rotational levels in the molecule. In fact, however, the interconversion rates are not zero, so the scientific questions become: How can these extremely slow rates be measured, and how can these rates be explained by theory? On page 1938 of this issue, Sun *et al.* (*2*) present answers to both of these questions in the case of the ethylene molecule.

In the case of hydrogen, it is well known that rotational levels with even and odd J quantum number belong to the *para* (where the nuclear spins are aligned in opposite directions and $I = 0$) and *ortho* (the spins are parallel and $I = 1$) nuclear spin modifications, respectively (I is the total nuclear spin angular momentum of the two H nuclei). Furthermore, nearly pure *para*-H_2 can be readily prepared by cooling hydrogen to low temperature on a paramagnetic catalyst as initially shown by Bonhoeffer and Harteck in 1929 (*3*). Once prepared, a *para*-H_2 sample can be preserved for months at room temperature in a glass container without converting to *ortho*-H_2. This remarkable stability of a single spin modification was ascribed by Wigner to the smallness of the nuclear spin interaction term that mixes *ortho* and *para* states (*4*).

Spin modifications are relevant also for polyatomic molecules with two or more identical and equivalent nuclei. Thus, for example, H_2O, H_2CO, etc., have *ortho* ($I = 1$) and *para* ($I = 0$) species; NH_3, CH_3F, etc., have *ortho* ($I = 3/2$) and *para* ($I = 1/2$) species; and CH_4 has *ortho* ($I = 1$), *meta* ($I = 2$), and *para* ($I = 0$) species. More complicated molecules such as C_2H_4 have more than three spin modifications, and their symmetry is used to label different spin modifications, as reported by Sun *et al.* (*2*). Polyatomic molecules have faster interconversion rates than H_2, not because their magnetic interactions are larger but because their rotational levels are closer. This is particularly true for spherical-top molecules in which levels are clustered and some levels with different spin modifications are very close. Thus, Ozier *et al.* observed a spectrum between *ortho* and *para* CH_4, by shifting an *ortho* level close to a *para* level with a magnetic field, and determined the small mixing term (*5*). For a heavy spherical top like SF_6 with very high rotational level ($J = 53$), the levels are so close that Bordé and colleagues naturally observed transitions between different spin species (*6*).

The theory for spin conversion in polyatomic molecules by collision was first formulated by Curl *et al.*, who enumerated mixing terms in the spirit of Wigner's theory—that is, choosing those nuclear spin interaction terms that are invariant with respect to exchange of the entire sets of nuclear coordinates but are not invariant to exchange of spin coordinates alone (*7*). They identified levels belonging to different spin modifications that are accidentally close and surmised that interconversion occurs through those pairs of levels. The validity of the theory of Curl *et al.* has been demonstrated by a series of beautiful experiments by Chapovsky and his collaborators since 1980. They introduced the method of light-induced drift developed in the former Soviet Union (see the figure) and succeeded in separating *ortho* and *para* species of CH_3F, the first such separation since H_2 and D_2 were separated several decades ago. [Readers are referred to an excellent review by Chapovsky and Hermans (*8*) for more details of history, experiments, and theory of the field.] This is the technique used by Sun *et al.* in their studies.

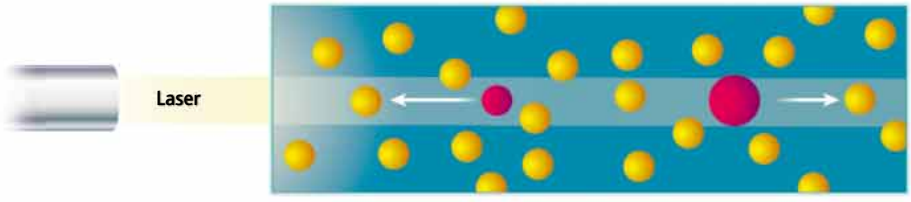

Getting the drift. Laser light tuned slightly below resonance excites a molecule moving away from the laser (red sphere on the right) and increases its size. The molecule is slowed down by collisions with buffer gas because of its larger size. A molecule in the same level moving toward the laser (red sphere on the left), however, is not excited and keeps moving with the normal speed. This causes a net drift toward the laser of molecules with selected spin modification. The increase of the molecular size is greatly exaggerated for clarity. [Adapted from (*8*)]

The exciting aspect of the experiment by Takagi and colleagues. (*2*) is that ethylene, C_2H_4, has symmetry with higher dimension than that of other molecules so far studied,

J. T. Hougen is in the Optical Technology Division, National Institute of Standards and Technology, Gaithersburg, MD 20899–8441, USA. E-mail: jon.hougen@nist.gov T. Oka is in the Department of Chemistry and Department of Astronomy and Astrophysics, The Enrico Fermi Institute, University of Chicago, Chicago, IL 60637, USA. E-mail: t-oka@uchicago.edu

and there are four nuclear spin modifications with different symmetry. This has allowed them to demonstrate yet another subtlety of the interconversion. Because the parity (the symmetry of the wave functions with respect to an inversion in space) is rigorous in atomic and molecular physics, the parity selection rule, unlike the *ortho*/*para* selection rule, should not be violated in these experiments. In other words, the nuclear spin interaction considered by Wigner and enumerated by Curl *et al*. may mix different spin species but cannot mix parity. This is clearly demonstrated in figure 2 of Sun *et al*. (*2*). Figure 2A (*2*) shows that there is an interconversion between the B_{2u} and B_{3u} species, and figure 2B shows that there is no interconversion between the B_{2u} and A_g species. The symbols g and u represent symmetric and antisymmetric states with respect to the molecule-fixed inversion operation, i.e., interchange of two pairs of H nuclei and inversion of space. However, all rotational functions are g with respect to this operation, and thus it turns out for a planar molecule like ethylene that g and u nuclear spin functions are associated with rotational–nuclear-spin wave functions of + and – parity. Thus, $B_{2u} \leftrightarrow B_{3u}$ conversion in ethylene is parity allowed but $B_{2u} \leftrightarrow A_g$ is parity forbidden, as indeed shown in figure 2 of Sun *et al*. (*2*).

This leaves an interesting problem to be solved. The authors should be able to determine the magnitude of the interaction term from the observed interconversion rate. In order to do this, the authors need to locate a pair or pairs of levels with the B_{2u} and B_{3u} symmetry that are accidentally or systematically (*9*) close through which the conversion proceeds. They also need to estimate collision cross sections that are temperature dependent. Experimentally, it will be interesting to measure the temperature dependence of the conversion rate. Also measuring the conversion rate caused by other gases will be interesting, especially paramagnetic gases such as oxygen. It is well known that *para*-H_2 converts to *ortho*-H_2 much faster in the presence of O_2. The mechanism of such conversion must be different from that considered by Curl *et al.*

Which other molecules will be interesting to study? Benzene, C_6H_6, has spin modifications with six different symmetries: A_{1g}, A_{2g}, E_{2g}, B_{1u}, B_{2u}, and E_{1u}. Here also, the molecule is planar, so one might expect that the parity selection rule will be equivalent to g ↔ g and u ↔ u. Because rotational levels in this symmetric-top molecule with $K = 6n$ (where $n \neq 0$) systematically consist of very nearly degenerate B_{1u}-B_{2u} nuclear spin pairs, rotational levels with quantum number $K = 6n + 3$ consist of very nearly degenerate A_{1g}-A_{2g} nuclear spin pairs, and the E nuclear spin functions do not cluster, one can further speculate (*9*) that conversion rates within the nuclear spin A species or within the B species will be much faster than rates between A and E or between B and E species. Ethane, C_2H_6, has spin modifications with seven different symmetries A_1, A_4, E_1, E_2, E_3, E_4, and G. Because the molecular symmetry group of ethane does not have any element corresponding exactly to inversion in space, the connection between symmetry species and parity is more complicated than for the planar molecules mentioned above. One can thus wonder if permutation-inversion symmetry species together with systematic level clustering will in the end provide a more unified way of discussing allowed nuclear spin conversions than parity together with accidental degeneracies does. In any case, a study of nuclear spin conversion rates in other highly symmetric molecules will almost certainly reveal further subtleties of the mechanism. However, the experiments will become more challenging as one goes to heavier molecules because of the larger rotational partition function.

References

1. G. Herzberg, *Molecular Spectra and Molecular Structure* (Krieger, Malabar, FL, 1989), vols. 1 and 2.
2. Z.-D. Sun, K. Takagi, F. Matsushima, *Science* **310**, 1938 (2005).
3. K. F. Bonhoeffer and P. Harteck, *Z. Phys. Chem.* **B4**, 113 (1929).
4. E. Wigner, *Z. Phys. Chem.* **B23**, 28 (1933).
5. I. Ozier, P. Yi, A. Khosla, and N. F. Ramsey, *Phys. Rev. Lett.* **24**, 642 (1970).
6. J. Bordé *et al.*, *Phys. Rev. Lett.* **45**, 14 (1980).
7. R. F. Curl Jr., J. V. V. Kasper, K. S. Pitzer, *J. Chem. Phys.* **46**, 3220 (1967).
8. P. L. Chapovsky, L. J. F. Hermans, *Annu. Rev. Phys. Chem.* **50**, 315 (1999).
9. W. G. Harter, C. W. Patterson, *J. Chem. Phys.* **80**, 4241 (1984).

10.1126/science.1122110

GEOCHEMISTRY

A Tale of Early Earth Told in Zircons

Yuri Amelin

No rock or mineral record has been preserved from Earth's "dark age"—the mysterious time after accretion of the planet about 4560 million years ago. Thanks to a continuous effort to find the oldest pieces of our planet, however, the duration of this unknown era is becoming shorter and shorter. Following the development of modern isotopic dating, the extent of the dark age was established at about 800 to 1000 million years by the discovery of exceptionally old rocks in western Greenland (*1*). The discovery of still older grains of zircon (zirconium silicate, a common if not very abundant component of crustal rocks, and an extraordinarily resilient mineral) in archean sedimentary rocks in Western Australia reduced the dark age to 400 to 300 million years (*2*, *3*) and recently to less than 200 million years (*4*), a mere 5% of Earth's life span. That this was an eventful time is clear from studies of the Moon and Mars, where internally driven magmatism and differentiation ceased quickly or slowed down. We know that the processes that shaped further evolution of these bodies—large-scale mantle differentiation and formation of the primary crust—were occurring within the first few hundred million years.

On page 1947 of this issue, Harrison *et al.* (*5*) report their use of some of the oldest known zircons to explore the prehistory of the source rocks of these minerals. Their approach relies on the slow radioactive decay of the rare isotope ^{176}Lu to ^{176}Hf (half-life 37 billion years). This decay process increases the ratio of ^{176}Hf to other isotopes of hafnium, usually expressed as $^{176}Hf/^{177}Hf$. The rate of growth of the $^{176}Hf/^{177}Hf$ ratio is proportional to the Lu/Hf ratio. In geochemical studies, the $^{176}Hf/^{177}Hf$ ratio in a mineral or rock is expressed as a deviation from this ratio in bulk silicate earth (thought to be broadly similar in composition to, and determined from, chondritic meteorites). This deviation is measured in parts per 10,000 and is denoted as $\varepsilon_{Hf}(T)$, where T is time. When primitive mantle differentiates to form continental crust (a cover of less dense aluminum- and silicon-rich rocks) and depleted mantle (the more dense and refractory magnesium- and iron-rich residue left after extraction of crust-forming melts), the depleted mantle acquires a Lu/Hf ratio several times that found in crustal rocks. As a result, the $^{176}Hf/^{177}Hf$ ratio in the mantle grows faster than in the crust and $\varepsilon_{Hf}(T)$ becomes positive, whereas the complemen-

The author is at the Geological Survey of Canada, Ottawa, Ontario K1A 0E8, Canada. E-mail: yamelin@nrcan.gc.ca

tary crust develops more and more negative $\varepsilon_{Hf}(T)$. When a melt derived from ancient crust or depleted mantle crystallizes and zircon is formed, the $^{176}Hf/^{177}Hf$ ratio in the melt is imprinted in the zircon and remains nearly unchanged over billions of years, owing to the low Lu/Hf ratio and high concentration of Hf in zircon (about 1%). If we measure the present-day $^{176}Hf/^{177}Hf$ and Lu/Hf ratios in the zircon crystal and determine the age of the zircon by decay of uranium isotopes to lead, we can trace the growth of the $^{176}Hf/^{177}Hf$ ratio backward and determine when primitive mantle separated into crust and depleted mantle. Alternatively, if the time of mantle differentiation is estimated independently, we can calculate the Lu/Hf ratios in the crust and depleted mantle, and try to infer the nature of these early Earth reservoirs by comparing these ratios to the Lu/Hf ratios measured in younger rocks of various compositions.

Most $^{176}Hf/^{177}Hf$ values determined by Harrison *et al.* (*5*) are close to or slightly below the primitive mantle evolution line, as would be expected for crustal rocks extracted from the mantle shortly before formation of the zircons. Some of the oldest zircon grains, however, plot well above or below the primitive mantle evolution line and require extreme fractionation of lutetium and hafnium and very early separation of their source rocks from the primitive mantle, probably around 4500 million years ago—less than 100 million years after the accretion of Earth. This result is interpreted by the authors as evidence for large-scale mantle differentiation and possibly an onset of plate tectonic activity between 4500 and 4400 million years ago. Whether the plate processes operated on a global scale or locally remains to be determined.

The report by Harrison *et al.* opens up many new questions. The first is the possibility that $\varepsilon_{Hf}(T)$ in zircon can be erroneously high or low if the zircon crystal includes domains that grew at different times (see the figure). Coexistence of domains with different ages within one crystal, very common in zircon, is the opposite side of the exceptional resistance of this mineral. If a zircon gets into magma, new layers can grow around the original crystal. The new zircon layer can have a chemical and isotopic composition different from the composition of the original crystal. Because the concentration of uranium and radiogenic lead (the decay product of uranium) can be quite different between the two domains while the concentration of hafnium remains relatively constant, the ages of the two components in a complex zircon crystal do not mix in the same proportion as their hafnium isotopic ratios. The $^{176}Hf/^{177}Hf$ ratio in zircon is arrested because of low Lu/Hf, but the $^{176}Hf/^{177}Hf$ in the reference reservoir (primitive mantle) evolves more rapidly. Hence, the use of a wrong age produces an erroneous $\varepsilon_{Hf}(T)$ that can mimic mantle differentiation. To avoid this problem, we need to study the internal structure and age distribution in ancient zircon in great detail. More reliable hafnium isotope data could be obtained from crystal domains that are shown to be homogeneous. However, analysis of these small crystal domains produces less precise data. Further progress in early Earth studies thus requires more sensitive and precise mass spectrometers for measuring $^{176}Hf/^{177}Hf$ ratios.

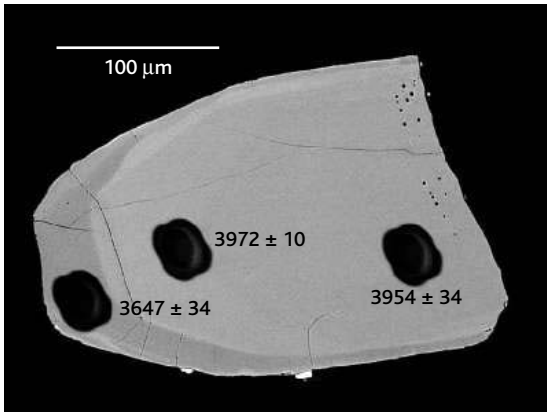

Messenger from an early era. This zircon crystal from Jack Hills, Western Australia (length 0.3 mm) contains a rim that is younger than the central part by 300 million years. The brightness in this image, taken in backscattered electrons, reflects the difference of average atomic mass (heavier is brighter) due to variable concentration of hafnium, uranium, thoriuim, and rare earth elements—the most common minor components of zircon. The ages (in millions of years) were determined by SHRIMP (sensitive high-resolution ion microprobe) U-Pb analysis, similar to the dating technique of Harrison *et al.* (*5*). (The black spots are sites of the ion microprobe analyses, where the charge-dissipating gold coating was removed by ion bombardment.)

CREDIT: P. HUNT/GEOLOGICAL SURVEY OF CANADA

A fundamental uncertainty is whether the bulk silicate Earth indeed has the same Lu/Hf and $^{176}Hf/^{177}Hf$ ratios as the accepted reference that is based on analyses of chondrites. Recent discovery of a difference in the Sm-Nd isotopic system (a geochemical cousin of Lu-Hf) between chondrites and Earth (*6*) raises the possibility that our planet and undifferentiated asteroids (the source of chondritic meteorites) were assembled from different reservoirs of matter that never completely mixed with each other. Moreover, the Lu/Hf ratios in chondrites are variable (*7*, *8*), and this makes choosing the accurate reference value for the bulk Earth even more difficult. The choice of bulk silicate Earth parameters would not change the spread of the earliest hafnium data, but it would change the proportion of those that show enriched crustal versus depleted mantle signatures. It also affects the mass balance of known reservoirs in the present-day Earth. Currently accepted parameters imply that these reservoirs are not in balance, which suggests either that the parameters are wrong or that there is an unknown reservoir that has sequestered lutetium and hafnium. Thus, the key to understanding the evolution of Earth's mantle and continents over time is establishing the precise chemical connection among Earth, meteorites, and the solar system as a whole, represented by the composition of the solar photosphere (*9*).

A final and perhaps most intriguing question is the mechanism whereby the signatures of extreme differentiation in the mantle-crust system during the first 500 million years were almost completely erased. Although there is some evidence for early differentiation in the oldest rocks, the average $^{176}Hf/^{177}Hf$ evolution curve defined by most mantle-derived rocks over the rest of Earth's history diverges from the chondritic curve at about 4 billion years, which is when the rock record begins (*10*). Something reset the clock on a planetary scale. On the basis of the lunar record, a period of massive meteorite bombardment is thought to have occurred at that time. If so, it must have induced homogenization of mantle and crust on a scale vastly greater than can be explained by recent plate tectonic processes. We are indeed fortunate that the fragmented memory of an earlier time has survived in the form of zircon crystals.

References and Notes

1. L. P. Black *et al.*, *Earth Planet. Sci. Lett.* **12**, 245 (1971).
2. D. O. Froude *et al.*, *Nature* **304**, 616 (1983).
3. W. Compston, R. T. Pidgeon, *Nature* **321**, 766 (1986).
4. S. A. Wilde, J. W. Valley, W. H. Peck, C. M. Graham, *Nature* **409**, 175 (2001).
5. T. M. Harrison *et al.*, *Science* **310**, 1947 (2005); published online 17 November 2005 (10.1126/science.1117926).
6. M. Boyet, R. W. Carlson, *Science* **309**, 576 (2005); published online 16 June 2005 (10.1126/science.1113634).
7. M. Bizzarro *et al.*, *Nature* **421**, 931 (2003).
8. P. J. Patchett *et al.*, *Earth Planet. Sci. Lett.* **222**, 29 (2004).
9. E. Anders, N. Grevesse, *Geochim. Cosmochim. Acta* **53**, 197 (1989).
10. J. D. Vervoort, J. Blichert-Toft, *Geochim. Cosmochim. Acta* **63**, 533 (1999).
11. Some ideas discussed in this paper were kindly contributed by D. W. Davis, Geology Department, University of Toronto. The text was also improved by his comments and by comments from W. J. Davis, Geological Survey of Canada.

10.1126/science.1121536

Richard E. Smalley (1943–2005)

W. Wade Adams and Ray H. Baughman

Richard Errett Smalley, who died on 28 October 2005 after a 7-year fight with cancer, unselfishly used his stature and wisdom to inspire a worldwide nanotechnology revolution. His breakthroughs, his inexhaustible enthusiasm for exciting young people about science, and his awakening the world to possible nanotech solutions to the energy crisis have all left an enduring legacy. In only 40 years of applying his powerful intellect to science and technology, his work led to entirely new types of materials and fields of study, revolutionary apparatus for scientific investigations and commercialization, and a deep understanding of behavior on nano and molecular scales. Along the way he shared the 1996 Nobel Prize in Chemistry for codiscovering the soccer-ball shaped C_{60} fullerene molecule.

Born in Akron, Ohio, on 6 June 1943, Smalley's interest in science began in his early teens as he and his mother collected single-cell organisms from a local pond and studied them with a microscope. He learned from his father how to build and fix mechanical and electrical equipment and from his mother mechanical drawing, so that he could be more systematic in design work. Many decades later, Rick's passion for creative design was still evident on his office walls—diagrams showing his most recent improvements on equipment for producing carbon nanotubes. Although his contributions to physics and engineering were landmarks, chemistry was his first love. The detailed periodic table of the elements that he drew on rafters in the attic where he studied as a youngster marked his early fascination with chemistry.

He pursued this love, from undergraduate studies at Hope College and the University of Michigan to the Shell Chemical Company, where he worked as a quality control chemist in a polypropylene plant. Rick said, "These were fascinating days, involving huge volumes of material, serious real-world problems, with large financial consequences." He learned about industrial-scale processes and the importance of efficient catalysts, which were useful much later when he initiated scale-up of carbon nanotube synthesis. After 4 years, he resumed academic studies and earned his Ph.D. in 1973 from Princeton University, focusing on the chemical physics of condensed phase and molecular systems with thesis adviser Elliott Bernstein.

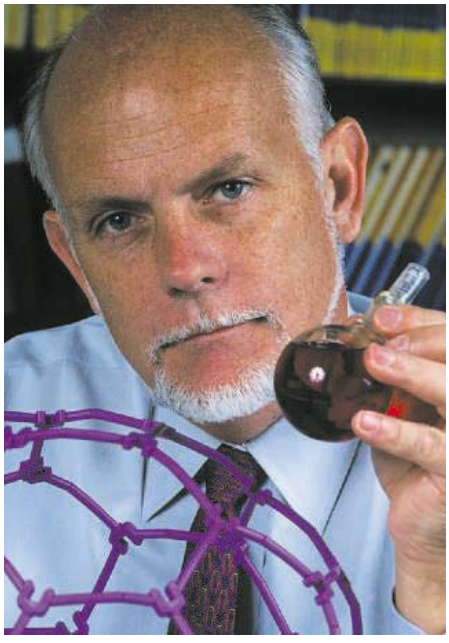

During postdoctoral study with Donald Levy and Lennard Wharton of the University of Chicago, and later with Daniel Auerbach, Rick helped develop a powerful technique: supersonic beam laser spectroscopy. As a result, chemical physicists can now drastically simplify the spectroscopy of complex molecules. Using the coldest part of the expanding gas, researchers could achieve temperatures below 1 K, thereby freezing the rotations of moderate-sized molecules and complexes. After joining the faculty of Rice University in 1976, Smalley worked together with Robert Curl to produce a sequence of pioneering advances applicable for making and characterizing very cold supersonic beams of large molecules, radicals, and atomic clusters having precisely known numbers of atoms.

In August 1985, Smalley and Curl were joined by Harold Kroto from the University of Sussex for a short summer project to study interesting carbon cluster distributions found by Andrew Kaldor at Exxon using an apparatus constructed by Smalley's group. After a legendary late night of taping together cardboard cutouts of hexagons and pentagons on his kitchen table, using Kroto's insights into the importance of five-carbon rings, Smalley presented the carbon "soccer ball" as the only sensible way that 60 carbon atoms could be assembled to produce the observed spectra. A new field of scientific investigation was thus born, and then fueled by a seemingly continuous barrage of exciting new results from both Rick's laboratory and others across the world, which showed the diversity of carbon cage types, how their production could be scaled up, the diverse ways they can be modified, and their novel physical and chemical properties.

In 1993, Rick redirected much of his group's work to carbon nanotubes, which can be viewed as cylindrical versions of the carbon cage molecules, and Rick and his co-workers became leaders in the field. His experimental skills were again critical as his team developed the laser ablation and the high-pressure carbon monoxide processes for making single-walled carbon nanotubes. Rapid worldwide scientific progress was assisted by Rick's providing access to these high-quality nanotubes, first through a nonprofit effort at Rice University, and then through the successful company he founded in 1999, Carbon Nanotechnologies, Inc.

Many call Rick the grandfather of nanotechnology. He was the most cited author in nanotechnology in the last decade, and his pivotal scientific and technological breakthroughs have inspired worldwide commercialization efforts. Because of Rick's key role in creating the National Nanotechnology Initiative, he was the only academic invited to the November 2003 Oval Office signing ceremony. His vision of using nanotechnology to help solve the energy crisis and to improve health through nanomedicine is motivating governments to fund effective programs. Many will dedicate themselves to a goal that Rick focused upon during his last 4 years of life: a carbon nanotube quantum wire cable much stronger than steel that would carry a current 10 times as high as that carried by copper wire and weigh one-sixth as much.

With his passing, the world lost a great intellect in chemistry, physics, and engineering, but we also lost a great advocate for science and technology and a great educator and mentor. Robert Curl said that "Rick was a visionary, and his charisma and logic made those he worked with buy into the vision. Rick convinced us that we could be better, stronger, and take more chances if we just tried. I hope that we don't forget—then his legacy…will make a lasting transformative difference." In his humble way, Rick simply said that science and life go on.

W. W. Adams is at the Center for Nanoscale Science and Technology, Rice University, Houston, TX 77251–1892, USA. E-mail: wade.adams@rice.edu
R. H. Baughman is at the NanoTech Institute, University of Texas at Dallas, Richardson, TX 75080, USA. E-mail: ray.baughman@utdallas.edu

10.1126/science.1122120

edited by Edward W. Lempinen

PROFILE

Holdren: Expand S&T Efforts to Meet Urgent Global Challenges

John P. Holdren is an expert on global environmental change, energy technology and policy, international science diplomacy, and nuclear arms control and nonproliferation. He has been a physicist, a professor, and a White House adviser, and he delivered the 1995 Nobel Peace Prize acceptance speech on behalf of the Pugwash Conferences on Science and World Affairs.

John P. Holdren

In February, when he assumes the presidency of AAAS, he hopes to bring his broad multidisciplinary vision and experience to bear on some of the most urgent problems facing humanity.

"I believe strongly in the power of partnerships, across institutions, sectors, and countries, for addressing the great challenges at the intersection of science and technology with the human condition—the challenges of poverty, disease, weapons of mass destruction, environmental impoverishment, climate change, terrorism, and more," Holdren said recently. "I also believe strongly in the power of education—of students, of professionals, of publics, of policy-makers—in increasing the capacity of society to meet and surmount these challenges."

Holdren, 61, is director of the Woods Hole Research Center, as well as Teresa and John Heinz Professor of Environmental Policy and director of the Science, Technology and Public Policy Program at Harvard University. He served as a member of President Bill Clinton's Committee of Advisors on Science and Technology from 1993 to 2001.

From an early age, Holdren remembers, he was equally fascinated with the natural world, with technology, and with people. As a high school student, he became persuaded "that many of the most interesting and important challenges facing the world—among them overpopulation, poverty, hunger, and weapons of mass destruction—could be solved only by combining insights from the natural sciences and technology with perspectives and approaches from the social sciences and the humanities."

This idea set him on a course to MIT, Stanford, Livermore, Caltech, the University of California-Berkeley, and Harvard, and helped position him for a career of remarkable influence at the intersection of science, technology, and society.

Holdren's MIT and Stanford degrees were in aeronautics and astronautics and plasma physics. In 1973 he co-founded the interdisciplinary graduate program in Energy and Resources at Berkeley, which he co-led until 1996. Since moving to Harvard that year, his work has focused on the causes and consequences of global climate change, challenges, and opportunities with advanced energy technologies and international cooperation to address problems of environment, development, and security.

He is a member of the National Academy of Sciences, the National Academy of Engineering, the American Academy of Arts and Sciences, and the Council on Foreign Relations, and is co-chair of the bipartisan, foundation-funded National Commission on Energy Policy.

Holdren was first invited to the Pugwash Conference in 1973, joining some of the world's leading thinkers for discussions about nuclear arms reductions and cooperative solutions for global problems. He was chair of the Pugwash executive committee when the organization won its Nobel, and he was chosen by his colleagues to give the acceptance speech.

He used the occasion to explore the connections between poverty, energy, environment, and security: "Either we will achieve an environmentally sustainable prosperity for all, in a world where weapons of mass destruction have disappeared or become irrelevant, or we will all suffer from the chaos, conflict, and destruction resulting from the failure to achieve this."

Holdren will assume the presidency of AAAS at the close of the Annual Meeting in St. Louis, Missouri, on 20 February, replacing Gilbert S. Omenn, who will become chairman of the AAAS Board of Directors.

In his candidacy statement, Holdren praised AAAS's diverse and wide-ranging programs at the intersection of science and technology with public policy. At the same time, he urged further strengthening of all of these efforts, arguing that as productive as the efforts of American science and engineering societies have been, they are still "not remotely commensurate with the challenges."

Above all, he said in the statement, "AAAS should continue and expand its efforts…to promote a more vigorous national discussion about the links between S&T and the human condition, and about the responsibilities of scientists and technologists and of government to work more thoughtfully and effectively to increase the societal benefits from S&T and to reduce the liabilities."

2006 ANNUAL MEETING

Evolution Event Will Rally Support for U.S. Teachers

The campaign against the teaching of evolution has put many public school science teachers in a difficult position: They want to teach science and preserve the integrity of science, but they sometimes risk objections and protests from students, parents, or school board members.

In collaboration with the National Research Council and many other leading U.S. scientific associations, AAAS is organizing a half-day special event at its upcoming Annual Meeting in St. Louis to give science teachers a voice on the issue and to give them aid in their schools and communities.

"Evolution on the Front Line," set for Sunday afternoon 19 February, will feature talks by the Rev. George Coyne, a Jesuit priest and director of the Vatican Observatory; U.S. Rep. Russ Carnahan of Missouri; and Linda Froschauer, president-elect of the National Science Teachers Association (NSTA). Teachers have been invited to talk about the pressures they face and the support they would like to receive from the U.S. science and technology community.

"K–12 teachers are the front line of efforts to preserve the integrity of science and evidence-based understanding of the physical and biological world. They are its unsung heroes," said AAAS President Gilbert S. Omenn. "We and they recognize how important math and science at all levels are to preparing our students for a knowledge-based, globally competitive economic future. We also respect the importance of religion and spirituality—in the home and places of

worship. Many teachers have told us that they would welcome help. We want to hear about their successes and stresses, share ideas, and offer them all the support we can."

The battle over evolution and the integrity of science has flared recently in at least 33 states, according to the National Center for Science Education, with Pennsylvania, Kansas, and Georgia most prominent among them. A 2005 NSTA survey indicated that nearly a third of teachers feel pressured to include creationism, intelligent design, or other nonscientific evolution alternatives in their science classrooms; a similar number reported pressure to de-emphasize or omit evolution.

Ray Cummings, who taught biology for 11 years in St. Louis public high schools before going on leave last year, said the pressure against evolution has become more acute in recent years, making teachers' jobs more difficult. Since students often come to class with a strong faith-based explanation for life's origins and development, the art of a teacher's work is in respecting students' beliefs while teaching them science and the scientific method.

"I'm a person of faith, but it doesn't mean that I've abandoned my faith because I can explain and accept the science of evolution," said Cummings, currently vice president for political education–St. Louis Teachers & School Related Personnel Union Local 420–American Federation of Teachers.

The AAAS Annual Meeting—the biggest general science meeting in the world—will bring thousands of scientists, educators, journalists, and others to St. Louis from 16 to 20 February. The Sunday evolution forum is considered especially important in light of events in neighboring Kansas and other heartland areas.

Carnahan is slated to give the keynote address. Froschauer, an eighth-grade teacher from Westport, Connecticut, will speak on the scope of the challenge facing public school teachers and administrators. *New York Times* science writer Cornelia Dean will moderate a panel of scientists who will explore teachers' questions on evolution facts and fiction. Omenn, professor of medicine, genetics, and public health at the University of Michigan, will moderate the event.

The evolution session will be tailored especially for St. Louis–area teachers, but is expected to attract educators from around the country. For example, the Geological Society of America (GSA) is underwriting travel expenses to St. Louis for science teachers from Dover, Pennsylvania; Cobb County, Georgia; and other hot spots.

"Members of the Geological Society of America understand very well the critical importance of teaching evolution and maintaining the integrity of the definition of science," said GSA Executive Director John W. Hess. "As a scientific society that includes K-12 teacher members, we are committed to supporting efforts that encourage the very best in science education."

For more information, see www.aaasmeeting.org/evolution.

SCIENCE COMMUNICATION

Study Probes "Open Access" and Scholarly Publishing

Open access journals are changing the landscape of scholarly publishing, but an ambitious new study suggests that with 40% of them operating in the red, the future of the no-subscription journals is uncertain.

"The Facts About Open Access," cosponsored by the AAAS Project on Science and Intellectual Property in the Public Interest (SIPPI), is the most comprehensive study to date on the revolution that is unsettling the world of traditional, subscription-based journals while attracting interest from some scholars and government officials.

Backed by data from extensive surveys and interviews, the report concluded that more than 1000 journals now embrace the philosophy that scientific and medical information should be provided freely to readers. Many, however, are struggling to attract authors and make ends meet. At the same time, open-access and online publishing generally are forcing traditional journals to address fundamental financial and philosophical challenges.

"Business models are changing," the report said. "Access models are changing. Experimentation is the order of the day."

Mark S. Frankel, co-director of AAAS's SIPPI Project, which helped fund and coordinate the study, acknowledged that it provides only a snapshot of a rapidly changing landscape.

Still, Frankel said, "Policy, whether made by government or the science journal community, should not rest merely on anecdotes, yet that has been the case. This study offers an initial foundation on which to make informed decisions about the future of journal publishing in science."

Other sponsors of the study were the Association of Learned and Professional Society Publishers and HighWire Press; the Association of American Medical Colleges also provided data. The full report is available at www.alpsp.org.

SCIENCE JOURNALISM

Winning Stories from the Universe of Science

Stories spanning the realm of nature—from cosmology and climate to extinct Siberian mammoths—were named winners in AAAS's prestigious Science Journalism Awards for 2005.

Large Newspaper (Circulation >100,000): Dennis Overbye, *The New York Times,* for "String Theory, at 20, Explains It All (or Not)," 7 December 2004; "Remembrance of Things Future: The Mystery of Time," 28 June 2005; and "The Next Einstein? Applicants Welcome," 1 March 2005.

Small Newspaper (Circulation <100,000): Richard Monastersky, *The Chronicle of Higher Education,* for "Women and Science: The Debate Goes On," 4 March 2005; "The Hidden Cost of Fish Farming," 22 April 2005; and "Come Over to the Dark Side," 3 June 2005.

Magazine: Elizabeth Kolbert, *The New Yorker,* for "The Climate of Man," 25 April 2005; 2 May 2005; 9 May 2005. And Atul Gawande, *The New Yorker,* for "The Bell Curve," 6 December 2004.

Television: Joseph McMaster, Martin Williams, Lara Acaster, and Alex Williams, NOVA-WGBH, for "The Wave that Shook the World," 29 March 2005.

Radio: John Nielsen, National Public Radio, for "Dolphin Necropsies," 21 March 2005.

Online: Daniel Grossman, wbur.org, for "Fantastic Forests: The Balance Between Nature & People of Madagascar," 3 June 2005.

Children's Science News: Elizabeth Carney, Scholastic's *SuperScience,* for "Mammoth Hunters," March 2005.

The awards are sponsored by Johnson & Johnson Pharmaceutical Research & Development, L.L.C. The competition attracted 386 entries, including 69 in the new children's category—32 of them from international reporters.

EARL LANE CONTRIBUTED TO THIS REPORT.

Appendage Regeneration in Adult Vertebrates and Implications for Regenerative Medicine

Jeremy P. Brockes* and Anoop Kumar

The regeneration of complex structures in adult salamanders depends on mechanisms that offer pointers for regenerative medicine. These include the plasticity of differentiated cells and the retention in regenerative cells of local cues such as positional identity. Limb regeneration proceeds by the local formation of a blastema, a growth zone of mesenchymal stem cells on the stump. The blastema can regenerate autonomously as a self-organizing system over variable linear dimensions. Here we consider the prospects for limb regeneration in mammals from this viewpoint.

The goal of regenerative medicine is to restore cells, tissues, and structures that are lost or damaged after disease, injury, or aging. The current approaches are influenced by our understanding of embryonic development, of tissue turnover and replacement in adult animals (*1*–*3*), and by tissue engineering and stem cell biology (*4*). The regeneration of organs and appendages after injury occurs in diverse animal groups and provides another important viewpoint, in addition to the demonstration that complex adult tissues can be rebuilt. The lessons of biological regeneration have not been extensively assimilated, in part because this attribute appears remote and exceptional from a mammalian perspective. This Review is concerned principally with lessons from regeneration in salamanders, the species of adult vertebrates that possesses the most extensive abilities (*5*, *6*). We identify three properties of regeneration in salamanders—autonomy, scaling, and plasticity—and discuss some of the cellular and molecular mechanisms underlying them. It may be desirable to implement these properties in the context of mammalian regeneration.

Regenerative medicine currently uses three approaches (Fig. 1) (*4*): the implantation of stem cells to build new structures, the implantation of cells pre-primed to develop in a given direction, and the stimulation of endogenous cells to replace missing structures. Each of the different aspects identified in the first two examples—the generation of an appropriate cohort of regenerative cells, their regulated division and differentiation, and the restoration of the appropriate part of the structure—must be evoked from endogenous cells in the third approach. These processes operate in adult animals that regenerate, and in addition, the regenerative response must be initiated by signals responsive to tissue injury or removal. One candidate signal in salamanders is the local activation of thrombin, a regulator of hemostasis and other aspects of the response to injury, as well as an activator of S phase (the phase of chromosome replication) reentry in differentiated cells (*7*–*9*).

A salamander can regenerate its limbs and tail, upper and lower jaws, ocular tissues such as the lens and retina, the intestine, and small sections of the heart (*10*–*13*). The various contexts for regeneration do not present an equivalent degree of difficulty. To restore the intricate and discontinuous pattern of the vertebrate limb is a different proposition from replacing a patch of cardiac tissue in the ventricle. Nonetheless, recent efforts at tissue engineering of heart muscle have underlined that even in the heart, it is quite challenging to achieve an appropriate vascular and electromechanical integration after implantation (*14*). The salamanders are unusual among adult vertebrates in their ability to regenerate an entire limb from a blastema, and this property is a particular focus here. Regeneration of the digit tip in fetal mammals does not proceed from a blastema but rather from progenitor cells in the nail bed (*15*). The limb blastema consists of a mound of mesenchymal stem cells at the end of the stump (Fig. 2A). The critical questions for research into limb regeneration are concerned with the blastema, and its properties offer a distinct perspective for regenerative medicine.

Autonomy of the Blastema

If a blastema is removed from its limb by transection at the amputation plane and is transplanted to an appropriate location, such as the anterior chamber of the eye or a tunnel bored in the connective tissue of the dorsal fin (Fig. 3A), then it forms a normal regenerate (Fig. 3B) (*16*, *17*). The blastemal cells derived after amputation at any level on the proximodistal (PD) axis give rise precisely to the distal structures—wrist-level cells regenerate a hand, shoulder cells regenerate an arm. This property is stably expressed by blastemas transplanted to the fin or eye and is called positional memory. The limb blastema, as illustrated in Fig. 2A, is a self-organizing system that is independent of any templating or inductive activities from the limb stump (*18*). The significance of this property can be illustrated by contrasting different strategies for the repair of a bone lesion resulting in a gap. The approach of tissue engineering depends on the implantation of a scaffold seeded with appropriate stem cells (Fig. 3C) (*19*, *20*). The salamander has no mechanism for local tissue regeneration of such a gap, but if the limb is amputated at an appropriate level, the blastema will reconstruct the distal skeletal elements (Fig. 3D). This outcome is independent of the presence of elements proximal to the amputation plane, as expected from blastemal autonomy (*21*). This property is a tantalizing one for attempts to regenerate complex structures in mammals, because it suggests that the isolation or engineering of a cell functionally

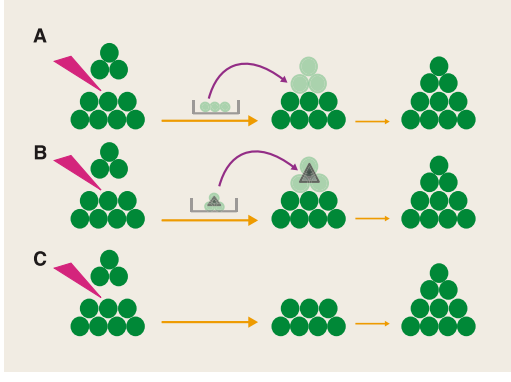

Fig. 1. Schematic of three approaches to regenerative medicine. (**A**) Implantation of stem cells (light green) from culture leads to the restoration of the structure. (**B**) Stem cells are provided with a scaffold (triangle) in order to guide restoration. (**C**) The residual cells of the structure are induced to make a regenerative response.

Department of Biochemistry and Molecular Biology, University College London, Gower Street, London WC1E 6BT, UK.

*To whom correspondence should be addressed. E-mail: j.brockes@ucl.ac.uk

equivalent to a salamander blastemal cell could obviate the necessity for much further intervention. What are the mechanisms that endow the limb blastema and its cells with this ability?

Blastemal cells are derived by dedifferentiation from adult mesenchymal cells at the plane of amputation, and they derive critical cues about their identity and potentiality from their precursors. Such cues include limb identity, and indeed when regenerative cells are transplanted between different tissue contexts in the salamander, they retain their original identity (*18*, *22*). The regenerative territories for forelimb, hindlimb, and tail identity have been mapped by inserting a peripheral nerve branch into the vicinity of a superficial wound at different locations on the body and observing the identity of the resulting appendage (*23*). The retention of such specification in adult differentiated cells may be one major step for the loss of regenerative ability in other vertebrates. The most striking example of local cues in blastemal cells is the specification of transverse and PD axial identity in limb regeneration (*24*, *25*). Positional memory is a critical aspect for the autonomy of limb regeneration, because it specifies the initial population of blastemal cells in relation to the extent of the axis to be regenerated. An understanding of its molecular basis is generally important for our appreciation of how stem cells are specified to give rise to different structures, rather than to different cell types.

When blastemal cells from different PD levels are juxtaposed in experimental configurations, this leads to the activation of cell division, movement, and adhesion (*26*, *27*). This mechanism operates even when single cells or small groups of cells in a distal location are respecified to a more proximal identity and then relocated over the distances characteristic of an adult salamander limb (*28*, *29*). The view that limb morphogenesis is driven by local differences between cells (*30*) has led to the hypothesis that PD identity is encoded by a molecule or molecules at the cell surface, possibly as a graded level of expression along the PD axis. This is consistent with the ability of retinoic acid (RA) and precursor retinoids such as vitamin A to respecify distal blastemal cells to a more proximal identity. Such respecification from wrist to shoulder levels occurs continuously over a 2.5-fold range of retinoid concentration, suggesting that the differences in gene expression that underlie PD identity may be relatively small (*31*, *32*).

These considerations have led to the identification of *Prod 1*, a gene that is regulated by PD location and RA. *Prod 1* encodes a small protein that is linked to the cell surface by a glycosylphosphatidylinositol (GPI) glycolipid anchor (*33*). It is apparently the newt ortholog of mammalian CD59, as evidenced by the prediction of secondary structure. The difference in expression at mRNA and protein levels is shown for mid-humerus and mid-radius blastemas, as well as for the gradient of expression in the normal limb (Fig. 4, A to C). The CD59 protein in mammals is associated with the inhibition of the terminal phase of complement activation, and it is also able to mediate activation of intracellular nonreceptor tyrosine kinases (*34*–*36*). When proximal and distal blastemas are confronted in culture (Fig. 4, B and C), the proximal member reproducibly engulfs the distal, and engulfment is selectively blocked by two antibodies against the protein Prod 1 (*33*). Compelling evidence for its relevance to PD identity has come from electroporating a Prod 1 expression vector into distal cells of the limb blastema of the larval axolotl. Whereas labeled cells in control blastemas maintain their distal location and give rise to tissues in the regenerated hand, labeled cells in the contralateral blastema receiving the Prod 1 vector relocate and contribute to the upper arm (Fig. 4D) (*28*). Taken together, the evidence suggests that Prod 1 is a cue for local cell identity that is expressed in the normal limb and persists in blastemal cells. Questions remain as to which extracellular and surface ligands may interact with it and how it mediates cell interactions based on differences in expression between neighbors. We have suggested that neighbors may titrate the relative expression of Prod 1 by homophilic adhesion between cells, leaving spare Prod 1 molecules on the proximal cell to interact with ligand (*33*). This mechanism may dictate the extent of growth, movement, and adhesion during patterning and hence define the morphogenetic autonomy of the blastema.

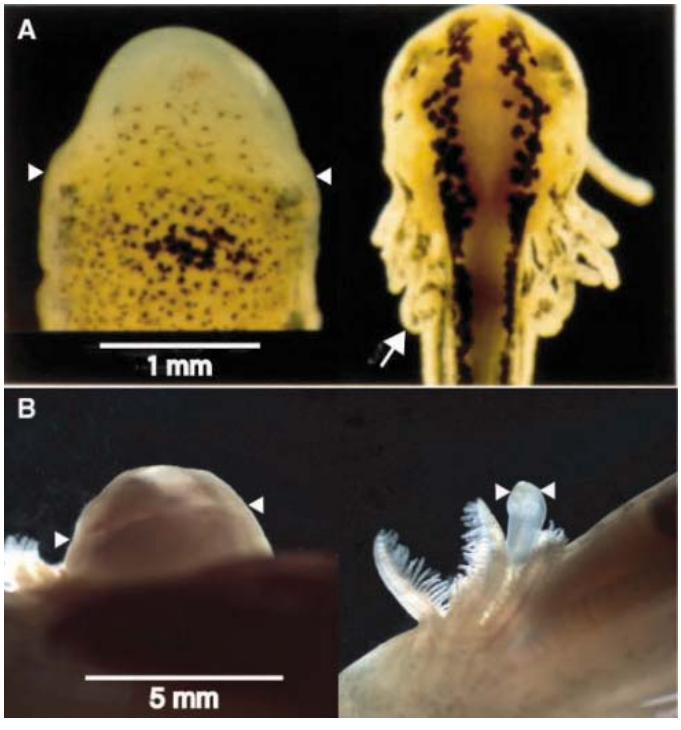

Fig. 2. Scaling differences in limb regeneration and development. (**A**) An adult newt (*Notophthalmus viridescens*) limb blastema (left) (arrowheads mark the original plane of amputation) next to a newt embryo (right) showing the developing limb bud (arrowed). The specialized epithelium surrounding the blastema is called the wound epidermis. (**B**) An adult axolotl limb blastema (left) (from an animal 16 cm in length) next to a 4-cm larval axolotl limb blastema (right) (arrowheads mark the amputation plane). The scale bars apply to the pair of (A) or (B) images, respectively.

Scale of Regeneration

There can be a major difference in the scale of limb development and adult limb regeneration (Fig. 2A), or of larval and adult limb regeneration (Fig. 2B). The difference in the time taken to generate the limb between members of each pair is only about twofold. In larger axolotls, there is a tendency for the cross-sectional area of the blastema to be smaller than the stump from which it arose (*37*); but nonetheless, regeneration can occur on a scale close to that of the limb bud or on the scale of an adult limb with a linear dimension that can be 10-fold greater. This property is important, because it would be inappropriate to regenerate a larval limb on an adult stump, but the mechanisms underlying it are not fully understood. One aspect of developmental mechanisms that is particularly hard to reconcile with scaling is the activity of morphogens, in particular, the principle that spatial localization can be derived from an extracellular diffusion gradient in conjunction with concentration thresholds (*38*, *39*). It seems difficult to implement this principle in the context of an adult limb, and historically, this has led to a substantial divergence in the mechanisms proposed for limb development and regeneration.

These differences between development and regeneration can be accommodated by recent findings in relation to the activity of RA on the PD axis and of sonic hedgehog (Shh) in digit specification on the anteroposterior (AP) axis. It has been proposed that an RA gradient operates in mouse limb development as a consequence of its synthesis near the midline of the animal and its degradation by the product of the *Cyp 26* gene, expressed at the distal end of the limb bud (*40*). If this mechanism

operates in salamander development, it apparently leads to a stable gradient of expression of *Prod 1*/*CD59* in the adult limb, as discussed above (Fig. 4A), so that regeneration may converge with development at a stage after the action of a putative extracellular gradient of RA. In the case of Shh, there is evidence that it is required in regeneration just as in development, because misexpression at the anterior margin of the axolotl blastema or treatment with the antagonist cyclopamine give the same phenotypes as the chick or mouse limb bud (*41*, *42*). Digit identity may depend on the time of exposure to Shh as cells move away from the source and their responsiveness is regulated, as opposed to a spatial gradient of Shh protein (*43*, *44*). These remarks are directed at the derivation of tissue pattern in the regenerate from extracellular concentration gradients, but not at the activity of diffusible ligands in general. The division of blastemal cells is dependent on signals provided initially by regenerating axons that ramify throughout the blastema (*45*–*47*) and later by the wound epidermis, a transient structure that surrounds the early regenerate (Fig. 2A) (*48*).

Plasticity of Differentiated Cells

One contribution to a mechanism that is able to operate at different scales is the founder population of blastemal cells, which is recruited from differentiated mesenchymal cell types across the amputation plane. The plasticity of differentiated cells is a notable feature in different contexts of non-neural regeneration in salamanders, but this term encompasses a range of phenomena (*49*). The regeneration of sections of the adult heart depends on the ability of cardiomyocytes to reenter the cell cycle in the vicinity of the lesion (*50*). Dissociated cardiomyocytes from the adult newt ventricle reenter S phase in culture, and about a third of the cells progress through mitosis and may enter successive cell divisions, in contrast with their mammalian counterparts. This is accomplished without major loss of differentiated properties, and cells promptly resume beating after cytokinesis (*51*). In lens regeneration, pigment epithelial cells at the dorsal margin of the iris reenter the cell cycle after removal of the lens, lose their pigmentation, and transdifferentiate into lens cells (*52*–*54*). In limb and tail regeneration, multinucleated myotubes or striated myofibers undergo cellularization to give rise to mononucleate progeny that resume division (*55*–*58*). In experiments where cultured myotubes are labeled by selective microinjection or by retroviral integration and then implanted into the limb blastema, transdifferentiation to labeled chondrocytes occurs only at a frequency of about 0.1% of mononucleate cells. The nuclei in multinucleate muscle cells may also reenter S phase, although this is apparently not required for cellularization to occur (*59*, *60*). The range of responses shown by these three cell types could occur for different mesenchmal cell types recruited into the limb blastema. For example, a critical contribution to tissue patterning comes from the connective tissue fibroblasts of the dermis, and the degree of change in their differentiated status is still unclear (*61*, *62*).

The plasticity of differentiated cells presents an interesting alternative to the familiar perspective for mammalian regeneration based on embryonic and adult stem cells. Salamanders can sustain an indefinite number of successive cycles of limb regeneration, and the renewable unit is the combination of a differentiated cell type and its derivative blastemal cell (or several cells for multinucleate muscle) (*49*). One example of mammalian regeneration that depends on the plasticity of differentiated cells is in the liver (*63*), where the retention of function by cycling hepatocytes resembles that of cardiomyocytes in the salamander. Another example is the regeneration of peripheral nerve, which depends on the ability of Schwann cells to reenter the cell cycle, lose their differentiated properties such as myelin expression, and acquire a phenotype that facilitates axonal regeneration (*64*). The mammalian Schwann cell is a regenerative cell in the sense familiar in salamander regeneration, and the pathways leading to its reversal of differentiation are currently under investigation (*65*). Current interest in differentiated cells as a target for mammalian renewal and regeneration is exemplified by evidence for renewal of rennin synthesizing cells (*66*) or pancreatic β cells (*67*) and by evidence for the division of adult postmitotic auditory hair cells after the removal of the retinoblastoma gene (*68*). The retinoblastoma protein in salamanders is a critical target for inactivation and S phase reentry in myotubes (*59*, *60*), cardiomyocytes (*51*), and iris epithelial cells (*69*). Another approach has been to screen combinatorial libraries for small molecules that are able to reverse the differentiated state in cultured mouse cells (*70*). For example, this has led to the identification of myoseverin, a substituted purine able to fragment myotubes into viable mononucleate cells (*71*, *72*).

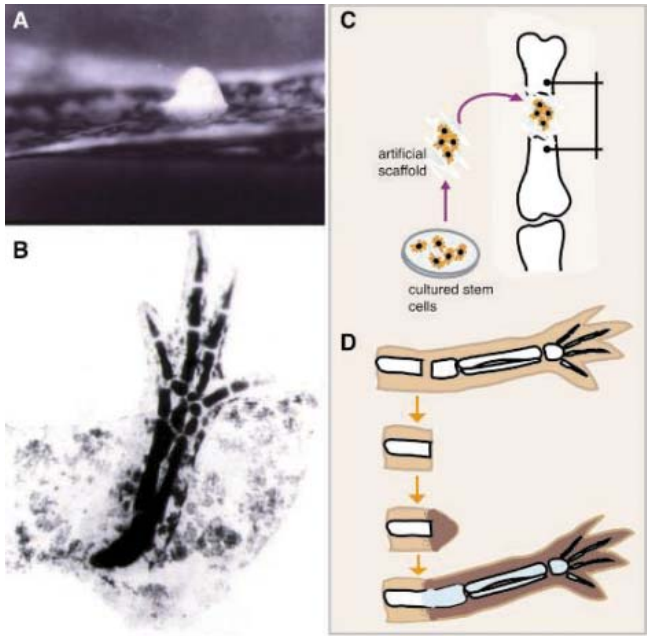

Fig. 3. Morphogenetic autonomy and its implications for regeneration. (**A**) A limb blastema from a salamander transplanted to the fin tunnel. (**B**) The limb structures formed from the blastema of (A). (**C**) Repair of a bone gap by grafting an artificial scaffold seeded with stem cells; an example of the approach of Fig. 1B. (**D**) Repair of a bone gap in a salamander by formation of a blastema and subsequent autonomous reconstruction of the distal skeletal elements.

Implementation in Mammals

These examples indicate that certain aspects of the regenerative mechanism in salamanders may become accessible in mammalian contexts, but what are the prospects for a more radical change in our potentiality, such as the regeneration of a limb? It is not understood why some animals are able to regenerate and others apparently are not (*73*, *74*); but even from our present limited perspective, there appear to be a number of differences between mammals and urodeles that prevent or limit regeneration, rather than any single defect or aberrant pathway. For example, mouse myotubes are refractory to the action of the thrombin pathway that leads to S phase reentry in newt myotubes, although mouse nuclei do respond in a mouse/newt heterokaryon (*75*). In another case, the Hox gene *C6* is turned off after limb development in the mouse, but its expression persists into the adult newt forelimb and limb blastemal cells (*76*–*78*). One aspect of adult wound healing in mammals that has been discussed in relation to the curtailment of regeneration is the occurrence of fibrosis, and also of immune and inflammatory responses (*79*, *80*). These are all potential targets for genetic and other manipulations. Existing variation in mouse strains and transgenics encompasses marked ability in tissue regeneration. For example, the MRL strain has the ability to heal punch wounds in the pinna of the ear (*81*), whereas transgenic mice expressing elevated levels of the muscle insulin-like growth factor–1 isoform

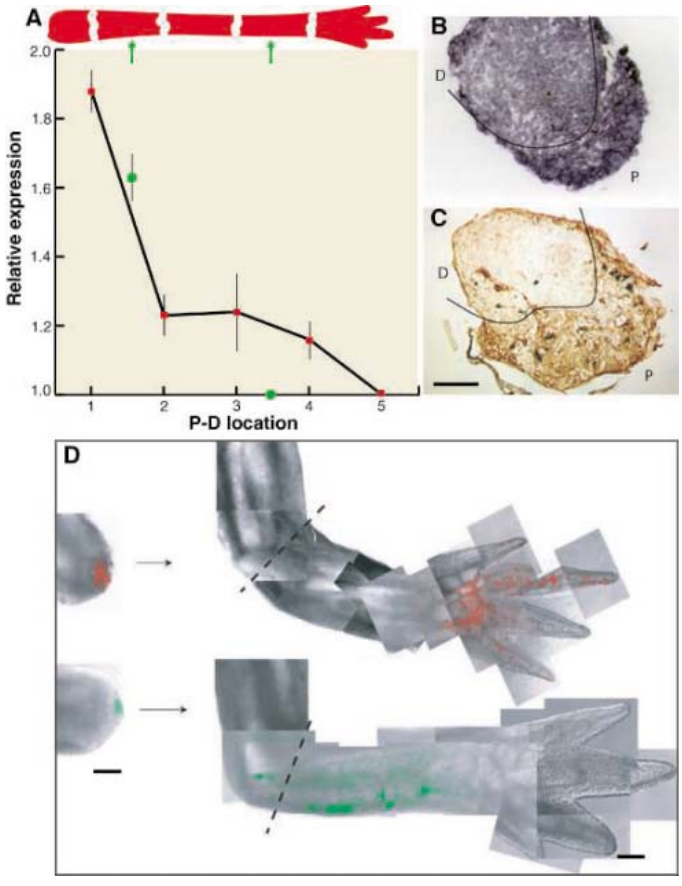

Fig. 4. Prod 1/CD59 as a local cue for PD identity in limb regeneration. (**A**) The graded expression of *Prod 1* mRNA along the PD axis in adult newt limb (outlined in red) is shown relative to the level in the hand (red points), whereas the expression in P and D blastemas is shown after amputation (green points) at the levels arrowed. (**B**) Expression of Prod 1 mRNA in P and D blastemas confronted in culture. (**C**) Expression of Prod 1 protein in confronted P and D blastemas. Scale bars in (B) and (C), 200 μm. (**D**) Elevated expression of Prod 1 converts distal blastemal cells to proximal. The left limb blastema of a larval axolotl (upper) was electroporated so as to express red fluorescent protein, and after regeneration, the labeled cells contribute to the hand. The right blastema (lower) was electroporated to express green fluorescent protein and Prod 1, and cells contribute to proximal tissue after regeneration, even to tissue proximal to the amputation plane (dashed line). Scale bars in the left panel, 200 μm; in the right panel, 1 mm. For experimental details, see (*89*). (B) and (C) are from (*33*) and (D) is from (*28*), with permission.

show enhanced recruitment of bone marrow cells and augmented repair mechanisms after injury (*82*). Nevertheless, it would be surprising if such approaches, even in combination, were to confer regeneration on a structure such as the limb.

Here we have outlined some of the distinctive properties of the limb blastema in salamanders, and a critical step forward for mammalian regeneration would be to engineer the equivalent of a founder blastemal cell. This goal should be facilitated first by increasing our understanding of stem cells in other contexts, including planarian regeneration (*83*) as well as limb development (*84*), which should help to define critical aspects of cellular regulation (*85*). Second, we need a better appreciation of how dedifferentiation operates to generate progenitor cells retaining local cues and specification. For example, the effects of cell cycle reentry in this process can be explored both in amphibian cells and in a mammalian context, such as the Schwann cell. In principle, it is possible that the blastemal phenotype could be approached either by modification of a generalized mesenchymal precursor, or by reversal from more differentiated cells. Third, we need a more extensive inventory of the properties of limb blastemal cells that takes advantage of the recently completed salamander expressed sequence tag (EST) projects (*86*, *87*). Finally, the approaches of systems biology should allow an integrated theoretical and experimental program to model the properties of blastmal cells. The value of such models as design tools has been noted previously (*88*), and this may allow for the derivation of a mammalian counterpart. This approach, although obviously challenging, seems more realistic than attempts to regulate externally the myriad processes of limb morphogenesis after beginning with relatively unspecified cells.

References and Notes

1. L. Alonso, E. Fuchs, *Proc. Natl. Acad. Sci. U.S.A.* **100**, 11830 (2003).
2. S. Harada, G. A. Rodan, *Nature* **423**, 349 (2003).
3. F. Radtke, H. Clevers, *Science* **307**, 1904 (2005).
4. D. L. Stocum, *Adv. Anat. Embryol. Cell Biol.* **176**, 1 (2004).
5. J. P. Brockes, *Science* **276**, 81 (1997).
6. D. L. Stocum, *Curr. Top. Microbiol. Immunol.* **280**, 1 (2004).
7. Y. Imokawa, J. P. Brockes, *Curr. Biol.* **13**, 877 (2003).
8. Y. Imokawa, A. Simon, J. P. Brockes, *Philos. Trans. R. Soc. London Ser. B* **359**, 765 (2004).
9. E. M. Tanaka, D. N. Drechsel, J. P. Brockes, *Curr. Biol.* **9**, 792 (1999).
10. G. Eguchi, in *Cellular and Molecular Basis of Regeneration*, P. Ferretti, J. Geraudie, Eds. (John Wiley & Sons, Chichester, 1998), pp. 207–228.
11. S. Ghosh, P. Thorogood, P. Ferretti, *Int. J. Dev. Biol.* **38**, 479 (1994).
12. J. O. Oberpriller, J. C. Oberpriller, *J. Exp. Zool.* **187**, 249 (1974).
13. W. K. O'Steen, B. E. Walker, *Anat. Rec.* **142**, 179 (1962).
14. J. Leor, Y. Amsalem, S. Cohen, *Pharmacol. Ther.* **105**, 151 (2005).
15. M. Han, X. Yang, J. E. Farrington, K. Muneoka, *Development* **130**, 5123 (2003).
16. P. Pietsch, R. H. Webber, *Anat. Rec.* **152**, 439 (1965).
17. D. L. Stocum, *Dev. Biol.* **18**, 457 (1968).
18. D. L. Stocum, *Differentiation* **27**, 13 (1984).
19. D. Logeart-Avramoglou, F. Anagnostou, R. Bizios, H. Petite, *J. Cell. Mol. Med.* **9**, 72 (2005).
20. H. Petite *et al.*, *Nat. Biotechnol.* **18**, 959 (2000).
21. C. S. Thornton, *J. Morphol.* **62**, 219 (1938).
22. R. W. Reyer, R. A. Woolfitt, L. T. Withersty, *Dev. Biol.* **32**, 258 (1973).
23. E. Guyenot, J. Dinichert-Favarger, M. Galland, *RSZ* **55**, (suppl. 2), 1 (1948).
24. V. French, P. J. Bryant, S. V. Bryant, *Science* **193**, 969 (1976).
25. D. M. Gardiner, T. Endo, S. V. Bryant, *Semin. Cell Dev. Biol.* **13**, 345 (2002).
26. K. Crawford, D. L. Stocum, *Development* **102**, 687 (1988).
27. M. J. Pescitelli Jr., D. L. Stocum, *Dev. Biol.* **79**, 255 (1980).
28. K. Echeverri, E. M. Tanaka, *Dev. Biol.* **279**, 391 (2005).
29. L. T. Pecorino, A. Entwistle, J. P. Brockes, *Curr. Biol.* **6**, 563 (1996).
30. S. V. Bryant, D. M. Gardiner, *Dev. Biol.* **152**, 1 (1992).
31. W. S. Kim, D. L. Stocum, *Rouxs Arch. Dev. Biol.* **195**, 455 (1986).
32. M. Maden, *Nature* **295**, 672 (1982).
33. S. M. da Silva, P. B. Gates, J. P. Brockes, *Dev. Cell* **3**, 547 (2002).
34. E. W. Murray, S. M. Robbins, *J. Biol. Chem.* **273**, 25279 (1998).
35. M. B. Powell, K. J. Marchbank, N. K. Rushmere, C. W. van den Berg, B. P. Morgan, *J. Immunol.* **158**, 1692 (1997).
36. S. A. Rollins, P. J. Sims, *J. Immunol.* **144**, 3478 (1990).
37. P. W. Tank, B. M. Carlson, T. G. Connelly, *J. Morphol.* **150**, 117 (1976).
38. J. B. Gurdon, P. Y. Bourillot, *Nature* **413**, 797 (2001).
39. T. Tabata, Y. Takei, *Development* **131**, 703 (2004).
40. K. Yashiro *et al.*, *Dev. Cell* **6**, 411 (2004).
41. S. Roy, D. M. Gardiner, S. V. Bryant, *Dev. Biol.* **218**, 199 (2000).
42. S. Roy, D. M. Gardiner, *J. Exp. Zool.* **293**, 186 (2002).
43. S. Ahn, A. L. Joyner, *Cell* **118**, 505 (2004).
44. B. D. Harfe *et al.*, *Cell* **118**, 517 (2004).
45. J. P. Brockes, *Science* **225**, 1280 (1984).
46. L. M. Mullen, S. V. Bryant, M. A. Torok, B. Blumberg, D. M. Gardiner, *Development* **122**, 3487 (1996).
47. M. Singer, *Q. Rev. Biol.* **27**, 169 (1952).
48. A. L. Mescher, *J. Exp. Zool.* **195**, 117 (1976).
49. J. P. Brockes, A. Kumar, *Nat. Rev. Mol. Cell Biol.* **3**, 566 (2002).
50. D. Bader, J. Oberpriller, *J. Exp. Zool.* **208**, 177 (1979).
51. M. Bettencourt-Dias, S. Mittnacht, J. P. Brockes, *J. Cell Sci.* **116**, 4001 (2003).
52. K. Del Rio-Tsonis, P. A. Tsonis, *Dev. Dyn.* **226**, 211 (2003).
53. G. Eguchi, R. Shingai, *Dev. Growth Differ.* **13**, 337 (1971).
54. T. S. Okada, *Transdifferentiation* (Clarendon Press, Oxford, 1991).
55. K. Echeverri, J. D. Clarke, E. M. Tanaka, *Dev. Biol.* **236**, 151 (2001).
56. A. Kumar, C. P. Velloso, Y. Imokawa, J. P. Brockes, *Dev. Biol.* **218**, 125 (2000).
57. A. Kumar, C. P. Velloso, Y. Imokawa, J. P. Brockes, *PLoS Biol.* **2**, E218 (2004).
58. D. C. Lo, F. Allen, J. P. Brockes, *Proc. Natl. Acad. Sci. U.S.A.* **90**, 7230 (1993).
59. E. M. Tanaka, A. A. Gann, P. B. Gates, J. P. Brockes, *J. Cell Biol.* **136**, 155 (1997).
60. C. P. Velloso, A. Kumar, E. M. Tanaka, J. P. Brockes, *Differentiation* **66**, 239 (2000).
61. T. Endo, S. V. Bryant, D. M. Gardiner, *Dev. Biol.* **270**, 135 (2004).
62. D. M. Gardiner, K. Muneoka, S. V. Bryant, *Dev. Biol.* **118**, 488 (1986).
63. R. Taub, *Nat. Rev. Mol. Cell Biol.* **5**, 836 (2004).
64. S. M. Hall, in *Peripheral Neuropathy* P. Dyck, P. K. Thomas, Eds. (Elsevier, London, 2005), pp. 1403–1434.

65. M. C. Harrisingh *et al.*, *EMBO J.* **23**, 3061 (2004).
66. M. L. Sequeira Lopez, E. S. Pentz, T. Nomasa, O. Smithies, R. A. Gomez, *Dev. Cell* **6**, 719 (2004).
67. Y. Dor, J. Brown, O. I. Martinez, D. A. Melton, *Nature* **429**, 41 (2004).
68. C. Sage *et al.*, *Science* **307**, 1114 (2005).
69. A. R. Thitoff, M. K. Call, K. Del Rio-Tsonis, P. A. Tsonis, *Anat. Rec.* **271**, 185 (2003).
70. S. Ding, P. G. Schultz, *Nat. Biotechnol.* **22**, 833 (2004).
71. A. Duckmanton, A. Kumar, Y. T. Chang, J. P. Brockes, *Chem. Biol.* **12**, 1117 (2005).
72. G. R. Rosania *et al.*, *Nat. Biotechnol.* **18**, 304 (2000).
73. J. P. Brockes, A. Kumar, C. P. Velloso, *J. Anat.* **199**, 3 (2001).
74. A. Sanchez Alvarado, *Bioessays* **22**, 578 (2000).
75. C. P. Velloso, A. Simon, J. P. Brockes, *Curr. Biol.* **11**, 855 (2001).
76. P. A. Khan, C. Tsilfidis, R. A. Liversage, *Dev. Genes Evol.* **209**, 323 (1999).
77. G. Oliver, C. V. Wright, J. Hardwicke, E. M. De Robertis, *Cell* **55**, 1017 (1988).
78. P. Savard, P. B. Gates, J. P. Brockes, *EMBO J.* **7**, 4275 (1988).
79. R. J. Goss, *Clin. Orthop. Relat. Res.* **151**, 270 (1980).
80. M. Harty, A. W. Neff, M. W. King, A. L. Mescher, *Dev. Dyn.* **226**, 268 (2003).
81. E. Heber-Katz, J. M. Leferovich, K. Bedelbaeva, D. Gourevitch, *Curr. Top. Microbiol. Immunol.* **280**, 165 (2004).
82. A. Musaro *et al.*, *Proc. Natl. Acad. Sci. U.S.A.* **101**, 1206 (2004).
83. P. W. Reddien, A. L. Bermange, K. J. Murfitt, J. R. Jennings, A. Sanchez Alvarado, *Dev. Cell* **8**, 635 (2005).
84. L. Niswander, *Nat. Rev. Genet.* **4**, 133 (2003).
85. L. A. Boyer *et al.*, *Cell* **122**, 847 (2005).
86. B. Habermann *et al.*, *Genome Biol.* **5**, R67 (2004).
87. S. Putta *et al.*, *BMC Genomics* **5**, 54 (2004).
88. D. Endy, R. Brent, *Nature* **409**, 391 (2001).
89. Materials and methods are available as supporting materials on *Science* Online.
90. We thank E. Amaya, J. Ladbury, P. Martin, and L. Wolpert for comments on the manuscript; P. Gates for Fig. 4A; and D. Stocum and E. Tanaka for permission to show Figs. 3, A and B, and Fig. 4D, respectively. J.P.B. thanks the H. Dudley Wright Foundation for the invitation to speak on this topic at their meeting in Geneva, November 2004. Supported by the Medical Research Council (UK) by a Research Professorship and Programme grant to J.P.B.

Supporting Online Material
www.sciencemag.org/cgi/content/full/310/5756/1919/DC1
Materials and Methods

10.1126/science.1115200

Torus-Margo Pits Help Conifers Compete with Angiosperms

Jarmila Pittermann, John S. Sperry,* Uwe G. Hacke, James K. Wheeler, Elzard H. Sikkema

Efficient water transport in plants allows for increased photosynthetic uptake of CO_2 for a given vascular investment and should improve fitness through enhanced growth and reproduction. The evolution of long, multicellular xylem vessels from short, unicellular tracheids reduces the number of times water must flow through high-resistance pits that link conduits end-to-end. Accordingly, the tracheid-based wood of conifers should have much higher flow resistance per length (resistivity) than the vesseled wood of angiosperms. However, despite the presumed tracheid handicap, conifers dominate many of the world's ecosystems and include the tallest plants (*Sequoia sempervirens*) and the oldest living organisms (*Pinus longaeva*). Just how handicapped is conifer xylem transport relative to that of angiosperms?

We found that conifers had lower sapwood-area resistivity than did angiosperms for the same average conduit diameter (Fig. 1A) (*1*). Even on the basis of an individual conduit, conifer tracheids averaged only 1.2 times the resistivity of vessels for the same diameter (*1*, *2*). Although vessels achieve a greater maximum diameter, in many species they are as narrow as tracheids (Fig. 1A). The similarity in resistivity is striking because the conifer tracheids were >10 times shorter than vessels of similar diameter (Fig. 1B). Compared with vessels, conifer tracheids must have low flow resistance through their end-walls, because these are encountered much more frequently as water ascends the tree.

Tracheid end-walls must have either a large area of connecting pits or have pits with a low flow resistance for their area (pit-area resistance). Total pit area was actually much lower in tracheids (0.016 ± 0.003 mm^2) than in vessels (0.95 ± 0.51 mm^2) (*1*, *2*). Instead, the pit-area resistance of conifers was 59 times lower than the angiosperm average (Fig. 1C) (*2*). This compensates for short tracheid length and low pit area and results in comparable resistivities of conifer tracheids and angiosperm vessels.

These findings indicate a function—minimal hydraulic resistance—for the unique torus-margo anatomy of the conifer pit membrane (Fig. 1, D and E). The large 0.1-μm–scale pores in the margo (Fig. 1D) are responsible for the reduced flow resistance. Low margo resistance more than compensates for the impermeable torus, which blocks much of the membrane. The torus is required for sealing the pit against the air seeding of cavitation (Fig. 1, F and G). In contrast, the angiosperm pit membrane is uniformly microporous (Fig. 1D). The narrow, nm-scale pores create high resistance to flow when the pit is conducting, but are required to seal the pit effectively by capillary force because there is no torus (Fig. 1, F and G). We found no difference in the range of cavitation pressure between conifer tracheids and angiosperm vessels (Fig. 1C) (*1*, *2*). The torus-margo pit not only has less flow resistance, but it is just as safe from air seeding as the angiosperm pit.

The superior hydraulics of the conifer pit are crucial for minimizing sapwood resistivity. If conifer tracheids had the pit resistance of angiosperms, their sapwood resistivity would increase by 38-fold (Fig. 1A, crosses) (*1*). This, added to the narrow diameter range of tracheids, would make it much more difficult for conifers to compete effectively with angiosperms.

The reduction in resistivity achieved by the torus-margo pit membrane is equivalent to a 7.7-fold increase in conduit length. This would require a tracheid to be as long as a vessel of equal diameter (Fig. 1B, crosses) (*1*). We conclude that the evolution of the torus-margo membrane within the gymnosperm lineage from homogenous pits was equivalent to the evolution of vessels within the angiosperms. The towering redwoods and the sweep of the boreal coniferous forest exist in no small part because of this clever microscopic valve.

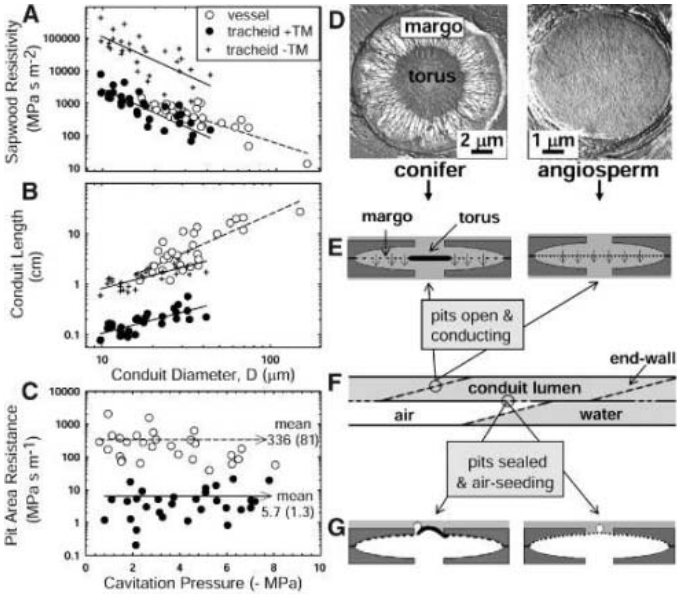

Fig. 1. (**A**) Sapwood-area resistivity versus average conduit diameter for conifer tracheids with torus-margo (+TM) pit membranes and for angiosperm vessels with homogenous pit membranes. Crosses are tracheids substituted with angiosperm pit resistance (–TM). (**B**) Average conduit length versus diameter. Crosses show the tracheid length required to compensate for the substitution of angiosperm pits. (**C**) Flow resistance through pits on a membrane-area basis versus cavitation pressure. (**D**) Scanning electron microscope image of pit membranes with secondary wall removed. (Left) Torus-margo membrane of conifer tracheids; (right) homogenous pit membrane of angiosperm vessels (*3*). (**E**) Schematic side view of conducting pits. (**F**) Conduit network with pits conducting water and sealed against air entry. (**G**) Side view of pits in sealed and air-seeding position. Air leakage nucleates cavitation in the xylem sap.

References and Notes

1. Materials and methods available as supporting material on *Science* Online.
2. U. G. Hacke, J. S. Sperry, J. K. Wheeler, L. Castro, *Tree Physiol.*, in press.
3. J. F. Siau, *Transport Processes in Wood* (Springer, Berlin, 1984), pp. 49 and 59.
4. This work was funded by the National Sciences and Engineering Research Council of Canada and by NSF grant no. DDIG-0308862 to J.P. and grant no. IBN-0416297 to J.S.S.

Supporting Online Material
www.sciencemag.org/cgi/content/full/310/5756/1924/DC1
Materials and Methods
Table S1
References

22 September 2005; accepted 7 November 2005
10.1126/science.1120479

Department of Biology, University of Utah, 257S 1400E, Salt Lake City, UT 84112, USA.

*To whom correspondence should be addressed. E-mail: sperry@biology.utah.edu

Radar Soundings of the Subsurface of Mars

Giovanni Picardi,[1] Jeffrey J. Plaut,[2]* Daniela Biccari,[1] Ornella Bombaci,[3] Diego Calabrese,[3] Marco Cartacci,[1] Andrea Cicchetti,[1] Stephen M. Clifford,[4] Peter Edenhofer,[5] William M. Farrell,[6] Costanzo Federico,[7] Alessandro Frigeri,[7] Donald A. Gurnett,[8] Tor Hagfors,[9] Essam Heggy,[4] Alain Herique,[10] Richard L. Huff,[8] Anton B. Ivanov,[2] William T. K. Johnson,[2] Rolando L. Jordan,[2] Donald L. Kirchner,[8] Wlodek Kofman,[10] Carlton J. Leuschen,[11] Erling Nielsen,[9] Roberto Orosei,[12] Elena Pettinelli,[14] Roger J. Phillips,[15] Dirk Plettemeier,[16] Ali Safaeinili,[2] Roberto Seu,[1] Ellen R. Stofan,[17] Giuliano Vannaroni,[13] Thomas R. Watters,[18] Enrico Zampolini[3]

The martian subsurface has been probed to kilometer depths by the Mars Advanced Radar for Subsurface and Ionospheric Sounding instrument aboard the Mars Express orbiter. Signals penetrate the polar layered deposits, probably imaging the base of the deposits. Data from the northern lowlands of Chryse Planitia have revealed a shallowly buried quasi-circular structure about 250 kilometers in diameter that is interpreted to be an impact basin. In addition, a planar reflector associated with the basin structure may indicate the presence of a low-loss deposit that is more than 1 kilometer thick.

The subsurface of Mars is unexplored territory. Glimpses of the third dimension of martian geology have been obtained by study of exposures on crater and valley walls (*1*) and by construction of cross sections inferred from geologic mapping of the surface (*2*, *3*). However, no direct measurements of the unexposed crust below a few meters depth were possible before the activation of the Mars Advanced Radar for Subsurface and Ionospheric Sounding (MARSIS) (*4*) onboard the European Space Agency's Mars Express (*5*) orbiter in June 2005. We report here on radar echoes obtained by MARSIS from the deep subsurface, to more than 1 km depth.

The MARSIS instrument and data. MARSIS is a multifrequency, synthetic-aperture, orbital sounding radar. Data are collected when the elliptical orbit of Mars Express brings the spacecraft to an altitude of 250 to 800 km above the surface; this condition is met during about 26 min of each 6.7-hour orbit. In its subsurface modes, MARSIS operates in four frequency bands between 1.3 and 5.5 MHz, with a 1-MHz instantaneous bandwidth that provides free-space range resolution of approximately 150 m. Lateral spatial resolution depends on surface roughness characteristics, but for most Mars surfaces, the cross-track footprint is 10 to 30 km and the along-track footprint, narrowed by onboard synthetic-aperture processing, is 5 to 10 km. Peak transmitted power out of the 40-m dipole antenna is ~10 W. Coherent azimuth sums are performed onboard on ~100 pulses taken at a pulse repetition frequency of 127 Hz, with a resulting signal-to-noise ratio for a typical Mars surface of 30 to 50 dB. The data described here were acquired during the commissioning and initial routine data-collection phases of the MARSIS experiment, in June and July 2005. During this period, the close approach of the orbit occurred near the evening terminator. MARSIS's sounding signals will not reach the surface when the ionospheric plasma frequency is close to or above the sounding frequency. The frequency bands were therefore chosen to minimize distortion by the ionosphere; typically, bands centered at 1.8 and 3.0 MHz were used on the nightside, and bands centered at 4.0 and 5.0 MHz were used on the dayside. Here we discuss data collected on orbits 1855, 1892, and 1903, on 26 June, 6 July, and 9 July 2005, respectively. Data were collected in a MARSIS subsurface-sounding mode, which returns complex spectra of summed pulses from three synthetic-aperture channels for each of two frequency bands. Once received on the ground, the spectra are transformed from the frequency domain to the time domain. Processing includes a correction for phase distortion in the ionosphere (*6*, *7*).

North polar layered deposits. Surrounding the north pole of Mars are the north polar layered deposits (NPLD) that consist mainly of an upper stratigraphic unit, thought to be dominated by water ice, which is typically finely layered because of varying fractions of included dust (*1*, *8*–*12*). A second, lower unit that is absent at some longitudes contains a substantial sand component that is probably ice-cemented (*10*–*12*). Previous compositional and stratigraphic interpretations of these deposits have been based on imaging, spectral, thermal, and topographic measurements. In an early MARSIS orbit, 1855, the NPLD were briefly observed in the longitude range from 10° to 40°E from altitudes of 800 to 900 km, on the nightside, in the frequency bands centered at 3.0 and 5.0 MHz. The radargrams show the surface reflection splitting into a pair of strong reflectors as the ground track passes from the northern plains onto the layered deposits (Fig. 1). The lower reflector extends to the end of the track, where it occurs at a time delay of 21 μs relative to the surface reflection. The interpretation of radar sounding data requires discriminating between signals arising from subsurface interfaces and those coming from surface topographic features at the same time delay (surface "clutter"). A high-fidelity model of the expected contribution of off-nadir topographic clutter, based on gridded Mars Orbiter Laser Altimeter (MOLA) data (*13*–*15*), shows no visible surface topographic feature that explains this reflector pair. Hence, we conclude that the second reflector is a subsurface ("basal") reflector.

The time delay to and the relative echo strength of the basal reflector are consistent with the overlying material (away from the boundary) having a dielectric constant and loss tangent (*16*) similar to that of fairly pure water ice. This is in accord with the absence of the lower, sandy stratigraphic unit in this region of the NPLD, as inferred from its lack of exposure in troughs in the longitude range from 290° to 90°E (*10*, *12*).

[1]Infocom Department, "La Sapienza" University of Rome, 00184 Rome, Italy. [2]Jet Propulsion Laboratory, California Institute of Technology, Pasadena, CA 91109, USA. [3]Alcatel Alenia Space Italia, 00131 Rome, Italy. [4]Lunar and Planetary Institute, Houston, TX 77058, USA. [5]Fakultaet fuer Elektrotechnik und Informationstechnik Ruhr-Universitaet Bochum, D-44780 Bochum, Germany. [6]NASA/Goddard Space Flight Center, Greenbelt, MD 20771, USA. [7]Dipartimento di Scienze della Terra, Università degli Studi di Perugia, 06123 Perugia, Italy. [8]Department of Physics and Astronomy, University of Iowa, Iowa City, IA 52242, USA. [9]Max Planck Institute for Solar System Research, 37191 Katlenburg-Lindau, Germany. [10]Laboratoire de Planetologie de Grenoble, 38041 Grenoble Cedex, France. [11]Applied Physics Laboratory, Johns Hopkins University, Laurel, MD 20723, USA. [12]Istituto di Astrofisica Spaziale e Fisica Cosmica, [13]Istituto di Fisica dello Spazio Interplanetario, Istituto Nazionale di Astrofisica, 00133 Rome, Italy. [14]Dipartimento di Fisica, University of Rome 3, 00146 Rome, Italy. [15]Department of Earth and Planetary Sciences, Washington University, St. Louis, MO 63130, USA. [16]Fakultaet fuer Elektrotechnik und Informationstechnik, Technische Universitaet Dresden, D-01062 Dresden, Germany. [17]Proxemy Research, Laytonsville, MD 20882, USA. [18]Center for Earth and Planetary Studies, National Air and Space Museum, Smithsonian Institution, Washington, DC 20560, USA.

*To whom correspondence should be addressed. E-mail: plaut@jpl.nasa.gov

The basal reflector time delay increases, with respect to the surrounding plains, as it proceeds inward from the NPLD boundary (Fig. 1). This is due to the slower velocity of the NPLD material relative to the martian atmosphere (approximately free-space velocity). Converting time to distance using a dielectric constant of pure ice (~3) brings the maximum basal reflector depth up to about the level of the plains; i.e., the depth to the reflector is approximately the height of the NPLD above its surroundings (about 1.8 km at the right edge in Fig. 1). Either this is a coincidence or the material in this region of the NPLD is dominated by ice sitting directly on the underlying plains material.

The wave attenuation properties strengthen the case for nearly pure ice. Among plausible geological materials, only pure or slightly dirty water ice has a sufficiently low value of loss tangent to explain the strength of the subsurface reflection observed. Simple two-layer modeling has been applied to estimate the loss tangent of the ~1.8-km NPLD layer. The two interfaces considered are one at the atmosphere/surface ice boundary and a second at the ice base at ~1.8-km depth. The MARSIS-measured ratio of the reflected power from these two interfaces at 5 MHz is approximately –10 dB. This ratio is consistent with an ice-layer dielectric of 3, an underlying material dielectric of 4.5 (basaltic regolith), and an ice-layer loss tangent that must be low, below 0.001 (conductivity $<10^{-6}$ siemens/m). The low loss tangent of the 1.8-km-thick ice layer gives rise to relatively low attenuation of MARSIS radar signals, thereby allowing the base to be easily detectable. Ice conductivity is temperature-dependent (*17–19*). The low loss and low conductivity of the ice indicate that it cannot contain more than a trace (2%) of impurities, and suggest a bulk temperature below 240 K. These observations are inconsistent with the presence of a melt zone at the base of the NPLD.

The NPLD will act as a load on the underlying elastic lithosphere and should cause a flexural/membrane downward deflection of the plains. In order to leave a residual deflection after the velocity conversion, the dielectric constant of the NPLD would have to be less than 3, which we deem unlikely. An elastic thickness in excess of 150 km would produce a deflection of 500 m or less (*20*), which is well within the resolution of our interface detection. Thus, a very thick elastic lithosphere (and a low crust/upper mantle temperature gradient) is implied for the north polar region.

Detection of ring structure. The mid-latitude northern lowlands region known as Chryse Planitia (Fig. 2) has long been recognized as a locus of deposition of sediments delivered in outflow flooding events from multiple sources in the highlands (*21–25*). In image data and MOLA topography, the surface is characterized by textures ranging from smooth to hummocky, with numerous iso-

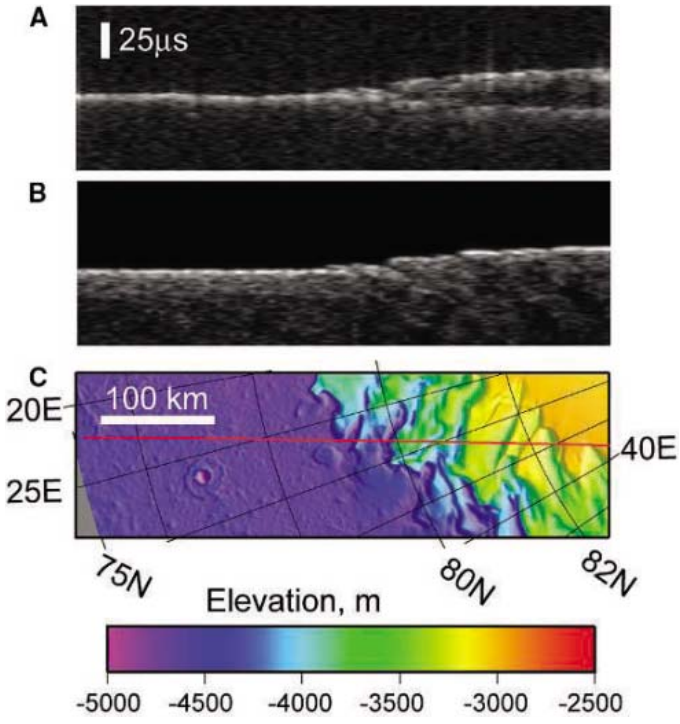

Fig. 1. (**A**) MARSIS data in radargram format for orbit 1855 as it crossed the margin of the NPLD. (**B**) Simulated MARSIS data if echoes are only from the surface (nadir and off-nadir clutter). (**C**) MOLA topography along the ground track (red line); elevation is relative to mean planetary radius. MARSIS data at 5 MHz show a split of the strong return into two as the ground track reaches the NPLD (higher terrain to the right). Maximum time delay to the second reflector is 21 μs, equivalent to 1.8-km depth in water ice.

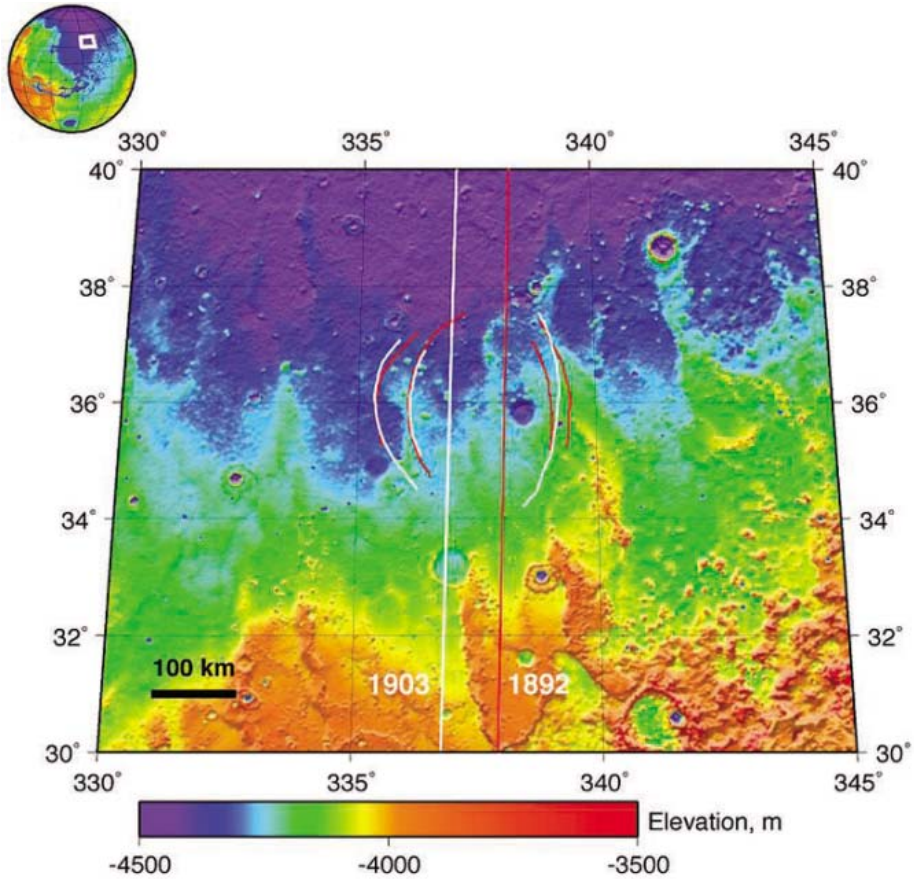

Fig. 2. Location of the ring structure, northeast Chryse Planitia, in MOLA topographic data (positive east longitude). The inset at top left shows the location of the detailed map on a globe of Mars. Ground track positions are shown as vertical lines (1903 and 1892). Traces of ring structures that match in the two orbits are shown in red (1892) and white (1903).

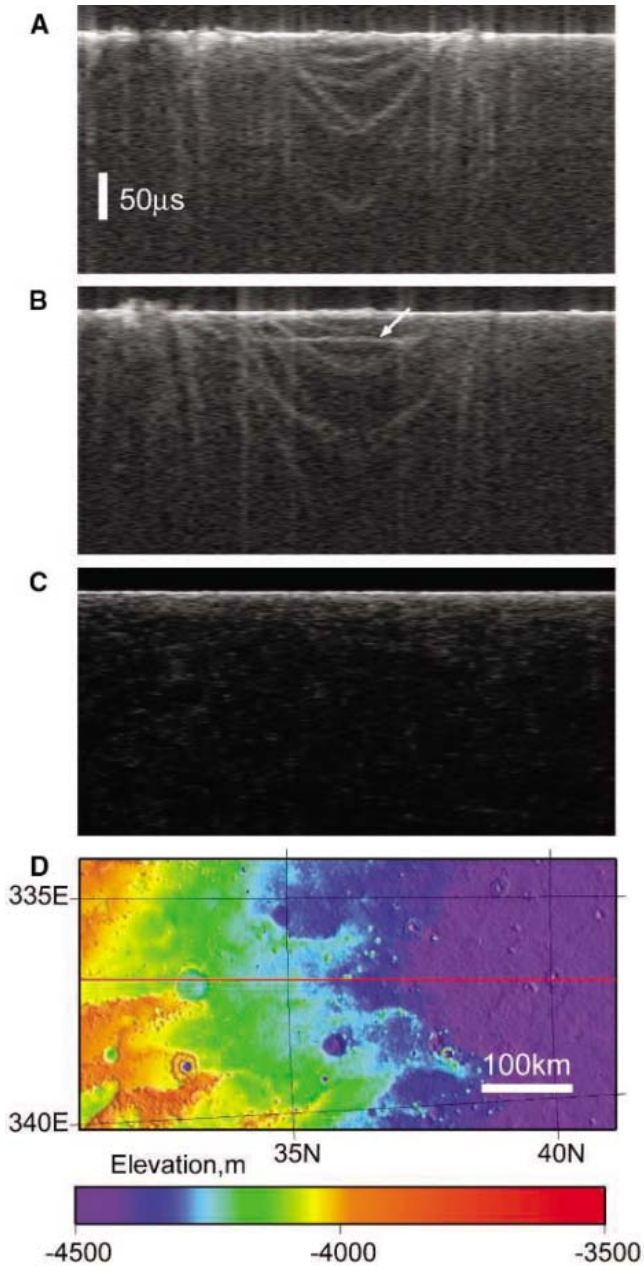

Fig. 3. MARSIS data for orbits (**A**) 1892 (3-MHz band) and (**B**) 1903 (4-MHz band). Note the multiple arc-shaped reflectors near the center of each panel, and the planar reflector associated with the arcs in orbit 1903 (arrow). (**C**) Model of the nadir surface and off-nadir clutter for orbit 1903. No arc-like or planar features are predicted in the clutter model. (**D**) MOLA topography along the ground track of orbit 1903.

lated knobs, several subdued wrinkle ridges, and highly degraded or buried crater forms. In northeastern Chryse Planitia, surficial units of Late Hesperian and Early Amazonian age (based on crater counts) have been interpreted primarily as aqueous sediments, though some workers did not rule out an origin as lava flows (*26*). The area has been mapped recently as the ''interior unit'' of the Vastitas Borealis Formation (VBF), near its southern contact with Hesperian channeled plains material (*25*). The materials underlying the VBF that resurfaced Chryse Planitia and much of the ancient crust of the northern lowlands appear to be volcanic in origin, based on numerous partially buried wrinkle ridges similar to those found in exposed volcanic plains in the highlands (*27*). Using MOLA data, numerous large (tens to hundreds of kilometers in diameter) subtle circular features were identified in the area (*28*, *29*) and were interpreted as surface expressions of a population of ancient degraded and/or buried impact craters. However, no structure corresponding to the feature described below has been identified previously.

MARSIS observed part of the Chryse Planitia region on two orbits (1892 and 1903), at 30° to 40°N latitude, 330° to 340°E longitude, when the spacecraft altitude was ~335 km (near periapsis) and the solar zenith angle was within a few degrees of 90° [the terminator (Fig. 2)]. The higher frequency band for each dual-frequency observation obtained the best data, which for orbit 1892 was the band centered on 3 MHz and for orbit 1903 the band centered on 4 MHz. A distinctive collection of echo structures arriving at time delays later than the surface echo were seen in both orbits, centered at a common latitude of about 36°N (Fig. 3). The structures include multiple parabolic arcs in each orbit, with a common axis of symmetry and an additional planar reflector parallel to the surface trace, 160 km in length along-track, seen only in orbit 1903. The time delays of the arc features relative to the surface echo range from nearly coincident to delays up to 180 μs. Such long delayed echoes are not expected from the nadir subsurface at these frequencies, because they imply implausible penetration depths as great as 15 km. Rather, these echoes are likely a form of off-nadir clutter. The model of topographic clutter (Fig. 3), however, shows no features corresponding to the arcs or planar feature in these orbits. We therefore attribute the arc echoes to off-nadir clutter, but from a source below the surface.

The radargrams, which are in a time-delay geometry (''slant range'') were transformed into a ground-range geometry, assuming that the detected features are at shallow depth. The ground-range projection transforms the parabolic echoes into arcs of constant curvature suggesting large circular features. Such a projection has a natural left/right ambiguity. The two orbit ground tracks are separated by about 50 km and provide a ''stereo'' viewing geometry. When the projected data are overlapped, some echoes from both orbits align (Fig. 2), suggesting that MARSIS imaged the same features twice and that the model of a near-surface structure is approximately correct. The matching arcs appear to trace out portions of several quasi-circular features. We interpret these rings as the rims of one or more buried impact basins, with a maximum diameter of ~250 km. A schematic representation of the detection of such a feature by a radar sounder is similar to the signature seen in the data (Fig. 4). We attribute the signature in the MARSIS data to reflections off of favorably oriented crater walls or related structures (such as rim-wall slump blocks or peak-ring features), where a contrast in electrical properties exists between the wall material and the basin fill or overlying materials. We note that no single circle or set of concentric circles exactly matches the ground range projection of the detected rings. This may be due to multiple overlapping structures, propagation effects not accounted for in the projection, or other unrecognized effects.

The planar reflector seen in orbit 1903 (Fig. 3) differs from the arc reflectors in several ways. First, it was seen at a remarkably uniform time delay from the surface echo (a mean delay of 29 μs, with a standard deviation of <2 μs in 26 measurements). Second, the intensity of the echo is significantly higher than that of the arcs, with a value of 16 ± 6 dB below the surface echo power in the same profiles. There is no obvious counterpart to this reflector in orbit 1892, although a subtle, shorter, early subhorizontal feature is observed that may be related. Here we explore the possibility that the feature in orbit

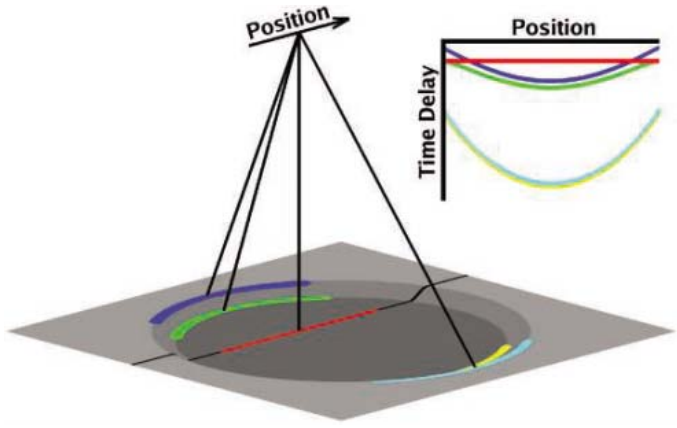

Fig. 4. Schematic showing the geometric relationships of a crater rim and floor in oblique view (**left**) and as seen in a sounder radargram (**right**). Note the appearance of multiple parabolic arcs and an associated planar reflector in the radargram. Compare with the radargram of orbit 1903 in Fig. 3.

1903 is a deep subsurface interface directly below the ground track of orbit 1903. This is consistent with the expected relationship of the geometric elements of a flat-floored circular basin when observed by a radar sounder (Fig. 4).

We again apply a simple two-layer model, in which the lower reflector occurs at the interface between a uniform upper layer and a lower layer of differing dielectric constant. The time delay translates to a depth to the interface of 2.0 to 2.5 km, for a plausible range of martian materials. The ratio of echo power between the two interfaces implies very low attenuation in the upper layer, with a loss tangent <0.005. This raises the intriguing possibility that a large volume of low-loss material, possibly ice-rich, at least partially fills the basin. The depth of the feature is roughly consistent with the observed depths of exposed 200- to 300-km-diameter basins on Mars. Thus, the feature could be the basin floor or a boundary between layers of basin fill. We cannot completely rule out the possibility that it is a ''hidden'' planar clutter structure that fortuitously lies almost exactly parallel to the orbital ground track. The putative interface extends ~160 km along-track, yet is not seen in the adjacent orbit 50 km to the east. Further observations are needed to understand this discrepancy. One possibility is that the eastern part of the basin floor was disrupted by a smaller, later impact event that formed a ~30-km-diameter crater (now degraded) that lies close to the ground track of orbit 1892 (Fig. 2). The ring feature and planar reflector occur near a crustal magnetic field anomaly (*30*). Our analysis does not show a major influence of the magnetic field on the radar signature, with the exception of some decorrelation (left side of Fig. 3) where there is a large gradient in the magnetic field (*31*).

Discussion and conclusions. MARSIS has demonstrated a capability to detect structures and layers in the subsurface of Mars that are not detectable by other sensors, past or present. In its only observation of the NPLD, the sounder has apparently penetrated >1 km of the ice-rich deposits, probably imaging the basal contact. The low attenuation observed in the NPLDs indicates a composition of nearly pure cold water ice. The lack of a significant deflection of the plains surface below the NPLD implies a very thick elastic lithosphere in this region. In the mid-latitude Chryse Planitia, MARSIS has detected a circular structure ~250 km in diameter, presumably of impact origin. Embedded in this structure is a continuous reflector that may be the basin floor beneath a thick volume of low-loss material, although other explanations cannot be ruled out. Data described here from the first month of MARSIS observations indicate that the experiment holds promise to address a number of issues in Mars geology through subsurface probing. For example, if further observations of the polar layered deposits show comparable penetration to that seen in the example here, we can expect to map in detail the base of the layered deposits and to obtain better estimates of the deposits' volume. The detection of a large buried impact basin suggests that MARSIS data may be used to further expose the population of impact craters hidden beneath the surface in the northern lowlands and elsewhere on the planet.

References and Notes

1. M. C. Malin, K. S. Edgett, *J. Geophys. Res.* **106**, 23429 (2001).
2. D. H. Scott *et al.*, *U.S. Geol. Surv. Misc. Invest. Ser.*, Maps I-1802-A, -B, and -C (1987).
3. N. E. Witbeck *et al.*, *U.S. Geol. Surv. Misc. Invest. Ser.*, Map I-2010 (1991).
4. G. Picardi *et al.*, in *Mars Express: A European Mission to the Red Planet* [SP-1240, European Space Agency (ESA) Publications Division, European Space Research and Technology Centre (ESTEC), Noordwijk, Netherlands, 2004)], pp. 51–69.
5. A. Chicarro, P. Martin, R. Trautner, in *Mars Express: A European Mission to the Red Planet* (SP-1240, ESA Publications Division, ESTEC, Noordwijk, Netherlands, 2004), pp. 313.
6. The ionosphere both attenuates the signal amplitude and scrambles its phase, resulting in defocusing of the radar echo return. The level of distortion depends on the electron content and collision frequency in the ionosphere, which in turn are related to the Sun elevation angle at the time of observation and the effects of solar activity on the martian plasma. Our ground processing includes a step that decodes the ionospheric phase distortion and refocuses the echo using redundant information in the data themselves and a priori information about local topography (*7*).
7. A. Safaeinili *et al.*, *Planet. Space Sci.* **51**, 505 (2003).
8. P. C. Thomas *et al.*, in *Mars*, H. H. Kieffer *et al.*, Eds. (Univ. of Arizona Press, Tucson, AZ, 1992), pp. 767–795.
9. E. Kolb, K. Tanaka, *Icarus* **154**, 22 (2001).
10. S. Byrne, B. C. Murray, *J. Geophys. Res.* **107**, 10.1029/2001JE001615 (2002).
11. K. S. Edgett *et al.*, *Geomorphology* **52**, 289 (2003).
12. K. E. Fishbaugh, J. W. Head III, *Icarus* **174**, 444 (2005).
13. D. E. Smith *et al.*, *Science* **284**, 1495 (1999).
14. MOLA topographic data at 1/128 degree per pixel grid spacing were used to simulate echoes from the cross-track region for each MARSIS subsurface sounding observation. Along-track sources were suppressed, because MARSIS data processing achieves this by aperture synthesis (*15*).
15. J.-F. Nouvel *et al.*, *Radio Sci.* **39**, 10.1029/2003RS002903 (2004).
16. We use the term "dielectric constant" to indicate the real part of the complex dielectric constant (relative permittivity) of a material ($\varepsilon = \varepsilon_r + i\varepsilon_i$), which is ratioed to the free-space value (*r*, real; *i*, imaginary). "Loss tangent" is the ratio $\varepsilon_i/\varepsilon_r$, or, equivalently, the ratio of electrical conductivity (s) to the product of angular frequency ($\omega = 2\pi f$) and ε_r.
17. D. C. Nunes, R. J. Phillips, in preparation.
18. W. M. Farrell *et al.*, *Geophys. Res. Lett.* **32**, L11204 (2005).
19. Y. Xu *et al.*, in preparation.
20. C. L. Johnson *et al.*, *Icarus* **144**, 313 (2000).
21. B. K. Lucchitta *et al.*, *Proc. Lunar Planet. Sci. Conf. 17th, Part 1, J. Geophys. Res.* **91**, E166 (1986).
22. S. Rotto, K. L. Tanaka, *U.S. Geol. Surv. Misc. Invest. Ser.*, Map I-2441 (1995).
23. K. L. Tanaka, *J. Geophys. Res.* **102**, 4131 (1997).
24. K. L. Tanaka *et al.*, *J. Geophys. Res.* **108**, 10.1029/2002JE001908 (2003).
25. K. L. Tanaka *et al.*, *U.S. Geol. Surv. Misc. Invest. Ser.*, Map I-2888 (2005).
26. G. E. McGill, *U.S. Geol. Surv. Misc. Invest. Ser.*, Map I-2811 (2005).
27. J. W. Head *et al.*, *J. Geophys. Res.* **107**, 10.1029/2000JE001445 (2002).
28. H. V. Frey *et al.*, *Geophys. Res. Lett.* **29**, 10.1029/2001GL013832 (2002).
29. H. V. Frey, *J. Geophys. Res.*, in press.
30. J. C. Cain *et al.*, *J. Geophys. Res.* **108**, 10.1029/2000JE001487 (2003).
31. The nearby magnetic anomaly has a peak magnitude of 310 nT (*30*). The depolarization of the radar wave due to the interaction of the magnetic field and ionosphere of Mars can cause ~1 μs of dispersion in the returned echo and cannot account for any of the features observed. Because the interaction of ionosphere with radar wave in the presence of a magnetic field is frequency-dependent, we plan to observe the feature in the future with different frequency bands.

32. MARSIS owes its existence to the funds and management of the Agenzia Spaziale Italiana (ASI) and NASA. The Mars Express mission is managed and operated by the European Space Agency. We thank the key instrument contractors, Alenia Spazio, University of Iowa, and Northrop Grumman Space Technology/Astro Aerospace, as well as the Mars Express flight team, whose efforts were instrumental in the successful deployment of the MARSIS antenna. We also thank S. Hensley, S. Madsen, E. Rodriguez, P. Rosen of the Jet Propulsion Laboratory for a technical review of the data used in this paper, and J. van Zyl for his contribution to the instrument concept. The research activities of the MARSIS principal investigator and Italian investigators are supported by grants under the Mars Express/ASI program. Work of the U.S. investigators is supported by grants under the Mars Express/NASA project. Some of the research described in this publication was carried out at the Jet Propulsion Laboratory, California Institute of Technology, under a contract with NASA.

2 November 2005; accepted 22 November 2005
Published online 30 November 2005;
10.1126/science.1122165
Include this information when citing this paper.

Radar Soundings of the Ionosphere of Mars

D. A. Gurnett,[1]* D. L. Kirchner,[1] R. L. Huff,[1] D. D. Morgan,[1] A. M. Persoon,[1] T. F. Averkamp,[1] F. Duru,[1] E. Nielsen,[2] A. Safaeinili,[3] J. J. Plaut,[3] G. Picardi[4]

We report the first radar soundings of the ionosphere of Mars with the MARSIS (Mars Advanced Radar for Subsurface and Ionosphere Sounding) instrument on board the orbiting Mars Express spacecraft. Several types of ionospheric echoes are observed, ranging from vertical echoes caused by specular reflection from the horizontally stratified ionosphere to a wide variety of oblique and diffuse echoes. The oblique echoes are believed to arise mainly from ionospheric structures associated with the complex crustal magnetic fields of Mars. Echoes at the electron plasma frequency and the cyclotron period also provide measurements of the local electron density and magnetic field strength.

The Mars Express spacecraft (*1*), currently in orbit around Mars, carries a low-frequency radar (*2*) called MARSIS. Here, we present the first ionospheric sounding results from MARSIS. Spacecraft radar sounders were originally developed in the 1960s to study Earth's ionosphere (*3*–*5*) and have proven to be a powerful tool for studying ionospheric physics. Currently, most of our knowledge of the Martian ionosphere comes from radio occultation measurements, which provide an average electron density along a line of sight from Earth to a spacecraft in orbit around Mars (*6*–*9*). The MARSIS measurements nicely complement these measurements by providing better spatial resolution and the ability to make observations in regions where radio occultation measurements cannot be made. Because of geometric constraints imposed by the orbits of Earth and Mars, radio occultation measurements are restricted to solar zenith angles from about 48° to 132°.

A horizontally stratified ionosphere provides an almost perfectly reflecting surface for radio echo sounding. The reflection (Fig. 1) occurs because free-space electromagnetic radiation cannot propagate at frequencies below the electron plasma frequency (*10*), which is given by $f_p = 8980\sqrt{n_e}$ Hz, where n_e is the electron number density in cm^{-3}. The MARSIS ionospheric soundings are carried out by transmitting a short pulse at a frequency f and then measuring the time delay, Δt, for the echo to return. The time delay is measured as a function of frequency by sequentially stepping the transmission frequency over the frequency range of interest. Three types of echoes usually occur (Fig. 1). The first is a very strong "spike" at the local electron plasma frequency, f_p(local). This response is caused by excitation of electrostatic oscillations at the electron plasma frequency (*10*). The second is an echo from the ionosphere that extends from f_p(local) to the maximum plasma frequency in the ionosphere, f_p(max), above which the radio wave can penetrate through the ionosphere to the surface. The third is a surface reflection that extends from f_p(max) to the maximum sounding frequency. The ionospheric echo and the surface reflection come together in a sharply defined cusp, centered on f_p(max). The cusp occurs because the propagation speed of the wave packet (i.e., the group velocity) is very small over an increasingly long path length as the wave frequency approaches f_p(max).

[1]Department of Physics and Astronomy, University of Iowa, Iowa City, IA 52242, USA. [2]Max Planck Institute for Solar System Research, 37191 Katlenburg-Lindau, Germany. [3]Jet Propulsion Laboratory, Pasadena, CA 91109, USA. [4]Infocom Department, "La Sapienza" University of Rome, 00184 Rome, Italy.

*To whom correspondence should be addressed. E-mail: donald-gurnett@uiowa.edu

Observations. The Mars Express spacecraft is in an eccentric orbit around Mars with a periapsis altitude of about 275 km, an apoapsis altitude of about 10,100 km, an orbital inclination of 86°, and a period of 6.75 hours. A typical MARSIS ionospheric sounding pass lasts about 40 min and starts at an altitude of about 1200 km on the inbound leg, extends through periapsis, and ends at an altitude of about 1200 km on the outbound leg. Because of gravitational perturbations, the local time and latitude of periapsis evolve rather rapidly. Most of the data collected so far (June to October 2005) have been from the day side of Mars, although a small amount is available from the night side near the evening terminator. The ionospheric soundings are typically displayed in the form of an ionogram, which is a plot of the echo strength versus frequency and time delay. Two ionograms (Fig. 2) have been selected to illustrate the range of phenomena typically observed. The closely spaced vertical lines in the upper left corner of the first ionogram (Fig. 2A) are at harmonics of the local electron plasma frequency and are caused by the excitation of electron plasma oscillations, in this case at a frequency that is slightly below the low-frequency cutoff (100 kHz) of the receiver. Even though the fundamental of the plasma frequency is not observed directly in this case, the plasma frequency can still be determined from the spacing of the harmonics and is f_p(local) = 44 kHz. At somewhat higher frequencies, from about 0.5 to 1.7 MHz, a strong, well-defined ionospheric echo can be seen with time delays ranging from about 4 to 5 ms. At even higher frequencies, from about 1.7 to 5.5 MHz, a strong reflected signal from the surface of Mars is apparent. The maximum plasma frequency in the ionosphere, f_p(max), can be identified from the cusp and is 1.71

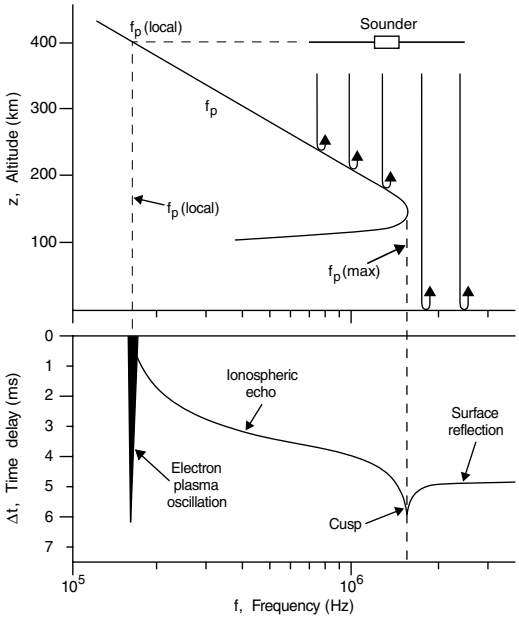

Fig. 1. The top panel shows a representative profile of the electron plasma frequency f_p in the martian ionosphere as a function of altitude z, and the bottom panel shows the corresponding ionogram, which is a plot of the delay time Δt for a sounder pulse at a frequency f to reflect and return to the spacecraft. The intense vertical "spike" at the local electron plasma frequency, f_p(local), is caused by electron plasma oscillations excited by the sounder pulse. At frequencies from f_p(local) to the maximum frequency in the ionosphere, f_p(max), an ionospheric echo is detected, followed at higher frequencies by a reflection from the surface. The ionospheric echo trace and the surface reflection trace form a cusp centered on f_p(max).

MHz. An unexpected feature is the presence of a second ionospheric echo with time delays ranging from about 6.3 to 7.1 ms. This echo has to arise from an oblique reflection, because the apparent range ($c\Delta t/2$, where c is the speed of light) given on the right side of the spectrogram is substantially greater than the distance to either the ionosphere or the surface. The origin of such oblique echoes will be discussed later.

Another unexpected effect, consisting of a series of echoes equally spaced in time, is seen along the left edge of the second ionogram (Fig. 2B). Comparisons of these echoes with the magnetic field model of Cain *et al*. (*11*) show that the repetition rate of these echoes, $1/T_c$, is almost exactly the local electron cyclotron frequency, $f_c = 28\ B$ Hz, where B is the magnetic field strength in nT. Because of the close relation to the electron cyclotron frequency, these echoes are called "electron cyclotron echoes." Such echoes are very common and are usually present whenever the magnetic field strength is greater than a few tens of nT. We believe that these echoes are caused by electrons accelerated by the strong electric fields near the antenna during each cycle of the transmitter waveform. The cyclotron motion of the electrons in the local magnetic field then causes these electrons to periodically return to the vicinity of the antenna, where they induce a signal on the antenna. For this process to occur, the magnetic field strength must be reasonably uniform over a spatial region comparable to the cyclotron radius. For a magnetic field strength of 100 nT, which is a typical crustal field strength at the spacecraft, and a voltage of 500 V, which is the typical antenna voltage, the cyclotron radius is about 1 km. Because the crustal magnetic fields have scale sizes of hundreds of kilometers, this condition is easily satisfied.

In contrast to the first ionogram (Fig. 2A), no surface reflection can be detected in the second ionogram (Fig. 2B). The intensity of the surface reflection is found to be highly variable, a topic of considerable importance for subsurface sounding. Some of this variability can be attributed to solar activity. For example, surface reflections disappeared completely about 2 days after a class X17 solar flare that occurred on 7 September 2005 and did not reappear until 23 September, nearly 2 weeks later. Although further analysis is needed, it seems almost certain that the absorption is caused by energetic charged particles produced by solar flares. The onset of the absorption is usually delayed by a day or more after a flare and tends to last many days, much longer than the typical time scale for decay of the ultraviolet and x-ray radiation associated with a flare. At Earth it is well known that energetic protons from solar flares cause enhanced ionization and absorption of radio waves in the lower levels of the ionosphere

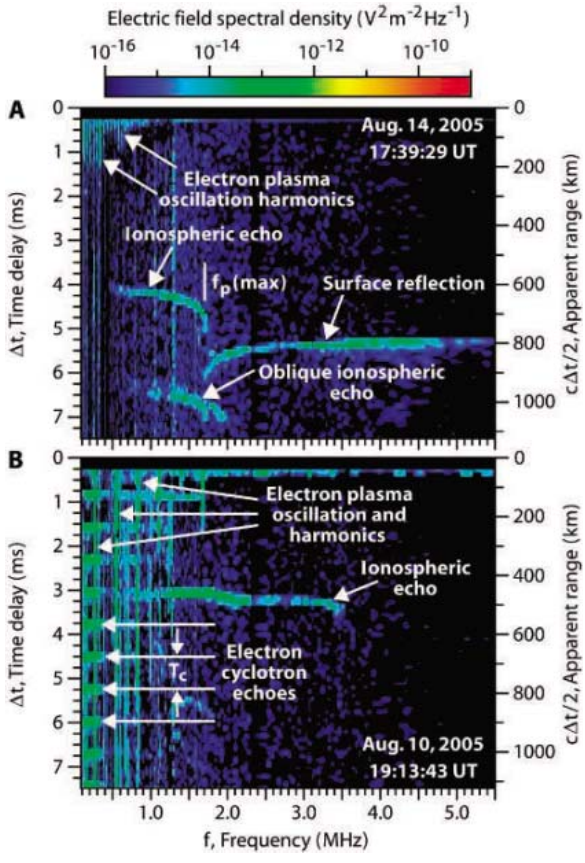

Fig. 2. Two ionograms selected to illustrate typical features found in the MARSIS ionospheric soundings. The ionograms display echo strength (color coded) as a function of frequency f and time delay Δt, with time delay plotted positive downward along the vertical axis. The apparent range to the reflection point $c\Delta t/2$, where c is the speed of light, is shown on the right. Ionogram (**A**) was obtained near the evening terminator at a solar zenith angle of $\chi = 89.3°$ and an altitude of 778 km. Ionogram (**B**) was obtained on the day side at a solar zenith angle of $\chi = 47.9°$ and an altitude of 573 km. Electron plasma oscillation harmonics can be seen in both ionograms, as well as strong echoes from the ionosphere. Ionogram (B) has a series of horizontal, equally spaced echoes along the left side. These echoes occur at the electron cyclotron period and are called electron cyclotron echoes. They are believed to be caused by the cyclotron motion of electrons accelerated by the transmitter pulse. Although a strong surface reflection is present in (A), no surface reflection is present in (B). Surface reflections are seldom seen at solar zenith angles less than about 40° or during periods of intense solar activity.

(*12*), and a similar process may occur at Mars. In addition to the solar flare control, the absorption also appears to increase with decreasing solar zenith angle. Even during periods of low solar activity, surface reflections are rarely observed when the solar zenith angle is less than about 40°.

Ionospheric density models. To compare the MARSIS ionospheric soundings to various ionospheric models, it is necessary to convert the soundings to usable electron density profiles. Although a rough estimate of the density profile can be obtained from the apparent range to the reflection point, for accurate measurements it is necessary to correct for dispersion, which is the effect the plasma has on the propagation speed of the wave. For vertical incidence on a horizontally stratified ionosphere, the round-trip delay time as a function of frequency, $\Delta t(f)$, is given by the integral

$$\Delta t(f) = \frac{2}{c}\int_{z(f_p)}^{z_{sc}} \frac{dz}{\sqrt{1 - \frac{f_p^2(z)}{f^2}}} \qquad (1)$$

where the integration is carried out from the reflection point altitude, $z(f_p)$, to the spacecraft altitude, z_{sc}. Because $\Delta t(f)$ is known from the ionospheric echo trace, the basic problem is to invert the integral to obtain $z(f_p)$, i.e., the altitude of the reflection point as a function of the plasma frequency. Once this is known, the equation $f_p = 8980\sqrt{n_e}$ can be used to obtain $z(n_e)$. Although the mathematical techniques for carrying out this inversion are straightforward, there are sometimes practical difficulties. For example, the ionospheric echo trace often does not extend down to the local plasma frequency (Fig. 2). In such cases it is necessary to make a reasonable guess as to how the echo trace extends from the lowest frequency measured to the local plasma frequency. Normally the inversion is not very sensitive to this choice, because the correction to the propagation speed becomes quite small when the plasma frequency is well below the wave frequency.

An example of an electron density profile obtained by inverting Eq. 1 is shown (Fig. 3A). This profile was obtained by using both the ionospheric echo trace and the surface reflection trace (Fig. 2A). Our approach was to select a theoretical model for the density profile and then adjust the parameters in the model to give the overall best fit to the measured time delays. For a density model, we use the following equation from Chapman (*13*)

$$n_e = n_0 \exp\left[\frac{1}{2}\left\{1 - \frac{z - z_0}{H} - \mathrm{Ch}(x,\chi)\exp\left(-\frac{z - z_0}{H}\right)\right\}\right] \qquad (2)$$

where z is the altitude, n_0 is the maximum electron density at the subsolar point, and z_0 is the altitude of this maximum. The function

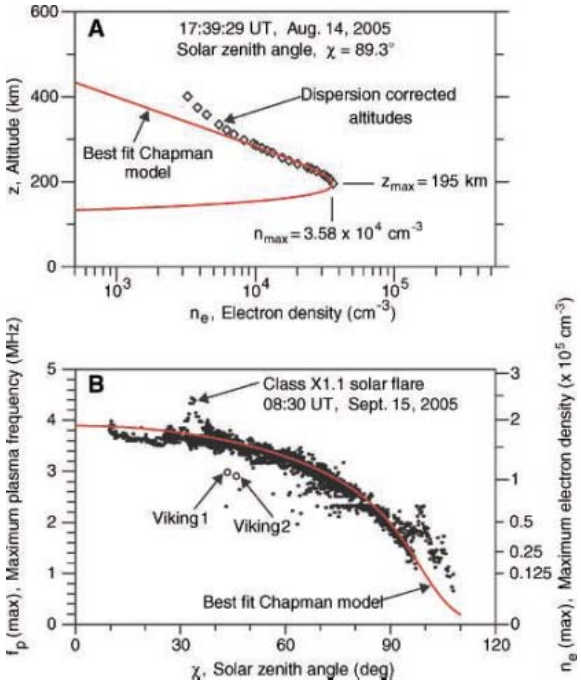

Fig. 3. Two illustrations comparing electron densities obtained from ionospheric soundings to the Chapman (*13*) ionospheric density model. The diamond-shaped points in (**A**) give the electron density profile computed from the ionospheric echo trace in Fig. 2A after correcting for dispersion. The red curve gives the best fit to this density profile, while simultaneously providing a good fit to the surface reflection trace. The best-fit parameters are $n_0 = 1.32 \times 10^5$ cm^{-3}, $z_0 = 130$ km, $z_{max} = 195$ km, $n_{max} = 3.58 \times 10^4$ cm^{-3}, $H = 25$ km, $x = 141$, and Ch(x, χ) = 13.5. Plot (**B**) shows the maximum plasma frequency in the ionosphere, f_p(max), as a function of solar zenith angle χ for 12 randomly selected orbits. The corresponding electron density is shown on the right side of the plot. The red line is the best fit to the Chapman electron density model using $(q_0/\alpha)^{1/2} = 1.98 \times 10^5$ cm^{-3}.

Ch(x, χ) is called Chapman's grazing incidence function and takes into account the absorption of the solar radiation as it passes obliquely through the atmosphere. This function depends on the solar zenith angle χ and a dimensionless parameter $x = (R_M + z_0)/H$, where $R_M = 3396$ km is the radius of Mars, and H is the scale height of the neutral atmosphere. Ch(x, χ) can be computed from a power series (*13*) or from a table provided by Wilkes (*14*). The fit to the top-side electron density profile is very good (Fig. 3A). The maximum electron density, $n_{max} = 3.58 \times 10^4$ cm^{-3}, and the altitude of the maximum, $z_{max} = 195$ km, are in reasonable agreement with radio occultation results at this solar zenith angle (*6*, *7*). Although the bottom-side electron density profile cannot be expected to represent complicated features such as multiple density layers, the model does accurately represent the top-side electron density profile near the peak and the total electron content (TEC) through the ionosphere, which is determined by the dispersion of the surface reflection. The total electron content is defined as the integral $\int n_e dz$ along a vertical line through the ionosphere and, in this case, is TEC = 3.7×10^{11} cm^{-2}. The deviation of the measured electron densities from the model at altitudes above about 300 km is probably caused by upward diffusion of plasma away from the region of photochemical equilibrium described by Chapman's model.

To study the dependence of the maximum electron density n_{max} on the solar zenith angle χ, the maximum frequencies of the ionospheric echo traces have been measured for 12 randomly selected passes from 5 July to 10 October 2005. During this time, the solar zenith angle at periapsis systematically decreased from 98° to 16°, thereby providing a good sampling of solar zenith angles. A scatter plot of the measured f_p(max) values is shown (Fig. 3B) as a function of solar zenith angle. As can be seen, the maximum plasma frequency has a very clear systematic dependence on solar zenith angle, varying from about 3.9 MHz near the subsolar point to less than 1 MHz on the night side. A scale showing the corresponding electron density values is given on the right side of the plot. These electron densities are in good agreement with the results from radio occultation measurements (*6*, *7*) but slightly higher than the in situ Viking 1 and 2 measurements (*15*), which were obtained during a less active phase of the solar cycle.

The solar zenith angle dependence (Fig. 3B) can be compared directly with the predictions of Chapman's electron density model. In Chapman's model, the maximum electron density in the ionosphere is given by

$$n_e(\max) = (q_0/\alpha)^{1/2}/\mathrm{Ch}(x,\chi)^{1/2} \qquad (3)$$

where q_0 is the ionization rate at the subsolar point and α is the recombination rate. The best fit of this equation to the measured n_e(max) values is shown by the red line. This fit uses the same basic parameters as in the first fit (Fig. 3A), with the exception of the parameter $(q_0/\alpha)^{1/2} = 1.98 \times 10^5$ cm^{-3}, which has been adjusted to give the best overall fit. The fit has been purposely selected near the most dense cluster of points, ignoring the outlying points. The outlying points are almost certainly influenced by solar events. For example, the sharp peak in the density that occurred during a pass at a solar zenith angle of about 34° coincides with a class X1.1 solar flare that occurred at 08:30 UT (Universal Time) on 15 September 2005. The enhanced electron densities during this event are almost certainly caused by an intense burst of ultraviolet radiation arriving from the Sun. Other large enhancements, well above the electron densities predicted by Chapman's equation, can also be seen on the night side at solar zenith angles of 98° and 104°. These events are not associated with any known solar flare activity. The ionospheric echoes in this region are often very diffuse and sometimes have unusual characteristics, such as a surface reflection that extends below the ionospheric echo trace. Such echoes are impossible in a horizontally stratified ionosphere and are suggestive of considerable small-scale structure, possibly consisting of low density "holes" like those that have been observed on the night side of Venus (*16*).

Oblique echoes. Oblique ionospheric echoes (Fig. 2A) are a common feature in the MARSIS ionograms. Inspection of successive ionograms shows that the range of these echoes systematically either increases or decreases with increasing time and sometimes merges with the vertical echoes. A good way to study these echoes is to make a plot of the echo strength at a fixed frequency as a function of time and apparent altitude (Fig. 4). Apparent altitude is defined as the spacecraft altitude minus the apparent range. In this display, the vertical echo is the nearly horizontal line at an altitude of about 120 km. The oblique echoes almost always have the shape of a downward-facing hyperbola, sometimes consisting of both branches, but more frequently consisting of only one branch or part of a branch. Sometimes the apex of the hyperbola merges with the vertical echo, as in the event marked A. In a radar display of this type, hyperbola-shaped echoes are characteristic of relative motion between the radar and an off-vertical target. The asymptotic slopes of the hyperbola-shaped echoes are consistent with the motion of the spacecraft relative to a feature that is fixed with respect to Mars. We have verified this hypothesis by comparing repeated passes over the same region of Mars. Such comparisons show that nearly identical hyperbola-shaped features often reappear over the same region. The ones that do not show a good pass-to-pass correlation often occur in very complicated regions with many overlapping echoes, such as near the center of Fig. 4.

Strong evidence exists that most of the oblique ionospheric echoes are related to ionospheric density structures caused by the crustal magnetic fields discovered by the Mars Global Surveyor spacecraft (*17*–*19*). In a comparison (bottom panel of Fig. 4) with the crustal magnetic field computed at an altitude of 150 km using the global magnetic field model developed by Cain *et al.* (*11*), the oblique echoes are seen to occur in the region where strong magnetic fields are present. Inspection of other

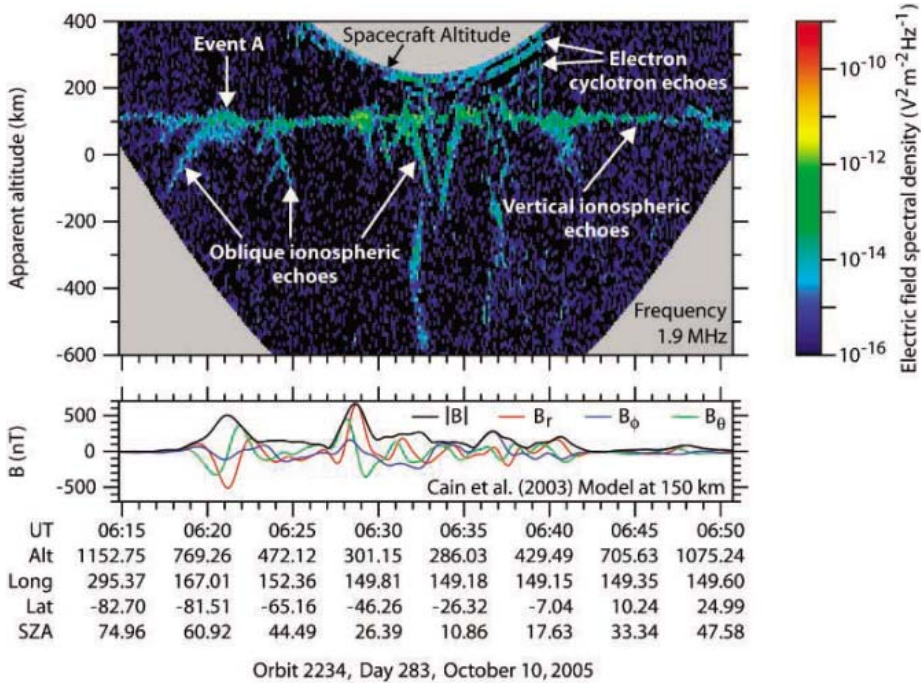

Fig. 4. The top panel shows echo strengths at a frequency of 1.9 MHz plotted as a function of time and apparent altitude, which is the spacecraft altitude minus the apparent range of the echo. The bottom panel shows three components, B_r, B_θ, and B_φ, of the crustal magnetic field and the magnitude of the magnetic field, |B|, computed from the Cain *et al*. magnetic field model at an altitude of 150 km. The nearly horizontal echoes at an altitude of about 120 km are vertical echoes, and the downward-facing hyperbola-shaped features are oblique echoes. This and other similar examples provide strong evidence that density structures related to crustal magnetic fields are responsible for most of the oblique echoes.

similar plots confirms this basic relationship. Although the detailed correlation between the oblique echoes and the magnetic field is often complicated and difficult to resolve, in some cases, such as event A in Fig. 4, the relationship is quite clear. For this event, the apex of the hyperbola-shaped echo is coincident with a well-defined peak in the magnetic field. Furthermore, near the apex, the altitude of the oblique echo (which has merged with the vertical echo) is clearly seen to be greater than the altitude of the surrounding ionosphere, which indicates an upward bulge in the ionosphere. Note also that the magnetic field is nearly vertical in this region, as can be seen by the radial (vertical) component, B_r, which is much stronger than either the southward, B_θ, or eastward, B_φ, components. These and numerous other similar observations lead us to conclude that the oblique echoes usually arise from an upward bulge in the ionosphere in a region where the magnetic field is nearly vertical (Fig. 5A). As the spacecraft approaches the bulge, oblique echoes start as soon as the constant density surface ($f = f_p$) is normal to the line of sight from the spacecraft (Fig. 5B). Two echoes are then detected until the spacecraft is nearly over the bulge, at which point the vertical echo disappears or merges with the oblique echo as the spacecraft passes over the bulge. This basic model is consistent with radar occultation measurements that show an increase in the scale height in regions where the crustal magnetic field is nearly vertical (*20*–*23*). The bulge is believed to be due to heating and the resulting increase in the scale height, caused by solar wind electrons that have access to the lower levels of the ionosphere along open magnetic field lines (*20*, *23*). More complex structures probably exist in regions where the magnetic field is very complex, such as near the middle of the plot in Fig. 4, or in regions where the crustal magnetic fields are strong enough to stand off the solar wind (*24*).

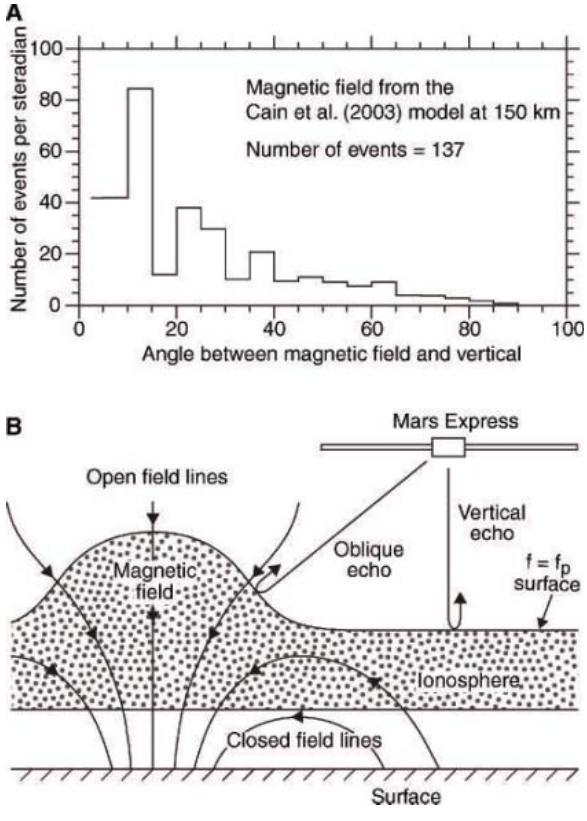

Fig. 5. (**A**) The distribution of oblique echo events as a function of the angle between the magnetic field and vertical. The angles were evaluated at the apex of the hyperbola-shaped time delay feature using the Cain *et al*. model. Most of the events occur at angles less than about 40°, indicating that the density structures responsible for the oblique echoes tend to occur in regions where the magnetic field is nearly vertical. (**B**) A sketch of the ionospheric density structures that are thought to be responsible for the oblique ionospheric echoes. As the spacecraft approaches the bulge in the ionosphere, the sounder detects two echoes, a vertical echo from the ionosphere and an oblique echo from the bulge. As the spacecraft passes over the bulge, the vertical echo either merges with the oblique echo or disappears entirely, depending on the exact shape of the bulge. The bulge in the ionosphere is believed to be due to ionospheric heating caused by hot solar wind electrons that reach the lower levels of the ionosphere along open magnetic field lines.

Although crustal magnetic fields are almost certainly involved in producing the majority of the oblique echoes, cases have been found where the echoes exist in regions where the Cain *et al*. model does not predict detectable crustal magnetic fields. We do not know if these cases involve a failure of the Cain *et al*.

model or whether there are other mechanisms for producing such echoes. Possible mechanisms are wind-driven atmospheric waves excited by topographic features and various types of wavelike structures in the ionosphere driven by interactions with the solar wind.

Conclusion. The MARSIS ionospheric soundings have shown that the ionosphere of Mars is in good agreement with the expectations of Chapman's 1931 photoequilibrium theory for the origin of planetary ionospheres. The soundings have also revealed a number of unexpected features. These include echoes that reoccur at the electron cyclotron period, large variations in the absorption apparently caused by energetic solar events, oblique echoes caused by ionospheric structures associated with the crustal magnetic fields of Mars, diffuse echoes apparently caused by scattering from ionospheric irregularities, and ionospheric holes. Because the subsurface soundings must occur at frequencies well above the maximum electron plasma frequency in the ionosphere and under conditions of low ionospheric absorption, these measurements have already proved to be quite useful for planning subsurface sounding operations. The electron cyclotron echoes also provide a new method of measuring the local magnetic field strength, which is useful because Mars Express does not have a magnetometer.

References and Notes

1. A. Chicaro, P. Martin, R. Traunter, *Mars Express: A European Mission to the Red Planet, SP-1240* (European Space Agency Publication Division, Noordwijk, Netherlands, 2004).
2. G. Picardi *et al.*, *Mars Express: A European Mission to the Red Planet, SP-1240* (European Space Agency Publication Division, Noordwijk, Netherlands, 2004).
3. C. A. Franklin, M. A. Maclean, *Proc. IEEE* **57**, 897 (1969).
4. E. L. Hagg, E. J. Hewens, G. L. Nelms, *Proc. IEEE* **57**, 949 (1969).
5. W. Calvert, J. R. McAfee, *Proc. IEEE* **57**, 1019 (1969).
6. M. H. G. Zhang, J. G. Luhmann, A. J. Kliore, *J. Geophys. Res.* **95**, 17095 (1990).
7. J. G. Luhmann, L. H. Brace, *Rev. Geophys.* **29**, 121 (1991).
8. D. P. Hinson, G. L. Tyler, L. J. Hollingsworth, R. J. Wilson, *J. Geophys. Res.* **106**, 1463 (2001).
9. M. Pätzold *et al.*, *Science* **310**, 837 (2005).
10. D. A. Gurnett, A. Bhattacharjee, *Introduction to Plasma Physics* (Cambridge Univ. Press, Cambridge, 2005), p. 114.
11. J. C. Cain, B. B. Ferguson, D. Mozzoni, *J. Geophys. Res.* **108** (E2), 5008 10.1029/2000JE001487 (2003).
12. J. D. Patterson, T. P. Armstrong, C. M. Laird, D. L. Detrick, A. T. Weatherwax, *J. Geophys. Res.* **106**, 149 (2001).
13. S. Chapman, *Proc. Phys. Soc.* **43**, 483 (1931).
14. M. V. Wilkes, *Proc. R. Soc. London B. Biol. Sci.* **67**, 304 (1954).
15. W. B. Hanson, S. Sanatani, D. R. Zuccaro, *J. Geophys. Res.* **82**, 4351 (1977).
16. L. H. Brace *et al.*, in *Venus*, D. M. Hunten, L. Colin, T. M. Donahue, V. I. Moroz, Eds. (Univ. of Arizona Press, Tucson, AZ, 1983), pp. 779–840.
17. M. H. Acuña *et al.*, *Science* **279**, 1676 (1998).
18. M. H. Acuña *et al.*, *Science* **284**, 790 (1999).
19. J. E. P. Connerney *et al.*, *Geophys. Res. Lett.* **28**, 4015 (2001).
20. N. F. Ness *et al.*, *J. Geophys. Res.* **105**, 15991 (2000).
21. A. M. Krymskii *et al.*, *J. Geophys. Res.* **107** (A9), 1245, 10.1029/2001JA000239 (2002).
22. A. M. Krymskii, T. K. Breus, N. F. Ness, D. P. Hinson, D. I. Bojkov, *J. Geophys. Res.* **108** (A12), 1431, 10.1029/2002JA009662 (2003).
23. A. M. Krymskii *et al.*, *J. Geophys. Res.* **109**, A11306, 10.1029/2004JA010420 (2004).
24. D. L. Mitchell *et al.*, *J. Geophys. Res.* **106**, 23419 (2001).

25. We thank the many members of scientific, technical, and management teams at NASA, the European Space Agency, the Italian Space Agency, and various industry groups for their considerable effort in making this project a success. The research at the University of Iowa was supported by NASA through contract 1224107 with the Jet Propulsion Laboratory.

26 October 2005; accepted 22 November 2005
Published online 30 November 2005;
10.1126/science.1121868
Include this information when citing this paper.

Animal Evolution and the Molecular Signature of Radiations Compressed in Time

Antonis Rokas,* Dirk Krüger,† Sean B. Carroll‡

The phylogenetic relationships among most metazoan phyla remain uncertain. We obtained large numbers of gene sequences from metazoans, including key understudied taxa. Despite the amount of data and breadth of taxa analyzed, relationships among most metazoan phyla remained unresolved. In contrast, the same genes robustly resolved phylogenetic relationships within a major clade of Fungi of approximately the same age as the Metazoa. The differences in resolution within the two kingdoms suggest that the early history of metazoans was a radiation compressed in time, a finding that is in agreement with paleontological inferences. Furthermore, simulation analyses as well as studies of other radiations in deep time indicate that, given adequate sequence data, the lack of resolution in phylogenetic trees is a signature of closely spaced series of cladogenetic events.

Detailed knowledge of the phylogenetic relationships among Metazoa and their eukaryotic relatives is critical for understanding the history of life and the evolution of molecules, phenotypes, and developmental mechanisms. Currently, with the exception of the well-resolved phylogenetic history of the deuterostomes (*1*), the relationships between and within protostome and diploblastic metazoan phyla remain unresolved (*2*–*5*). The uncertainty surrounding metazoan relationships may result from analytical and biological factors such as insufficient amounts of available sequence data, mutational saturation, the occurrence of unequal rates of evolution between lineages, or the rapidity with which metazoan phyla diversified (*3*–*7*).

Recent investigations concerning two critical variables of phylogenetic experimental design—the number of taxa and amount of data used—have guided our approach to metazoan relationships. It has been shown that taxon number may not be as critical a determinant of phylogenetic accuracy (*8*, *9*) as the choice of taxa (*10*). Thus, to investigate relationships among phyla at the base of the metazoan tree and within protostomes, we selected metazoans and closely related eukaryotes that included representatives from choanoflagellates, poriferans (one representative from each of the three poriferan classes), cnidarians (one representative from each of two of the three cnidarian classes), platyhelminths (two representatives), priapulids, annelids, mollusks, arthropods, nematodes, urochordates, and vertebrates (three representatives) (all taxa are listed in table S1).

The use of single or few genes is now recognized to be insufficient for the confident resolution of many clades (*4*, *11*, *12*). In contrast, analyses of larger amounts of data have robustly resolved relationships in many taxonomic groups (*11*–*14*), even after allowance for a high percentage of missing data (*12*–*14*). Thus, to increase resolution of metazoan relationships, we used experimental and bioinformatic approaches to assemble a data matrix composed of 50 genes from the 17 selected taxa (*15*). Gene sequences from five key taxa were obtained through an automated polymerase chain reaction and sequencing approach we devised for the systematic amplification of large amounts of gene sequence data from cDNA of any metazoan (*15*) (table S2). Gene sequences from the 12 other taxa were retrieved through bioinformatic means from public databases (*15*).

Howard Hughes Medical Institute, Laboratory of Molecular Biology, R. M. Bock Labs, University of Wisconsin–Madison, 1525 Linden Drive, Madison, WI 53706, USA.

*Present address: The Broad Institute of MIT and Harvard, 320 Charles Street, Cambridge, MA 02141, USA.
†Present address: Departments of Bacteriology and Plant Pathology, University of Wisconsin–Madison, 420 Henry Mall, Madison, WI 53706, USA.
‡To whom correspondence should be addressed. E-mail: sbcarrol@wisc.edu

A 50-gene data matrix does not resolve relationships among most metazoan phyla. Despite the large amount of data from taxa spanning the Metazoa, analyses of this data matrix and subsets thereof under maximum likelihood (ML) and maximum parsimony (MP) (*15*) still failed to resolve most relationships (Fig. 1 and fig. S1). There was no significant support (defined as >70% bootstrap support) for the order of relationships between early branching metazoans or within protostomes. Resolution of well-established "superclades" (protostomes, bilaterians, vertebrates, and deuterostomes; and metazoans with choanoflagellates as an outgroup) was attained with moderate to high support, depending on the optimality criterion used. The recovery of these superclades suggests that our failure to resolve relationships within them is either due to aspects of our experimental design [such as systematic error artifacts resulting from violation of phylogenetic assumptions (*16*)] or may reflect a prevailing limit to the resolution of certain clades in deep time.

One recurrent problem for phylogenetic inference in deep time is the phenomenon of long branch attraction (*17*), under which unrelated taxa with long branches can artifactually be placed together. To test whether the inclusion of taxa with long branches [as visually identified on the ML tree (fig. S1)] had an effect on support values, we analyzed the data matrix, excluding long-branched taxa singly or in combination. For example, a clade joining platyhelminths and nematodes received moderate support, but all taxa in the clade are characterized by conspicuously long branches (fig. S1). The removal of long-branched taxa had a negligible effect on support for most internodes (table S3). For example, although support for protostomes and bilaterians did increase after the exclusion of nematode and platyhelminth taxa, the resolution of nodes within these superclades was not improved.

Clade support values can be very sensitive to the presence of "rogue" taxa whose placement on the tree may be unstable (*17*). To test whether the presence of rogue taxa could be responsible for the low support in many internodes of the metazoan phylogeny, the least stable metazoan taxa in this data matrix were identified using leaf stability indices (*15*). Removal of these taxa had a negligible effect on support (table S3). Furthermore, tests of additional parameters, such as deviations in amino acid composition, did not account for the lack of resolution (*15*). These results suggest that the low support values obtained are not due to the instability (or deviation) of a small subset of taxa but are the result of a systemic lack of support for relationships among most taxa.

Because the choice of taxa did not account for the lack of resolution in many key branches of the metazoan tree, we then considered two potential analytical explanations: the amount of missing data contained in the data matrix and the total amount of data used. By necessity of experimental design, the data matrix lacked, on average, 20% of the potential data per taxon (table S4). However, large data sets can be surprisingly tolerant to a high fraction of missing data (*13*, *14*, *18*), and reanalyses of the data matrix excluding the priapulid and the mollusk (the two taxa with the highest percentages of missing data; 68 and 54%, respectively) did not lead to noticeable changes in support (table S3). A second potential explanation may be that the data matrix still contains too few informative characters to robustly resolve phylogenetic relationships among protostomes and early branching metazoans. However, sequence variation is abundant between metazoan taxa, with 56% of the 12,060 amino acid sites being variable and 31% of the sites being parsimony-informative (Table 1). Furthermore, MP site pattern and ML mapping (*15*) analyses suggest that the differences in resolution between clades do not result from the number of informative sites per se, but in how these sites are distributed among alternative topologies (fig. S2). In agreement with these results, two- to eightfold increases in the number of characters resampled by bootstrapping (*15*) led to small improvements in the resolution of most internodes (fig. S3 and table S3). These data

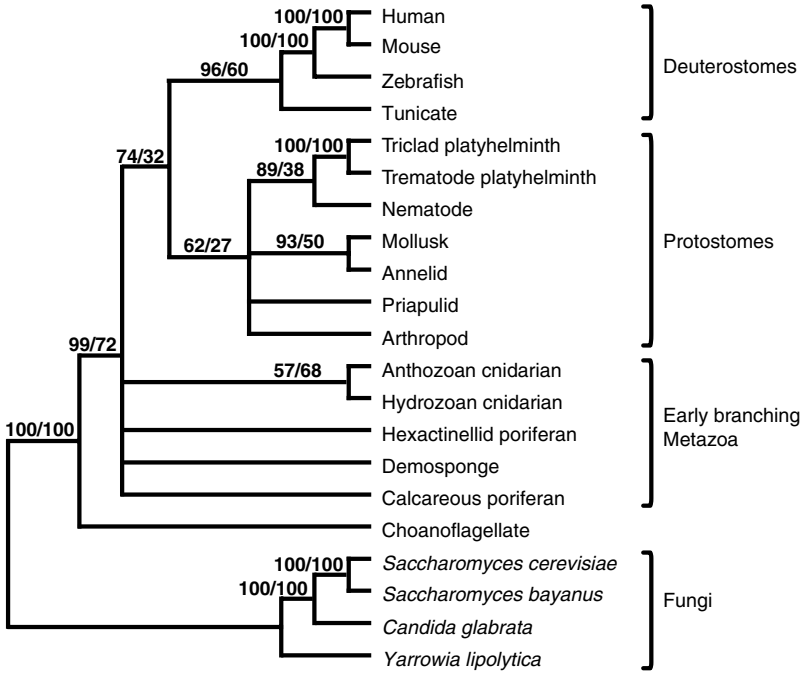

Fig. 1. The lack of resolution in phylogenetic relationships among major metazoan phyla. Values above internodes correspond to support values from ML and MP analyses, respectively. Only internodes with significant support in at least one of the two analyses (ML and MP) or internodes present in majority-rule consensus trees of both analyses are drawn. Analyses were also performed by Bayesian inference (*15*) (fig. S1). Although certain analyses provided strong support for particular clades, analyses of different subsets of taxa produced significantly different and conflicting results (table S3).

Table 1. Statistical attributes of the amino acid sequence data matrix. Numbers of variable, parsimony-informative, and singleton sites for the 50-gene data matrix are shown, including 16 metazoan, 1 choanoflagellate, and 15 fungal taxa. Percentages are reported in parentheses. All statistical attributes for the metazoan taxon set were calculated with choanoflagellates included. The mean observed distance (± standard deviation) corresponds to the average proportion of amino acid sites that are different in all pairwise sequence comparisons in a taxon set. The mean estimated distance (± standard deviation) corresponds to the ML-estimated average proportion of amino acid sites that are different in all pairwise sequence comparisons in a taxon set (*15*).

Taxon set	Number of sites	Variable sites	Informative sites	Singleton sites	Observed distance	Estimated distance
All taxa	12060	8257 (68%)	6669 (55%)	1588 (13%)	29.2 ± 6.7	35.7 ± 11.1
Metazoa	12060	6782 (56%)	3701 (31%)	3080 (26%)	21.8 ± 4.6	23.4 ± 6.2
Fungi	12060	6533 (54%)	5015 (42%)	1518 (13%)	27.1 ± 5.8	31.7 ± 8.2

suggest that neither the percentage of potential data missing nor the total amount of data in this data matrix can explain the lack of resolution among protostomes and early branching metazoans.

A remarkable contrast in phylogenetic resolution between two kingdoms. Given the time since the origin of Metazoa, another hypothesis is that mutational saturation (*19*–*21*) may have erased the phylogenetic signal originally contained in proteins' variable sites. Alternatively, the lack of resolution may be the signature of a closely spaced series of cladogenetic events occurring early in the evolution of Metazoa (*7*). One means of testing these alternative explanations is by comparing the phylogeny of Metazoa to that of their natural sister kingdom, the Fungi (*22*). The validity of this comparison rests on the inference that both lineages originated within approximately the same geological time frame, which is supported by the fossil record of both Fungi (*23*) and Metazoa (*24*, *25*), particularly recent finds in the Doushantuo Formation (551 to 635 million years old) (*23*, *26*, *27*), as well as molecular clock analyses in which multiple representatives of both kingdoms are included (*28*–*30*).

The availability of genome sequence data from many species spanning the fungal kingdom enabled us to sample exactly the same type and amount of data across Fungi as we did for Metazoa. We generated a data matrix containing 49 of the same 50 genes used for the metazoan phylogeny from a select set of 15 taxa representing most major taxonomic groups within Ascomycetes and Basidiomycetes (table S1). Examination of evolutionary distances and models of amino acid evolution for the 49 orthologs in each of the two kingdoms suggests that the tempo and mode of molecular evolution in this set of 49 genes has remained similar across the two kingdoms (table S5). Furthermore, comparisons of evolutionary distances within this set of fungi and within their metazoan counterparts suggest that both clades have undergone similar amounts of evolutionary change, with Fungi exhibiting slightly higher mean distances [mean observed/estimated distances ± standard error: Metazoa, 21.8 ± 4.6%/23.4 ± 6.2%; Fungi, 27.1 ± 5.8%/31.7 ± 8.2% (Table 1)], a finding consistent with a similar date of origin (table S6).

Phylogenetic analyses of the data matrix containing both Metazoa and Fungi showed a remarkable contrast in the resolution obtained within each of the two kingdoms. The fungal clade was robustly resolved, with the overwhelming majority of fungal internodes (11 out of 13) being significantly supported, irrespective of optimality criterion used (Fig. 2 and fig. S4). These relationships are generally in agreement with previous studies (*31*). In contrast, again only 4 of 14 metazoan internodes were significantly supported under both optimality criteria.

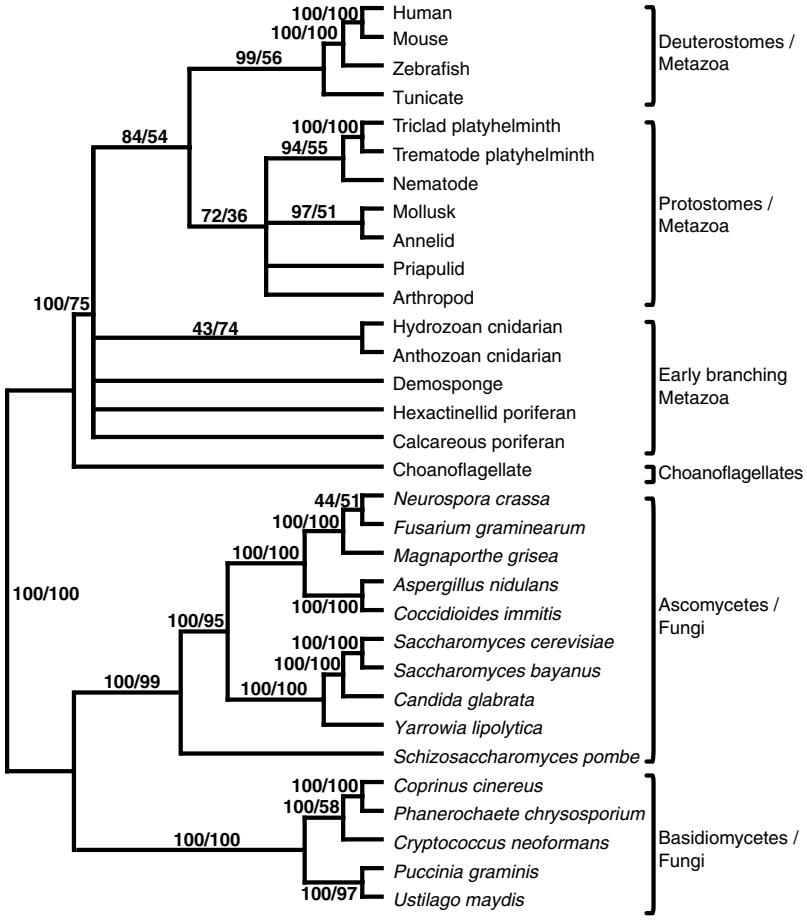

Fig. 2. The contrast in phylogenetic resolution between the clades of Metazoa and Fungi. Values above internodes are as in Fig. 1. Eleven out of 13 internodes in the fungal clade are significantly supported by both optimality criteria (ML and MP), whereas only 4 out of 14 internodes in the metazoan clade are significant. Analyses were also performed by Bayesian inference (*15*) (fig. S4 and table S3).

The early history of Metazoa as a radiation compressed in time. The contrast in the resolution of the fungal and metazoan trees shows that neither the type nor the amount of data is a limit to the resolution of relationships within metazoan superclades. Therefore, the explanation for the sharp contrast in resolution may lie in differences in the tempo and pattern of cladogenesis within the kingdoms. One explanation for the contrasting resolution observed in the metazoan and fungal trees may be differences in "stemminess: (*32*): a measure of the relative length of internal versus external branches. Theoretical work indicates that the accuracy of reconstruction is higher for trees exhibiting high stemminess (that is, trees with longer internodes and shorter terminal branches) (*32*). In agreement with these studies, phylogenetic resolution is higher in the fungal tree, which is characterized by long internodes (Fiala and Sokal's stemminess index F = 0.201), and poorer in the metazoan clade, where internodes are much shorter (F = 0.121) (*15*). These differences in degree of stemminess between the two kingdoms are also reflected in the distributions of parsimony-informative sites (Fungi/Metazoa = 5015/3701 sites) and singleton sites (Fungi/Metazoa = 1518/3080 sites) along the branches of the two trees (Table 1).

These contrasts in resolution depth, stemminess, and distribution of site categories between the two kingdoms are consistent with a history of major metazoan lineages characterized by closely spaced (tempo) series of cladogenetic events (pattern). Paleontological evidence also suggests a rapid tempo of cladogenesis near the origin of Metazoa approximately 600 million years ago, with poriferans (*26*), cnidarians (*33*), and at least certain bilaterians (*34*) making their first appearance within 50 million years. Thus, inferences from these two independent lines of evidence (molecules and fossils) support a view of the origin of Metazoa as a radiation compressed in time.

Identifying the limits to resolution of cladogenetic events in deep time by simulation analysis. It has been proposed that, given adequate data, phylogenetic resolution for cladogenetic events of Cambrian age occurring as close as 1 million years apart will be achieved (*35*). If true, with the amount of data

used here, the lack of observed resolution would indicate extreme compression of the metazoan radiation. Alternatively, the limit of resolution for internodes in deep time may be much larger than previously suggested.

To better understand the potential limits to the resolution of series of closely spaced cladogenetic events in deep time, and to explore how to interpret the lack of resolution when large amounts of data are available, we conducted a simulation analysis. The radiation of mammalian orders is particularly well suited for addressing this issue because it occurred within a small window of time (42 million years) an estimated 107 million years ago (*36*), with many internodes estimated to span between 1 and 10 million years in length. We simulated the effect of increasing the elapsed time since the radiation on the phylogenetic accuracy of internodes within this 42-million-year window, given adequate data and a rigorous model of sequence evolution (*15*, *20*, *37*). If the proposed limits of resolution are in fact very small, the degree of resolution for all in-

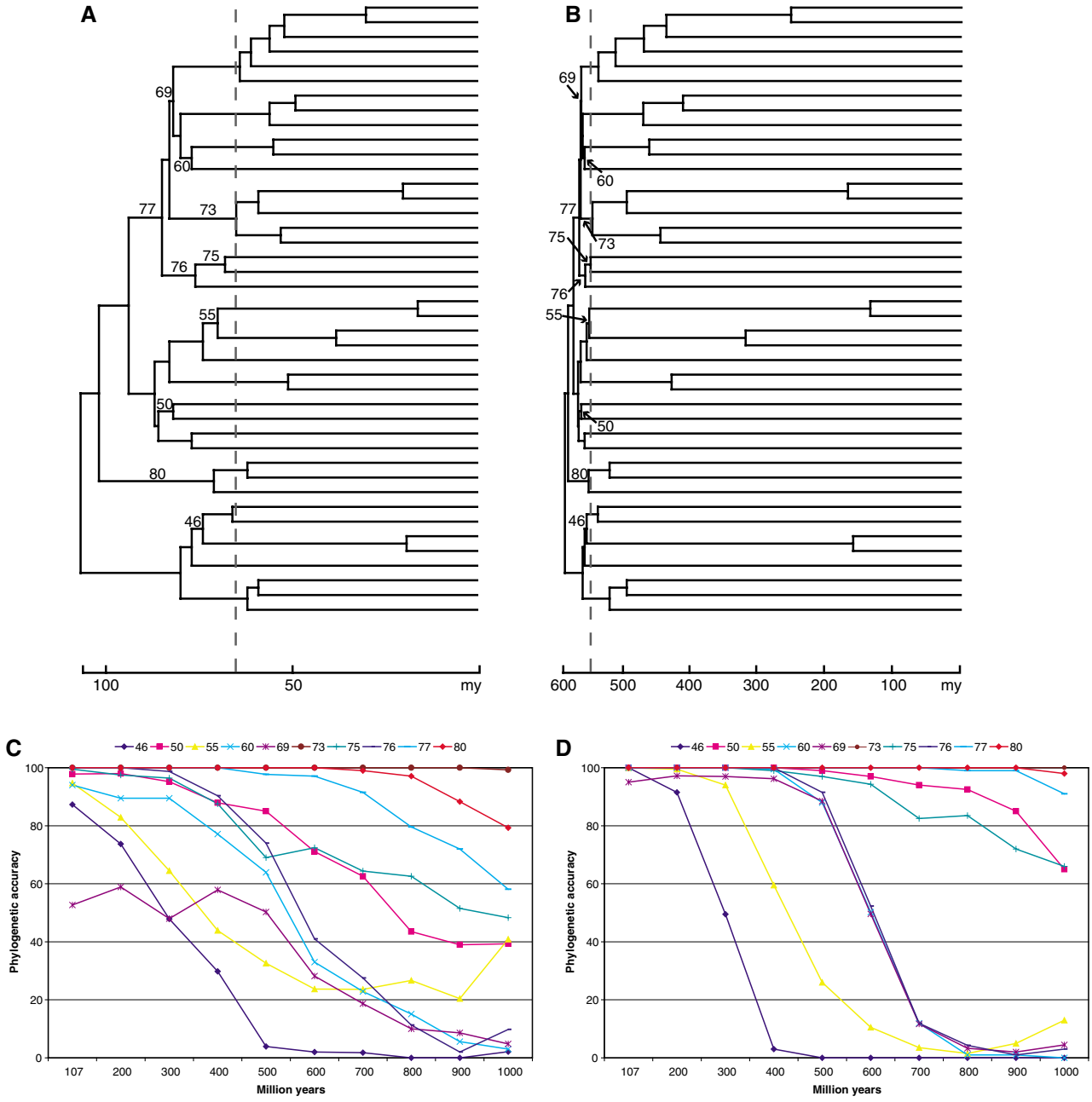

Fig. 3. Phylogenetic accuracy is inversely correlated with the length of time elapsed since a closely spaced series of cladogenetic events. A simulation analysis of increasing the age of origin of the 42-million-year window of mammalian order diversification is shown. (**A**) The best estimate of the mammalian phylogenetic tree at present under the molecular clock assumption (*36*) (time span of 107 million years). (**B**) The mammalian phylogenetic tree, assuming a 600-million-year time span. Branch lengths are shown in million-year time units. The topology and branch lengths within the 42-million-year window (left of the dashed grey line) of trees in (A) and (B) are identical. There is a compression in the lengths of internodes in the 42-million-year window of the tree in (B), due to the longer time span elapsed. (**C**) Graph showing the relationship between phylogenetic accuracy of internodes in the 42-million-year window and total time span simulated, after MP analysis of 100 simulated data matrices, each containing 16,000 characters (of which roughly 6000 are variable). (**D**) The same graph as in (C), but with simulated data matrices, each containing 73,000 characters (of which roughly 28,000 are variable). Similar results were obtained by neighbor-joining (NJ) analyses (fig. S5). Only 10 exemplar internodes are shown (all the internodes are shown in fig. S5). The numbers of internodes in all panels are according to (*36*).

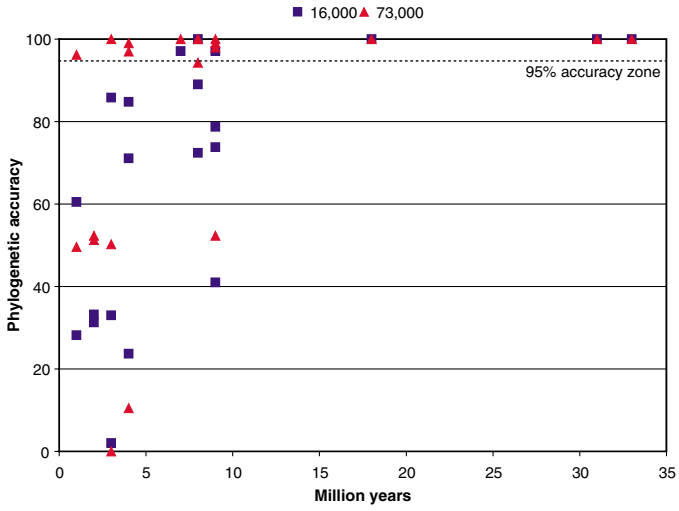

Fig. 4. The limit for resolution of cladogenetic events of Cambrian age, under the best of circumstances, may be an order of magnitude higher than previously thought. The phylogenetic accuracy with which internodes are resolved (the ordinate) is plotted against the length of each internode in million years (the abscissa). Data sets of two different lengths (data set in blue, 16,000 characters, of which 6000 are variable; data set in red, 73,000 characters, of which 28,000 are variable) were generated by simulation, assuming a tree with a 600-million-year time span. For many internodes with lengths much higher than 1 million years, resolution accuracy values are low, irrespective of data set size. Not all internodes of a given age exhibit the same resolution accuracy. For example, certain 3-million-year internodes are resolved with 100% accuracy, whereas other internodes of similar (or greater) age exhibit much lower values of resolution accuracy. Results are shown for analyses using MP [similar results are obtained by NJ analyses (fig. S7)].

ternodes should not be affected, because all internodes are dated as 1 million years in length or longer. However, if the limits of resolution are greater than has been postulated, then the degree of resolution for several internodes should decrease as we move deeper in time.

The results of the simulations show a negative correlation between the amount of time elapsed and the accuracy with which internodes are resolved (Fig. 3 and fig. S5). For example, whereas almost all internodes in simulations assuming a 107-million-year time span are resolved near 100% accuracy (Fig. 3A), the accuracy of several internodes in data sets simulating the lapse of a 600-million-year time span is low (Fig. 3, B to E), contrary to predictions that data matrices of this size and properties should attain accuracy levels of 95% across all internodes (*35*). These results suggest that the actual limits of resolution for closely spaced events in deep time is larger than previously thought (*38*). To estimate the actual limit of resolution, we plotted the phylogenetic accuracy for each internode against the internode's length (in million years), assuming a 600-million-year time span. Results suggest that, even when very large data matrices are used, and under simulation assumptions that most likely represent the best of circumstances when compared to biological data, many internodes with lengths much larger than 1 million years are resolved with accuracies well below 50% (Fig. 4). Thus, the limit of resolution of large data sets in deep time may differ by an order of magnitude from previous estimates (*35*).

The lack of resolution as a signature of events compressed in time. The resolution of other clades of the metazoan tree, in which cladogenetic events are thought to be much further apart than 1 million years, has also proved challenging, despite the use of large amounts of data. For example, fossil evidence suggests that the three major lineages of lobe-limbed vertebrates (lungfish, coelacanths, and tetrapods) first appeared within a time span of 20 to 30 million years approximately 390 million years ago (*39*). However, resolution of the relationships among these three lobe-limbed vertebrate lineages has not been obtained, despite analyses of more than 40 gene sequences from key taxa (*40*). The lack of resolution of lobe-limbed vertebrates, of metazoan phyla here and of other problematic groups that diverged in deep time such as the arthropods, coupled with the simulation studies, suggest that, given adequate sequence data, the lack of phylogenetic resolution is a positive signature of closely spaced cladogenetic events.

Of course, the ultimate objective of phylogenetics is to resolve the true branching order within such important groups. So what are the prospects for doing so? It has been argued that the use of even more gene sequences will increase the resolution of such radiations compressed in deep time (*35*, *40*). However, the number of genes identifiable as orthologs, or usable in taxa that diverged in deep time, may actually turn out to be on the order of the number of genes currently being used in some studies (*13*, *40*). If the maximum number of genes that could further be added to existing data matrices is not much greater, even the use of all conserved gene sequences across metazoan phyla or lobe-limbed vertebrates may not suffice for accurate reconstruction of certain clades. Furthermore, although increasing the gene number greatly reduces sampling error (*11*), the vulnerability to systematic error artefacts also increases (*16*), perhaps explaining how different phylogenetic analyses can reach contradicting inferences with absolute support (*41*–*43*). In such cases, the use of alternative types of molecular characters, such as rare genomic changes (*44*–*46*), and the development of more realistic models of character evolution (*47*) may hold the key to further progress in resolving closely spaced ancient diversification events.

References and Notes

1. T. Rowe, in *Assembling the Tree of Life*, J. Cracraft, M. J. Donoghue, Eds. (Oxford Univ. Press, New York, 2004), pp. 384–409.
2. G. Giribet, *Mol. Phylog. Evol.* **24**, 345 (2002).
3. A. Adoutte *et al.*, *Proc. Natl. Acad. Sci. U.S.A.* **97**, 4453 (2000).
4. A. Rokas, N. King, J. Finnerty, S. B. Carroll, *Evol. Dev.* **5**, 346 (2003).
5. K. M. Halanych, *Annu. Rev. Ecol. Evol. Syst.* **35**, 229 (2004).
6. D. H. Erwin, *Trends Ecol. Evol.* **6**, 131 (1991).
7. D. M. Raup, *Paleobiology* **9**, 107 (1983).
8. A. Rokas, S. B. Carroll, *Mol. Biol. Evol.* **22**, 1337 (2005).
9. M. S. Rosenberg, S. Kumar, *Proc. Natl. Acad. Sci. U.S.A.* **98**, 10751 (2001).
10. S. Poe, D. L. Swofford, *Nature* **398**, 299 (1999).
11. A. Rokas, B. L. Williams, N. King, S. B. Carroll, *Nature* **425**, 798 (2003).
12. E. Bapteste *et al.*, *Proc. Natl. Acad. Sci. U.S.A.* **99**, 1414 (2002).
13. H. Philippe *et al.*, *Mol. Biol. Evol.* **21**, 1740 (2004).
14. A. C. Driskell *et al.*, *Science* **306**, 1172 (2004).
15. Materials and methods are available as supporting material on *Science* Online.
16. M. J. Phillips, F. D. Delsuc, D. Penny, *Mol. Biol. Evol.* **21**, 1455 (2004).
17. M. J. Sanderson, H. B. Shaffer, *Annu. Rev. Ecol. Syst.* **33**, 49 (2002).
18. J. J. Wiens, *Syst. Biol.* **52**, 528 (2003).
19. E. Sober, M. Steel, *J. Theor. Biol.* **218**, 395 (2002).
20. D. Penny, B. J. McComish, M. A. Charleston, M. D. Hendy, *J. Mol. Evol.* **53**, 711 (2001).
21. E. Mossel, M. Steel, in *Mathematics of Evolution and Phylogeny*, O. Gascuel, Ed. (Oxford Univ. Press, Oxford, 2005), pp. 384–412.
22. S. L. Baldauf, A. J. Roger, I. Wenk-Siefert, W. F. Doolittle, *Science* **290**, 972 (2000).
23. X. Yuan, S. Xiao, T. N. Taylor, *Science* **308**, 1017 (2005).
24. A. H. Knoll, S. B. Carroll, *Science* **284**, 2129 (1999).
25. J. W. Valentine, D. H. Erwin, D. Jablonski, *Dev. Biol.* **173**, 373 (1996).
26. S. H. Xiao, Y. Zhang, A. H. Knoll, *Nature* **391**, 553 (1998).
27. C. W. Li, J. Y. Chen, T. E. Hua, *Science* **279**, 879 (1998).
28. S. B. Hedges, J. E. Blair, M. L. Venturi, J. L. Shoe, *BMC Evol. Biol.* **4**, 2 (2004).
29. D. S. Heckman *et al.*, *Science* **293**, 1129 (2001).
30. E. J. Douzery, E. A. Snell, E. Bapteste, F. Delsuc, H. Philippe, *Proc. Natl. Acad. Sci. U.S.A.* **101**, 15386 (2004).
31. F. Lutzoni *et al.*, *Am. J. Bot.* **91**, 1446 (2004).
32. K. I. Fiala, R. R. Sokal, *Evolution* **39**, 609 (1985).
33. J. Y. Chen *et al.*, *Dev. Biol.* **248**, 182 (2002).
34. M. A. Fedonkin, B. M. Waggoner, *Nature* **388**, 868 (1997).
35. H. Philippe, A. Chenuil, A. Adoutte, *Dev. Suppl.* **1994**, 15 (1994).
36. M. S. Springer, W. J. Murphy, E. Eizirik, S. J. O'Brien, *Proc. Natl. Acad. Sci. U.S.A.* **100**, 1056 (2003).
37. C. Ane, J. G. Burleigh, M. M. McMahon, M. J. Sanderson, *Mol. Biol. Evol.* **22**, 914 (2005).
38. We also conducted simulations in which the effect of increasing elapsed time on phylogenetic accuracy was measured, using trees in which all branches are proportionally scaled as time span increases. Results from these simulations show that most internodes are resolved near 100% accuracy, irrespective of

time span simulated (fig. S6 and table S8). These results, combined with the lack of resolution within superclades of the metazoan tree, argue against models of metazoan radiation in which the temporal window of diversification is much larger (*48*).
39. J. A. Clack, *Gaining Ground: the Origin and Evolution of Tetrapods* (Indiana Univ. Press, Bloomington, IN, 2002).
40. N. Takezaki, F. Figueroa, Z. Zaleska-Rutczynska, N. Takahata, J. Klein, *Mol. Biol. Evol.* **21**, 1512 (2004).
41. Y. I. Wolf, I. B. Rogozin, E. V. Koonin, *Genome Res.* **14**, 29 (2004).
42. J. E. Blair, K. Ikeo, T. Gojobori, S. B. Hedges, *BMC Evol. Biol.* **2**, 7 (2002).
43. H. Philippe, N. Lartillot, H. Brinkmann, *Mol. Biol. Evol.* **22**, 1246 (2005).
44. S. L. Baldauf, J. D. Palmer, *Proc. Natl. Acad. Sci. U.S.A.* **90**, 11558 (1993).
45. J. L. Boore, D. Lavrov, W. M. Brown, *Nature* **393**, 667 (1998).
46. A. Rokas, P. W. H. Holland, *Trends Ecol. Evol.* **15**, 454 (2000).
47. A goodness-of-fit test using parametric bootstrapping (*15*) showed that even the best-fit model of sequence evolution does not adequately describe the evolution of the sequence data from these 32 fungal and metazoan taxa (fig. S8).
48. G. A. Wray, J. S. Levinton, L. H. Shapiro, *Science* **274**, 568 (1996).
49. We thank D. Arendt for providing RNA for *Platynereis dumerilii;* C. Ané for providing the modified version of the Seq-Gen simulation software with an implementation of a covarion model; and B. Prud'homme, B. Williams, and T. Rokas for comments on the manuscript. A.R. was funded by a Human Frontier Science Program Long-Term Fellowship. This work was funded by the Howard Hughes Medical Institute.

29 June 2005; accepted 4 November 2005
10.1126/science.1116759

REPORTS

Separation and Conversion Dynamics of Four Nuclear Spin Isomers of Ethylene

Zhen-Dong Sun,* Kojiro Takagi, Fusakazu Matsushima

Molecules with three or more nuclei of nonzero spin exist as discrete spin isomers whose interconversion in the gas phase is generally considered improbable. We have studied the interconversion process in ethylene by creating a sample depleted in the B_{2u} nuclear spin isomer. The separation was achieved through spatial drift of this isomer induced by resonant absorption of narrow-band infrared light. Evolution of the depleted sample revealed conversion between B_{2u} and B_{3u} isomers at a rate linearly proportional to pressure, with a rate constant of 5.5 (±0.8) $\times$ 10^{-4} s^{-1} $torr^{-1}$. However, almost no change was observed in the A_g isomer populations. The results suggest a spin conversion mechanism in C_2H_4 via quantum relaxation within the same inversion symmetry.

Nuclear spin isomers and their stability are fundamental concepts in quantum mechanics (*1*). In accordance with Pauli's principle, all molecules possessing identical nuclei with nonzero spin have distinct nuclear spin isomers (*1*). However, despite continuous study following the first separation and conversion of *ortho*- and *para*-H_2 in 1929 (*2*), the interconversion dynamics of three or more isomers in larger polyatomic molecules remain poorly understood. In astronomy and astrophysics, the abundance ratios of nuclear spin isomers in the interstellar medium (ISM) are key parameters in probing the formation conditions in the past and anticipating subsequent processes in the future evolution of planetary materials and protostellar environments (*3*–*5*). It is widely assumed that the conversion probabilities among nuclear spin isomers for the various molecules in the ISM are zero, even over time spans of millions of years. However, this is not necessarily the case (*6*–*10*).

Department of Physics, University of Toyama, Toyama 930-8555, Japan.

*To whom correspondence should be addressed. E-mail: zdsun@unbsj.ca

To date, separation and conversion of nuclear spin isomers have been successfully studied for only a small number of polyatomic molecules: CH_3F (*6*, *7*), $^{13}C^{12}CH_4$ (*8*), H_2CO (*9*), and H_2O (*11*). Among the separation methods (*6*, *9*, *11*), the light-induced drift (LID) (*12*) technique is one of the more powerful and sensitive tools. The principle of LID can be briefly described as follows: Let a powerful laser pass through a closed cell containing a low-pressure gas mixture of a laser-absorbing species and a nonabsorbing buffer gas. When the laser frequency is tuned to, for example, the red wing of the spectral Doppler absorption profile, a certain velocity class of absorbing molecules moving toward the laser will be excited as a result of the Doppler effect. Because the excited molecules usually have a larger cross section than the ground-state molecules, their mean free path will be smaller than that of the ground-state molecules. This produces a drift of the absorbing species moving in the direction of the laser beam with respect to the buffer gas and results in a concentration difference between the two ends of the closed cell. So far, however, insights from LID studies have been limited to molecules with only *ortho* and *para* isomers (gaseous CH_3F and $^{13}C^{12}CH_4$). For a molecule with more than two nuclear spin isomers, such as the four isomers (A_g, B_{1g}, B_{2u}, and B_{3u}) of $^{12}C_2H_4$ ethylene, the possibility of interconversion remains experimentally unexplored. To address this question, we have assembled a spectrometer, following the design of Nagels *et al.* (*7*), to separate and monitor potential interconversion among the $^{12}C_2H_4$ nuclear spin isomers.

Ethylene has a simple structure and a point group (D_{2h}) of high symmetry. There are two zero-spin ^{12}C nuclei and four hydrogens with active spins of ½. However, unlike *ortho*/*para* hydrogen, one cannot visualize the isomers by flipping the spin of individual nuclei. The symmetry characteristics of the four nuclear spin isomers of C_2H_4 are listed in Table 1 (*13*). Here the coordinate system and group theoretical definitions are the same as those given in the textbook by Herzberg (*14*) and that by Landau and Lifshitz (*1*); the *x*-*y* plane with the *x* axis parallel to the C=C double bond is the molecular plane, and the *z* axis is vertical to it. The four nuclear spin species correspond to different classes of J_{K_a,K_c} rotational levels in the ground rovibrational state, where *J*, K_a, and K_c refer to the quantum numbers for rotational angular momentum and its projections along the *x* and *z* axes, respectively. An energy level of C_2H_4 is of even or odd parity with regard to the inversion operation E^* in D_{2h}(M) in the molecular symmetry group (*10*). As the parity is given by $(-1)^{Kc}$ (*15*), the subscripts *g* or *u* in

Table 1. Species of nuclear spin isomers (NSI) of C_2H_4 (*1*, *14*). *W* is the statistical weight, *I* is the total spin of four equivalent hydrogen nuclei, and even and odd refer to whether K_a and K_c are even or odd integers.

NSI	*W*	*I*	K_a	K_c
A_g	7	2, 0	Even	Even
B_{1g}	3	1	Odd	Even
B_{3u}	3	1	Even	Odd
B_{2u}	3	1	Odd	Odd

Table 2. Experimental schemes and determined absorption coefficient β (cm^{-1} $torr^{-1}$), the percentage of enrichment or depletion (negative values) at a pressure of 1 torr for a 3-min separation period, and pressure dependence of conversion rate $\gamma = kp + y$ of C_2H_4 at a temperature of 300 K, where k, p, and y are in units of s^{-1} $torr^{-1}$, torr, and s^{-1}, respectively. Rovibrational transition is from the ground state to the $\nu_7 = 1$ state. Frequency offset Δf denotes the C_2H_4 transition frequency minus the CO_2 laser frequency.

Case and number	Rovibrational transition	NSI	Laser line	Δf (MHz)	β	Enrichment	k (10^{-4})	y (10^{-4})
Separation	$9_{0,9} \leftarrow 10_{1,9}$	B_{2u}	10*P*44	61				
Probe 1	$9_{0,9} \leftarrow 10_{1,9}$	B_{2u}	10*P*44	61	0.019 ± 0.001	–2.55 ± 0.50	5.76 ± 1.12	1.02 ± 1.98
2	$5_{0,5} \leftarrow 4_{1,3}$	B_{2u}	10*P*10	–100	0.059 ± 0.002	–3.55 ± 0.50	5.79 ± 0.59	1.59 ± 1.17
3	$6_{1,5} \leftarrow 6_{2,5}$	B_{3u}	10*P*26	112	0.097 ± 0.003	0.91 ± 0.10	5.05 ± 0.57	2.57 ± 0.83
4	$4_{3,1} \leftarrow 3_{2,1}$	B_{3u}	10*R*22	102	0.083 ± 0.002	0.94 ± 0.10	5.41 ± 0.92	2.14 ± 1.13
5	$6_{3,4} \leftarrow 5_{2,4}$	A_g	10*R*28	–228	0.191 ± 0.001	0.76 ± 0.15		
Average of cases 1 to 4							5.5 ± 0.8	1.8 ± 1.3

the symmetry representations correspond to even or odd parity of an energy level.

We now report the successful use of LID to deplete the population of the B_{2u} isomer in a sample of gaseous ethylene, followed by monitoring of the subsequent spin conversions for the return to equilibrium. We measured isomer concentrations by recording the absorption intensities of spectral lines with appropriate J, K_a, and K_c quantum numbers. Our experimental setup uses two CO_2 lasers (Edinburgh Instruments PL3 as the separation laser and a home-built laser as the probe) and three glass cells (for separation, test, and reference) (*16*). We measured the spin conversion rates for $^{13}CH_3F$ with this setup and obtained good agreement with the published results (*6*, *7*).

For the ethylene study, the experimental schemes are shown in Table 2, where the reported results from high-resolution infrared spectroscopy (*17*) were used to calculate the frequency offsets between the C_2H_4 transition frequencies and the CO_2 laser frequencies. Application of the LID technique for the separation of nuclear spin isomers requires that a molecular transition be near-coincident with a CO_2 laser line. Here, the 10*P*44 laser line with a power of 6 W was used. Its frequency was tuned about 20 MHz above the center frequency by adjusting the laser cavity length to set it in the red wing of the $9_{0,9} \leftarrow 10_{1,9}$ line of the ν_7 band of ethylene. This frequency selectively excited the B_{2u} isomer, with the other three isomers acting as a buffer gas. The B_{2u} molecules drift, by the LID effect, along the direction of the separation laser beam in the separation cell, thereby depleting the B_{2u} species and enriching the A_g, B_{1g}, and B_{3u} species at the entrance end of the cell; this direction of drift corresponds to an increase in the collision cross section upon excitation. The nonequilibrium population was then transferred through a valve from the near end of the separation cell to the test cell. For high sensitivity, we measured differential absorption by splitting the probe beam to acquire simultaneous data from the test cell and the reference cell with a population at thermal equilibrium. We determined normalized absorption intensity differences for appropriate probe lines to observe the initial degree of isomer depletion or enrichment. At an ethylene pressure of 1 torr, the probe was tuned through five absorption lines belonging to one of the species B_{2u}, B_{3u}, or A_g (cases 1 to 5 in the seventh column of Table 2 together with the corresponding absorption coefficients in the sixth column) (*18*). The depletion of the B_{2u} species was about 3%, with 1% or less enrichment of the other three isomers.

The equilibration kinetics of the B_{2u}-depleted sample were measured as follows: For the first 1-min period, the separation laser was blocked and the valve was kept open to record the zero baseline of the differential signal in the first period. Then, in the second period, the separation laser was unblocked and its beam was introduced into the separation cell for 3 min to generate the nonequilibrium distribution in the test cell. Then the valve was closed, and the decay curves due to isomeric conversion were monitored during the third period. Typical signals are shown for probing B_{2u} (Fig. 1), B_{3u} (Fig. 2A) and A_g (Fig. 2B)

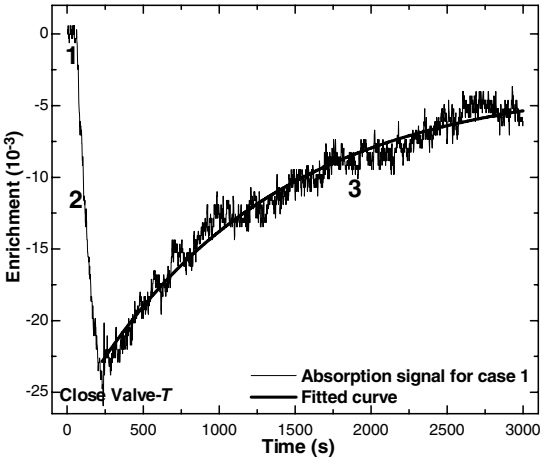

Fig. 1. Recorded differential absorption signal at lock-in time constant of 0.3 s using the 10*P*44 probe CO_2 laser line at a pressure of 1.44 torr. The trace in the first period is the zero-difference baseline. The trace in the second period shows depletion of 2.46% (±0.20%) for 3 min, and the trace in the third period shows the conversion after the valve is closed.

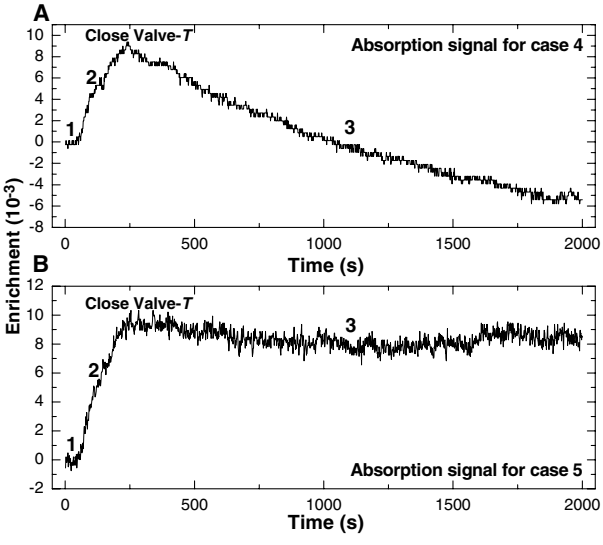

Fig. 2. Recorded differential absorption signals at lock-in time constant of 0.3 s using probe CO_2 laser lines of (**A**) 10*R*22 at a pressure of 0.98 torr and (**B**) 10*R*28 at a pressure of 1.02 torr. The enrichments are 0.91% (±0.05%) and 0.89% (±0.05%) at the end of the second period of (A) and (B), respectively. The spin conversion rates observed in the third periods of (A) and (B) are 7.55 (±0.04) × 10^{-4} s^{-1} and 5 (±5) × 10^{-5} s^{-1}, respectively.

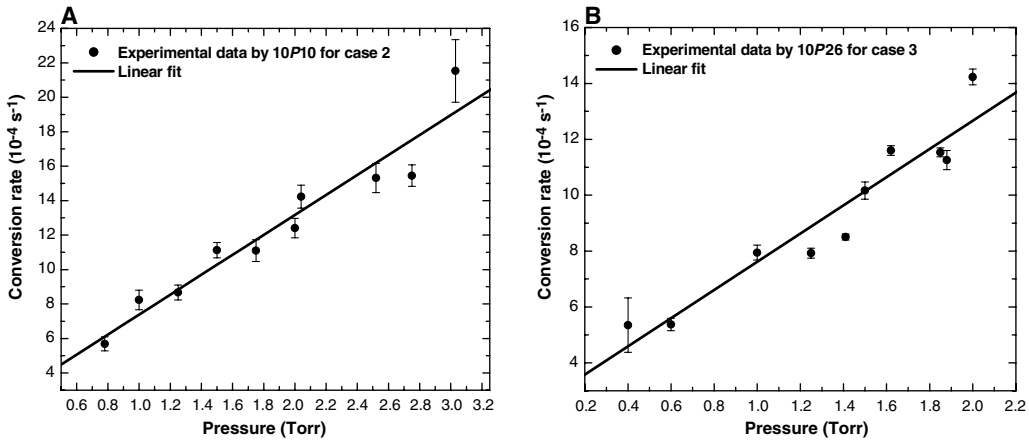

Fig. 3. Observed conversion rates as a function of pressure for probing (**A**) the B_{2u} species by the 10*P*10 line and (**B**) the B_{3u} species by the 10*P*26 line of probe CO_2 laser.

populations. Very similar signals were also observed for alternative B_{2u} and B_{3u} probe resonances (cases 2 and 3 in Table 2). We tried to monitor the B_{1g} population dynamics but were not successful because the line intensity of the resonant $26_{10,16} \leftarrow 27_{9,18}$ transition was too weak. The signals in the third period show the relaxation due to the conversion among spin isomers. A model function $A \exp(-\gamma t) + B$ (where A is the integrated intensity, γ is the observed conversion rate constant, and B is the baseline offset) was fitted to the decay data of Fig. 1 to give the solid smooth curve shown with a rate constant $\gamma = 8.09\ (\pm 0.10) \times 10^{-4}\ s^{-1}$.

The data clearly show that the concentration of the A_g species is almost constant in time, whereas monoexponential kinetics are observed for recovery of the depleted B_{2u} population and decay of the enriched B_{3u} population. Furthermore, the B_{2u} signal does not return to the original zero-difference baseline, and the B_{3u} signal overshoots the baseline and asymptotically approaches a new equilibrium level. These general phenomena can be qualitatively explained using Curl's theory of state mixing (*19*). We assume that conversion of nuclear spin isomers of C_2H_4 is allowed between the B_{2u} and B_{3u} isomers, and between the A_g and B_{1g} isomers, but forbidden between species of opposite inversion symmetry. Specifically, molecular "doorway" states are posited, between either B_{2u} and B_{3u} or A_g and B_{1g}, that are so close in energy that the weak intramolecular nuclear spin-rotation and spin-spin interactions of C_2H_4 can induce mixing between them. This mixing is interrupted by collisions, which promote interconversion between either the B_{2u} and B_{3u} or the A_g and B_{1g} states, through the quantum relaxation process proposed by Chapovsky for *ortho*- and *para*-CH_3F (*20*). Therefore, the time rate of change of the number density of one species is determined by the net number of doorway transitions within species of like inversion symmetry. The concentrations of the B_{2u} and B_{3u} species relax exponentially toward a common depleted equilibrium level, whereas those of the A_g and B_{1g} species retain their initial enriched level with no large relaxation. Net population is thus transferred from the B_{3u} to the B_{2u} state (reflected in the absorption signal of the B_{2u} population not reaching the zero-difference baseline, and the B_{3u} signal passing the baseline).

From the near-constancy of the signal in the third period of Fig. 2B, it appears that spin isomer conversion between states of opposite inversion symmetry is negligible, as is the impact of molecular collisions with the cell wall over the 30-min time range studied. However, over a longer time frame, it is speculated that these factors could cause eventual reequilibrium of the isomer populations to the initial thermal ratios (zero-difference baseline).

The theory of quantum relaxation in *ortho-para* conversion (*20*) predicts that, at low pressure, the spin conversion rate should vary linearly with the total gas concentration p. Thus, the observed first-order rate constant is $\gamma = kp + y$, and varying the pressure allows extraction of the bimolecular rate constant k. So far, this behavior has been observed for CH_3F (*6*, *7*) and $^{13}C^{12}CH_4$ (*8*). For C_2H_4, we measured more than 100 conversion tracks at different pressures and observation times, probing at each of the four B_{2u} and B_{3u} resonances (Table 2, cases 1 to 4). The mean values of γ are plotted in Fig. 3 as a function of pressure. The data fit reasonably well to a linear pressure dependence. Rate constants from the fits for each probe wavelength agree well within the experimental errors (Table 2) and give an average of $5.5\ (\pm 0.8) \times 10^{-4}\ s^{-1}\ torr^{-1}$.

Thus, our spin conversion observations for C_2H_4 are well accounted for by the model of quantum relaxation. The results provide evidence of the weak intramolecular hyperfine interactions in C_2H_4 and suggest that the conversion mechanism among nuclear spin isomers of polyatomic molecules in general is quantum relaxation with conserved inversion symmetry.

References and Notes

1. L. D. Landau, E. M. Lifshitz, *Quantum Mechanics* (Pergamon, Oxford, ed. 3, 1981).
2. A. Farkas, *Orthohydrogen, Parahydrogen, and Heavy Hydrogen* (Cambridge Univ. Press, London, 1935).
3. H. Kawakita *et al.*, *Science* **294**, 1089 (2001).
4. J. E. Dickens, W. M. Irvine, *Astrophys. J.* **518**, 733 (1999).
5. N. Dello Russo *et al.*, *Astrophys. J.* **621**, 537 (2005).
6. P. L. Chapovsky, *JETP* **70**, 895 (1990).
7. B. Nagels, M. Schuurman, P. L. Chapovsky, L. J. F. Hermans, *Phys. Rev. A* **54**, 2050 (1996).
8. P. L. Chapovsky, J. Cosléou, F. Herlemont, M. Khelkhal, J. Legrand, *Chem. Phys. Lett.* **322**, 424 (2000).
9. G. Peters, B. Schramm, *Chem. Phys. Lett.* **302**, 181 (1999).
10. P. R. Bunker, P. Jensen, *Molecular Symmetry and Spectroscopy* (NRC Research Press, Ottawa, ed. 2, 1998), pp. 407–409.
11. V. I. Tikhonov, A. A. Volkov, *Science* **296**, 2363 (2002).
12. F. Kh. Gel'mukhanov, A. M. Shalagin, *JETP Lett.* **29**, 711 (1979).
13. In Table 1, the A_g species corresponds to all four spins aligned, as well as to the case of no net spin. This species corresponds to the symmetric state with respect to the 180° rotations (or interchanges of H nuclei caused by these rotations) about the *x*, *y*, and *z* axes and belongs to the rotational states with the same symmetry $[(K_a, K_c) = (\text{even, even})]$ because of the Pauli principle. The B_{1g}, B_{2u}, and B_{3u} species correspond to the case for one total spin. The B_{1g} state is symmetric with respect to the 180° rotation about the *z* axis and antisymmetric to the rotations about the *x* and *y* axes, belonging to the rotational state with the same symmetry $[(K_a, K_c) = (\text{odd, even})]$; the B_{2u} and B_{3u} states are symmetric with respect to the 180° rotations about the *y* and *x* axes, respectively, and antisymmetric to those about the other two axes (*x* and *z*; *y* and *z*), respectively, belonging to the rotational states shown in Table 1. The A_g, B_{3g}, B_{2u}, and B_{1u} species of nuclear spin isomers of C_2H_4 given by Bunker and Jensen (*10*) correspond to the A_g, B_{1g}, B_{2u}, and B_{3u} species, respectively, used in this work.
14. G. Herzberg, *Molecular Spectra and Molecular Structure. II. Infrared and Raman Spectra of Polyatomic Molecules* (Van Nostrand Reinhold, New York, 1945).
15. T. Oka, *J. Mol. Spectrosc.* **48**, 503 (1973).
16. See supporting material on *Science* Online.
17. I. Cauuet *et al.*, *J. Mol. Spectrosc.* **139**, 191 (1990).
18. In these measurements, the probe laser was locked to the 4.3-μm Lamb-dip fluorescence signal in an external CO_2 cell via a closed servo feedback loop (*21*). To shift the probe CO_2 laser frequency by 100 or 200 MHz, we used one set (for cases 2 to 4) or two sets in tandem (for case 5) of an acousto-optic modulator (IntraAction AGM-1003A1) and an RF modulator driver (GE-10020), respectively.

19. R. F. Curl Jr., J. V. V. Kasper, K. S. Pitzer, *J. Chem. Phys.* **46**, 3220 (1967).
20. P. L. Chapovsky, *Phys. Rev. A.* **43**, 3624 (1991).
21. Z.-D. Sun, F. Matsushima, S. Tsunekawa, K. Takagi, *J. Opt. Soc. Am. B* **17**, 2068 (2000).
22. We express sincere thanks to P. L. Chapovsky for valuable guidance when he visited our laboratory. We thank P. L. Chapovsky and R. M. Lees for critical reading and commenting on the manuscript; T. Oka and J. T. Hougen for helpful discussions; Y. Moriwaki, K. Uehara, and group members for assistance in this work; and the anonymous referees for their insightful comments. Supported by the Japan Society for the Promotion of Science (JSPS) and grant-in-aid P04063 for JSPS Fellows from the Ministry of Education, Science, Sports, and Culture of Japan (Z.-D.S.).

Supporting Online Material
www.sciencemag.org/cgi/content/full/310/5756/1938/DC1
Materials and Methods
Fig. S1

12 September 2005; accepted 27 October 2005
10.1126/science.1120037

Synthesis of Imido Analogs of the Uranyl Ion

Trevor W. Hayton,[1] James M. Boncella,[1]* Brian L. Scott,[1] Phillip D. Palmer,[1] Enrique R. Batista,[2] P. Jeffrey Hay[2]

Here we describe the synthesis of two imido analogs of the uranyl ion, UO_2^{2+}, in which the oxygens are replaced by divalent alkyl or aryl nitrogen groups: $U(N^tBu)_2I_2(THF)_2$ (1) and $U(NPh)_2I_2(THF)_3$ (2) (where ^{t}Bu is *tert*-butyl and THF is tetrahydrofuran). Both compounds have been fully characterized by standard analytical techniques, including x-ray crystallography, and the chemical bonding between the metal center and the nitrogen ligands was quantified by using hybrid density functional theory calculations. As expected for a uranyl analog, these complexes exhibit linear N-U-N linkages and very short U-N bonds. In addition, the theoretical calculations show strong involvement of the 5f and 6d electrons in the U-N bonding.

The uranyl (UO_2^{2+}) species is the most common functional unit in the chemistry of U(VI) and has been known for more than 150 years (*1*). With the advent of nuclear energy and the use of uranium oxide as reactor fuel, the chemistry of the uranyl ion has played an essential role in the processing of uranium ore, nuclear fuel, and waste (*2*). The linear arrangement of the oxo ligands, extremely short U-O bond lengths, and high thermal and chemical stability reflect some of the unusual properties of this functional group (*3*). Given the prevalence of uranyl, it is surprising that metal-ligand multiple bonding in the actinides is not better understood. For instance, it is generally agreed that the uranium-oxygen bonds in uranyl involve six U-O interactions; however, the ordering of the frontier orbitals is still being debated (*4*). Furthermore, recent high-profile reports, such as the synthesis of a molecular uranium nitride (*5*) and the isolation of an η^1-*O*-bound uranium-CO_2 complex (*6*), point to a general deficiency in our knowledge of the chemistry of the f elements relative to the transition metals. The importance of multiple bonding in the actinides and the extent that the f orbitals participate in bonding are still open questions that can be addressed through the synthesis of new classes of compounds.

The imido ligand (NR^{2-}) is isoelectronic with the oxo ligand, and the two groups can often be interchanged in transition metal complexes. The alkyl or aryl substituent of the imido ligand provides a variable unavailable in oxo chemistry, because changes in the steric and electronic properties of the imido substituent can affect the chemistry of the metal center to which it is bound. The synthesis of the isoelectronic imido analogs of uranyl has therefore been of interest for many years (*7*). However, direct imido analogs of the uranyl ion have remained elusive despite a great deal of effort toward their synthesis. For instance, Denning and co-workers were able to isolate the phosphorane-iminato ($UNPR_3$) and sulfilimine ($UNSR_2$) substituted analogs of uranyl, which are heteroatom approximations to the imido ligand (*7–9*). Burns and co-workers were able to synthesize $Cp^*_2U(NR)_2$ (where R was either Ph or adamantyl and Cp* was C_5Me_5), but with imido groups in a cis configuration (*10*, *11*). The difficulty in isolating a *trans*-bis(alkyl or aryl imido) complex led Denning to speculate that their isolation was not possible because uranium(VI) is too oxidizing (*9*).

Here we report the synthesis and full characterization of both alkyl and aryl *trans*-bis(imido) analogs of the uranyl ion: $U(NR)_2^{2+}$. By using hybrid density functional theory (DFT), we also compare the calculated and experimental properties of these compounds and analyze the nature of the U-N bonding (*12–15*).

Reaction of uranium turnings with 3 equivalents of I_2 and 6 equivalents of *tert*-butylamine in tetrahydrofuran (THF) quickly results in metal dissolution and the formation of an orange solution (Scheme 1). Isolation of a crude orange solid and recrystallization from a toluene/hexanes solution provides crystalline $U(N^tBu)_2I_2(THF)_2$ (**1**) in 68% yield (*16*).

Replacing *tert*-butylamine with aniline in Scheme 1 does not provide any tractable products. However, by starting with well-known

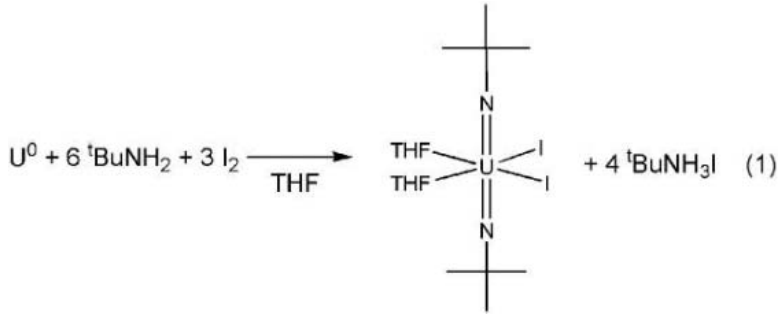

Scheme 1.

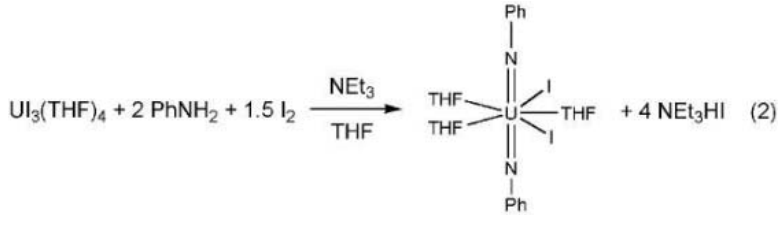

Scheme 2.

[1]Chemistry Division, MS J514, [2]Theoretical Division, MS B268, Los Alamos National Laboratory, Los Alamos, NM 87545, USA.

*To whom correspondence should be addressed. E-mail: boncella@lanl.gov

$UI_3(THF)_4$ (*17*) instead of uranium metal, a bis(imido) complex could be made in 84% yield. Thus, addition of 1.5 equivalents of I_2 to a THF solution of $UI_3(THF)_4$, aniline (2 equivalents), and NEt_3 (4 equivalents) generates orange-brown solutions containing $U(NPh)_2I_2(THF)_3$ (**2**) (Scheme 2) (*18*).

Complex **1** is an orange, moisture-sensitive, crystalline solid, which is soluble in THF and toluene. The ^1H nuclear magnetic resonance (NMR) spectrum of **1** displays resonances for both THF ligands and *tert*-butyl groups in a 1:1 ratio. One THF resonance occurs at 4.56 parts per million (ppm), whereas the other occurs at 1.54 ppm. Complex **2** is a red-brown crystalline solid with similar solubility properties to **1**. Its ^1H NMR spectrum exhibits resonances for three equivalent THF ligands and two equivalent phenyl moieties. Its two THF resonances are observed at 4.38 ppm and 1.41 ppm. Addition of excess THF to NMR samples of **1** or **2** causes these resonances to shift to the values anticipated for free THF, suggesting rapid exchange of coordinated and uncoordinated THF molecules on the NMR time scale.

The infrared (IR) spectra of complexes **1** and **2** show strong vibrations at 1170 cm^{-1} and 1270 cm^{-1}, respectively, which is in the region expected for a *trans* imido complex (*19*). Normal mode analysis of the model complex $U(NMe)_2I_2(THF)_2$ and of **2** (from DFT calculations) further confirms this (*20*). With use of this technique, we identified a strong IR active vibrational mode at 1229 cm^{-1} in complex **1** and one at 1326 cm^{-1} in complex **2**, corresponding to the N-U mode coupled out of phase with the N-C stretch mode (*21*). The ultraviolet-visible (UV-vis) spectra of **1** and **2** are similar, and each display two intense, broad maxima. For **1**, the absorption bands occur at 291 nm [molar absorptivity (ε) = 3500 $l{\cdot}mol^{-1}{\cdot}cm^{-1}$] and 353 nm ($\varepsilon$ = 2200 $l{\cdot}mol^{-1}{\cdot}cm^{-1}$), whereas for **2** they are observed at 291 nm (ε = 7900 $l{\cdot}mol^{-1}{\cdot}cm^{-1}$) and 352 nm ($\varepsilon$ = 1900 $l{\cdot}mol^{-1}{\cdot}cm^{-1}$). The vibronic coupling fine structure often seen in uranyl UV-vis spectra is not observed in the spectra for **1** and **2**. The lack of fine structure is understandable given that the U-N stretching modes are coupled with other vibrational modes of the substituents of the imido ligands.

It is unexpected that the synthesis of **1** and **2** can be achieved with I_2 as the oxidant. Iodine is not a potent enough oxidant to access the U(VI) oxidation state under other circumstances. For instance, neither UI_6 nor UI_5 are known to exist, and UI_4 slowly disproportionates, forming UI_3 and I_2 (*22*). The formation of the U-N multiple bonds must play a substantial role in providing a thermodynamic driving force over and above the oxidizing power of I_2 to facilitate this reaction. The strength of the U-N interactions in **1** and **2** is demonstrated by the short U-N bond lengths that have been observed in the crystal structures of these compounds.

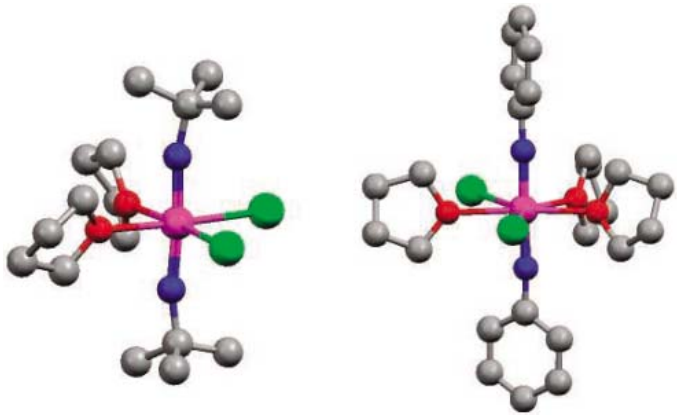

Fig. 1. Ball-and-stick representation of $U(N^tBu)_2I_2(THF)_2$ (**left**) and $U(NPh)_2I_2(THF)_3$ (**right**). Uranium, magenta; carbon, gray; iodine, green; nitrogen, blue; and oxygen, red.

In the solid state (Fig. 1) (*23*), complex **1** has an octahedral geometry, whereas **2** exhibits pentagonal bipyramidal coordination. Both geometries are common for uranyl-containing complexes. The two imido ligands in **1** exhibit a trans geometry (N1-U1-N2 = 175.4° ± 0.2°) and very short U-N bonds (U1-N1 = 1.848 ± 0.004 Å and U1-N2 = 1.840 ± 0.004 Å). Both imido ligands are linear (U1-N1-C1 = 167.7° ± 0.3° and U1-N2-C5 = 168.9° ± 0.4°). The bis(imido) unit in **2** is nearly identical to that of **1** (U1-N1 = 1.866 ± 0.002 Å, U1-N2 = 1.859 ± 0.002 Å, N1-U1-N2 = 177.42° ± 0.09°, U1-N1-C1 = 177.7° ± 0.2°, and U1-N2-C7 = 176.2° ± 0.2°). The U-N bonds are significantly shorter than the U-N interactions reported for $[PPh_4][UOCl_4(NSPh_2)]$ and $[PPh_4][UOCl_4(NPPh_3)]$ (1.920 ± 0.003 Å and 1.912 ± 0.003 Å, respectively) (*7*). The U-N bonds in **1** and **2** are also much shorter than those observed in other uranium imido species, e.g., $Cp^*_2U(NPh)_2$ (U-N = 1.952 ± 0.007 Å) (*24*), $Cp^*_2U(NAd)_2$ (average U-N = 1.95 Å) (*11*), and $U[NSiMe_3][N(SiMe_3)_2]_3$ (U-N = 1.910 ± 0.006 Å) (*25*). Futhermore, the trans arrangement of the imido ligands is rare, even in transition metal chemistry (*19*, *26*, *27*).

The optimal structures of $U(NMe)_2I_2(THF)_2$ and **2** as predicted by DFT calculations agree very well with experiment, with the U-N and U-I bond lengths predicted to within 0.005 Å of the experimental values and the computed N-U-N angle predicted to within 2° (*28*, *29*). The molecular orbitals involved in the U-N bonds for the model complex $U(NMe)_2I_2(THF)_2$, along with the percentage participation of the uranium orbitals, are shown in Fig. 2 in descending order of orbital energy. The calculations clearly demonstrate the importance of the 5f orbitals in the U-N interaction. Overall, there are six orbitals with strong interactions between the uranium center and the nitrogen ligands, indicating the presence of two triple bonds. Each of these six orbitals contains a large 5f or 6d component, as indicated in Fig. 2. The top two bonding orbitals correspond to π interactions where the uranium participates in the bonding via the 5f electrons. The following two molecular orbitals also represent π bonds in which the 5f and 6d atomic orbitals of the metal center take part. The remaining two U-N bonding orbitals correspond to two σ interactions with the uranium participation composed of mostly 5f (mixed with smaller 6d and 6p components) in one and mostly 6d in the other. Overall, the U-N bonding in $U(NMe)_2I_2(THF)_2$ follows a similar pattern to that of the UO_2^{2+} fragment, which has six bonding orbitals, σ_g, σ_u, two π_u, and two π_g (*30*), although with slightly smaller participation of the uranium orbitals.

In each orbital the uranium contribution is large, indicating a strong covalent interaction. This is consistent with the Mulliken population analysis, which assigns an effective total charge on uranium of +1.50. This contrasts with a completely ionic description in which the formal charge on U(VI) would be +6. Furthermore, the natural bond orbital (NBO) analysis assigns an effective total charge of +1.27. For comparison, an NBO analysis of uranyl assigns a higher charge on uranium of +2.84, indicating a more ionic interaction. Our conclusions are in agreement with those of Kaltsoyannis (*4*), who carried out an extensive analysis of the six bonding orbitals in the naked UN_2 and $U(NPR_3)_2^{4+}$ fragments and found that the U-N bonds were more covalent than the analogous U-O interactions in uranyl.

Complexes **1** and **2** are excellent starting materials for the synthesis of new uranium imido complexes; the THF ligands of **1** and **2** are readily displaced by addition of other donor ligands, and addition of alkali metal salts exchanges the iodide groups for other anionic ligands. In addition, the methodology outlined in Scheme 2 appears to be a general reaction, allowing the synthesis of many new uranium imido species by simply

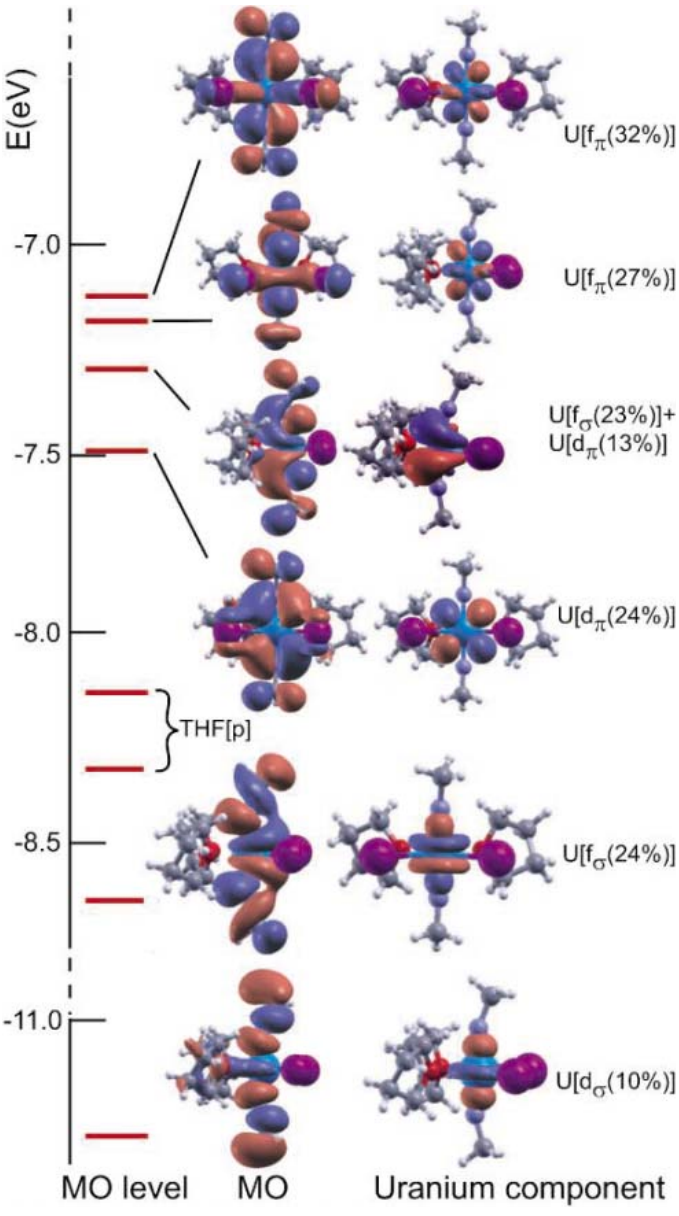

Fig. 2. Molecular orbital (MO) diagram of the bonding orbitals involved in the U-N bonds of $U(NMe)_2I_2(THF)_2$. The energy scale is in eV with the zero corresponding to the highest occupied level. The top six MOs belonging to the iodine ligands were omitted. The total MO and the metal component are shown. The column on the right indicates the type of uranium atomic orbital participating in the MO, along with its percentage contribution to the total MO.

changing the primary amine used in the reaction, thus allowing exceptional steric and electronic control at the metal center (*31*). Detailed spectroscopic investigations of compounds **1** and **2** and their derivatives will allow further quantification of the extent of f-orbital participation in the imido interaction.

References and Notes

1. A. E. Comyns, *Chem. Rev.* **60**, 115 (1960).
2. J. J. Katz, G. T. Seaborg, L. R. Morss, *The Chemistry of the Actinide Elements* (Chapman and Hall, New York, ed. 2, 1986).
3. R. G. Denning, *Struct. Bonding* (*Berlin*) **79**, 215 (1992).
4. N. Kaltsoyannis, *Inorg. Chem.* **39**, 6009 (2000).
5. W. J. Evans, S. A. Kozimor, J. W. Ziller, *Science* **309**, 1835 (2005).
6. I. Castro-Rodriguez, H. Nakai, L. N. Zakharov, A. L. Rheingold, K. Meyer, *Science* **305**, 1757 (2004).
7. V. C. Williams, M. Müller, M. A. Leech, R. G. Denning, M. L. H. Green, *Inorg. Chem.* **39**, 2538 (2000).
8. D. R. Brown, R. G. Denning, R. H. Jones, *Chem. Commun.* **2004**, 2601 (1994).
9. D. R. Brown, R. G. Denning, *Inorg. Chem.* **35**, 6158 (1996).
10. D. S. J. Arney, C. J. Burns, *J. Am. Chem. Soc.* **117**, 9448 (1995).
11. B. P. Warner, B. L. Scott, C. J. Burns, *Angew. Chem. Int. Ed.* **37**, 959 (1998).
12. All the calculations were carried out with use of the B3LYP functional. The Stuttgart relativistic effective core potential was used for the uranium atom, and the double zeta basis 6-31G* was used for all the other atoms.
13. X. Cao, M. Dolg, H. Stoll, *J. Chem. Phys.* **118**, 487 (2003).
14. W. Küchle, M. Dolg, H. Stoll, H. Preuss, *J. Chem. Phys.* **100**, 7535 (1994).
15. A. D. Becke, *J. Chem. Phys.* **98**, 5648 (1993).
16. Complete details of the synthesis and characterization of **1** and **2** can be found on *Science* Online.
17. D. L. Clark, A. P. Sattelberger, *Inorg. Synth.* **31**, 307 (1997).
18. Complex **1** could also be made from $UI_3(THF)_4$ in 87% yield.
19. Z.-Y. Li, J.-S. Huang, M. C.-W. Chan, K.-K. Cheung, C.-M. Che, *Inorg. Chem.* **36**, 3064 (1997).
20. For the computer simulations of complex **1**, we used a model system that replaced the ^{t}Bu (^{t}Bu is *tert*-butyl) substituents with methyl groups, and the molecules were studied in gas phase. We do not expect this simplification to affect the understanding of the U-N bonding because the predicted bond distances are in very good agreement with the experimental ones. The 70-cm^{-1} difference between the calculated and observed bands that are assigned as having a great deal of U-N stretching character to them is expected given the ability of the DFT method to calculate vibrational frequencies of complex molecules.
21. A. V. Korolev, A. L. Rheingold, D. S. Williams, *Inorg. Chem.* **36**, 2647 (1997).
22. F. A. Cotton, G. Wilkinson, C. A. Murillo, M. Bochmann, *Advanced Inorganic Chemistry* (Wiley, New York, ed. 6, 1999), pp. 1146–1147.
23. Crystal data for $U(N^tBu)_2I_2(THF)_2$ (**1**): $C_{16}H_{34}I_2N_2O_2U$, M_w = 778.28, monoclinic, $P2_1/n$, a = 12.3751 ± 0.0007, b = 15.3700 ± 0.0008, c = 12.4804 ± 0.0007, β = 90.507 ± 0.001, V = 2373.7 ± 0.2 Å^3, Z = 4. For 5822 reflections and 245 parameters collected at 141 K with $F^2 > 2\sigma(F^2)$, R = 0.0288 and wR = 0.0613. Crystal data for $U(NPh)_2I_2(THF)_3$ (**2**): $C_{24}H_{34}I_2N_2O_3U$, M_w = 890.36, monoclinic, $P2_1/n$, a = 10.9867 ± 0.0008, b = 17.7376 ± 0.00013, c = 14.2243 ± 0.00011, β = 90.070 ± 0.001, V = 2772.0 ± 0.4 Å^3, Z = 4. For 6802 reflections and 289 parameters collected at 141 K with $F^2 > 2\sigma(F^2)$, R = 0.0181 and wR = 0.0414.
24. D. S. J. Arney, C. J. Burns, D. C. Smith, *J. Am. Chem. Soc.* **114**, 10068 (1992).
25. A. Zalkin, J. G. Brennan, R. A. Andersen, *Acta Crystallogr.* **C44**, 1553 (1988).
26. J. T. Anhaus, T. P. Kee, M. H. Schofield, R. R. Schrock, *J. Am. Chem. Soc.* **112**, 1642 (1990).
27. A. A. Danopoulos, G. Wilkinson, B. Hussain-Bates, M. B. Hursthouse, *Polyhedron* **11**, 2961 (1992).
28. The equivalent complex with the iodide ligands in a trans configuration was calculated to have essentially the same energy as complex **1**. The U-I bond distances in the trans configuration are longer by 0.025 Å and 0.046 Å with respect to the cis isomer, whereas the U-N bond distances remain almost unaltered.
29. The U-N-C angle in the calculated structure of $U(NMe)_2I_2(THF)_2$ differs from 180°. However, this angle is known to be easily perturbed and is not a good indicator of the strength of the imido interaction with the metal (*32*).
30. M. Pepper, B. E. Bursten, *Chem. Rev.* **91**, 719 (1991).
31. Initial studies have demonstrated that a variety of substituted aryl amines are viable substrates. The chemistry and characterization of these compounds will be reported in due course.
32. P. Barrie, T. A. Coffey, G. D. Forster, G. Hogarth, *Dalton Trans.* **1999**, 4519 (1999).

33. We are grateful to the Seaborg Institute at Los Alamos National Laboratory for support of this work. T.W.H. wishes to acknowledge the Natural Sciences and Engineering Research Council (Canada) and the Seaborg Institute for postdoctoral fellowships. E.R.B. and P.J.H. were supported by the Division of Chemical Sciences, Office of Basic Energy Sciences, U.S. Department of Energy, under the Heavy Element Chemistry program at Los Alamos National Laboratory. Metrical details for the solid state structures of **1** and **2** are available free of charge from the Cambridge Crystallographic Data Centre under deposition numbers CCDC 283336 and CCDC 283337, respectively.

Supporting Online Material

www.sciencemag.org/cgi/content/full/310/5756/1941/DC1
Materials and Methods
Figs. S1 and S2
Tables S1 to S3
References

12 September 2005; accepted 15 November 2005
10.1126/science.1120069

Trading Water for Carbon with Biological Carbon Sequestration

Robert B. Jackson,[1]* Esteban G. Jobbágy,[1,2] Roni Avissar,[3] Somnath Baidya Roy,[3] Damian J. Barrett,[4] Charles W. Cook,[1] Kathleen A. Farley,[1] David C. le Maitre,[5] Bruce A. McCarl,[6] Brian C. Murray[7]

Carbon sequestration strategies highlight tree plantations without considering their full environmental consequences. We combined field research, synthesis of more than 600 observations, and climate and economic modeling to document substantial losses in stream flow, and increased soil salinization and acidification, with afforestation. Plantations decreased stream flow by 227 millimeters per year globally (52%), with 13% of streams drying completely for at least 1 year. Regional modeling of U.S. plantation scenarios suggests that climate feedbacks are unlikely to offset such water losses and could exacerbate them. Plantations can help control groundwater recharge and upwelling but reduce stream flow and salinize and acidify some soils.

Tree plantations feature prominently among tools for carbon sequestration (*1–8*). Plantations typically combine higher productivity and biomass with greater annual transpiration and rainfall interception, particularly for evergreen species such as pines and eucalypts (*9–12*). In addition to influencing water budgets, plantations require additional base cations and other nutrients to balance the stoichiometry of their extra biomass. In consequence, trade-offs of sequestration with water yield and soil fertility, including nutrient depletion and increased acidity, are likely. The goal of our research was to account for the trade-offs and benefits of carbon sequestration, identifying potential problems and management needs for a sustainable sequestration policy. We examined changes in hydrology and biogeochemistry with afforestation, using global synthesis data, fieldwork, and regional modeling. We evaluated the extent to which plantations altered water yield, soil chemistry, and acidity at plot (ha), catchment (ha to km^2), and regional ($>10^4$ km^2) scales, comparing environmental benefits of carbon sequestration with effects on other environmental services (*13*).

Our global analysis of 504 annual catchment observations shows that afforestation dramatically decreased stream flow within a few years of planting (Fig. 1, A and C) ($P < 0.0001$). Across all ages in the database, afforestation of grasslands, shrublands, or croplands decreased stream flow by 180 mm $year^{-1}$ and 38% on average (Fig. 1) ($P < 0.001$). After slight initial increases in some cases (Fig. 1), substantial annual decreases of 155 mm and 42% were observed on average for years 6 to 10, and average losses for 10- to 20-year-old plantations were even greater, 227 mm $year^{-1}$ and 52% of stream flow (Fig. 1, A and C). Perhaps most important, 13% of streams dried up completely for at least 1 year (Fig. 1C), with eucalypts more likely to dry up streams than pines. Afforestation in drier regions [<1000 mm mean annual precipitation (MAP)] was more likely to eliminate stream flow completely than in wetter regions. Mean annual renewable water (percentage of annual precipitation lost as runoff) decreased ~20% with afforestation (Fig. 1D) ($P < 0.0001$). For many nations with total annual renewable freshwater <30% of precipitation (Fig. 1B), afforestation is likely to have large impacts on water resources.

Climate feedbacks at regional scales could potentially offset some of these water losses through increased transpiration and convective rainfall (*14–17*), depending on site location, climate, and biophysical characteristics. To assess potential climate feedbacks, we first used the Forest and Agricultural Sector Optimization Model–Greenhouse Gases (FASOMGHG) (*7*, *18*) to estimate the U.S. lands projected to convert to plantations for C sequestration payments of 50 and 100 $US per Mg C (*13*); at a simulated price of $100 per Mg C, FASOMGHG estimates that 72 million ha of land would initially convert to forestry from nonirrigated agriculture and pasture (Fig. 2, A and B). We then used the Regional Atmospheric Modeling System (RAMS) (*19*) to examine potential hydroclimate feedbacks using these economically based scenarios of land-use change (*13*).

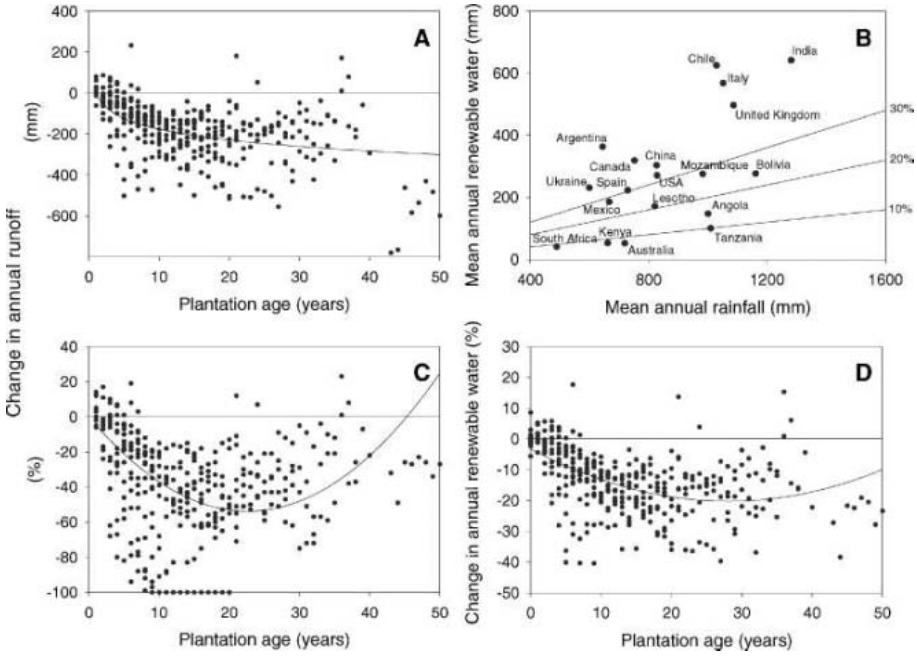

Fig. 1. Changes in stream flow and annual renewable water as a function of plantation age, and the relative abundance of renewable water by country. Changes in stream flow in mm (**A**) and proportion (%) (**C**) as a function of plantation age. (**D**) Changes in annual renewable water (annual stream flow in mm divided by annual precipitation). (**B**) Average renewable freshwater (mm) versus mean annual precipitation (mm) by nation. The lines define 10%, 20%, and 30% renewable water as a percentage of MAP. See (*13*).

[1]Department of Biology, Nicholas School of the Environment and Earth Sciences, and Center on Global Change, Duke University, Durham, NC 27708–1000, USA. [2]Grupo de Estudios Ambientales–Instituto de Matematica Aplicada de San Luis (IMASL), Universidad Nacional de San Luis and Consejo Nacional de Investigaciones Cientificas y Tecnicas (CONICET), San Luis 5700, Argentina. [3]Department of Civil and Environmental Engineering, Duke University, Durham, NC 27708, USA. [4]Commonwealth Scientific and Industrial Research Organisation (CSIRO) Land and Water, Canberra, ACT, Australia 2601. [5]Natural Resources and Environment CSIR, Stellenbosch 7599, South Africa. [6]Department of Agricultural Economics, Texas A&M University, College Station, TX 77843, USA. [7]Center for Regulatory Economics and Policy Research, Research Triangle Institute, Research Triangle Park, NC 27709, USA.

*To whom correspondence should be addressed. E-mail: jackson@duke.edu

On the basis of simulations for the United States, the higher water use of plantations and decreased stream flow is unlikely to be offset by atmospheric feedbacks operating at larger scales (Fig. 2). Climate simulations showed that plantations typically increased summer evapotranspiration (ET) by >0.3 mm day^{-1} and decreased both summer surface air temperature by as much as 0.3°C and precipitation by as much as 30 mm per month in the most densely afforested areas, compared with the crop and pasture lands they replaced (Fig. 2) ($P < 0.10$ for each). No evidence for increased rainfall from local convection was observed with afforestation except in northern Florida and southern Georgia (Fig. 2). Increased ET did not generate more rain because, unlike in the tropics (*17*, *20*), the temperate regions modeled here did not have sufficient energy to lift the additional atmospheric moisture high enough to condense and form clouds. Furthermore, the lack of sensible heating over plantations reduced the energy available for convection, reducing rainfall in general and the convective component in particular (Fig. 2F).

Plantations not only have greater water demands than grasslands, shrublands, or croplands, they typically have increased nutrient demands as well. These demands change soil chemistry in ways that affect fertility and sustainability. Global synthesis data show that the afforestation of grasslands or shrublands significantly increased Na concentrations, exchangeable sodium percentage (ESP), and soil acidity and decreased base saturation, suggesting potential soil salinization and sodicity in some cases (Fig. 3). Saturation of the soil exchange complex with bases decreased by one-quarter on average for 26 paired observations globally (from 59% to 45%; $P = 0.002$) (Fig. 3). Declines in exchangeable Ca, Mg, and K caused this result, because exchangeable Na doubled across 42 paired observations ($P = 0.007$) (Fig. 3). In addition, exchangeable sodium percentage more than doubled for 36 pairs, increasing on average from 3.4% to 7.8% in plantations ($P = 0.001$). ESP increased in 29 of 36 pairs globally, in four cases crossing the severe sodic threshold of 15% associated with physical degradation of soils. Differences in nutrient cycling, root depth distributions, and water consumption between plantations and native vegetation (*9*–*12*, *21*, *22*) likely explained these patterns, with Ca, Mg, and K redistributed from soil to biomass pools and Na excluded by roots and concentrated in the soil (*22*).

In addition to redistributing and excluding soil nutrients, plantations produce acidic litter, canopy leachates, and decomposition products. Globally, plantation soils were more acidic in 98 of 114 cases, with afforestation resulting in a median decrease of 0.3 pH units ($P < 0.0001$) (Fig. 3). Declines of 0.5 to 1.6 pH units were observed in a quarter of observations (Fig. 3). Plantations that did not acidify soils tended to grow on highly buffered parent material such as limestone.

The dual characteristics of increased water use and higher nutrient demands quantified above should help scientists and land managers predict the environmental costs and benefits of plantations. In some regions, establishing extensive plantations can have strong negative effects on soil fertility and salinity (Fig. 4). For example, the Pampas of Argentina, one of the world's largest uncultivated grasslands, has brackish groundwater under shallow freshwater lenses that provide drinking water (*22*). Our vertical electric sounding (VES) measurements along three grassland-to-plantation transects show eucalypts eliminating this freshwater lens, with decreased resistivity at the plantation boundary and higher electrical conductivity (EC) and salinity in plantation groundwater (Fig. 4, A to D). The VES transect data were confirmed by direct sampling of groundwater chemistry from wells and boreholes showing EC under plantations to be larger by a factor of 15 compared with the surrounding grasslands and agricultural fields ($P < 0.001$) (Fig. 4D).

Additional analyses at eight sites across the Pampas using 17 paired native grassland and

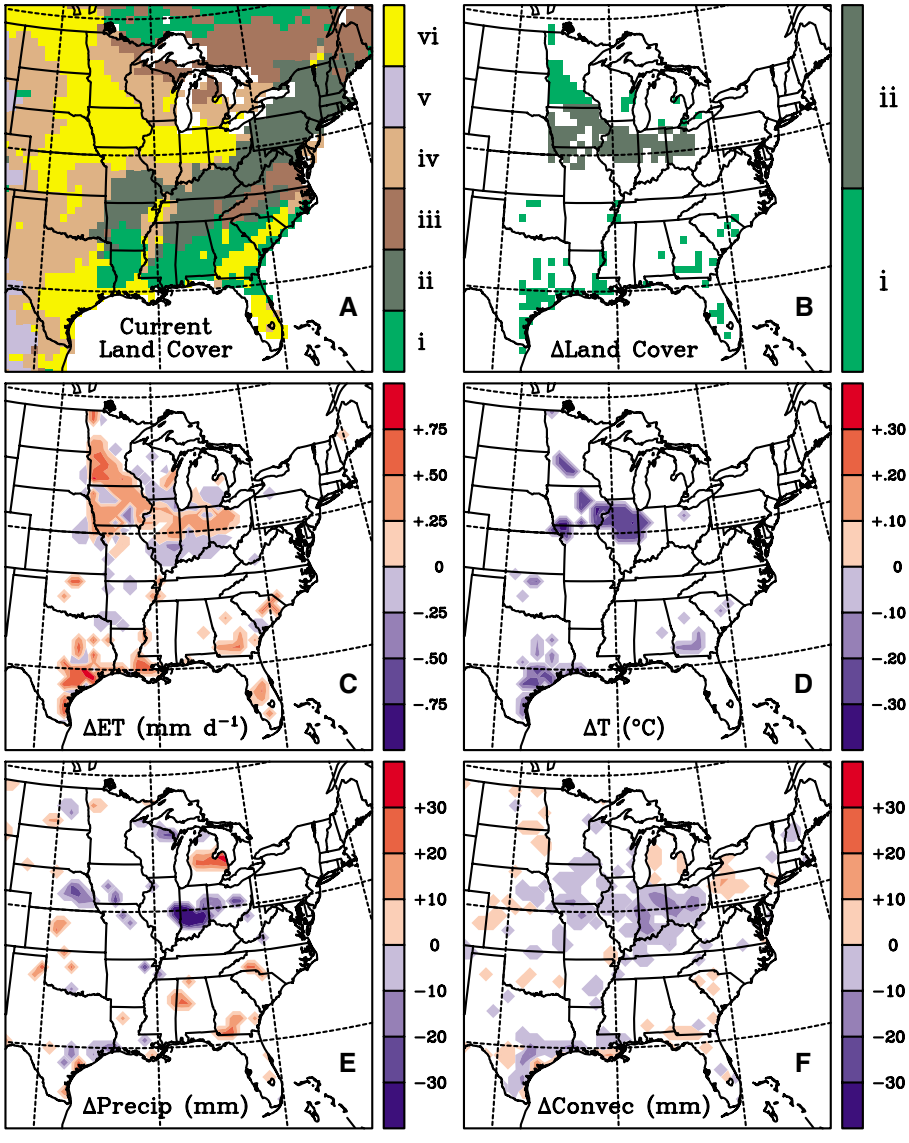

Fig. 2. Vegetation-climate feedbacks for economically based carbon sequestration scenarios using plantations. (**A**) Dominant land-cover type for each model grid cell aggregated into the following categories: (i) evergreen needleleaf forest, (ii) deciduous broadleaf forest, (iii) other forest, (iv) grass/shrubland, (v) desert/semi-desert, and (vi) farmland. (**B**) Model grid cells where crops and pasture were replaced by softwood (i) and hardwood (ii) plantations ($100 sequestration scenario). Difference between the $100 payment scenario (B) and current vegetation (A) for an ensemble average of monthly mean: (**C**) Evapotranspiration rate (mm/day) and (**D**) near-surface air temperature (°C), (**E**) accumulated total precipitation (mm), and (**F**) subgrid convective precipitation (mm). Plots (C) to (F) show only regions where the differences are significant at the 90% level using the Wilcoxon signed-rank test.

plantation stands revealed that the observed salinization was independent of tree species planted but depended strongly on soil texture (Fig. 4E). Intermediately textured loess soils showed 10-fold increases in salinity (Fig. 4E); finer soils likely had hydraulic conductivities too low for sufficient lateral movement of groundwater, and coarser soils underwent sufficient leaching of salts through the rooting zone to remove salt buildup. Increased salinity in intermediately textured soils occurred through at least two mechanisms. One was the buildup of salts, such as Na and Cl, excluded by tree roots. The other was upwelling of saline groundwater. These mechanisms have been linked to >5-fold increases in groundwater salinization in southern Australia (*23*) and in the Caspian steppes of Russia (*24*). Grassland and agricultural regions around the world with shallow groundwater and similar intermediately textured soils include Hungary's Hortobágy grasslands, Russia's western Siberian steppes, and the eastern Chaco croplands of Paraguay and Argentina (*22*). We predict that plantations could salinize soils in these locations as well if planted broadly.

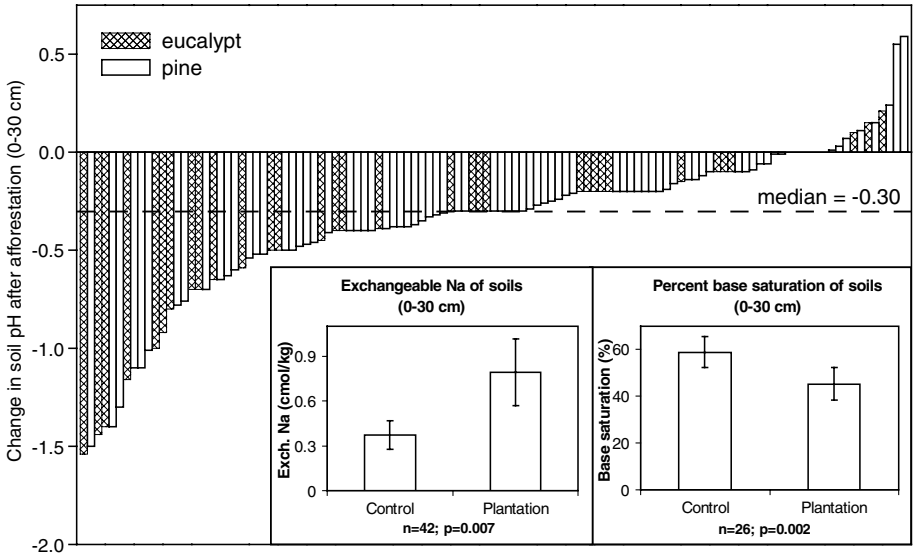

Fig. 3. The effects of plantations on soil pH and chemical properties (mean ± SE). We analyzed data from 52 published studies (*13*) that compared soil chemistry in grasslands or shrublands with that in adjacent plantation plots. Comparisons were made for soil pH (main panel), base saturation (%), and exchangeable soil Na concentrations (cmol kg^{-1}).

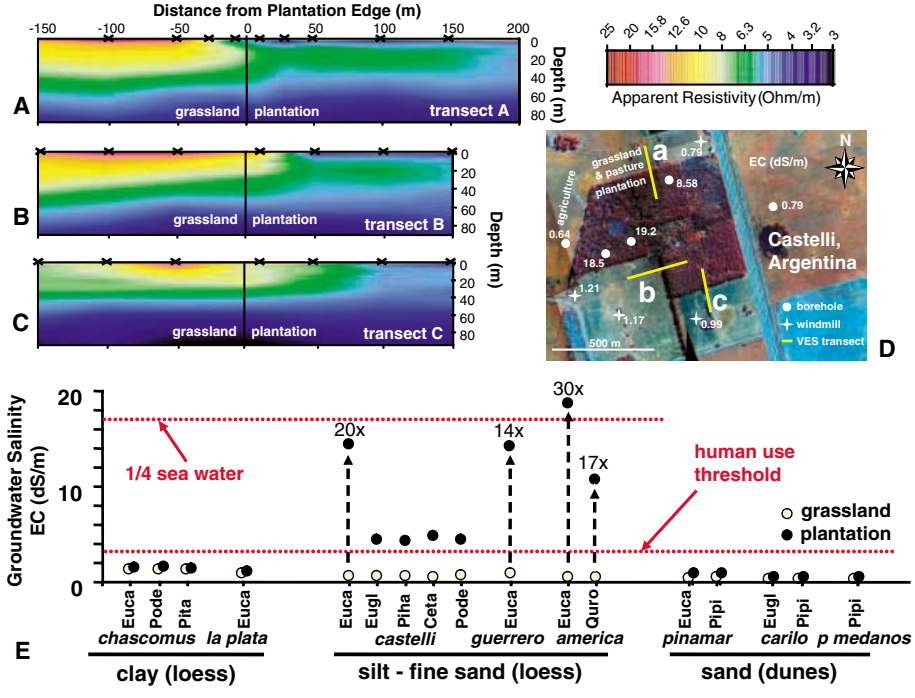

Fig. 4. Effects of plantations on groundwater salinity and electrical conductivity in the Argentine Pampas. (**A** to **C**) Three transects across plantation/grassland borders at Castelli made using vertical electric soundings, with reds indicating fresher water (higher resistivity) and blues indicating saltier water (lower resistivity). (**D**) Direct measurements of groundwater electrical conductivity (dS m^{-1}) from nine locations inside and outside the Castelli plantation. (**E**) Electrical conductivity of shallow groundwater samples (dS m^{-1}) in 17 grassland/plantation pairs at eight sites. Ceta, *Celtis tala*; Euca, *Eucalyptus camaldulensis*; Eugl, *Eucalyptus globulus*; Piha, *Pinus halepensis*; Pipi, *Pinus pinaster*; Pita, *Pinus taeda*; Pode, *Populus deltoides*; Quro, *Quercus robur*.

General trends in water use and soil chemistry found in our global analyses and field work must be adjusted to include local factors, including site history, soil texture, and the availability and quality of groundwater. In regions such as southern Australia and the African Sahel, plantations are being used successfully to keep saline groundwater below crop rooting zones, although the recovered area is often a small proportion of the original area (*27*). Plantations are also being used successfully to help dry waterlogged soils and alleviate flooding (*27*, *28*). The co-benefits of reforestation on water and soil resources may be the greatest where former forests have been replaced by crops, potentially restoring water quality and recharge to pre-agricultural levels (*28*). Reforestation of floodplains can also be beneficial for maintaining biodiversity, reducing erosion, improving water quality, mitigating peak flows, and controlling groundwater discharge (upwelling).

These cases contrast with monoculture plantations that maximize carbon sequestration but have considerable impact on runoff and groundwater recharge, as shown in our analysis. In these situations, plantations are likely to have adverse side effects, including reduced stream flow (*10*, *12*, *29*) and decreased soil pH and base saturation. In extreme cases, salinization and sodicity are possible. Although few

data are available from second-rotation plantations, these effects would likely be exacerbated after harvesting, owing to the export of cations and other nutrients off site. In the framework described above, the potential positive and negative benefits of plantations for salinity are predictable based on the presence and type of groundwater available, biophysical evaporative demand, and soil texture.

Plantations provide a proven tool for managing Earth's carbon cycle. The Clean Development Mechanism of the Kyoto Protocol allows countries to offset part of their CO_2 emissions through carbon sequestration, when consistent with a country's sustainable development objectives. New carbon trading exchanges such as the European Union's Greenhouse Gas Emission Trading Scheme help make such offsets a reality. As demand increases for land to accommodate plantations, more comprehensive environmental planning will be needed to avoid problems and to manage land successfully and sustainably. One way to do this is to compare the value of other ecosystem services gained or lost with those of carbon sequestration. The field of ecosystem services valuation is becoming increasingly sophisticated, and markets are opening up for some other services. The co-benefits and trade-offs of plantations need to be taken into account when negotiating exchange agreements. We believe that decreased stream flow and changes in soil and water quality are likely as plantations are increasingly grown for biological carbon sequestration.

References and Notes

1. P. M. Vitousek, *J. Environ. Qual.* **20**, 348 (1991).
2. R. A. Houghton, J. L. Hackler, K. T. Lawrence, *Science* **285**, 574 (1999).
3. M. I. Hoffert *et al.*, *Science* **298**, 981 (2002).
4. R. B. Jackson, J. L. Banner, E. G. Jobbágy, W. T. Pockman, D. H. Wall, *Nature* **418**, 623 (2002).
5. S. Pacala, R. Socolow, *Science* **305**, 968 (2004).
6. R. B. Jackson, W. H. Schlesinger, *Proc. Natl. Acad. Sci. U.S.A.* **101**, 15827 (2004).
7. B. A. McCarl, U. A. Schneider, *Science* **294**, 2481 (2001).
8. J. A. Wright, A. DiNicola, E. Gaitan, *J. Forestry* **98**, 20 (2000).
9. A. J. Pearce, L. K. Rowe, *J. Hydrol. N.Z.* **18**, 73 (1979).
10. L. Zhang, W. R. Dawes, G. R. Walker, *Water Resour. Res.* **37**, 701 (2001).
11. M. G. R. Cannell, *New For.* **17**, 239 (1999).
12. K. A. Farley, E. G. Jobbágy, R. B. Jackson, *Glob. Change Biol.* **11**, 1565 (2005).
13. Materials and methods and supporting material are available on *Science* Online.
14. Y. Xue, M. J. Fennessy, P. J. Sellers, *J. Geophys. Res.* **101**, 7419 (1996).
15. R. A. Pielke, R. Avissar, *Landscape Ecol.* **4**, 133 (1990).
16. S. Baidya Roy, R. Avissar, *J. Geophys. Res.* **107**, (D20), 8037 (2002).
17. W. A. Hoffmann, R. B. Jackson, *J. Clim.* **13**, 1593 (2000).
18. D. M. Adams, R. J. Alig, J. M. Callaway, B. A. McCarl, S. M. Winnett, "The forest and agriculture sector optimization model (FASOM): Model structure and policy applications" (Research Paper PNW-RP-495, USDA Forest Service, Pacific Northwest Research Station, Portland, Oregon, 1996).
19. W. R. Cotton *et al.*, *Meteor. Atmos. Phys* **82**, 5 (2003).
20. R. E. Dickinson, P. Kennedy, *Geophys. Res. Lett.* **19**, 1947 (1992).
21. D. C. Le Maitre, D. F. Scott, C. Colvin, *Water S.A.* **25**, 137 (1999).
22. E. G. Jobbágy, R. B. Jackson, *Glob. Change Biol.* **10**, 1299 (2004).
23. A. Heuperman, *Agric. Water Manage.* **39**, 153 (1999).
24. M. K. Sapanov, *Eurasian Soil Sci.* **33**, 1157 (2000).
25. G. R. Walker, L. Zhang, T. W. Ellis, T. J. Hatton, C. Petheram, *Hydrogeol. J.* **10**, 68 (2002).
26. S. K. Pattanayak *et al.*, *Clim. Change* **71**, 341 (2005).
27. R. J. George *et al.*, *Agric. Water Manage.* **39**, 91 (1999).
28. A. J. Plantinga, J. Wu, *Land Econ.* **79**, 74 (2003).
29. D. F. Scott, W. Lesch, *J. Hydrol.* **199**, 360 (1997).

30. We gratefully acknowledge the Duke University Center on Global Change and Provost's Office, the U.S. National Science Foundation, the National Institute for Global Environmental Change of the U.S. Department of Energy, the Inter-American Institute for Global Change Research, the Andrew W. Mellon Foundation, and the CSIR for financial support. A. Mendoza assisted with the database, and W. H. Schlesinger and two anonymous reviewers provided helpful suggestions on the manuscript.

Supporting Online Material

www.sciencemag.org/cgi/content/full/310/5756/1944/DC1
Materials and Methods
Tables S1 to S3
References

24 August 2005; accepted 21 November 2005
10.1126/science.1119282

Heterogeneous Hadean Hafnium: Evidence of Continental Crust at 4.4 to 4.5 Ga

T. M. Harrison,[1,2]* J. Blichert-Toft,[3] W. Müller,[1,4] F. Albarede,[3] P. Holden,[1] S. J. Mojzsis[5]

The long-favored paradigm for the development of continental crust is one of progressive growth beginning at ~4 billion years ago (Ga). To test this hypothesis, we measured initial $^{176}Hf/^{177}Hf$ values of 4.01- to 4.37-Ga detrital zircons from Jack Hills, Western Australia. ε_{Hf} (deviations of $^{176}Hf/^{177}Hf$ from bulk Earth in parts per 10^4) values show large positive and negative deviations from those of the bulk Earth. Negative values indicate the development of a Lu/Hf reservoir that is consistent with the formation of continental crust (Lu/Hf ≈ 0.01), perhaps as early as 4.5 Ga. Positive ε_{Hf} deviations require early and likely widespread depletion of the upper mantle. These results support the view that continental crust had formed by 4.4 to 4.5 Ga and was rapidly recycled into the mantle.

A fundamental question of Earth's evolution is: When did the growth of continental crust begin? One model is that the first crust formed after 4 Ga and grew slowly until the present day (*1*, *2*). This view reflects the absence of a >4-Ga rock record (*3*) and the broadly coherent post–4 Ga evolution of depleted mantle $^{143}Nd/^{144}Nd$ (*4*) and $^{176}Hf/^{177}Hf$ (*5*). Long-standing observations of early Nd (*6*) and Hf (*7*, *8*) depletions, however, leave open the possibility of even earlier global fractionations. Another view (*9*, *10*) is that continental crust was widespread during the Hadean Eon [the first 500 million years (My) of Earth history]. In such a scenario, the lack of direct evidence of earlier depletion events reflects subsequent remixing. Detrital zircons from Jack Hills, Western Australia, with 4.0- to 4.4-Ga U-Pb ages (*11*–*13*) represent pieces of crust that have been sequestered for up to ~4.4 Ga. Hf isotopic compositions vary because of radioactive decay of ^{176}Lu, and such variations in zircons constitute an excellent tracer of Earth's crust/mantle differentiation. This is because zircons have very low Lu/Hf ratios and thus record near-initial $^{176}Hf/^{177}Hf$ at the time given by their U-Pb age. Amelin and co-workers (*14*) investigated Hf isotopes in Jack Hills zircons as old as 4.14 Ga and inferred the existence of reworked Hadean crust. We have now extended this application by undertaking Lu-Hf analyses of grains ranging in age up to 4.37 Ga, thereby narrowing the gap to less than 200 My from the end of Earth's accretion to the first mineral record. We document significant Hf isotopic heterogeneity during the early Hadean and conclude that major differentiation of the silicate Earth, possibly the formation of continental crust with a volume similar in magnitude to the present day, may have occurred by 4.4 to 4.5 Ga.

Using the multicollector Sensitive High Resolution Ion Microprobe II, we have surveyed the radiogenic $^{207}Pb/^{206}Pb$ ($^{207}Pb/^{206}Pb^*$) ratio

[1]Research School of Earth Sciences, Australian National University, Canberra, ACT 0200, Australia. [2]Department of Earth and Space Sciences and Institute of Geophysics and Planetary Physics, University of California at Los Angeles, Los Angeles, CA 90095, USA. [3]Ecole Normale Supérieure, CNRS Unité Mixte de Recherche 5570, 69364 Lyon Cedex 7, France. [4]Department of Geology, Royal Holloway University of London, Egham, TW20 0EX, UK. [5]Department of Geological Sciences, University of Colorado, Boulder, CO 80309, USA.

*To whom correspondence should be addressed. E-mail: mark.harrison@anu.edu.au

of over 50,000 Jack Hills zircons separated from a large conglomerate sample (JH992) obtained from the original locality of Compston and Pidgeon (*11*). Hadean grains thus identified were dated by the U-Pb method (*11–13*). Zircons between 4.01 and 4.37 Ga were then analyzed for Lu/Hf and Hf isotopic composition (tables S1 and S2). Although $^{207}Pb/^{206}Pb^*$ ages can be variable within Hadean zircons (*11–13*), it is rarely the case (*15*) that an individual grain exhibits more than two generations of crystal growth. In the cases of concordant or nearly concordant (<12% discordant) results, we assume that the $^{207}Pb/^{206}Pb^*$ age records the time of crystallization, which we then use to calculate $\varepsilon_{Hf(T)}$, where T is age. For grains that showed evidence of zoning or yielded apparent $\varepsilon_{Hf(T)}$ values that strongly deviated from those of bulk Earth, we undertook additional ion microprobe dating investigations to assess whether multiple generations of zircon growth were present (table S2 and fig. S2).

Of the 104 multicollector–inductively coupled plasma–mass spectrometry (MC-ICP-MS) zircon $^{176}Hf/^{177}Hf$ results we present, 44 were measured by solution MC-ICP-MS (table S1) (*16*) and 60 by laser ablation MC-ICP-MS (table S2) (*16*). We deliberately used both approaches, because each has potential limitations that are in part compensated for by the other. Solution MC-ICP-MS provides a bulk Hf isotope composition, but does not suffer from isobaric interferences on ^{176}Hf from Yb and Lu. Although laser ablation MC-ICP-MS measurements require peak stripping to correct for Yb and Lu interferences on ^{176}Hf, they allow spatially resolved analysis using spots of 60 to 80 μm in diameter, which facilitates the identification of zircons zoned with respect to $^{176}Hf/^{177}Hf$. Because these analyses retain some of the zircon under analysis, subsequent ion microprobe investigations of potential age heterogeneity are possible.

We calculated $\varepsilon_{Hf(T)}$ using the "terrestrial" ^{176}Lu decay constant (λ_{176}) of $1.867 \pm 0.008 \times 10^{-11}$ year^{-1} [(*17*) and references therein] and the present day chondritic parameters $^{176}Lu/^{177}Hf = 0.0332 \pm 0.0002$ and $^{176}Hf/^{177}Hf = 0.282772 \pm 29$ (*18*) [λ_{176} and solar system initial $^{176}Hf/^{177}Hf$ deduced from meteorite Lu-Hf isochrons appear to reflect irradiation effects in the solar nebula (*19*)]. Using the chondritic averages of Patchett and co-workers (*20*) instead would not significantly change our calculated values of $\varepsilon_{Hf(T)}$, because their $^{176}Hf/^{177}Hf$ and Lu/Hf values all fall on the same 4.5-Ga isochron as those in (*18*).

Our data (tables S1 and S2) show a high degree of Hf isotope heterogeneity, with variation in $\varepsilon_{Hf(T)}$ values at 4.2 Ga of over 20 ε units. Before we examine the geological significance of these data, we investigate possible artifacts of combined interpretation of Lu-Hf and U-Pb systematics in a complex zircon population that could lead to incorrect inferences of early deviations from chondritic evolution. A key link in using zircon to assess initial Hf isotopic ratios is that the age ascribed accurately reflects the time at which the Hf isotopic composition was incorporated into the zircon. In the case of a zircon zoned in U-Pb age, relating an older age component to the bulk Hf isotope composition could result in an incorrect estimate of $\varepsilon_{Hf(T)}$.

For example, consider the case of grain CU05 8.5, which yields an ion microprobe age of 4123 ± 18 Ma and age-corrected solution MC-ICP-MS $^{176}Hf/^{177}Hf = 0.280415 \pm 0.000015$ (2 SE) (table S1), corresponding to an apparent $\varepsilon_{Hf(T)} = +10.7 \pm 0.5$. However, because the bulk solution ICP-MS $^{207}Pb/^{206}Pb$ age is only 3624 Ma (*21*), we infer that this grain is substantially heterogeneous with respect to age and that the ~4.1-Ga ion microprobe date represents only a small portion of the total U-Pb system. If we instead use the bulk 3.62-Ga age, the apparent ε_{Hf} drops to a near–bulk Earth value of $+1.2 \pm 0.5$. We thus eliminated this sample from further consideration.

Less obvious is that mixtures of concordant components with contrasting U concentrations each plotting on bulk Earth could also yield substantial positive and negative deviations in ε_{Hf}. This is because of the strongly nonlinear relationship between $^{207}Pb/^{206}Pb^*$ (or Pb/U) and age, whereas the long half-life of ^{176}Lu resulted in essentially linear growth in $^{176}Hf/^{177}Hf$ over the past 4.56 Gy. To assess this effect, we developed a model in which concordant core (T1) and rim (T2) ages are characterized by $\varepsilon_{Hf(T)}$ at T1 and T2, respectively. If the bulk age of this composite is characterized by a U-Pb date obtained by ion microprobe spot analysis in the core, but associated with a $^{176}Hf/^{177}Hf$ ratio that is a mixture of the two end-members, an incorrect value of ε_{Hf} results. Even in the case for which U-Pb age and Hf isotopes are measured on the same spot overlapping these two zones, aberrant values can result. Figure 1 illustrates possible trajectories in $\varepsilon_{Hf(T)}$ resulting from mixing two such components. Because variations in U concentration are far greater than those in Hf concentration (*22*), we only varied U concentrations.

Consider the case of a 4.4-Ga core ($^{176}Hf/^{177}Hf_{4.4\ Ga} = 0.279930$) and a 3.7-Ga rim ($^{176}Hf/^{177}Hf_{3.7\ Ga} = 0.280398$) (i.e., an age contrast of 1 half-life of ^{235}U). Mixtures of these two components between 0 and 100%, shown in 10% increments, are indicated by the black symbols (Fig. 1). The variation in symbol shape represents differing U concentrations of the 4.4-Ga core (T1) and the 3.7-Ga rim (T2). For the case of equal U concentration (diamonds), mixing produces a roughly symmetric trajectory in positive ε_{Hf} space, reaching an ε_{Hf} value of +2 at ~4 Ga. Doubling the U concentration in the core relative to the rim (squares) increases the apparent ε_{Hf} value to close to +5. This is expected because the Hf isotope composition at every intermediate position is associated with an older apparent $^{207}Pb/^{206}Pb^*$ age and thus appears to originate in a higher Lu/Hf environment. Where the rim U concentration is a factor of 1.6 greater than in the core (circles), no variation from bulk Earth is seen (because $^{207}Pb/^{206}Pb^*$ drops by a factor of 1.6 for each half-life of ^{235}U). Thus, the reduced rate of generation of Pb* at 3.7 Ga is in this case exactly offset by the 160% greater U content of the rim. Where U in the core is 10 times less than in the rim (triangles), ε_{Hf} values as negative as –7 result.

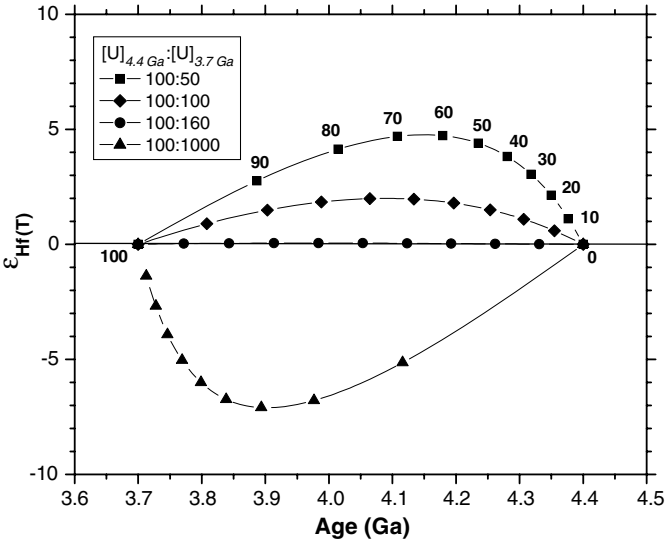

Fig. 1. Results of a model illustrating possible trajectories in $\varepsilon_{Hf(T)}$ versus age space ensuing from mixing zircon components of differing age, U concentration, and Hf isotope composition. The model assumes concordant ages of T1 (core) and T2 (rim), which are characterized by the Hf isotope composition of bulk Earth at T1 and T2, respectively. Mixtures of the two components are shown adjacent the relevant curve in % of the rim component for the case of a 4.4-Ga core and 3.7-Ga rim. Where the bulk age of a mixture is characterized by a U-Pb age in the core, but incorrectly associated with a $^{176}Hf/^{177}Hf$ ratio that is a mixture of the two end-members, the potential exists for incorrect ε_{Hf} values to be calculated. More surprising is that in the case where U-Pb age and Hf isotopes are measured on the same spot overlapping these two zones, aberrant values result, as shown in the mixing curves.

For many grains analyzed by laser ablation MC-ICP-MS, further age investigations are possible, because the method is not completely destructive, compared with solution chemistry. Grains with calculated ε_{Hf} that differ from bulk Earth by more than 5 ε units were, where sufficient sample remained, redated near their rims to assess age homogeneity. In the majority of cases, $^{207}Pb/^{206}Pb$* ages were reproduced at a satisfactory level (table S2). In one case (RSES17 2.9), we were able to resolve a time-dependent $^{176}Hf/^{177}Hf$ signal that dropped by 4 ε units upon penetrating a 3469 ± 12–Ma rim from a 4127 ± 64–Ma core, yielding $\varepsilon_{Hf(4.13\ Ga)} = 10 \pm 1.3$ (table S2 and fig. S1).

Where rims are demonstrably younger than core ages, we were able to rule out mixing between domains by the lack of a time-resolved variation in the $^{176}Hf/^{177}Hf$ signal and by visual evidence from imaging studies. Even where mixing may have occurred below our ability to resolve time variations in $^{176}Hf/^{177}Hf$, we have ruled out this effect as a cause for overestimating variations in $\varepsilon_{Hf(T)}$ from bulk Earth by using our mixing model (table S2, comments). For example, grain ANU39 15.15 yields a $^{207}Pb/^{206}Pb$ age of 4234 ± 10 Ma (0% discordant), which corresponds to a high apparent $\varepsilon_{Hf(T)}$ of 15.3 ± 1.8 (table S2 and fig. S2). Both the ion microprobe spot for the U-Pb age and the laser ablation pit for the Hf isotope analysis were obtained from the central portion of the grain, which was imaged as a homogenous core (fig. S2). Although the overgrowth region was later found to yield an age of 3548 ± 10 Ma (table S2 and fig. S2), our modeling shows that the relationship between U concentrations in the core [82 parts per million (ppm)] and rim (440 ppm) would likely increase the estimated value of ε_{Hf} if a portion of the rim had inadvertently been included in the analysis. Thus, the value of ~+15 is a minimum estimate of the true ε_{Hf} of the grain core.

In four cases, measured $^{174}Hf/^{177}Hf$ and $^{178}Hf/^{177}Hf$ were outside accepted values (*16*), and these data were eliminated from consideration. Figure 2 shows the results for which we are confident that all the aforementioned effects have not affected the true ε_{Hf} values. Concordant or near-concordant results are shown as solid symbols, whereas >12% discordant results are shown as open symbols. The diagonal line extending into the negative ε_{Hf} field from an age of 4.5 Ga, labeled Lu/Hf = 0, demarcates the "forbidden region," corresponding to Lu/Hf < 0. Data plotting near this line must have been derived from an environment in which Lu was essentially completely fractionated from Hf shortly after Earth formation. If that event was the formation of continental crust, then the average continental crust $^{176}Lu/^{177}Hf$ value of ~0.01 (*23*) is a more appropriate comparator. The many results that plot along this line require formation of an enriched reservoir by 4.4 to 4.5 Ga.

Positive $\varepsilon_{Hf(T)}$ deviations observed in the same age interval have not previously been documented (*14*) and imply derivation from reservoirs with high Lu/Hf ratios. These data almost surely reflect the rapid development of depleted mantle with single-stage $^{176}Lu/^{177}Hf$ ratios within the possible range of values (0.05 and 0.2) for rocks residual from mantle melting (*24*). Whereas the depleted signature we observe is roughly symmetrical with the enriched reservoir (Fig. 2), negative ε_{Hf} values outnumber positive ε_{Hf} by 2.5:1. This is in part expected, because rocks originating from a source with a depleted signature are less petrogenetically suited to crystallizing zircon.

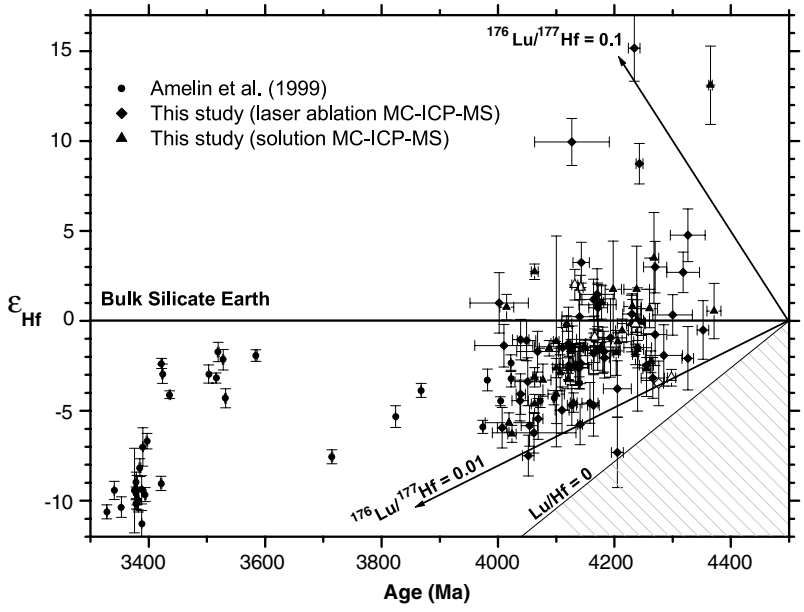

Fig. 2. Plot of $\varepsilon_{Hf(T)}$ versus age for new MC-ICP-MS Hf isotope analyses together with results of Amelin and co-workers (*14*) recalculated using the "terrestrial" ^{176}Lu decay constant (*17*). Solid symbols are concordant to <12% discordant, whereas open symbols are >12% discordant. The line marked Lu/Hf = 0 corresponds to $^{176}Hf/^{177}Hf$ ratios equivalent to the bulk silicate Earth value at 4.5 Ga. The stippled region indicates values not attainable (i.e., lower than solar system initial $^{176}Hf/^{177}Hf$). Error bars indicate 2 SE.

Most models for the growth of continental crust have emphasized delayed, slow growth (*1*, *2*, *4*). The existence of Hadean Jack Hills zircons has been known for 20 years (*11*) but has been largely considered as a curiosity rather than a fundamental record of the origin of continental crust (*25*). Investigations of Jack Hills zircons [$\delta^{18}O$, inclusion assemblages, zircon thermometry (*12*, *13*, *26–28*)] indicate that the vast majority formed in a continental environment (*26*) characterized by two forms of convergent margin magmatism (crustal anatexis and calc-alkaline magmatism at or close to water saturation) throughout the Hadean. Together, these data indicate that Earth was experiencing continental crust formation during the Hadean and that a mature sediment recycling system similar to that of the known era of plate tectonics had developed by ~4.4 Ga.

Jack Hills zircons are largely of continental origin (*12*, *13*, *26–28*), and our preferred interpretation of the variation of $\varepsilon_{Hf(T)}$ (Fig. 2) is that a major differentiation event occurred at 4.4 to 4.5 Ga, producing continental crust and a complementary depleted mantle reservoir. Because the production of modern continental crust is intimately connected with orogenic magmas, our interpretation implies that plate boundary interactions may have begun within the first ~100 My of Earth history. If the relative fraction of depleted versus enriched samples (Fig. 2) is representative of the general ongoing process, the volume of depleted mantle must have been a substantial fraction of the silicate Earth.

Positive $\varepsilon_{Hf(T)}$ deviations of +15 at ~4.2 Ga imply a reservoir with Lu/Hf of ~0.1 (Fig. 2). This extrapolates to ε_{Hf} of over +200 today, whereas values as negative as –7 at 4.2 Ga project to $\varepsilon_{Hf(0)}$ of about –100. No evidence for these reservoirs has yet been recognized in the post-Hadean rock record (*5*, *29*). Although it is conceivable that such reservoirs exist but have remained hidden for 4 Gy (*30*), their disappearance is well explained by the recycling of continental crust during the Hadean at rates ~10 times greater than those at present (*9*, *31*), coupled with vigorous stirring in a hotter and thus less-viscous mantle.

Armstrong (*9*) emphasized that all large terrestrial planets, including Earth, must have immediately differentiated into relatively constant volume core, depleted mantle, enriched crust, and fluid reservoirs. Recent investigations of $^{142,143}Nd/^{144}Nd$ variations indicate that a major silicate differentiation event occurred within 50 to 150 My (*32*, *33*), and possibly even

within 30 My (*30*) of Earth's formation. Our results support the view that continental crust was at least a component of the enriched counterpart that formed at ~4.5 Ga, but this original crust was largely recycled back into the mantle by the onset of the Archean (<4 Ga).

References and Notes

1. J. Veizer, S. L. Jansen, *J. Geol.* **87**, 341 (1979).
2. S. R. Taylor, S. M. McLennan, *The Continental Crust: Its Composition and Evolution* (Blackwell Scientific, Oxford, 1985).
3. S. A. Bowring, I. Williams, *Contrib. Mineral. Petrol.* **134**, 3 (1999).
4. M. T. McCulloch, V. C. Bennett, *Lithos* **30**, 237 (1993).
5. J. D. Vervoort, J. Blichert-Toft, *Geochim. Cosmochim. Acta* **63**, 533 (1999).
6. C. G. Chase, P. J. Patchett, *Earth Planet. Sci. Lett.* **91**, 66 (1988).
7. J. Blichert-Toft, N. T. Arndt, *Earth Planet. Sci. Lett.* **171**, 439 (1999).
8. J. Blichert-Toft, N. T. Arndt, G. Gruau, *Chem. Geol.* **207**, 261 (2004).
9. R. L. Armstrong, *Philos. Trans. R. Soc. London Ser. A* **301**, 443 (1981).
10. R. L. Armstrong, *Aust. J. Earth Sci.* **38**, 613 (1991).
11. W. Compston, R. T. Pidgeon, *Nature* **321**, 766 (1986).
12. S. J. Mojzsis, T. M. Harrison, R. T. Pidgeon, *Nature* **409**, 178 (2001).
13. S. A. Wilde, J. W. Valley, W. H. Peck, C. M. Graham, *Nature* **409**, 175 (2001).
14. Y. Amelin, D. C. Lee, A. N. Halliday, R. T. Pidgeon, *Nature* **399**, 252 (1999).
15. J. Hermann, R. Rubatto, *J. Metamorphic Geol.* **21**, 833 (2003).
16. Materials and methods are available as supporting material on *Science* Online.
17. U. Soderlund, P. J. Patchett, J. D. Vervoort, C. E. Isachsen, *Earth Planet. Sci. Lett.* **219**, 311 (2004).
18. J. Blichert-Toft, F. Albarède, *Earth Planet. Sci. Lett.* **148**, 243 (1997).
19. F. Albarède *et al.*, *Geochim. Cosmochim. Acta,* in press.
20. P. J. Patchett, J. D. Vervoort, U. Soderlund, V. J. M. Salters, *Earth Planet. Sci. Lett.* **222**, 29 (2004).
21. J. Blichert-Toft, unpublished data.
22. P. W. O. Hoskin, U. Schaltegger, *Rev. Mineral. Geochem.* **53**, 27 (2003).
23. J. D. Vervoort, P. J. Patchett, *Geochim. Cosmochim. Acta* **60**, 3717 (1996).
24. D. G. Pearson, G. M. Nowell, *J. Petrol.* **45**, 439 (2004).
25. S. J. G. Galer, S. L. Goldstein, *Geochim. Cosmochim. Acta* **55**, 227 (1991).
26. E. B. Watson, T. M. Harrison, *Science* **308**, 841 (2005).
27. D. Trail, S. J. Mojzsis, T. M. Harrison, *Geochim. Cosmochim. Acta* **68**, A743 (2004).
28. R. Maas, P. D. Kinny, I. S. Williams, D. O. Froude, W. Compston, *Geochim. Cosmochim. Acta* **56**, 1281 (1992).
29. J. D. Vervoort, P. J. Patchett, J. Blichert-Toft, F. Albarede, *Earth Planet. Sci. Lett.* **168**, 79 (1999).
30. M. Boyet, R. W. Carlson, *Science* **309**, 576 (2005).
31. G. F. Davies, *Geochim. Cosmochim. Acta* **66**, 3125 (2002).
32. M. Boyet *et al.*, *Earth Planet. Sci. Lett.* **214**, 427 (2003).
33. G. Caro, B. Bourdon, J. L. Birck, S. Moorbath, *Nature* **423**, 428 (2003).

34. We thank M. McCulloch, P. Lanc, Z. Bruce, A. Schmitt, T. Ireland, and S. Mussett for their major contributions to this project. The work was supported at the Australian National University by Australian Research Council grant DP0342709 to T.M.H., by the French Institut National des Sciences de l'Univers and the Programme National de Planétologie grants to J.B.T. and F.A., and by NASA Exobiology grant NAG5-13497 to S.J.M.

Supporting Online Material

www.sciencemag.org/cgi/content/full/1117926/DC1
Materials and Methods
Figs. S1 and S2
Tables S1 to S3
References

25 July 2005; accepted 2 November 2005
Published online 17 November 2005;
10.1126/science.1117926
Include this information when citing this paper.

X-ray Structure of the EmrE Multidrug Transporter in Complex with a Substrate

Owen Pornillos, Yen-Ju Chen, Andy P. Chen, Geoffrey Chang*

EmrE is a prototype of the Small Multidrug Resistance family of efflux transporters and actively expels positively charged hydrophobic drugs across the inner membrane of *Escherichia coli*. Here, we report the x-ray crystal structure, at 3.7 angstrom resolution, of one conformational state of the EmrE transporter in complex with a translocation substrate, tetraphenylphosphonium. Two EmrE polypeptides form a homodimeric transporter that binds substrate at the dimerization interface. The two subunits have opposite orientations in the membrane and adopt slightly different folds, forming an asymmetric antiparallel dimer. This unusual architecture likely confers unidirectionality to transport by creating an asymmetric substrate translocation pathway. On the basis of available structural data, we propose a model for the proton-dependent drug efflux mechanism of EmrE.

A major obstacle to effective treatment of bacterial infections is the emergence of strains that are resistant to available antibiotics. Of particular concern are multidrug-resistant strains that cause common diseases such as tuberculosis, gonorrhea, and hospital-acquired staphylococcal infections (*1*). Multidrug resistance arises, in part, through the action of integral membrane proteins called multidrug transporters (*1*, *2*). Each of these transporters can actively expel a wide variety of drugs and toxic compounds from the cell. There are two broad classes of transporters: ATP-binding cassette (ABC) proteins directly couple drug efflux to adenosine 5′-triphosphate (ATP) hydrolysis, whereas secondary transporters use the energy derived from proton or cation electrochemical gradients across the lipid bilayer.

EmrE is a proton-dependent secondary transporter from *Escherichia coli* and is a prototype of the Small Multidrug Resistance (SMR) family (*3*, *4*). SMRs represent the smallest transporters in nature; each polypeptide has only 105 to 120 amino acid residues and four transmembrane helices, and forms homo- or heterooligomers (*3*). EmrE is well documented to function as a homooligomer (*5*–*9*) and confers resistance to positively charged hydrophobic antibiotics, such as tetracycline, ethidium, and tetraphenylphosphonium (TPP) (*3*, *4*). EmrE exchanges two or more protons per drug molecule through a "hydrophobic" translocation pathway (*10*, *11*).

The general model for multidrug efflux by EmrE and other secondary transporters is the alternating access mechanism (*12*, *13*). In this model, the EmrE transporter has at least two conformations, inward-facing and outward-facing, with the drug-binding site accessible to the cytoplasm or periplasm, respectively. Interconversion between the two conformations is promoted by drug and/or proton binding. Here, we describe the x-ray crystal structure of one conformation of the EmrE transporter in complex with the drug TPP. The structure was determined to 3.7 Å resolution by anomalous dispersion methods, using the arsonium analog of TPP and selenomethionine (SeMet)–substituted proteins (Fig. 1A) (*14*).

SeMet-labeled proteins used for this study were produced in a cell-free system, because SeMet-EmrE did not express well in vivo. Briefly, EmrE was expressed by use of the T7 promoter in *E. coli* lysates supplemented with nucleotide triphosphates, T7 polymerase, and appropriate amino acids (*14*). Experimental maps derived from Se and As data are very well correlated, indicating that in vitro– and in vivo–expressed EmrE proteins adopt a similar structure. Our work shows that cell-free methods are a viable alternative to traditional large-scale protein expression systems.

Consistent with biochemical studies showing that EmrE is primarily a dimer in detergent and binds drugs with a 2:1 protein/drug ratio (*9*, *15*), the asymmetric unit of the EmrE-TPP crystal is composed of two molecules of EmrE and one molecule of TPP (Fig. 1). The minimally functional unit of EmrE is therefore

Department of Molecular Biology, The Scripps Research Institute, 10550 North Torrey Pines Road, CB-105, La Jolla, CA 92037, USA.

*To whom correspondence should be addressed. E-mail: gchang@scripps.edu

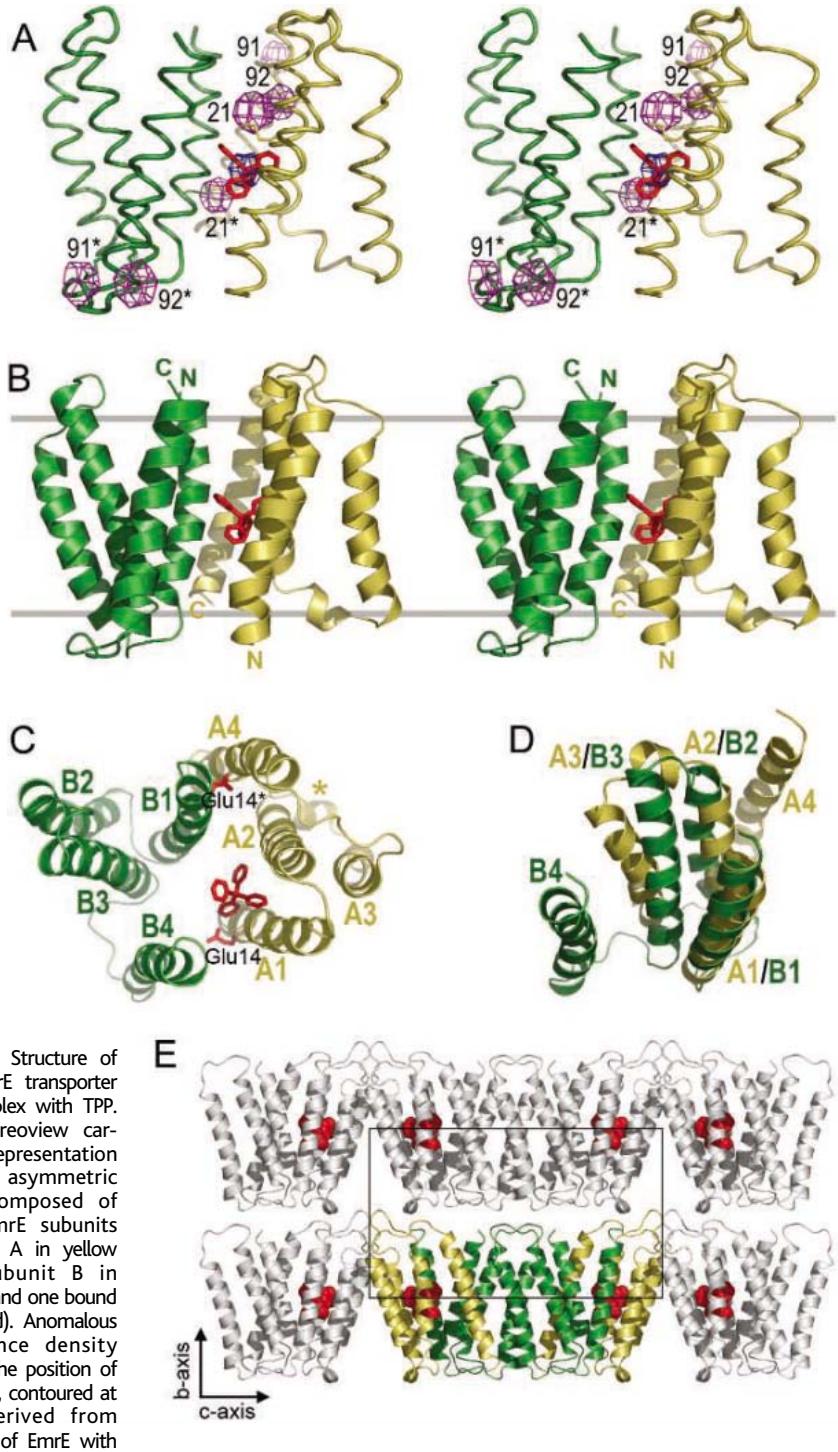

Fig. 1. Structure of the EmrE transporter in complex with TPP. (**A**) Stereoview cartoon representation of the asymmetric unit, composed of two EmrE subunits (subunit A in yellow and subunit B in green), and one bound TPP (red). Anomalous difference density shows the position of As (blue, contoured at 1σ), derived from crystals of EmrE with tetraphenylarsonium (an analog of TPP). Methionine positions are indicated by Se atoms (magenta, 4σ), derived from SeMet-EmrE-TPP crystals. Methionine side chains are shown explicitly and labeled; corresponding residues in subunit B and subunit A are distinguished by the asterisks. The coloring scheme in this panel is maintained throughout Figs. 1 to 3. (**B**) Stereoview of the EmrE homodimer. The N and C termini of the two subunits are indicated. The boundaries of the lipid bilayer, deduced from the positions of aromatic groups, are shown by the gray lines. (**C**) Top view of the dimer, with the four transmembrane helices in each subunit labeled. The short helix connecting helices A2 and A3 is indicated by an asterisk. This view clearly shows that TPP is bound at the dimerization interface. The two Glu-14 residues are shown in red. (**D**) Best-fit superposition of subunits A (yellow) and B (green) (root mean square deviation of 3.5 Å over equivalent Cα positions). The first three helices form a left-handed bundle, whereas the fourth helices are positioned differently. (**E**) Crystal packing of EmrE-TPP. The lattice is stabilized by side-by-side transmembrane contacts and loop interactions, reminiscent of type I and 2D membrane protein crystals. A potential dimer of dimers is colored as above; the symmetry-related elements are colored gray. The unit cell is boxed in black. This view is perpendicular to the *bc* plane.

likely to be a homodimer. In contrast to the simple, symmetric organization expected from genetic and biochemical data, the EmrE structure shows an unusual architecture. The two subunits pack in an inverted orientation relative to each other, forming an antiparallel dimer (Fig. 1, A and B). SeMet sites in the two subunits are related by an approximate twofold axis in the middle of the dimer perpendicular to the transmembrane axis (Fig. 1A). X-ray studies of unbound EmrE (*16*) and electron microscopic analysis of EmrE-TPP in reconstituted lipid bilayers (*13*) also suggested an antiparallel arrangement for the EmrE dimer. Although a previous study suggested that EmrE has a unique topology (*17*), the structure is consistent with more recent analyses of the *E. coli* inner-membrane proteome by von Heijne and colleagues, which indicate that indeed, EmrE and other homomeric SMR proteins are likely to have a dual topology (*18*, *19*). Antiparallel arrangement of EmrE is also supported by studies of heterooligomeric SMR transporters, such as the YdgE/YdgF proteins of *E. coli* and EbrA/EbrB of *Bacillus subtilis* (*20*, *21*). These transporters are composed of two similar but distinct polypeptides, which appear to form heterodimers analogous to the EmrE homodimer. The two subunits are inserted in unique but opposite orientations in the bacterial membrane, as predicted by the "positive-inside rule" and determined experimentally for YdgE/YdgF (*18*). Thus, the emerging structural paradigm for SMR transporters is that they are probably built from antiparallel dimers, which can be composed of two copies of a single polypeptide as in EmrE, or two different polypeptides as in YdgE/YdgF. This is in line with an increasing number of known membrane protein structures, primarily transporters and channels, which contain tandem antiparallel domains (*22*).

Antiparallel dimerization of identical subunits can symmetrize the substrate translocation pathway, which could result in a nonproductive transporter that simply cycles back and forth. Although coupling to an electrochemical gradient may be sufficient to drive directional transport in such a system, the EmrE transporter has an additional feature that likely confers unidirectionality—the dimer is asymmetric. The two subunits, A and B, adopt slightly different tertiary folds, despite having identical primary sequence (Fig. 1). In each subunit, the first three helices form a loose left-handed three-helix bundle, as viewed from the N terminus (Fig. 1, C and D). However, the disposition of the fourth helix is different in the two subunits. In subunit A, helix A4 is packed against helix A2, whereas in subunit B, helix B4 is packed against B3 (Fig. 1D). These helices form part of the dimer interface, suggesting that the alternate EmrE folds may be required for dimerization. In addition, a single-turn helix, which forms part of the loop

connecting helices A2 and A3, is absent in subunit B (asterisk in Fig. 1C).

Viewed along the transmembrane axis, the two three-helix bundles are on opposite sides of the dimer, flanked by helices A4 and B4 (Fig. 1C). Helices A1 and B1 are located in the middle of the dimer and form part of the TPP-binding site, in accord with their essential role in drug transport (Fig. 1, B and C). These two helices form an approximate V shape with a ~30° crossing angle, consistent with predictions from electron paramagnetic resonance (EPR) spin-labeling studies of unbound EmrE (*23*). The relative positions of the first and fourth transmembrane helices are also in general agreement with predictions from cross-linking experiments (*7*).

Biochemical studies also suggest that EmrE can form a dimer of dimers (*8*), and examination of packing interactions in the EmrE-TPP crystal suggests a possible tetramerization interface. Helices A4, B1, and B2 from one dimer pack against their symmetry-related mates in another dimer, burying a total surface area of ~1600 Å^2 (Fig. 1E). Although it remains to be confirmed by mutagenesis and other biophysical methods, EmrE tetramerization could, in principle, increase the efficiency of drug recognition and efflux through avidity effects.

A possible drug translocation pathway is evident in the structure, consisting of two cone-shaped pockets that open to opposite sides of the lipid bilayer (shown by arrows in Fig. 2A). The two pockets are demarcated by helices A1 and B1. Consistent with the asymmetric nature of the EmrE dimer, this putative translocation pathway is also asymmetric. In addition to A1 and B1, the larger pocket is surrounded by helices A2, B3, and B4, whereas the smaller one is lined by helix A2. TPP appears bound at the bottom of the larger pocket, wedged between helices A1, A2, and B1 (Fig. 2B). We presume that these three helices act as a "gate," controlling passage of the drug into the smaller pocket. Extensive mutagenic studies of EmrE by Schuldiner and co-workers have previously identified residues required for drug binding and translocation (*10*, *11*, *24*–*28*). These residues nicely map to the proposed translocation pathway (Fig. 2A).

The volume of the binding pocket is considerably larger than TPP (Fig. 2B) and can accommodate a wide range of substrate sizes and shapes, explaining EmrE's polyspecificity. The binding site complements the positively charged hydrophobic nature of TPP and other EmrE substrates (*3*, *4*). Hydrophobic residues in the pocket are well positioned to participate in van der Waals contacts with the four phenyl rings of TPP (Fig. 2B). The electrostatic component is provided by a membrane-embedded acidic residue located at the bottom of the pocket, Glu-14 in helix A1 (colored red in Fig. 2B). Mutagenesis indicates that this glutamate is absolutely required for proper EmrE function (*24*–*26*), although such studies cannot readily distinguish between the two Glu-14 residues in the homodimer. In this EmrE conformation, the second Glu-14 in helix B1 does not appear to contact TPP (Glu14* in Fig. 2B). Its carboxylate group is located ~16 Å away from the TPP phosphate atom and appears to face the smaller pocket. Thus, the two glutamates do not necessarily contact the bound drug simultaneously, as previously proposed (*4*), and we suggest that instead they bind TPP sequentially (see below).

A structure of the EmrE-TPP complex has also been reported by electron microscopy (EM) of two-dimensional (2D) crystals to resolutions of 7.5 Å in-plane and 16 Å perpendicular to the lipid bilayer (*13*). The EM model also shows EmrE as an asymmetric dimer with the drug-binding site located between the two monomers, and also suggests an antiparallel arrangement. The x-ray and EM structures appear to have captured two different conformations of drug-bound EmrE transporter (Fig. 3). Independent superposition of the two EmrE subunits in the x-ray structure with the EM model allowed us to define the subunit boundaries and propose helical assignments for the EM structure (Fig. 3A). This

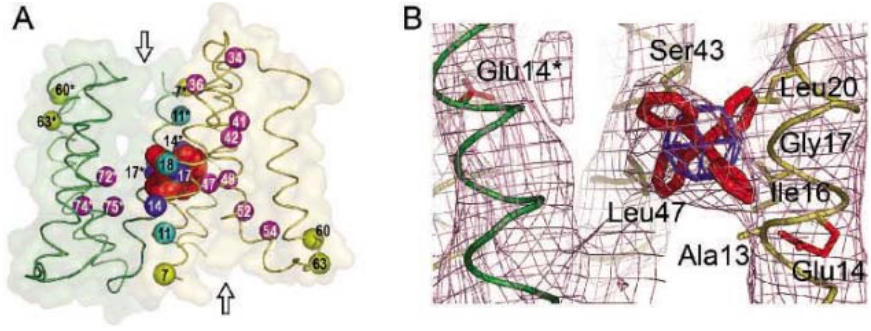

Fig. 2. A possible drug translocation pathway in the EmrE transporter. (**A**) Side view of the EmrE dimer, superimposed with a semitransparent surface rendering. The openings to the two pockets, facing opposite sides of the lipid bilayer, are indicated by arrows. Residues that have been shown by cysteine-scanning mutagenesis to be important for drug binding and transport (*10*, *11*, *24*–*28*) are indicated by spheres, using the following color scheme: blue, absolutely required for TPP binding; cyan, substitutions show partial TPP binding and impaired transport; magenta, residues that confer altered drug specificity when mutated. Residues in subunit B are indicated by asterisks. Note that EmrE mutagenesis alters two residues in the dimer, which are in nonequivalent positions. We have therefore only shown the positions that are close to the putative translocation pathway. Residues that are important for drug transport but have both copies removed from the pathway are shown in yellow (Leu-7, Tyr-60, Trp-63). These residues likely perform essential structural roles. (**B**) Close-up view of the bound drug, with protein, TPP, and As densities (contoured at 1σ). The three helices are B1 (left), A2 (middle), and A1 (right). The two Glu-14 residues are shown and colored red. The position of the phosphate atom is unambiguously defined by the anomalous As peak from the arsonium analog of TPP (blue), and the positions of the Glu-14 residues are relatively well defined based on the positions of Se atoms in Met-21, two helical turns away. Hydrophobic residues within van der Waals distance of TPP are also indicated. Close packing of TPP to helix A1 appears facilitated by the absence of a side chain in Gly-17. Mutation of this glycine to cysteine abolishes TPP binding (*27*).

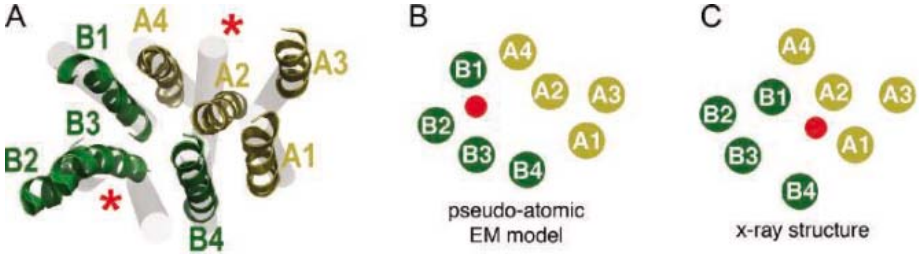

Fig. 3. Comparison of the x-ray and EM structures of EmrE-TPP. (**A**) Independent superposition of EmrE subunits A and B in the x-ray structure with a cylinder model (colored gray) derived from the EM structure of EmrE-TPP (European Molecular Biology Laboratory–EBI accession code EMD-1087) (*13*). A unique match was found using two constraints: Three-helix bundles on opposite sides of the dimer were assumed to be helices 1 to 3, and the helix closest to the density attributed to TPP in the EM map was assumed to be helix 1. In this pseudo-atomic model, three helices have notably different tilt angles: A2, B2, and B3 (shown by red asterisks). The x-ray position of helices B2 and B3, which appear to move as a unit, is likely due to crystal packing interactions along the putative tetramerization interface (see also Fig. 1E). We speculate that the conformational change in helix A2 is relevant to the drug transport mechanism. (**B** and **C**) The TPP molecule is bound to different sites in the x-ray structure (C) and EM model (B), suggesting a possible mechanism for drug transport. The relative positions of the EmrE helices are indicated, viewing toward the binding pockets (in the same orientation as in Fig. 1C). The positions of the TPP molecules are shown by red circles.

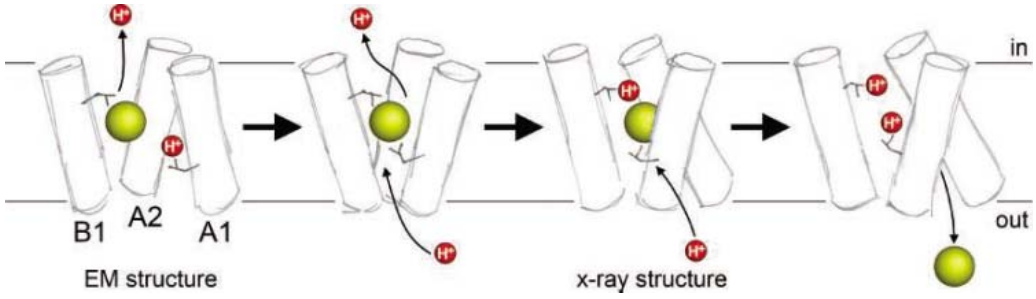

Fig. 4. A potential mechanism for proton-dependent drug translocation by EmrE. For clarity, only the three putative gating helices (A1, A2, and B1) and two membrane-embedded Glu-14 side chains are shown explicitly. Drug substrates and protons are represented by the yellow sphere and red balls, respectively.

unique match was obtained because the dimer is asymmetric, and with the constraint that the helix closest to the putative TPP density in the EM map is helix 1 (*13*). The transformation between the two structures can be approximated by a relative twist of ~30° between the two subunits, although helical tilt angles also change within individual monomers. Curiously, the binding pockets open to the same side in both models.

There are several interesting differences between the x-ray and EM models of EmrE-TPP. (i) TPP appears bound to subunit B in the EM structure, and not subunit A (Fig. 3B). Although this remains to be confirmed by other methods, it suggests that the two subunits may alternately bind drug during the transport cycle and explains the requirement for both membrane-embedded glutamates in the dimer. (ii) The drug-binding pocket in the EM model appears larger and more open, surrounded by six helices (Fig. 3B) (*13*). In the x-ray model, the binding site is more closed, surrounded by only five helices (Fig. 3C). We speculate that these differences reflect conformational changes that occur upon transfer of TPP between subunits A and B. (iii) In the EM model, the second pocket on the opposite side of the drug translocation pathway is absent. This is because the three gating helices, A1, A2, and B1, are in different positions. Helices A1 and B1 in the EM model are more parallel and >20 Å apart, whereas helix A2 is tilted differently (Fig. 3A). Conformational mobility in these helices is evident from both EPR and nuclear magnetic resonance data (*23*, *29*), and we speculate that helix-coil conversion in the A2-A3 loop may help facilitate movement. An attractive model is that the x-ray and EM structures represent the two EmrE conformations deduced from the EPR studies: one where helices A1 and B1 form a V-shaped configuration and another where they are >20 Å apart (*23*). We speculate that interconversion of the EmrE transporter between these two (and perhaps other) conformations may drive drug transport.

On the basis of the above observations, we propose the following outline for proton-dependent drug transport by EmrE and other SMR transporters (Fig. 4). With its large, open binding site, we suggest that the EM structure represents an inward-facing conformation of EmrE. With two potential entry points to the binding site (*13*), this EmrE conformation could act as an effective "hydrophobic vacuum cleaner" (*30*), filtering both the cytoplasm and the inner leaflet of the lipid bilayer for substrates. We envision that TPP first binds to Glu-14 in subunit B in exchange for one proton. As a next step, the bound drug is transferred to subunit A (that is, the translocation pathway) in exchange for the second proton. Conformational changes in the dimer could serve to bring the two Glu-14 side chains in proximity, facilitating the exchange. In support of this idea, the Glu-14→Asp EmrE mutant forms a transporter that binds TPP with high affinity but with impaired transport function (*24*), likely because the Asp side chain is too short. The x-ray structure may represent the postexchange conformation in which the drug is bound to subunit A, and Glu-14 in subunit B is oriented toward the outer pocket and reprotonated. Rearrangement of helices A1, A2, and B1 in the putative translocation pathway could transfer TPP to this pocket, where it would rapidly dissociate owing to favorable proton exchange at the periplasmic space.

In the proposed mechanism, the two subunits in the EmrE dimer are structurally and functionally nonequivalent, an arrangement that would favor unidirectional transport. Indeed, this is a recurring theme in structural studies of the different transporter families (*12*, *22*, *31*). The large conformational changes that appear to occur during drug translocation are consistent with the low turnover number for this transporter (*32*).

References and Notes

1. S. B. Levy, *Sci. Am.* **278**, 46 (March 1998).
2. Reviewed in X. Z. Li, H. Nikaido, *Drugs* **64**, 159 (2004).
3. Reviewed in Y. J. Chung, M. H. Saier Jr., *Curr. Opin. Drug Discov. Dev.* **4**, 237 (2001).
4. S. Schuldiner *et al.*, *News Physiol. Sci.* **16**, 130 (2001).
5. H. Yerushalmi, M. Lebendiker, S. Schuldiner, *J. Biol. Chem.* **271**, 31044 (1996).
6. D. Rotem, N. Sal-man, S. Schuldiner, *J. Biol. Chem.* **276**, 48243 (2001).
7. M. Soskine, S. Steiner-Mordoch, S. Schuldiner, *Proc. Natl. Acad. Sci. U.S.A.* **99**, 12043 (2002).
8. Y. Elbaz, S. Steiner-Mordoch, T. Danieli, S. Schuldiner, *Proc. Natl. Acad. Sci. U.S.A.* **101**, 1519 (2004).
9. P. J. Butler, I. Ubarretxena-Belandia, T. Warne, C. G. Tate, *J. Mol. Biol.* **340**, 797 (2004).
10. M. Lebendiker, S. Schuldiner, *J. Biol. Chem.* **271**, 21193 (1996).
11. S. S. Mordoch, D. Granot, M. Lebendiker, S. Schuldiner, *J. Biol. Chem.* **274**, 19480 (1999).
12. J. Abramson *et al.*, *FEBS Lett.* **555**, 96 (2003).
13. I. Ubarretxena-Belandia, J. M. Baldwin, S. Schuldiner, C. G. Tate, *EMBO J.* **22**, 6175 (2003).
14. Materials and methods and structure statistics are available as supporting material on *Science* Online.
15. C. G. Tate, I. Ubarretxena-Belandia, J. M. Baldwin, *J. Mol. Biol.* **332**, 229 (2003).
16. C. Ma, G. Chang, *Proc. Natl. Acad. Sci. U.S.A.* **101**, 2852 (2004).
17. S. Ninio, Y. Elbaz, S. Schuldiner, *FEBS Lett.* **562**, 193 (2004).
18. D. O. Daley *et al.*, *Science* **308**, 1321 (2005).
19. E. Granseth, D. O. Daley, M. Rapp, K. Melen, G. von Heijne, *J. Mol. Biol.* **352**, 489 (2005).
20. K. Nishino, A. Yamaguchi, *J. Bacteriol.* **183**, 5803 (2001).
21. Y. Masaoka *et al.*, *J. Bacteriol.* **182**, 2307 (2000).
22. For a recent example, see C. Hunte *et al.*, *Nature* **435**, 1197 (2005).
23. H. A. Koteiche, M. D. Reeves, H. S. McHaourab, *Biochemistry* **42**, 6099 (2003).
24. T. R. Muth, S. Schuldiner, *EMBO J.* **19**, 234 (2000).
25. H. Yerushalmi, S. Schuldiner, *J. Biol. Chem.* **275**, 5264 (2000).
26. H. Yerushalmi, S. S. Mordoch, S. Schuldiner, *J. Biol. Chem.* **276**, 12744 (2001).
27. N. Gutman, S. Steiner-Mordoch, S. Schuldiner, *J. Biol. Chem.* **278**, 16082 (2003).
28. Y. Elbaz, N. Tayer, E. Steinfels, S. Steiner-Mordoch, S. Schuldiner, *Biochemistry* **44**, 7369 (2005).
29. M. Schwaiger *et al.*, *Eur. J. Biochem.* **254**, 610 (1998).
30. Y. Raviv, H. B. Pollard, E. P. Bruggemann, I. Pastan, M. M. Gottesman, *J. Biol. Chem.* **265**, 3975 (1990).
31. J. Abramson, S. Iwata, H. R. Kaback, *Mol. Membr. Biol.* **21**, 227 (2004).
32. H. Yerushalmi, M. Lebendiker, S. Schuldiner, *J. Biol. Chem.* **270**, 6856 (1995).

33. We thank C. Ma for invaluable contributions to EmrE-TPP crystallization; T. Kudlicki and J. Fletcher (Invitrogen) for in vitro translation reagents; S. Lieu for general lab support; and the staff at Stanford Synchrotron Radiation Laboratory, Advanced Light Source, and Advanced Photon Source for assistance with data collection. We thank C.G. Tate (MRC Laboratory of Molecular Biology) for providing the EM map of EmrE-TPP, and S. H. White, P. E. Wright, H. J. Dyson, R. A. Milligan, C. L. Reyes, and Y. Yin for critical reading of the manuscript. This study was supported by grants from the NIH (GM67644 and GM073197) and NASA (NAG8-1834) to G.C. O.P. is supported by an NIH postdoctoral fellowship. Coordinates have been deposited in the Protein Data Bank (PDB code: 2f2m).

Supporting Online Material

www.sciencemag.org/cgi/content/full/310/5756/1950/DC1
Materials and Methods
Table S1
References and Notes

6 September 2005; accepted 21 November 2005
10.1126/science.1119776

A Developmental Timing MicroRNA and Its Target Regulate Life Span in *C. elegans*

Michelle Boehm and Frank Slack*

The microRNA *lin-4* and its target, the putative transcription factor *lin-14*, control the timing of larval development in *Caenorhabditis elegans*. Here, we report that *lin-4* and *lin-14* also regulate life span in the adult. Reducing the activity of *lin-4* shortened life span and accelerated tissue aging, whereas overexpressing *lin-4* or reducing the activity of *lin-14* extended life span. Life-span extension conferred by a reduction in *lin-14* was dependent on the DAF-16 and HSF-1 transcription factors, suggesting that the *lin-4*–*lin-14* pair affects life span through the insulin/insulin-like growth factor–1 pathway. This work reveals a role for microRNAs and developmental timing genes in life-span regulation.

Life span is highly variable among species, and it has become clear that a genetic program of senescence in the soma is responsible for this variation (*1*). Recent studies have suggested that gene expression changes in the aged adult are developmentally timed at the transcriptional level. For example, in both the nematode *Caenorhabditis elegans* and the fly *Drosophila melanogaster*, a characteristic gene expression profile associated with age can be detected in young adulthood, well before the accumulation of molecular damage has begun (*2*). Thus, conserved genes may act temporally to initiate a program of aging that starts early in adult life (*3*, *4*). We hypothesized that if such an aging program exists, it may be controlled by mechanisms similar to those used in developmental timing (*3*). The heterochronic genes of *C. elegans* constitute one such genetic pathway that regulates developmental timing (*5*–*7*).

Heterochronic genes, such as *lin-4* and *lin-14* (*5*, *8*, *9*), are temporal identity genes that affect the fate choices that cells make at specific times during development, and mutations in heterochronic genes result in temporal alterations to stage-specific patterns of cellular development (*6*, *7*). Expression of the *lin-4* microRNA (miRNA) is up-regulated near the end of the first larval stage, and *lin-4* binds with imperfect complementarity to the 3′UTR of its target, *lin-14*, to prevent its translation (*8*–*11*) and allow stage two larval cell fates to occur. The molecular function of *lin-14* is unknown, but it encodes a nuclear protein (*12*) that associates with DNA (*13*) and has sequence similarities to transcription factors (fig. S1). LIN-14 is down-regulated in the hypodermis at the first to second larval-stage transition (*12*), but its expression persists weakly in other tissues throughout larval development (*13*) and into adulthood (fig. S2). Similarly, *lin-4* is also expressed in the adult (*14*, *15*) (fig. S2). Although the roles of *lin-4* and *lin-14* during larval development have been extensively studied, the function of these genes in the adult has not been investigated. Therefore, we tested whether genes that direct the timing of early developmental events may also function in the adult to regulate the timing of later processes, such as life span and aging.

We assayed heterochronic mutants for life-span length and found that mutations in *lin-4* and *lin-14* resulted in aging defects. Animals with a loss-of-function (*lf*) mutation in *lin-4* displayed a life span that was significantly shorter than that of the wild type (Fig. 1A), suggesting that *lin-4* is required to prevent premature death. Conversely, overexpressing *lin-4* from an extrachromosomal array led to a lengthened life span (Fig. 1C). This result demonstrates that the *lin-4(lf)* mutant did not die prematurely solely as the result of an unrelated, general pathology, but rather that *lin-4* functions to extend life span. Consistent with our *lin-4* data, we found that a *lf* mutation in a target of *lin-4*, *lin-14*, produced the opposite life-span phenotype. Animals carrying a temperature-sensitive *lf* mutation in *lin-14* had a 31% longer life span than the wild type (Fig. 1B). The longevity

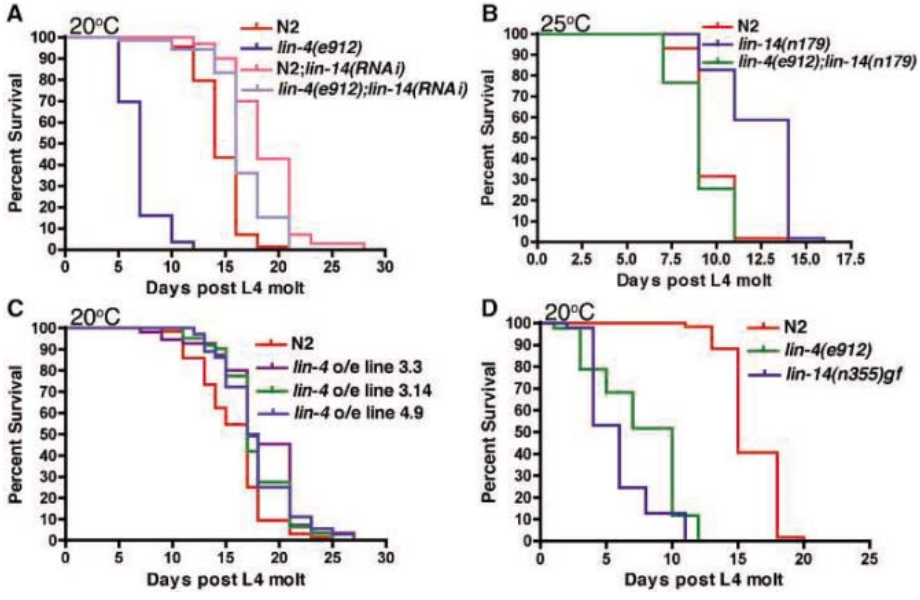

Fig. 1. *lin-4* and *lin-14* mutants have opposite life-span phenotypes. (**A**) Red, survival of wild-type (N2) animals on control bacteria containing empty vector (mock RNAi); blue, *lin-4(e912)lf*; mock RNAi; pink, *lin-14(RNAi)*; light blue, *lin-4(e912)lf*; *lin-14(RNAi)* at 20°C. N2: $n = 69$, $m = 14.6$. *lin-4(e912)lf*: $n = 56$, $m = 6.9$, $P < 0.0001$*. N2 ;*lin-14(RNAi)*: $n = 68$, $m = 18.7$, $P < 0.0001$*. *lin-4(e912)lf*; *lin-14(RNAi)*: $n = 72$, $m = 16.6$, $P < 0.0001$#. (**B**) A *lin-14(lf)* mutation extends life span when grown and assayed at the restrictive temperature of 25°C. N2: $n = 57$, $m = 9.5$. *lin-14(n179)lf*: $n = 58$, $m = 12.5$, $P < 0.0001$*. *lin-4(e912)lf*; *lin-14(n179)lf*: $n = 51$, $m = 9.0$, $P = 0.0906$*. (**C**) *lin-4* overexpression extends life span. Three lines overexpressing (o/e) *lin-4* are shown in purple, blue, and green; wild-type animals are in red. N2: $n = 64$, $m = 15.8$. *lin-4* o/e line 3.3: $n = 54$, $m = 18.3$, $P < 0.0001$*. *lin-4* o/e line 3.14: $n = 62$, $m = 17.7$, $P = 0.0023$*. *lin-4* o/e line 4.9: $n = 37$, $m = 17.8$, $P = 0.0113$*. (**D**) A *lin-14* gain-of-function mutant, *n355*, has a short-lived phenotype similar to that of the *lin-4(e912)lf* mutant. Red, wild-type animals; green, *lin-4(e912)lf*; blue, *lin-14(n355 gf)*. N2: $n = 59$, $m = 15.9$. *lin-4(e912)lf*: $n = 85$, $m = 7.7$, $P < 0.0001$*. *lin-14(n355 gf)*: $n = 94$, $m = 5.9$, $P < 0.0001$*. All experiments were repeated at least once with similar effects. *n*, number of animals observed in each experiment. *m*, mean adult life span (days). *P** values refer to experimental strain and N2 control animals in a single experiment, and *P#* values refer to a strain on control and experimental RNAi treatment in a single experiment.

Department of Molecular, Cellular, and Developmental Biology, Yale University, New Haven, CT 06511, USA.

*To whom correspondence should be addressed. E-mail: frank.slack@yale.edu

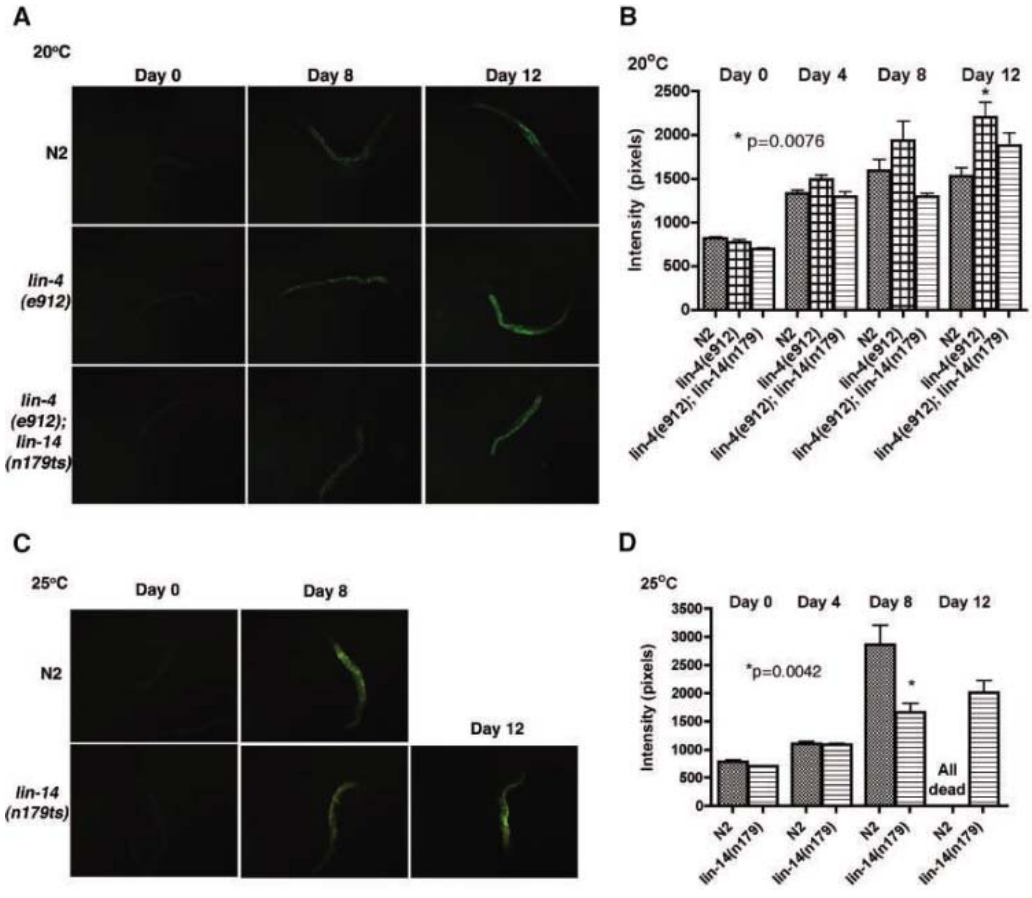

Fig. 2. *lin-4* and *lin-14* mutants display accelerated and delayed rates, respectively, of lipofuscin accumulation. (**A**) *lin-4(e912)lf* mutants display an increase of lipofuscin as compared with similarly aged wild-type animals at 20°C. This effect is suppressed by the *lin-14(n179)lf* mutation. (**B**) Quantification of the N2, *lin-4(e912)lf*, *lin-4(e912)lf;lin-14(n179)lf* populations' gut autofluorescence at days 0, 4, 8, and 12 after the larval-to-adult transition at 20°C. (**C**) *lin-14(n179)lf* mutants display a decrease in lipofuscin accumulation compared with wild-type animals at 25°C. (**D**) Quantification of the N2 and *lin-14(n179)lf* populations' gut autofluorescence at 25°C as for (B). For (A) and (C), photographs shown are representative examples (n = 10 for each time point per strain). Photographs were taken at 100× magnification. All animals were photographed on the same day under identical conditions, and photographs were treated identically. For (B) and (D), autofluorescence was quantified using Axiovision 4.4 software (n = 10 for each time point per strain). P values were calculated using the Mann-Whitney nonparametric t test comparing mutant to wild-type results at day 12 in (B) and day 8 in (D). Error bars represent the standard error of the mean.

phenotype produced by the *lin-14(lf)* lesion was reproduced by RNA interference (RNAi) of *lin-14* (Fig. 1A). Thus, *lin-14* normally acts to promote a short life span. A *lin-14* gain-of-function (*gf*) mutant (*16*), which lacks the *lin-4* complementary sites in the *lin-14* 3′ untranslated region (UTR) and overexpresses LIN-14 at later stages (*12*), closely phenocopied the short-lived phenotype of the *lin-4(lf)* mutant (Fig. 1D). Additionally, *lin-14(RNAi)* suppressed the short life span of the *lin-4(e912)lf* mutant (Fig. 1A). Taken together, the data suggest that the major role of *lin-4* in regulating life span is to repress its target, *lin-14*.

To determine whether the short life span of *lin-4(lf)* mutants is due to accelerated aging or to an unrelated, pleiotropic cause, we monitored the accumulation of intestinal autofluorescence in adult animals. Intestinal autofluorescence, which is caused by lysosomal deposits of lipofuscin, accumulates over time in the aging animal and is an established marker for aging (*17*). In agreement with its short life span, the *lin-4(lf)* mutant accumulated intestinal autofluorescence more rapidly than the wild type (Fig. 2, A and B). These results resemble those found for the short-lived strain with a *daf-16(lf)* mutation (fig. S3, A and B). *daf-16* encodes a FOXO transcription factor that regulates life span through insulin-like signaling (*1*, *18*–*20*). The premature lipofuscin accumulation caused by *lin-4(lf)* was suppressed when combined with the *lin-14(n179)lf* lesion (Fig. 2, A and B), consistent with the ability of *lin-14(lf)* to suppress the short life span of the *lin-4(lf)* mutant.

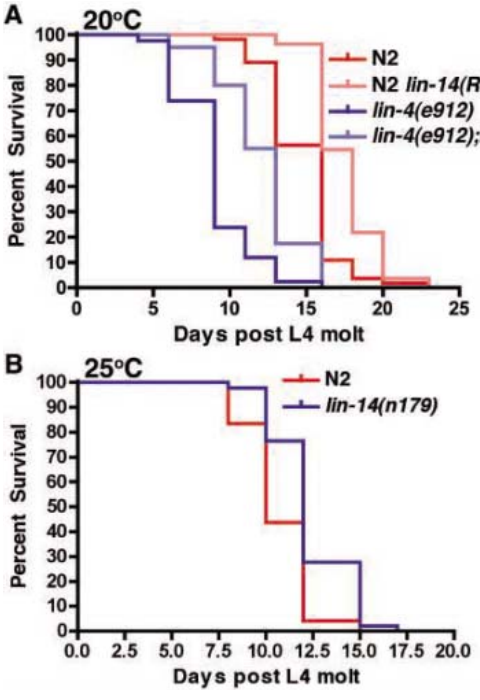

Fig. 3. Loss of *lin-14* function during adulthood is sufficient to extend life span. (**A**) Wild-type animals treated with *lin-14(RNAi)* (pink) only in the adult stage have extended life spans compared with mock RNAi animals (red). *lin-4(e912)lf* mutants treated with *lin-14(RNAi)* (light blue) only in the adult stage display an extended life span compared with *lin-4(e912)lf* mutants on mock RNAi (blue) at 20°C. N2: n = 55, m = 14.8. *lin-14(RNAi)*: n = 55, m = 17.6, $P < 0.0001$*. *lin-4(e912)lf*: n = 43, m = 9.0. *lin-4(e912)lf*; *lin-14(RNAi)*: n = 40, m = 12.1, $P < 0.0001$#. (**B**) *lin-14(n179)lf* animals (blue) display extended life spans compared with wild-type animals (red) when grown at the permissive temperature of 15°C until the larval-to-adult transition and then moved to the restrictive temperature of 25°C. N2: n = 48, m = 10.7. *lin-14(n179)lf*: n = 53, m = 12.4, $P < 0.0001$*. All experiments were repeated at least once with similar effects. P* and P# are defined in the legend to Fig. 1.

In contrast to *lin-4(lf)*, the *lin-14(n179)lf* mutant displayed a slower rate of intestinal autofluorescence accumulation as compared with the wild type (Fig. 2, C and D), in agreement with

its extended life span. The decreased rate of gut autofluorescence accumulation is similar to that observed in the long-lived *daf-2(lf)* mutant (fig. S3, C and D) (*17*). *daf-2* encodes an insulin/insulin-like growth factor–1 (IGF-1) receptor that lies upstream of *daf-16* in insulin-like signaling (*18*, *20*, *21*).

The stress response of the *lin-4(lf)* and *lin-14(lf)* strains was also examined. *C. elegans* mutants that display life-span phenotypes also display altered responses to stress treatments, including heat shock (*22*, *23*). For instance, the long-lived *daf-2(lf)* mutant is highly tolerant to heat shock, and this heightened stress resistance is believed to be essential for life-span extension (*22*). In accordance with its life-span phenotype, the *lin-4(e912)lf* mutant displayed a greater sensitivity to heat shock as compared with the wild type (fig. S4B), whereas the *lin-14(n179)lf* mutant displayed a greater resistance to heat shock as compared with the wild type (fig. S4C).

To rule out the possibility that life-span modulation directed by *lin-14* and *lin-4* is merely due to their role in larval development, we examined the effect of reducing the function of *lin-14* only in the postmitotic adult. RNAi-mediated inhibition of *lin-14* expression after the final larval molt extended the life span of wild-type animals, similar to the extension observed when animals were exposed to *lin-14(RNAi)* just after hatching (Fig. 3A). Additionally, growing the *lin-14(n179)lf* mutant at the permissive temperature until young adulthood and then shifting to the restrictive temperature also produced an extended life span (Fig. 3B). These results demonstrate that *lin-14* functions in the adult to restrict life span. Furthermore, the short life span of the *lin-4(e912)lf* mutant was also rescued to a significant extent when exposed to *lin-14(RNAi)* only during adulthood. This result supports the idea that the *lin-4(e912)lf* accelerated-aging phenotype is not due to developmental abnormalities or an unrelated pleiotropic cause. Thus, the *lin-4* miRNA appears to suppress senescence in *C. elegans* through repression of *lin-14* in the adult.

We tested whether *lin-4* and *lin-14* extend life span by acting through one of the known *C. elegans* life-span regulatory pathways, such as the insulin/IGF-1 signaling pathway. Several insulin/IGF-1 signaling pathway members regulate life span through mechanisms dependent on the downstream DAF-16/FOXO and HSF-1 transcription factors (*1*, *18*–*21*, *24*, *25*). As with *lin-4*, inhibiting *daf-16* or *hsf-1* activity shortens life span, whereas elevating their activity lengthens life span (*25*, *26*). The *daf-16(mu86)* null mutant strain, when treated with *lin-14(RNAi)*, did not display an extended life span (Fig. 4B), nor did *lin-14(n179)lf*; *daf-16(RNAi)* animals (Fig. 4A). These data demonstrate that *daf-16* is required for the *lin-14(lf)*–mediated longevity phenotype. *lin-4(lf)* animals grown on *daf-16(RNAi)* had shortened life-span lengths that are identical to that of the *lin-4(lf)* strain grown on mock RNAi (Fig. 4C), indicating that *lin-4* and *lin-14* genetically interact with *daf-16*. However, the *lin-4(lf)* mutant had a shorter life span than the *daf-16(lf)* mutant, indicating that *lin-14* does not exert its effect on life span by negative regulation of DAF-16 alone. Consistent with this idea, the *lin-14(lf)*; *hsf-1(RNAi)* animals had a short life span, indicating that the *lin-14(lf)*–mediated longevity phenotype is dependent on *hsf-1* (fig. S4A) as well as on *daf-16*.

To further explore the possibility that *lin-4* and *lin-14* might function through the insulin/IGF-1 pathway, we analyzed their interactions with the *daf-2*-insulin/IGF-1 receptor. Consistent with previous studies, *daf-2(RNAi)* animals had a significant extension in life span compared with wild-type animals (Fig. 4C) (*25*). This life-span extension was significantly reduced by the *lin-4(e912)lf* lesion (Fig. 4C), such that *lin-4(e912)lf*; *daf-2(RNAi)* animals displayed life spans similar to those of the wild type. This phenotype is different from that of the *hsf-1(lf)* mutation, which wholly abolishes the life-span extension conferred by *daf-2(lf)* and results in a shortened life span (*25*). An epistatic relationship between *lin-4* and *daf-2* cannot be determined because the *daf-2* allele is non-null. However, our data suggests that a wild-type copy of *daf-2* is necessary for the short life span phenotype conferred by *lin-4(lf)*. The life span of the *daf-2(e1370)lf* mutant was modestly extended by *lin-14(RNAi)* (Fig. 4B), and *lin-14(n179)lf*; *daf-2(RNAi)* animals also displayed an extended life span as compared with *daf-2(RNAi)* animals (Fig. 4A). Null alleles were not used for either analysis, and thus concrete epistatic relationships cannot be determined. However, our data support a model whereby *lin-4* and *lin-14* modulate life span through the canonical *daf-2* insulin/IGF-1 pathway. Alternatively, *lin-4* and *lin-14* may converge onto the DAF-16/FOXO transcription factor in a pathway parallel to the *daf-2* insulin/IGF-1 pathway to control aging.

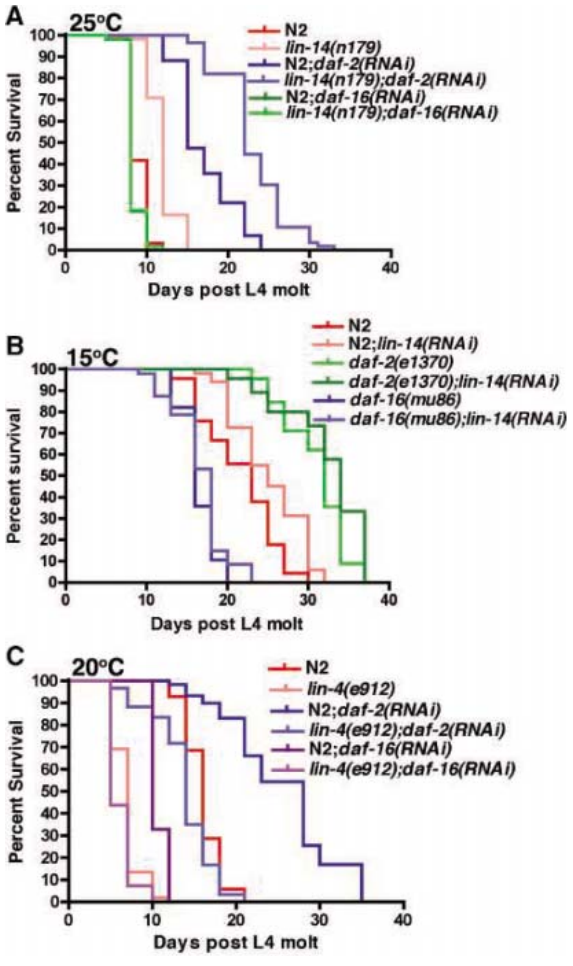

Fig. 4. The life-span extension of a *lin-14(lf)* mutant is *daf-16* dependent. (**A**) The life-span extension conferred by the *lin-14(n179)lf* mutation is abolished with *daf-16(RNAi)* (light green); *daf-16(RNAi)* animals (green—obscured by light green). *lin-14(lf)*; *daf-2(RNAi)* (light blue) displays a further lengthening of the life-span extension conferred by *daf-2(RNAi)* (blue) at 25°C. Wild-type (red) and *lin-14(n179)lf* (pink) animals on mock RNAi are shown for comparison. N2: n = 60, m = 8.9. *lin-14(n179)lf*: n = 56, m = 11.9, $P <$ 0.0001*. *daf-2(RNAi)*: n = 58, m = 17.1. *lin-14(n179)lf*; *daf-2(RNAi)*: n = 56, m = 23.0, $P <$ 0.0001*. *daf-16(RNAi)*: n = 55, m = 8.3. *lin-14(n179)lf*; *daf-16(RNAi)*: n = 54, m = 8.4, P = 0.9330*. (**B**) *lin-14(RNAi)* is unable to extend the life span of *daf-16(mu86)* (light blue) or *daf-2(e1370)lf* (light green) mutants as compared with these strains grown on mock RNAi (blue and green, respectively) at 15°C. Wild-type animals on mock RNAi (red) and on *lin-14(RNAi)* (pink) are shown for comparison. N2: n = 45, m = 21.6. *lin-14(RNAi)*: n = 51, m = 25.1, P = 0.0003*. *daf-2(e1370)lf*: n = 49, m = 32.3. *daf-2(e1370)lf*; *lin-14(RNAi)*: n = 53, m = 31.1, P = 0.0100#. *daf-16(mu86)*: n = 28, m = 16.4. *daf-16(mu86)*; *lin-14(RNAi)*: n = 42, m = 16.7, P = 0.2300#. (**C**) A wild-type copy of *lin-4* is required for full life-span extension by *daf-2(RNAi)* (blue versus light blue), and is also required for the life-span phenotype conferred by *daf-16(RNAi)* (purple versus light purple). Wild-type (red) and *lin-4(e912)lf* (pink) animals grown on mock RNAi are shown for comparison. N2: n = 70, m = 16.0. *lin-4(e912)lf*: n = 52, m = 6.8, $P <$ 0.0001*. *daf-2(e1370)*: n = 67, m = 25.5. *lin-4(e912)lf*; *daf-2(RNAi)*: n = 55, m = 13.8, $P <$ 0.0001*. *daf-16(RNAi)*: n = 64, m = 10.7. *lin-4(e912)lf*; *daf-16(RNAi)*: n = 55, m = 6.1, $P <$ 0.0001*. All experiments were repeated at least once with similar results. P* and P# are defined in the legend to Fig. 1.

In key *C. elegans* adult tissues, the *lin-4* miRNA may act to suppress the translation of *lin-14*, preventing *lin-14* from affecting the transcription of a yet unidentified factor that regulates or interacts with the *daf-2* insulin/IGF-1 pathway. By demonstrating that *lin-4* and *lin-14*, two key temporal regulators of development, also influence the rate of aging, we provide support for the theory that life span is affected by an innate, programmed timing mechanism. However, our data are also consistent with an alternative theory of aging, antagonistic pleiotropy, which posits that genes with primary roles in development can later secondarily influence life span (*27*). miRNAs are important regulators of development, apoptosis, and metabolism (*28–31*), and our work demonstrates that a miRNA can regulate aging, possibly through the insulin-like signaling pathway. It is possible that the mammalian *lin-4* miRNA homologs, the *miR-125* family, may regulate processes responsible for life-span determination in vertebrates.

References and Notes

1. C. Kenyon, *Cell* **120**, 449 (2005).
2. S. A. McCarroll *et al.*, *Nat. Genet.* **36**, 197 (2004).
3. C. Kenyon, in *C. elegans II: Monograph 33*, D. L. Riddle, Ed. (Cold Spring Harbor monograph series, Cold Spring Harbor Laboratory, Plainview, New York, 1997), p. xvii, p. 796.
4. T. Lu *et al.*, *Nature* **429**, 883 (2004).
5. V. Ambros, H. R. Horvitz, *Genes Dev.* **1**, 398 (1987).
6. D. Banerjee, F. Slack, *Bioessays* **24**, 119 (2002).
7. F. Slack, G. Ruvkun, *Annu. Rev. Genet.* **31**, 611 (1997).
8. R. C. Lee, R. L. Feinbaum, V. Ambros, *Cell* **75**, 843 (1993).
9. B. Wightman, I. Ha, G. Ruvkun, *Cell* **75**, 855 (1993).
10. P. H. Olsen, V. Ambros, *Dev. Biol.* **216**, 671 (1999).
11. R. Feinbaum, V. Ambros, *Dev. Biol.* **210**, 87 (1999).
12. G. Ruvkun, J. Giusto, *Nature* **338**, 313 (1989).
13. Y. Hong, R. C. Lee, V. Ambros, *Mol. Cell. Biol.* **20**, 2285 (2000).
14. L. P. Lim *et al.*, *Genes Dev.* **17**, 991 (2003).
15. A. Esquela-Kerscher *et al.*, *Dev. Dyn.* **234**, 868 (2005).
16. B. Wightman, T. R. Burglin, J. Gatto, P. Arasu, G. Ruvkun, *Genes Dev.* **5**, 1813 (1991).
17. D. Garigan *et al.*, *Genetics* **161**, 1101 (2002).
18. C. Kenyon, J. Chang, E. Gensch, A. Rudner, R. Tabtiang, *Nature* **366**, 461 (1993).
19. K. Lin, J. B. Dorman, A. Rodan, C. Kenyon, *Science* **278**, 1319 (1997).
20. P. L. Larsen, P. S. Albert, D. L. Riddle, *Genetics* **139**, 1567 (1995).
21. K. D. Kimura, H. A. Tissenbaum, Y. Liu, G. Ruvkun, *Science* **277**, 942 (1997).
22. G. J. Lithgow, T. M. White, S. Melov, T. E. Johnson, *Proc. Natl. Acad. Sci. U.S.A.* **92**, 7540 (1995).
23. S. S. Lee *et al.*, *Nat. Genet.* **33**, 40 (2003).
24. S. Ogg *et al.*, *Nature* **389**, 994 (1997).
25. A. L. Hsu, C. T. Murphy, C. Kenyon, *Science* **300**, 1142 (2003).
26. K. Lin, H. Hsin, N. Libina, C. Kenyon, *Nat. Genet.* **28**, 139 (2001).
27. K. A. Hughes, R. M. Reynolds, *Annu. Rev. Entomol.* **50**, 421 (2005).
28. D. P. Bartel, *Cell* **116**, 281 (2004).
29. J. Brennecke, D. R. Hipfner, A. Stark, R. B. Russell, S. M. Cohen, *Cell* **113**, 25 (2003).
30. M. N. Poy *et al.*, *Nature* **432**, 226 (2004).
31. B. J. Reinhart *et al.*, *Nature* **403**, 901 (2000).

32. We thank A. Esquela-Kerscher, D. Banerjee, and K. Carter for critical reading of this manuscript; K. Carter and L. Bai for providing the *zals1* strain; S. S. Lee for technical advice; and R. Lee and V. Ambros, and the *C. elegans* Genetic Center, for supplying strains. This work was supported by an NIH grant (GM64701) to F.S.

Supporting Online Material

www.sciencemag.org/cgi/content/full/310/5756/1954/DC1
Materials and Methods
Figs. S1 to S4
Table S1
References and Notes

1 June 2005; accepted 10 November 2005
10.1126/science.1115596

fgf20 Is Essential for Initiating Zebrafish Fin Regeneration

Geoffrey G. Whitehead, Shinji Makino, Ching-Ling Lien, Mark T. Keating*

Epimorphic regeneration requires the presence or creation of pluripotent cells capable of reproducing lost organs. Zebrafish fin regeneration is mediated by the creation of blastema cells. Here, we characterize the *devoid of blastema* (*dob*) mutant that fails fin regeneration during initial steps, forms abnormal regeneration epithelium, and does not form blastema. This mutation has no impact on embryonic survival. *Dob* results from an *fgf20a* null mutation, Y148S. *Fgf20a* is expressed during initiation of fin regeneration at the epithelial-mesenchymal boundary and later overlaps with the blastema marker *msxb*. Thus, *fgf20a* has a regeneration-specific requirement, initiating fin regeneration, and controlling blastema formation.

Vertebrate regeneration is of scientific and medical interest. Although acute tissue regeneration in humans is limited, other vertebrates possess extraordinary regenerative capabilities. Zebrafish are amenable to genetic analyses and regenerate an impressive array of structures, including spinal cord, optic nerve, heart, and fins (*1–3*). Zebrafish fin regeneration is marked by five stages: regeneration epithelialization, mesenchymal disorganization, blastema formation, regenerative outgrowth, and termination. Although genetic analyses have enhanced our understanding of fin regeneration (*1*, *4–6*), the specific signaling factor(s) that initiate regeneration and blastema formation are unknown.

To discover genes that initiate regeneration, we treated zebrafish with *N*-ethyl-*N*-nitrosourea (ENU) and screened adults for mutants (*1*, *4–6*). We looked for temperature-sensitive (ts) effects on regeneration, because many genes involved in regeneration also function during embryogenesis (*1*, *4–7*). The *dob* mutant displayed an early, genetically recessive regeneration block at 2 days post-amputation (dpa) at 33°C (Fig. 1). Mutant fins were covered only by epithelium, whereas wild-type fins grew beyond the amputation plane and later fully regenerated (Fig. 1). Most (72%, 34/47) mutants showed an identical regeneration defect at 25°C (fig. S2A). *dob* also failed to regenerate pectoral, dorsal, and anal fins. Thus, a regenerative block in *dob* is observed at both temperatures.

We expected that *dob* would also disrupt embryogenesis (*1*, *4–6*). However, at 33°C, *dob* viability was comparable with wild type (fig. S1A). Half (23/46) of *dob* adults developed asymmetric caudal fin lobes when heat-shocked as embryos, yet all wild type (41/41) developed symmetric fin lobes (fig. S1B). The total size of wild-type and *dob* caudal fins was comparable (fig. S1B). Therefore, there appears to be an incompletely penetrant ts patterning defect in *dob* (*8*). Survival of *dob* adults at 33°C was also comparable to wild type (fig. S1C). These data suggest a regeneration-specific requirement for *dob*.

To determine the cellular nature of *dob* regenerative failure, we examined histology of regenerates at 33°C. The first stage of regeneration, formation of regeneration epithelium, appeared abnormal. At 6 and 12 hours post-amputation (hpa), *dob* regenerates demonstrated a thickened regeneration epithelium (Fig. 2A). Epithelial proliferation levels in *dob* at 6 and 12 hpa were similar to wild type (fig. S3A). Therefore, thickened regeneration epithelium likely results from aberrant epithelial migration (*9*, *10*).

To determine whether *dob* resulted from a primary defect in wound healing, we performed a longitudinal incision along the caudal fin and allowed healing at 33°C. The wild-type response to this injury is nonregenerative, as the wound is covered by epithelium and leaves a slit down the fin. We found no difference in the timing, histochemistry, or bromodeoxyuridine (BrdU) immunohistochemistry of wound-healing between wild type and *dob* (fig. S3B). The possibility remains that the *dob* mutant may have a subtle defect in wound-healing not identified by our observations.

Howard Hughes Medical Institute, Department of Cell Biology, Harvard Medical School, Department of Cardiology, Children's Hospital, Boston, MA 02115, USA.

*To whom correspondence should be addressed. E-mail: mark.keating@novartis.com

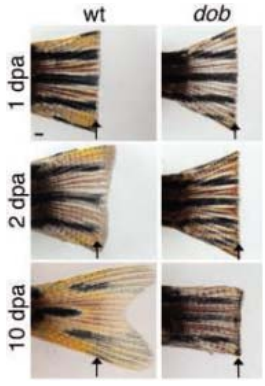

Fig. 1. *dob*, a mutant with early fin regeneration block. Regenerating wild-type (wt) and *dob* fins at 33°C following amputation. Arrows mark amputation plane. At 1 dpa, both wt and *dob* have covered the amputation with epithelium. By 2 dpa, wt fins have regenerated beyond the amputation plane, whereas *dob* mutants have not. At 10 dpa, wt has undergone full reconstitution, but *dob* fails to regenerate. Scale bars, 400 μm.

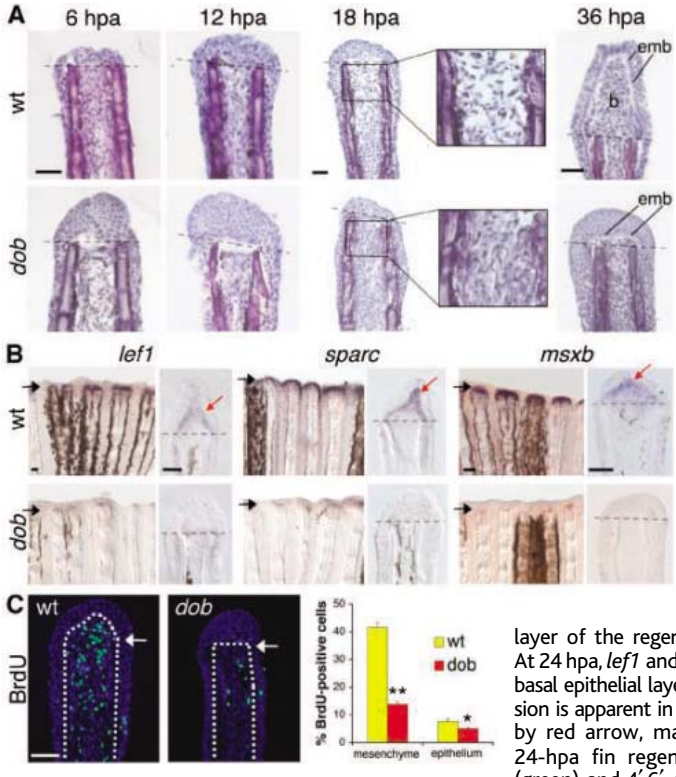

Fig. 2. *dob* fails to initiate fin regeneration and does not form a blastema. Dashed line or arrow marks amputation plane. (**A**) Hematoxylin-stained sections of caudal fin regenerates. At 6 and 12 hpa, the regeneration epithelium in *dob* is thicker than wild type (wt). At 18 hpa, disorganization of mesenchyme beneath the regeneration epithelium is apparent in wt fins but was not observed in *dob*. At 36 hpa, a blastema is seen in wt regenerates, yet *dob* lacks blastema. b, blastema; emb, epithelial-mesenchymal boundary. (**B**) *lef1* and *sparc* mark the basal epidermal layer of the regeneration epithelium in wt. At 24 hpa, *lef1* and *sparc* are absent from the basal epithelial layer in *dob*. No *msxb* expression is apparent in *dob*. Violet stain, indicated by red arrow, marks gene expression. (**C**) 24-hpa fin regenerates stained for BrdU (green) and 4′,6′-diamidino-2-phenylindole (blue). White dashed line marks epithelial-mesenchymal boundary. During blastema formation, mutants had reduced mesenchymal and epithelial proliferation ($n = 19$). Graph displays the indices of proliferation in mesenchyme and epithelium of wt and *dob* regenerates. **, $P \ll 0.01$; *, $P < 0.05$. Scale bars, 50 μm (A), 100 μm [(B) and (C)].

To further characterize the *dob* defect in regeneration epithelialization, we performed in situ hybridization experiments. The wild-type regeneration epithelium at 24 hpa is molecularly and histochemically distinct. Specifically, the basal epithelium in wild-type regenerates consists of ordered linear cuboidal epithelial cells (*11*). In *dob*, the basal epithelium lacked the distinctive cuboidal shape and was nonlinear. *Lef1*, a transcription factor downstream of Wnt (*12*), and *sparc*, a matricellular protein (*13*), both demarcate regeneration basal epithelium. *Lef1* and *sparc* in situ hybridization in *dob* revealed absent basal epithelial expression (Fig. 2B). Thus, normal formation of a basal regeneration epithelium appears essential for fin regeneration.

At 18 hpa in wild-type regenerates, disorganized mesenchymal cells beneath the amputation plane are considered evidence of dedifferentiation (*9*, *11*). *dob* mutants did not undergo mesenchymal disorganization (Fig. 2A). In 18 hpa wild-type regenerates, *hsp60* is up-regulated in mesenchymal cells destined to form blastema (*6*). However, *dob* did not express *hsp60* in these cells (fig. S2B). These data suggest a mesenchymal disorganization defect in *dob*.

Mesenchymal disorganization is followed by cell proliferation, migration, and blastema formation (*9*, *10*). The blastema is a mass of undifferentiated mesenchymal cells that have proliferated beyond the amputation plane to drive fin regrowth. At 36 hpa, wild-type regenerates show proper blastema formation; however, *dob* is devoid of blastema (Fig. 2A). These data indicate that *dob* does not initiate fin regeneration and fails to form regeneration epithelium and blastema.

To determine the effect of *dob* on blastema formation, we performed in situ hybridization experiments. In 24 hpa wild-type fins, *msxb* marks rudimentary blastema cells, the mesenchyme distal to the amputation plane. At 72 hpa, during regenerative outgrowth, *msxb* marks distal blastema (*7*, *9*). No *msxb* expression was apparent in *dob* at 24 hpa during blastema formation (Fig. 2B). Faint *msxb* expression was present in *dob* at 72 hpa at the central tip of mesenchyme (fig. S2C). These *msxb*-positive cells may represent a later, inadequate attempt at blastema formation. These data demonstrate that *dob* lacks early *msxb* expression and does not form blastema.

During blastema formation, mesenchymal cells reenter the cell cycle and begin to proliferate (*9*, *10*). These cells migrate toward regeneration epidermis and form the rudimentary blastema. To further define the mechanism of the *dob* regenerative defect, we examined DNA replication, through BrdU labeling. At 24 hpa, *dob* mesenchymal proliferation levels were one-third of wild type, and epithelial proliferation was slightly lower (Fig. 2C). These data indicate that *dob* fails to form a blastema through an early defect in mesenchymal proliferation.

To identify the *dob* gene, we raised 2027 zebrafish from $dob^{-/-} \times dob^{+/-}$ mapping crosses to adulthood at 25°C, scored for regenerative defects at 33°C, and genotyped these animals (*1*, *4*–*6*). Two markers, bef7 and tof24, flanked the 0.2 centimorgan (cM) *dob* critical region on chromosome 1. *fgf20a* was the only transcript within this region, genetically excluding neighboring transcripts (Fig. 3A). Syntenic multicontig alignments demonstrated that no transcripts were located between *efha2* and *fgf20a* in human or fugu databases.

To identify the *dob* mutation, we performed DNA sequence analysis of *fgf20a*. We discovered one missense mutation, an adenine-443 to cytosine (A443C) transversion, in the *fgf20a* gene of *dob* that converted tyrosine-148 to serine (Y148S) (Fig. 3B). We genotyped 140 *dob* mutants, 30 *dob* heterozygotes, and 20 wild-type controls and verified that the A443C transversion cosegregated with the *dob* phenotype. *Dob* was isolated in the SJD background, and DNA sequence of *fgf20a* in wild-type SJD revealed no mutation. Therefore, the A443C transversion in *dob* was caused by ENU mutagenesis. This point mutation was not found among five commonly used laboratory strains, indicating that A443C is not a polymorphism. These data indicate that the *dob* phenotype results from *fgf20a* Y148S.

Fgf20 is a newly identified member of the Fgf family. Fgf20 is overexpressed in cancer cell lines, promotes proliferation and differentiation of myocardial cells, and enhances survival of dopaminergic neurons in the adult brain, functions consistent with a role in regeneration (*14*–*16*). Y148 exists in the highly

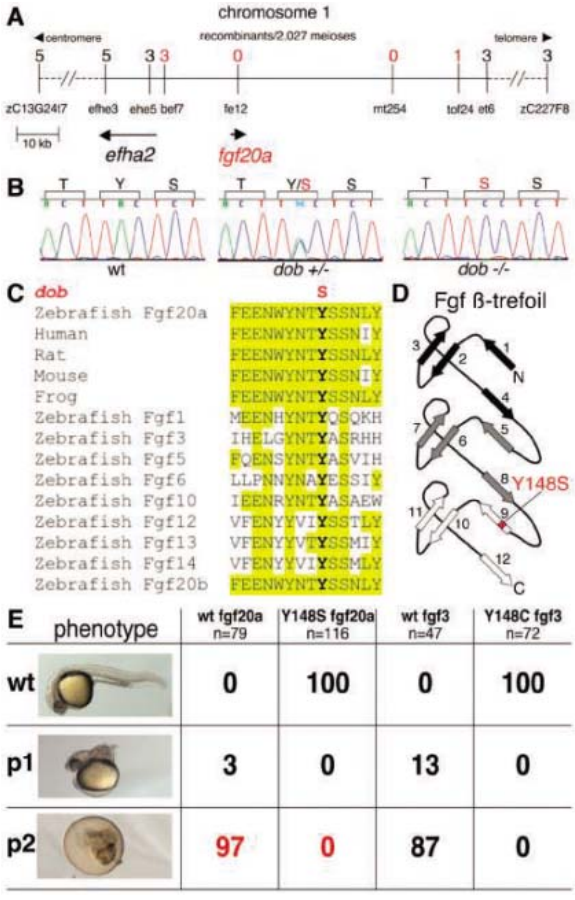

Fig. 3. *fgf20a* Y148S missense mutation causes *dob*. (**A**) Genetic map of *dob* on chromosome 1. Refined linkage analysis mapped *dob* to the 0.2 cM region between bef7 and tof24. The only gene between flanking recombinant markers is *fgf20a*. Numbers above linear map quantify recombination events between *dob* and linked markers from 2027 meioses. Bef7, fe12, mt254, tof24, and et6 are polymorphic genetic markers between AB and SJD strains identified by random DNA amplification and sequencing within the *dob* critical region. (**B**) DNA sequence chromatograms of wild-type, $dob^{+/-}$, and $dob^{-/-}$ fish. A443C transversion leads to Y148S amino acid substitution. (**C**) Tyr-148 is conserved across vertebrates and among most zebrafish Fgfs. (**D**) Fgf secondary β-trefoil structure. Tyr-148 is located in the β9 strand of Fgf20a. (**E**) Phenotypic classes and frequencies (%) obtained after injection of wild-type *fgf20a*, Y148S *fgf20a*, wild-type *fgf3*, or Y148C *fgf3* mRNAs (10 ng/μl) into wild-type embryos. Y148S *fgf20a* had no effect on the embryo, suggesting loss of function. Wt, normal; p1, head reduction, loss of tail; p2, lysis.

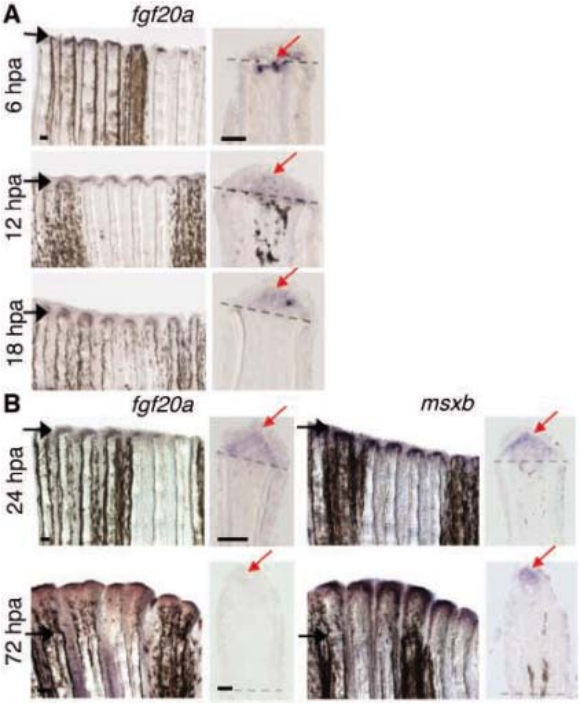

Fig. 4. *fgf20a* expression localizes to epithelial-mesenchymal boundary during initiation of fin regeneration. (**A**) Whole-mount in situ hybridization and sections showing *fgf20a* expression. During initiation of fin regeneration (6 to 12 hpa), *fgf20a* expression is localized to mesenchymal cells directly underneath the regeneration epithelium. During early blastema formation (18 hpa), *fgf20a* is confined to the blastema. (**B**) During blastema formation (24 hpa), *fgf20a* and *msxb* colocalize in blastema cells. *fgf20a* and *msxb* expression domains overlap at 72 hpa, when *fgf20a* is concentrated at the distal tip of *msxb*-positive distal blastema. Violet stain indicated by red arrow marks expression. Scale bars, 100 μm.

conserved Fgf-core domain in the β9 strand of the 12-strand β-trefoil, adjacent to residues (WYN) (Fig. 3, C and D) that make essential Fgf receptor contacts (*17*). Y148 is invariant across vertebrate species of Fgf20 and most zebrafish Fgfs (Fig. 3C). Thus, Y148 is evolutionarily conserved among species and within the Fgf family.

To determine the effect of Y148S on the activity of Fgf20a protein, we carried out overexpression studies in zebrafish embryos. Injection of wild-type *fgf* mRNA leads to dorsalization of the embryo and death (*18*). Injected *fgf20a* Y148S mRNA failed to recapitulate this phenotype (Fig. 3E). Similar results have been demonstrated for the null $fgf3^{t21142}$ allele, a Y148C mutation, the same tyrosine mutated in *dob* (*18*). These data indicate that Y148S is likely a null mutation and that Y148 is crucial for Fgf function.

To ensure that *fgf20a* Y148S is responsible for the *dob* phenotype, we injected wild-type and *dob* embryos with wild-type *fgf20a* mRNA. We found that 87.8% of wild-type embryos showed dorsalization and lethality, compared with 53.5% of *dob* embryos ($P = 0.02$) (table S1). These data support the view that the *dob* phenotype results from reduced *fgf20a* and that *fgf20a* Y148S causes *dob*.

To define the timing and pattern of *fgf20a* expression during fin regeneration, we performed reverse transcriptase polymerase chain reaction and in situ hybridization experiments. *fgf20a* was expressed as early as 1 hpa. Expression peaked at 6 hpa, gradually declined, peaked again at 24 hpa, then declined (fig. S2D). During initiation of fin regeneration (6 to 12 hpa), *fgf20a* expression was localized to mesenchyme at the epithelial-mesenchymal boundary (Fig. 4A). *fgf20a* was later expressed in blastema during early blastema formation (18 hpa) (Fig. 4A). These data indicate that *fgf20a* is expressed in key regeneration cells during initiation of fin regeneration, consistent with the *dob* phenotype.

We further characterized the expression of *fgf20a* during fin regeneration and compared *fgf20a* and *msxb* expression. At 24 hpa, *msxb* marks rudimentary blastema cells. *fgf20a* expression colocalized with *msxb* in early blastema cells (Fig. 4B). During regenerative outgrowth, at 72 hpa, *msxb* expression marks stem cell–like distal blastema cells (*6*, *9*). *fgf20a* expression was restricted to a subset of *msxb*-positive distal blastema cells (Fig. 4B). These data indicate that *fgf20a* and *msxb* expression overlap during blastema formation and regenerative outgrowth.

We conclude that the *dob* phenotype is caused by a Y148S mutation in Fgf20a. Data implicating *fgf20a* in *dob* include (i) genetic linkage of *dob* to a 70-kb critical interval on chromosome 1, the presence of *fgf20a* in this interval, and the absence of other transcripts; (ii) the presence of an Fgf20a missense mutation (Y148S) in a completely conserved amino acid linked with the *dob* phenotype ($P = 4.22 \times 10^{-42}$, Fisher's Exact test); (iii) the absence of Y148S in five wild-type strains, indicating that this variant is not a polymorphism; (iv) in situ hybridization showing that *fgf20a* is expressed in mesenchymal cells adjacent to regeneration epithelium as early as

6 hpa; (v) functional studies showing that the Y148S mutation leads to loss of function; (vi) DNA microarray data demonstrating disrupted Fgf signaling in *dob* (fig. S4A and table S2); and (vii) insensitivity of *dob* embryos to wild-type *fgf20a* mRNA overexpression (table S1). Thus, the early regenerative defect observed in *dob* results from Fgf20a dysfunction.

We have genetically identified a specific growth factor, Fgf20a, that is essential for initiating fin regeneration, regeneration epithelialization, and blastema formation. These findings provide a genetic foothold on the early signaling events of regeneration that will enable further identification of key regeneration genes. This information will broaden our understanding of regenerative mechanisms and may enable regenerative medicine.

References and Notes

1. S. L. Johnson, J. A. Weston, *Genetics* **141**, 1583 (1995).
2. T. Becker, M. F. Wullimann, C. G. Becker, R. R. Bernhardt, M. Schachner, *J. Comp. Neurol.* **377**, 577 (1997).
3. K. D. Poss, L. G. Wilson, M. T. Keating, *Science* **298**, 2188 (2002).
4. A. Nechiporuk, K. D. Poss, S. L. Johnson, M. T. Keating, *Dev. Biol.* **258**, 291 (2003).
5. K. Poss, A. Nechiporuk, A. Hillam, S. L. Johnson, M. T. Keating, *Development* **129**, 5141 (2002).
6. S. Makino *et al.*, *Proc. Natl. Acad. Sci. U.S.A.* **102**, 14599 (2005).
7. M. A. Akimenko, S. L. Johnson, M. Westerfield, M. Ekker, *Development* **121**, 347 (1995).
8. Materials and methods are available as supporting material on *Science* Online.
9. A. Nechiporuk, M. T. Keating, *Development* **129**, 2607 (2002).
10. G. Poleo, C. W. Brown, L. Laforest, M. A. Akimenko, *Dev. Dyn.* **221**, 380 (2001).
11. K. D. Poss, M. T. Keating, A. Nechiporuk, *Dev. Dyn.* **226**, 202 (2003).
12. K. D. Poss, J. Shen, M. T. Keating, *Dev. Dyn.* **219**, 282 (2000).
13. A. D. Bradshaw, E. H. Sage, *J. Clin. Invest.* **107**, 1049 (2001).
14. M. N. Chamorro *et al.*, *EMBO J.* **24**, 73 (2005).
15. K. J. Lavine *et al.*, *Dev. Cell* **8**, 85 (2005).
16. S. Ohmachi, T. Mikami, M. Konishi, A. Miyake, N. Itoh, *J. Neurosci. Res.* **72**, 436 (2003).
17. A. N. Plotnikov, S. R. Hubbard, J. Schlessinger, M. Mohammadi, *Cell* **101**, 413 (2000).
18. W. Herzog *et al.*, *Development* **131**, 3681 (2004).

19. See supporting online text for acknowledgments.

Supporting Online Material

www.sciencemag.org/cgi/content/full/310/5756/1957/DC1
Materials and Methods
SOM Text
Figs. S1 to S4
Tables S1 and S2
References

19 July 2005; accepted 29 November 2005
10.1126/science.1117637

Protein Synthesis upon Acute Nutrient Restriction Relies on Proteasome Function

Ramunas M. Vabulas* and F. Ulrich Hartl*

The mechanisms that protect mammalian cells against amino acid deprivation are only partially understood. We found that during an acute decrease in external amino acid supply, before up-regulation of the autophagosomal-lysosomal pathway, efficient translation was ensured by proteasomal protein degradation. Amino acids for the synthesis of new proteins were supplied by the degradation of preexisting proteins, whereas nascent and newly formed polypeptides remained largely protected from proteolysis. Proteasome inhibition during nutrient deprivation caused rapid amino acid depletion and marked impairment of translation. Thus, the proteasome plays a crucial role in cell survival after acute disruption of amino acid supply.

Protein biosynthesis in mammalian cells relies on the continuous uptake of essential amino acids from the environment. Acute amino acid restriction can occur in several physiological and pathophysiological conditions, such as after disruption of the trans-placental nutrient supply in neonates or during organ ischemia. Up-regulation of the autophagosomal-lysosomal pathway is known to provide free amino acids for protein synthesis under these nutrient stress conditions through the bulk degradation of cytoplasmic proteins and organelles (*1*, *2*). However, this adaptation requires hours to become fully effective (*2*, *3*), suggesting the existence of constitutive mechanisms that protect cells during short-term fluctuations in amino acid supply. Moreover, certain organs, such as the brain, are inefficient in up-regulating autophagy (*3*). Nonlysosomal degradation by means of the proteasomal system is known to be induced during long-term fasting (*4*), but the role of the proteasome in maintaining the intracellular amino acid pool during acute nutrient deprivation has remained unexplored. The proteasome, a ~2.5-MD protein complex acting together with ubiquitin and ubiquitin-processing enzymes, is responsible for most cytosolic protein degradation under normal nutrient conditions and has a variety of essential functions in cell regulation and protein quality control (*5*, *6*).

A constitutive function of the proteasome in buffering fluctuations in external amino acid availability would be consistent with a recent report that 30% or more of newly formed proteins are proteasomally degraded immediately upon synthesis (*7*). To explore a possible role of the proteasome in supplying amino acids for translation, we established conditions to measure the immediate effects of proteasome inhibition in human HeLa cells. A rapidly degraded ubiquitin–enhanced green fluorescent protein fusion protein (Ub-EGFP) served as a reporter of proteasome activity (*8*, *9*). Ub-EGFP accumulated to a low steady-state level in transiently transfected cells, reflecting the equilibrium between its synthesis and degradation. As expected, upon inhibition of protein synthesis with cycloheximide (CHX), Ub-EGFP was degraded within minutes (Fig. 1A). In contrast, the addition of the proteasome inhibitor MG132 caused the virtually immediate accumulation of Ub-EGFP (Fig. 1A). To determine whether proteasome inhibition was complete, we analyzed the combined effect of MG132 and CHX. Inhibition of translation by CHX is known to be very rapid and efficient (*10*, *11*). Thus, if MG132 were to block proteasome function only partially, the arrest of translation would lead to a decrease in Ub-EGFP level due to degradation. The simultaneous addition of CHX and MG132 instantaneously stabilized the Ub-EGFP reporter (Fig. 1A). Similar observations were made with the proteasome inhibitors clasto-lactacystin-β-lactone and epoxomicin (*11*). Thus, under the conditions chosen proteasome inhibition was immediate and essentially complete.

The effect of proteasome inhibition on translation was analyzed under conditions of acute amino acid restriction. The concentrations of the essential amino acids—leucine, phenylalanine, or methionine—were maintained in the range of normal adult plasma levels (*12*) or were reduced individually 100-fold to create insufficiency in external supply (*13*). Newly synthesized proteins were labeled with ^{35}S-methionine (^{35}S-Met), followed by cell lysis in SDS and precipitation of proteins with trichloroacetic acid (TCA). Proteasome inhibition with MG132, clasto-lactacystin-β-lactone or epoxomicin markedly impaired translation within 5 to 10 min, but only when cells were incubated in medium deficient in at least one essential amino acid (leucine or phenylalanine) (Fig. 1, B to D, and fig. S1, A and B). Similar results were obtained when cells were incubated in methionine-deficient medium with ^{3}H-leucine (^{3}H-Leu) as the tracer

Department of Cellular Biochemistry, Max Planck Institute of Biochemistry, Am Klopferspitz 18, D-82152 Martinsried, Germany.

*To whom correspondence should be addressed: E-mail: vabulas@biochem.mpg.de (R.M.V.); uhartl@biochem.mpg.de (F.U.H.)

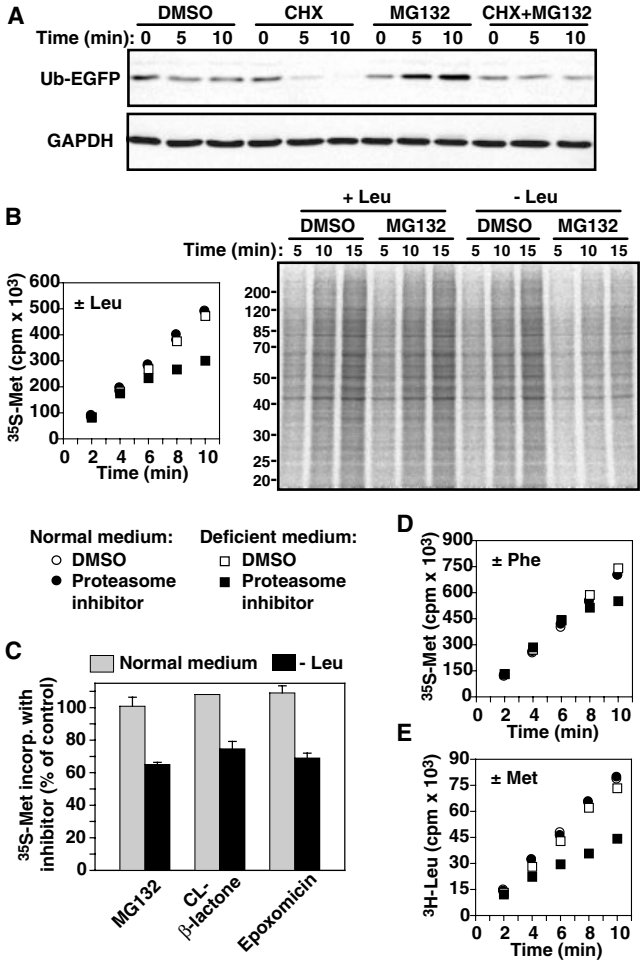

Fig. 1. Proteasome activity is required to sustain protein synthesis upon amino acid restriction. (**A**) Amounts of Ub-EGFP reporter protein were analyzed in transiently transfected HeLa cells at 0, 5, and 10 min after addition of dimethyl sulfoxide (DMSO) alone, 5 mM CHX, 100 μM MG132 in DMSO, or CHX and MG132 combined by anti-GFP immunoblotting. Glyceraldehyde-3-phosphate dehydrogenase (GAPDH) was used as a loading control. (**B**) Translation was followed by measuring the incorporation of ^{35}S-Met into TCA-insoluble material (left) or analyzing newly synthesized proteins by 10% SDS-PAGE and phosphorimaging (right). At time 0, 50 μCi/ml ^{35}S-Met and MG132 were added. Circles, normal medium (80 μM Leu); squares, deficient medium (0.8 μM Leu). Solid symbols, MG132 addition; open symbols, DMSO controls. (**C**) Translation was analyzed as in (B). In addition to MG132, 40 μM clasto-lactacystin-β-lactone (CL-β-lactone) or 40 μM epoxomicin were used, and translation was observed for 15 min (fig. S1, A and B). Protein synthesis is expressed in percentage of controls lacking inhibitor. Means + SD of three independent experiments are shown. Gray bars, normal medium; black bars, Leu-deficient medium. (**D**) Same as (B), except that Phe-sufficient (40 μM) and Phe-deficient (0.4 μM) media were used. (**E**) Same as (B), except that the amount of Met was varied from 20 μM (normal medium) to 0.2 μM (deficient medium) and labeling was with 100 μCi/ml ^{3}H-Leu. Representative results of at least three independent experiments are shown.

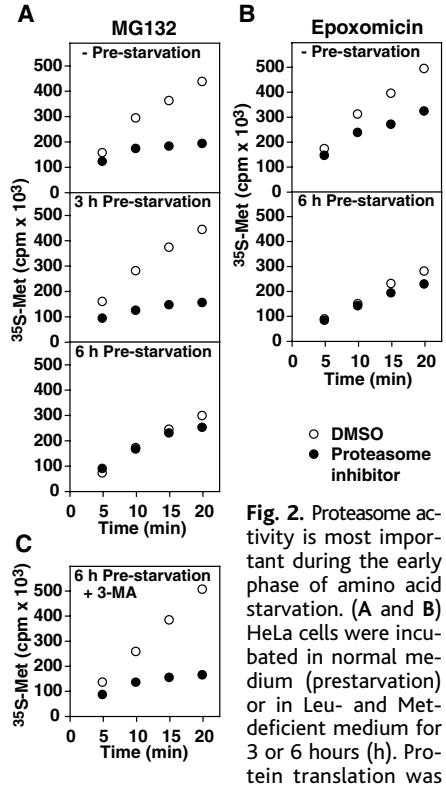

Fig. 2. Proteasome activity is most important during the early phase of amino acid starvation. (**A** and **B**) HeLa cells were incubated in normal medium (prestarvation) or in Leu- and Met-deficient medium for 3 or 6 hours (h). Protein translation was then analyzed in Leu-deficient medium by adding 50 μM Ci/ml ^{35}S-Met with either DMSO (open symbols), MG132 (A), or epoxomicin (B) (solid symbols) (*13*). (**C**) Same as (A), except that 10 mM 3-MA was added at the beginning of prestarvation. DMSO (open symbols) or MG132 (solid symbols) was added during labeling. Representative results of at least three independent experiments are shown. cpm, counts per minute.

(Fig. 1E), except that proteasome inhibition affected translation earlier. These observations were reproduced in human embryonic kidney 293T cells (fig. S1C). Thus, the proteasome had a critical role in buffering the sudden disruption of the external amino acid supply, allowing translation to proceed normally.

The use of the specific proteasome inhibitors clasto-lactacystin-β-lactone and epoxomicin (*14*) (Fig. 1C and fig. S1, A and B) excluded an inhibition of lysosomal proteolysis as the cause of the observed reduction in translation. Moreover, translation was unimpaired when cells deficient in amino acids were treated with lysosomal inhibitors bafilomycin A or chloroquine (*15*, *16*) (fig. S2A). In contrast, bestatin methyl ester, an inhibitor of the aminopeptidase hydrolyzing di- and tripeptides downstream of the proteasome (*17*, *18*), caused a substantial inhibition of translation (fig. S2B), similar to proteasome inhibition. These results corroborate the critical role of the proteasome in sustaining translation upon acute amino acid restriction. In contrast, prolonged amino acid starvation for several hours should induce the autophagosomal-lysosomal system (*3*), and this could reduce the dependence of protein synthesis on proteasome activity. Indeed, after 6 hours of amino acid starvation, the effect of proteasome inhibition on translation was substantially reduced (Fig. 2, A and B), suggesting that at this time lysosomal protein degradation contributed increasingly to providing amino acids. This adaptation was not seen when cells were treated with 3-methyladenine (3-MA), which prevents the formation of autophagosomes (*19*, *20*). In cells treated with 3-MA, the addition of a proteasome inhibitor after 6 hours of prestarvation caused a reduction in translation similar to that in cells without prestarvation (Fig. 2C).

Lack of intracellular amino acids results in the accumulation of uncharged tRNAs and leads to the formation of active, phosphorylated general control nonderepressible 2 (GCN2) kinase (*21*, *22*). As detected by a phospho-GCN2 antibody, GCN2 was activated upon shifting cells to leucine-deficient medium, but only when the proteasome was simultaneously inhibited (Fig. 3A). This is indicative of a physiologically relevant depletion of the intracellular leucine pool under these conditions. Efficient translation resumed rapidly upon re-addition of the lacking amino acid, even when the block of proteasome function was maintained (Fig. 3B). Amino acid analysis demonstrated directly that the proteasome supplied building blocks for protein synthesis. The addition of translation inhibitor (CHX) to cells growing in normal medium resulted in a measurable increase in intracellular leucine within 10 min (table S1). This effect was less pronounced in the presence of the proteasome inhibitor. In leucine-deficient medium, intracellular leucine was only detectable upon addition of CHX when the proteasome was not inhibited (table S1), indicating that combined amino acid deficiency and proteasome inhibition severely depleted the intracellular amino acid pool.

At least 30% of newly synthesized proteins are thought to be degraded by the proteasome during and immediately after translation, presumably reflecting a general inefficiency of protein biosynthesis and folding (*7*). How-

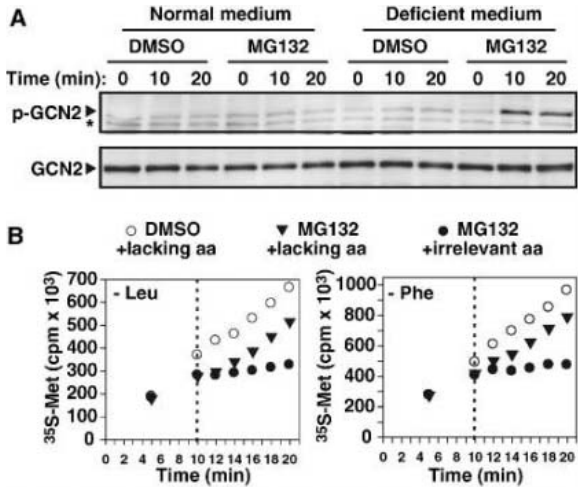

Fig. 3. Immediate cellular effects of amino acid restriction and proteasome inhibition. (**A**) Activation of GCN2 kinase in HeLa cells by reducing the medium concentration of Leu from 80 to 0.8 μM and simultaneous proteasome inhibition. Activated GCN2 kinase (pGCN2) was detected by immunoblotting with an antibody to pGCN2. Asterisk, nonspecific band. Equal loading was confirmed with antibodies detecting GCN2 independent of its phosphorylation (GCN2). At time 0, 100 μM MG132 or DMSO was added. (**B**) Translation was analyzed in Leu-deficient medium (–Leu) or Phe-deficient medium (–Phe). Incorporation of ^{35}S-Met into TCA-precipitable material was measured. 50 μCi/ml ^{35}S-Met was added either together with MG132 (solid symbols) or with DMSO (open symbols). After 10 min (dashed line), the respective lacking amino acid (triangles) or control amino acid (circles) (Phe in case of –Leu medium, Leu in case of –Phe medium) was added to normal concentration. aa, amino acid. Representative results of at least three independent experiments are shown.

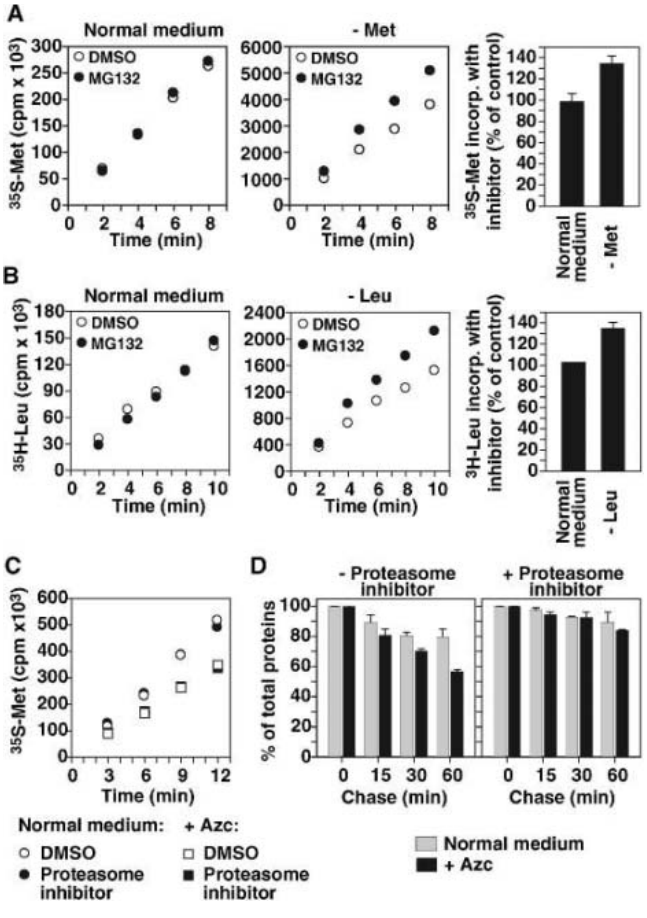

Fig. 4. Effect of proteasome activity on radiolabeling of newly synthesized proteins and degradation of faulty proteins. (**A** and **B**) Newly synthesized proteins in HeLa cells were labeled with 50 μCi/ml ^{35}S-Met in Met-deficient medium (A), or with 100 μCi/ml ^{3}H-Leu in Leu-deficient medium (B). Radioactivity of TCA-insoluble material was measured. MG132 (solid symbols) or DMSO (open symbols) were added with radioactive tracers at time 0. (Right) Protein synthesis after 8 min (A) or 10 min (B) of labeling is expressed in percentage of controls lacking inhibitor. Means + SD of three independent experiments are shown. (**C**) Labeling with 50 μCi/ml ^{35}S-Met in normal medium lacking nonessential amino acids. Circles, cells in normal medium; squares, cells preincubated for 15 min in 20 mM L-azetidine-2-carboxylic acid (Azc) before and during labeling. Open symbols, DMSO; solid symbols, MG132-containing cultures. cpm, counts per minute. (**D**) Proteins were labeled as in (C). Gray bars, control cells; black bars, Azc-treated cells. After labeling for 10 min, a chase was performed with 20 mM unlabeled Met. Half of the cultures received 100 μM MG132 and 10 μM clasto-lactacystin-β-lactone during labeling and chase (+ proteasome inhibitor), and the other half received DMSO (– proteasome inhibitor). TCA-precipitable radioactivity at time 0 was set as 100%. Means + SD of three experiments are shown.

ever, our experiments revealed a notable degree of protection of newly made proteins against immediate degradation. In contrast to the reported observations, cells did not accumulate an additional amount of newly synthesized, radiolabeled protein when proteasome function was blocked (Fig. 1, B to E). How can this discrepancy be explained?

For labeling, cells are usually preincubated in media lacking the respective nonradioactive amino acid to increase the incorporation of radiolabel into newly made proteins (*7*). Based on our findings, preincubation with a proteasome inhibitor (*7*) should enhance this effect as a result of severe intracellular amino acid depletion (table S1 and Fig. 3A). Indeed, the incorporation of ^{35}S-Met into newly synthesized protein increased more than 10-fold when labeling was performed in methionine-deficient medium (Fig. 4A). As predicted, proteasome inhibition during amino acid starvation resulted in a substantial further increase in incorporated radioactivity (Fig. 4A), even though the efficiency of translation was reduced (Fig. 1). This effect was independent of the specific ratio of labeled-to-unlabeled amino acid (fig. S3) and was equally observed when cells were labeled with ^{3}H-Leu in leucine-deficient medium (Fig. 4B). Double-labeling experiments with ^{3}H-Leu and ^{35}S-Met in methionine-deficient medium showed that proteasome inhibition increased the incorporation of ^{35}S-Met into equal amounts of newly synthesized, ^{3}H-Leu-labeled protein by twofold (fig. S4A). A threefold increase in ^{35}S-Met-tRNA was detected in cells after 15 min of proteasome inhibition, which would explain the increased incorporation of ^{35}S-Met into newly formed protein (fig. S4B). Thus, the higher incorporation of radiolabel observed upon proteasome inhibition in amino acid deficient medium was due to an increase in specific radioactivity of the intracellular amino acid pool, not to the stabilization of a large fraction of newly synthesized proteins. At most, only a few percent of total protein was rapidly degraded immediately upon translation in the cell types analyzed here.

To test whether translating polypeptides remain protected against proteasomal degradation even when unable to fold, we incubated cells in the presence of the proline analog L-azetidine-2-carboxylic acid (Azc). Whereas the addition of Azc resulted in a reduced incorporation of ^{35}S-Met, no notable additional accumulation of radiolabeled protein was detectable upon proteasome inhibition within 12 min (Fig. 4C). This suggested that removal by the proteasome of misfolded proteins containing Azc occurred only after a substantial lag period. To address this possibility, cells were labeled with ^{35}S-Met for 10 min, followed by a chase with excess unlabeled methionine. More than 40% of the proteins synthesized in the presence of Azc were degraded within 60 min and this effect was largely prevented by proteasome inhibition (Fig. 4D). The extent of protein degradation observed in normal medium (~20% over 60 min) is in agreement with previous studies demonstrating the proteasomal turnover of short-lived proteins (*23*, *24*). Thus, when cells produce a substantial amount of protein chains

that are unable to fold correctly, the majority of these chains are not degraded during translation, but rather through a relatively slow, posttranslational process.

Our results provide evidence for a critical role of the proteasome in supplying amino acids for sustained protein synthesis. This function of the proteasome is most critical upon acute amino acid restriction, where the uninduced lysosomal system is unable to maintain a sufficient intracellular amino acid pool. Amino acids for translation are predominantly generated by the proteasomal degradation of preexisting proteins. Newly synthesized proteins are largely protected from degradation during and immediately after translation, both under normal conditions and upon amino acid starvation. Faulty proteins are predominantly degraded through a posttranslational process that is likely to involve a functional cooperation between molecular chaperones assisting in folding and the proteasome system (*25*, *26*). The proteasome has a demonstrated capacity to degrade polypeptides during synthesis, provided they carry specialized N-terminal degradation signals (*27*), but this mechanism is likely to be more extensively used in cell regulation rather than during basic housekeeping processes.

References and Notes

1. G. E. Mortimore, A. R. Poso, *Annu. Rev. Nutr.* **7**, 539 (1987).
2. A. Kuma *et al.*, *Nature* **432**, 1032 (2004).
3. N. Mizushima, A. Yamamoto, M. Matsui, T. Yoshimori, Y. Ohsumi, *Mol. Biol. Cell* **15**, 1101 (2004).
4. S. H. Lecker, V. Solomon, W. E. Mitch, A. L. Goldberg, *J. Nutr.* **129**, 227S (1999).
5. A. Hershko, A. Ciechanover, *Annu. Rev. Biochem.* **67**, 425 (1998).
6. A. Varshavsky, *Trends Biochem. Sci.* **30**, 283 (2005).
7. U. Schubert *et al.*, *Nature* **404**, 770 (2000).
8. E. S. Johnson, B. Bartel, W. Seufert, A. Varshavsky, *EMBO J.* **11**, 497 (1992).
9. N. P. Dantuma, K. Lindsten, R. Glas, M. Jellne, M. G. Masucci, *Nat. Biotechnol.* **18**, 538 (2000).
10. Addition of 5 mM CHX together with radioactive tracer amino acid immediately blocked biosynthesis of polypeptides as evidenced by SDS–polyacrylamide gel electrophoresis (PAGE) analysis or from the lack of TCA-precipitable radioactivity.
11. R. M. Vabulas and F. U. Hartl, data not shown.
12. N. W. Tietz, Ed., *Clinical Guide to Laboratory Tests* (W. B. Saunders Company, Philadelphia, PA, 1995).
13. Materials and methods are available as supporting material on *Science* Online.
14. A. F. Kisselev, A. L. Goldberg, *Chem. Biol.* **8**, 739 (2001).
15. T. Yoshimori, A. Yamamoto, Y. Moriyama, M. Futai, Y. Tashiro, *J. Biol. Chem.* **266**, 17707 (1991).
16. I. Mellman, R. Fuchs, A. Helenius, *Annu. Rev. Biochem.* **55**, 663 (1986).
17. V. Botbol, O. A. Scornik, *J. Biol. Chem.* **264**, 13504 (1989).
18. K. Sekine, H. Fujii, F. Abe, K. Nishikawa, *Int. J. Cancer* **94**, 485 (2001).
19. P. O. Seglen, P. B. Gordon, *Proc. Natl. Acad. Sci. U.S.A.* **79**, 1889 (1982).
20. P. O. Seglen, P. B. Gordon, H. Hoyvik, *Biomed. Biochim. Acta* **45**, 1647 (1986).
21. S. A. Wek, S. Zhu, R. C. Wek, *Mol. Cell. Biol.* **15**, 4497 (1995).
22. H. P. Harding *et al.*, *Mol. Cell* **6**, 1099 (2000).
23. A. Ciechanover, D. Finley, A. Varshavsky, *Cell* **37**, 57 (1984).
24. K. L. Rock *et al.*, *Cell* **78**, 761 (1994).
25. A. J. McClellan, M. D. Scott, J. Frydman, *Cell* **121**, 739 (2005).
26. C. Esser, S. Alberti, J. Hohfeld, *Biochim. Biophys. Acta* **1695**, 171 (2004).
27. G. C. Turner, A. Varshavsky, *Science* **289**, 2117 (2000).

28. We thank K. Mann and W. Straβhofer for performing the amino acid analyses; J. M. Barral, P. Breuer, H.-C. Chang, N. Tzvetkov, and J. C. Young for stimulating discussion; and J. M. Barral and S. Broadley for critical reading of the manuscript. This work was supported by the Deutsche Forschungsgemeinschaft (SFB 596).

Supporting Online Material

www.sciencemag.org/cgi/content/full/310/5756/1960/DC1
Materials and Methods
Figs. S1 to S4
Table S1

27 October 2005; accepted 18 November 2005
10.1126/science.1121925

Category-Specific Cortical Activity Precedes Retrieval During Memory Search

Sean M. Polyn,[1]* Vaidehi S. Natu,[2] Jonathan D. Cohen,[2,3] Kenneth A. Norman[2,3]

Here we describe a functional magnetic resonance imaging study of humans engaged in memory search during a free recall task. Patterns of cortical activity associated with the study of three categories of pictures (faces, locations, and objects) were identified by a pattern-classification algorithm. The algorithm was used to track the reappearance of these activity patterns during the recall period. The reappearance of a given category's activity pattern correlates with verbal recalls made from that category and precedes the recall event by several seconds. This result is consistent with the hypothesis that category-specific activity is cueing the memory system to retrieve studied items.

Human memory can be characterized as an elaborate network of stored representations (*1*, *2*). Recalling a particular event involves reactivating the constellation of representations that was active during that event, a phenomenon that Tulving has referred to as "mental time travel" (*3*). One of the major puzzles of human memory is how we enact this process of mental time travel. More concretely: When we are instructed to recall a particular event, how do we manage to select representations corresponding to that event, as opposed to representations from other events (*4*, *5*)?

Several theorists have argued that recalling an event involves a process of contextual reinstatement (*6*, *7*). When asked to recall memories of a certain type, a person activates knowledge about the general properties of those events and then uses this general knowledge to constrain the search for memories of the target events. For example, in trying to remember a trip to the zoo, a person could use their general knowledge of the kinds of animals that are typically found at zoos as a contextual cue for specific memories of seeing those animals. If specific details are recalled, these details can be used to further refine the retrieval cue, which leads to recall of additional details, and so on. Over time, the person continues to probe memory, and the set of representations that are active at recall increasingly comes to resemble the set of representations that were active during the targeted event. Whereas a number of behavioral memory studies have found evidence consistent with the contextual reinstatement hypothesis (*8*–*10*), this kind of evidence is necessarily indirect. We can infer (based on theoretical grounds) that the observed patterns of behavioral data arise from increased match between cues at test and stored memory traces, but these studies do not directly measure cue-trace match.

We used functional magnetic resonance imaging (fMRI) to more directly test the contextual reinstatement hypothesis. In neural terms, the contextual reinstatement hypothesis leads to a number of predictions. The most basic prediction is that, when subjects try to recall specific details from a particular episode or type of episode, the pattern of brain activity (during recall) will progressively come to resemble the pattern of activity that was present during the to-be-remembered episode. Furthermore, it should be possible to relate the reinstatement of

[1]Department of Psychology, University of Pennsylvania, Philadelphia, PA 19104, USA. [2]Department of Psychology, [3]Center for the Study of Brain, Mind, and Behavior, Princeton University, Princeton, NJ 08544, USA.

*To whom correspondence should be addressed. E-mail: polyn@psych.upenn.edu

brain activity to behavioral recall performance on a time-varying basis. The likelihood of recalling details from a particular episode (at a particular moment during the recall test) should be strongly related to how well subjects—at that moment—have reinstated activity from the to-be-remembered episode. According to the contextual reinstatement hypothesis, this association occurs because subjects use reinstated activity in a top-down fashion to cue for additional details (i.e., better reinstatement creates a better cue). However, this association could also occur if reinstated activity passively reflects recall of specific details (i.e., more recall leads to more reinstatement) and has nothing to do with cueing. To tease apart these ideas, we need to examine the temporal dynamics of how brain activity from the study phase is reinstated during recall. The contextual reinstatement hypothesis posits that if subjects use reinstated activity to cue memory, reinstatement should precede the recall of specific details. The alternative hypothesis (that reinstated brain activity is a passive reflection of the recall of specific details) posits that reinstated activity should occur during and after behavioral recall, but not before.

The main predictions of the contextual reinstatement hypothesis are summarized as follows: (i) Contextual reinstatement should build up gradually during the recall period. (ii) Fluctuations in contextual reinstatement should correlate with fluctuations in recall performance. (iii) Contextual reinstatement should precede recall of individual items. Recent neuroimaging studies of human memory retrieval have found that components of brain activity recorded during the study period are reinstated during the recall period, but these studies did not measure how contextual reinstatement changes over time during the recall test (*11*–*15*).

To test the predictions of the contextual reinstatement hypothesis, we designed a study that would allow us to directly measure contextual reinstatement in a time-varying manner. Unlike the aforementioned imaging studies (which used recognition or cued recall tests), our study used a free-recall paradigm in which subjects were asked to recall studied items in the absence of specific cues. The lack of specific environmental information driving retrieval in the free-recall paradigm places stronger demands on contextual reinstatement processes (*16*). Also, we used newly developed, multivariate pattern-analysis methods (*17*–*20*) to compare patterns of brain activity at the time of recall (test) to those observed during the initial encoding (study). This method increased our sensitivity in measuring how well study-phase brain activity was being reinstated at test.

Over the course of the experiment, subjects studied three lists, each of which contained 30 study items. Each list was composed of three different types of study items: photographs of famous faces, photographs of famous locations, and photographs of common objects. These photographs were presented with a name written in text above them (for example, a photograph of actor Jack Nicholson with the words "Jack Nicholson" above the picture). Subjects performed a different judgment on each class of stimuli to orient them to the salient features of those stimuli (*21*). Overall, the goal was to create a distinctive mental context associated with each stimulus class at study that could subsequently be tracked during the recall phase. At the end of the experiment, subjects were given a final free-recall test (lasting 3 min) where they were asked to recall all of the items they studied, in any order and regardless of category. fMRI data were acquired during both the study and recall periods (*21*).

The goal of the fMRI analysis was to track reinstatement (at the time of retrieval) of the contexts associated with studying face, location, and object stimuli. In order to do this, we first sought to identify patterns of brain activity associated with each category during study. Data analysis was carried out on an individual-subject basis. For each subject, we trained a neural-network pattern classifier to discriminate between patterns of whole-brain activity associated with face, location, and object stimuli during the study phase (*21*). Next, the trained network was used to classify whole-brain patterns of activity in the same individual (each pattern corresponding to 1.8 s of scanning) during the recall period. For each brain volume (scan), the classifier was used to produce an estimate of how well that scan matched the patterns of activity associated with the face, location, and object contexts from the study phase. By applying the classifier to successive brain scans acquired during the recall phase, we were able to derive a graded, time-varying estimate of the extent to which subjects were reinstating the face, location, and object study contexts. These time-varying estimates of the reinstatement of each context were then compared to the record of actual verbal recalls made by the subject.

Consistent with the contextual reinstatement hypothesis, we found that category-specific brain activity during the final free-recall period corresponded to the category of verbal recall (Fig. 1). This correspondence was quantified by correlating the classifier's estimates of category-specific activity (for each 1.8-s scan) with the record of verbal recalls for each category. A nonparametric statistical analysis confirmed that the classifier estimates correlated more with recall from the matching category than with recall from other categories; this effect was significant ($P < 0.05$) in seven of the nine individual subjects. A second nonparametric statistical analysis revealed that these effects were significant at the group level at $P < 0.001$ (table S3) (*21*).

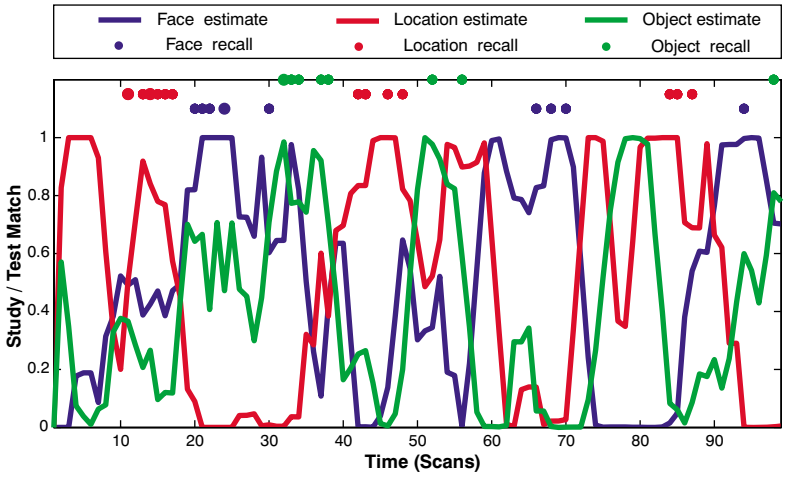

Fig. 1. Correspondence between the classifier's estimates of contextual reinstatement and verbal recalls for a single representative subject. Time is represented on the *x* axis; each time point represents one complete brain scan (lasting 1.8 s). For each brain scan, the classifier produced an estimate of the match between the current testing pattern and each of the three study contexts (strength of estimate appears on the *y* axis). The blue, red, and green lines correspond to the face, location, and object classifier estimates, respectively. The blue, red and green dots correspond to the face, location, and object recalls made by the subject (larger dots correspond to multiple items recalled during a single scan). The recall events are shifted forward by three time points to account for lag to the peak hemodynamic response (*27*). For illustrative purposes, the classifier estimate lines were temporally smoothed by replacing each point with the mean of that point and the immediately neighboring estimates (however, the correlations reported here were computed based on unsmoothed classifier estimates, as was the event-related average shown in Fig. 2).

An event-related average of the classifier estimates, constructed based on a subset of recall events (see below), revealed that category-specific brain activity reliably appeared before the verbalization of the recalled item (Fig. 2). This anticipatory rise was significant beginning at 5.4 s before recall, suggesting that subjects cue with general information about a category when trying to recall specific items from that category. To minimize the possibility that estimates of category-related activity (before recall) would be influenced by other recall events, we only included recall events in the event-related average if no same-category items were recalled in the preceding 14.4 s. For qualifying recall events, Fig. 2 plots the average classifier estimate for the currently recalled category in the time intervals surrounding the time of recall ($t = 0$). The anticipatory rise was computed relative to a baseline plot, showing classifier estimates for categories that were not recalled at $t = 0$ or in the 14.4 s preceding $t = 0$. This analysis was not corrected for the lag in the hemodynamic response; thus, the increase in category-related brain activity most likely preceded recall by substantially more than the 5.4 s observed in the blood oxygen level–dependent response.

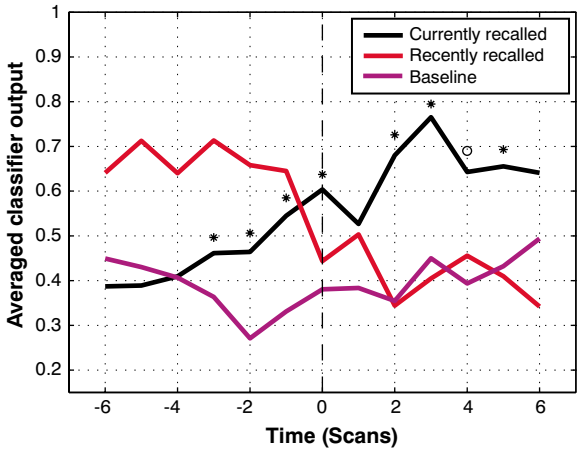

Fig. 2. Event-related average of the classifier's estimates of contextual reinstatement for the time intervals surrounding recall events. Recall events were excluded from the event-related average if a same-category recall was made in the preceding 8 scans (equivalent to 14.4 s). The dotted line at $t = 0$ represents the scan on which the verbal recall was made. The "currently recalled" plot (black line) was constructed by averaging together classifier estimates for categories that were recalled at $t = 0$, but not in 14.4 s preceding $t = 0$. The "baseline" plot (purple line) was constructed by averaging together classifier estimates for categories that were not recalled at $t = 0$ or in the 14.4 s preceding $t = 0$. The "recently recalled" plot (red line) was constructed by averaging together classifier estimates for categories that were not recalled at $t = 0$, but were recalled (at some point) during the 14.4 s preceding $t = 0$ (*28*). The three plots have not been shifted to account for hemodynamic lag effects. Statistical comparisons focused on the difference between the currently recalled and baseline plots, because these two plots were matched for lack of recalls in the 14.4 s preceding $t = 0$. The currently recalled and baseline plots differ significantly starting at $t = -3$ (i.e., 3 scans or 5.4 s before the verbal recall). Significance was calculated using a one-tailed, paired-samples t test on the within-subject difference between the two plots (points marked with stars and circles differ at $P < 0.01$ and $P < 0.05$, respectively).

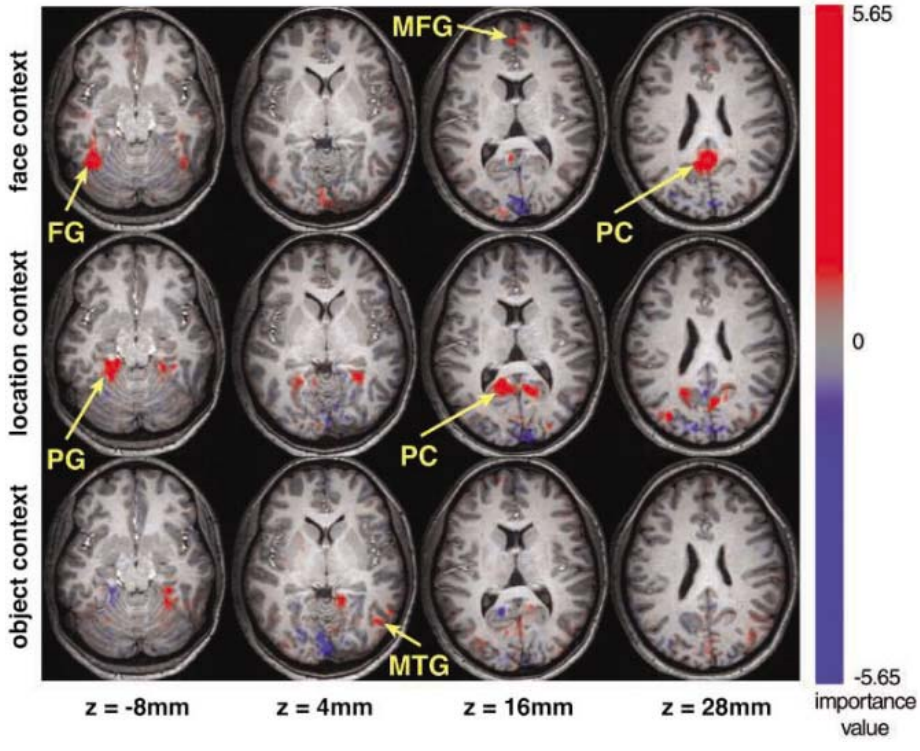

Fig. 3. The classifier-derived importance maps. Each voxel was assigned an "importance value" for each study context based on its influence on the classifier's estimate of reinstatement for that context (*21*). These maps average over all 9 subjects (whereas all classification was done on a within-subject basis). Each row depicts the map for a different study context, and each column depicts a different axial slice, spaced 12 mm apart. Voxels with positive importance values are colored red; voxels with negative importance values are colored blue. The colors fade into transparency as importance values approach zero, as shown on the color bar. FG, fusiform gyrus; PG, parahippocampal gyrus; MFG, medial frontal gyrus; PC, posterior cingulate; MTG, middle temporal gyrus (*24*).

Given the neural network classifier's success at predicting overt recall based on patterns of brain activity, we ran an analysis to determine which brain regions were contributing to the classification. Figure 3 presents maps displaying which voxels exerted the strongest influence in detecting each of the three study contexts (*21*). The four representative axial slices show that canonical category-selective areas [such as the fusiform face area and parahippocampal place area (*22–24*)], in addition to textured patterns in other brain areas, activate during the study of these item types.

The finding that canonical category-selective areas were contributing to the classification suggests that these areas could be driving the observed increase in contextual reinstatement before recall. However, follow-up analyses indicated that voxels outside of peak category-selective areas are also important for establishing this result (*21*). We identified peak category-selective regions of interest (ROIs) by using a group general linear model analysis, applied to study-phase data (see table S5 for a list of identified regions). In one analysis, we tracked category-related activity at recall by computing (at each time point) the average activity of each category-specific ROI. In another analysis, we used our standard pattern-classification procedure, but we limited the analysis to the union of the voxels in the peak category-selective ROIs. Both ROI-based analyses showed a significant correspondence between category-specific brain activity and behavior (tables S7 and S8). However, in both cases the observed correspondence was smaller than the correspondence obtained using our primary analysis method, and neither of the ROI-based analysis methods was sensitive enough to detect

the anticipatory rise in category-selective activity shown in Fig. 2 (figs. S10 and S11). Taken together, these results suggest that including voxels outside of the peak category-selective ROIs improves our ability to detect subtle changes in the reinstatement of category-related activity.

The work described here is one of a growing number of fMRI studies illustrating the benefits of multivoxel pattern-classification techniques (*17*–*20*, *25*, *26*). These studies have demonstrated that, by efficiently extracting the information present in multivoxel patterns of brain activity, it is possible to detect subtle distinctions between cognitive states using relatively thin time slices of brain data (on the order of seconds). Whereas previous applications of classification techniques have focused on brain activity elicited by specific perceptual cues, our study shows that classification algorithms can be used to extract a time-varying trace of the subjects' cognitive state as they search through memory in the absence of specific cues. Our results ground Tulving's speculations about mental time travel in neural fact. As subjects search for memories from a particular event, their brain state progressively comes to resemble their brain state during the sought-after event, and the degree of match predicts what kinds of information the subjects will retrieve. By providing a direct view of how subjects are cueing memory, the methods presented here constitute a powerful new tool that researchers can use to test and refine theories of how people mine the recesses of the past.

References and Notes

1. J. L. McClelland, D. E. Rumelhart, in *Parallel Distributed Processing: Explorations in the Microstructure of Cognition*, J. L. McClelland, D. E. Rumelhart, PDP Research Group, Eds. (Massachusetts Institute of Technology Press, Cambridge, MA, 1986), vol. 2, chap. 17, p. 170.
2. J. L. McClelland, in *Memory Distortion: How Minds, Brains, and Societies Reconstruct the Past*, D. L. Schacter, Ed. (Harvard Univ. Press, Cambridge, MA, 1995), chap. 2, p. 69.
3. E. Tulving, *Curr. Dir. Psychol. Sci.* **2**, 67 (1993).
4. K. A. Norman, D. L. Schacter, *Implicit Memory and Metacognition*, L. M. Reder, Ed. (Erlbaum, Hillsdale, NJ, 1996).
5. M. W. Howard, M. J. Kahana, *J. Math. Psychol.* **46**, 269 (2002).
6. E. Tulving, D. Thompson, *Psychol. Rev.* **80**, 352 (1973).
7. F. C. Bartlett, *Remembering: A Study in Experimental and Social Psychology* (Cambridge Univ. Press, Cambridge, 1932).
8. L. Sahakyan, C. M. Kelley, *J. Exp. Psychol. Learn. Mem. Cogn.* **28**, 1064 (2002).
9. S. M. Smith, in *Memory in Context: Context in Memory*, G. M. Davies, D. M. Thomson, Eds. (Wiley, Oxford, UK, 1988), pp. 13–34.
10. M. W. Howard, M. J. Kahana, *J. Exp. Psychol. Learn. Mem. Cogn.* **25**, 923 (1999).
11. M. E. Wheeler, S. E. Petersen, R. L. Buckner, *Proc. Natl. Acad. Sci. U.S.A.* **97**, 11125 (2000).
12. L. Nyberg, R. Habib, E. Tulving, *Proc. Natl. Acad. Sci. U.S.A.* **97**, 11120 (2000).
13. M. E. Wheeler, R. L. Buckner, *J. Neurosci.* **23**, 3869 (2003).
14. I. Kahn, L. Davachi, A. D. Wagner, *J. Neurosci.* **24**, 4172 (2004).
15. A. P. R. Smith, R. N. A. Henson, R. J. Dolan, M. D. Rugg, *Neuroimage* **22**, 868 (2004).
16. R. Shiffrin, R. Ratcliff, S. Clark, *J. Exp. Psychol. Learn. Mem. Cogn.* **16**, 179 (1990).
17. J. V. Haxby *et al.*, *Science* **293**, 2425 (2001).
18. T. M. Mitchell *et al.*, *Mach. Learn.* **5**, 145 (2004).
19. S. J. Hanson, T. Matsuka, J. V. Haxby, *Neuroimage* **23**, 156 (2004).
20. D. D. Cox, R. L. Savoy, *Neuroimage* **19**, 261 (2003).
21. Materials and methods—including behavioral paradigm, scanning parameters, classifier methods, data preprocessing details, details regarding nonparametric statistics, and details of map creation—are available as supporting material on *Science* Online.
22. N. Kanwisher, J. McDermott, M. M. Chun, *J. Neurosci.* **17**, 4302 (1997).
23. R. Epstein, N. Kanwisher, *Nature* **392**, 598 (1998).
24. A listing of the brain regions that were most reliably activated by each study context across subjects (as identified by a group general linear model analysis) is available (*21*).
25. Y. Kamitani, F. Tong, *Nat. Neurosci.* **8**, 679 (2005).
26. J. D. Haynes, G. Rees, *Nat. Neurosci.* **8**, 686 (2005).
27. When computing the correlation between classifier estimates and recall behavior, we adjusted for the hemodynamic response in two ways. In our primary analysis, we shifted the recall record forward by three time points (as in Fig. 1). We also ran a secondary analysis, where we convolved the recall record with a model of the hemodynamic response. The two analyses yielded very similar results (*21*).
28. The following example details how a set of hypothetical recall events are assigned to the currently recalled, recently recalled, and baseline plots. Assume that a subject recalls nothing for 20 s, then recalls a location ("Taj Mahal"), then recalls a face ("Bruce Lee") 5 s after recalling the location. The location recall ("Taj Mahal") qualifies for inclusion in the event-related average, because no other locations were recalled in the preceding 14.4 s. For the location recall, the currently recalled category is location, and both the face and object categories are assigned to the baseline plot (because neither faces nor objects were recalled in the 14.4 s preceding the location recall). The face recall ("Bruce Lee") also qualifies for inclusion in the event-related average, because no other faces were recalled in the preceding 14.4 s. With regard to the face recall, the currently recalled category is face; the location category is assigned to the recently recalled plot, because a location item was recalled during the 14.4 s preceding the face recall; and the object category is assigned to the baseline plot, because no items were recalled from that category in the 14.4 s preceding the face recall.

29. This study was supported by grants from the National Institute of Mental Health (NIMH) to K.A.N. (R01MH069456) and to J.D.C. (R01MH052864). S.M.P. was supported by a Ruth L. Kirschstein National Research Service Award predoctoral fellowship from NIMH (MH070177-01). Special thanks to R. Schapire, J. Haxby, P. Sederberg, and M. Kahana for comments; to C. Buck for assisting with running the subjects; and to S. Takerkart and L. Nystrom for assistance with the analysis.

Supporting Online Material

www.sciencemag.org/cgi/content/full/310/5756/1963/DC1
Materials and Methods
SOM Text
Figs. S1 to S11
Tables S1 to S8
References

19 July 2005; accepted 11 November 2005
10.1126/science.1117645

Inducible Nitric Oxide Synthase Binds, S-Nitrosylates, and Activates Cyclooxygenase-2

Sangwon F. Kim,[1] Daniel A. Huri,[1] Solomon H. Snyder[1,2,3]*

Cyclooxygenase-2 (COX-2) and inducible nitric oxide synthase (iNOS) are two major inflammatory mediators. Here we show that iNOS specifically binds to COX-2 and S-nitrosylates it, enhancing COX-2 catalytic activity. Selectively disrupting iNOS–COX-2 binding prevented NO-mediated activation of COX-2. This synergistic molecular interaction between two inflammatory systems may inform the development of anti-inflammatory drugs.

Inflammatory processes are mediated by multiple molecular mechanisms. Two of the most prominent are the production of nitric oxide (NO) by inducible NO synthase (iNOS) and the formation of prostaglandins by cyclooxygenase-2 (COX-2; prostaglandin H_2 synthase) (*1*, *2*). COX-2 inhibitors have attained widespread use as anti-inflammatory agents, although they elicit potentially adverse side effects (*1*, *3*, *4*), whereas iNOS inhibitors are not presently employed therapeutically. Inflammatory stimuli elicit the synthesis of iNOS and COX-2 proteins with similar time courses, which suggests that the two systems may interact (*5*, *6*). Stimulants of iNOS such as bradykinin (*7*) and lipopolysaccharide (LPS) plus interferon-γ (IFN-γ), two components of endotoxin, enhance prostaglandin formation (*8*). NOS inhibitors prevent the formation of prostaglandins (*9*).

To determine whether iNOS and COX-2 interact, we used a murine macrophage cell line (RAW264.7) in which LPS and IFN-γ massively activate both iNOS and COX-2. INOS immunoprecipitated with COX-2–specific antibodies from lysates of cells treated with LPS–IFN-γ (Fig. 1A). This was also observed in transfected human embryonic kidney cells (HEK293T) overexpressing both proteins (fig. S1A). The two enzymes also coimmuno-

[1]Department of Neuroscience, [2]Department of Pharmacology and Molecular Sciences, and [3]Department of Psychiatry and Behavioral Sciences, The Johns Hopkins University School of Medicine, 725 North Wolfe Street, Baltimore, MD 21205, USA.

*To whom correspondence should be addressed. E-mail: ssnyder@jhmi.edu

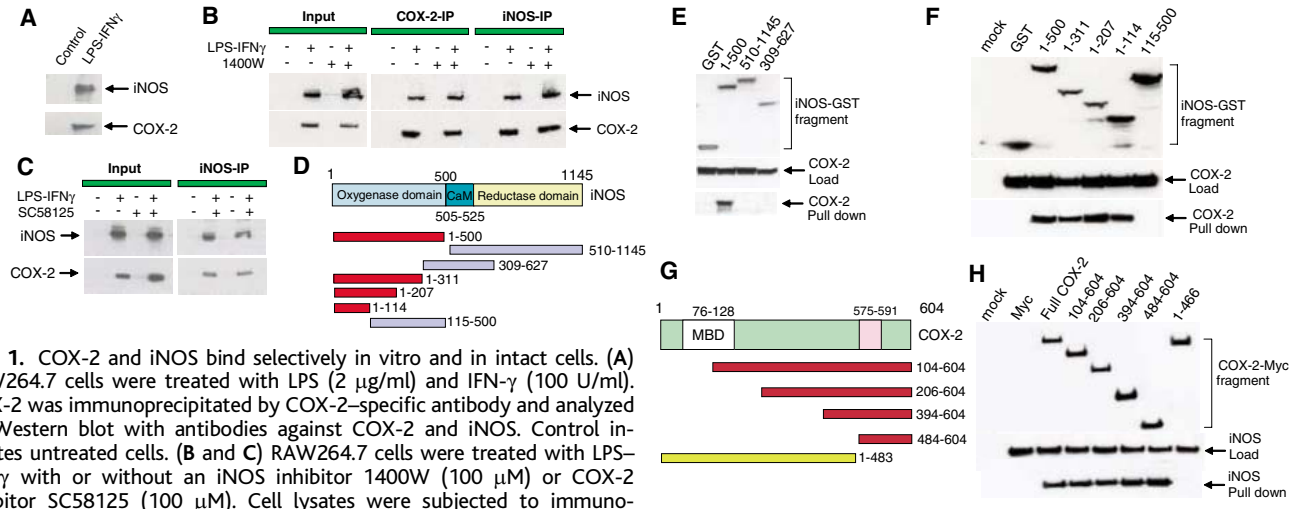

Fig. 1. COX-2 and iNOS bind selectively in vitro and in intact cells. (**A**) RAW264.7 cells were treated with LPS (2 μg/ml) and IFN-γ (100 U/ml). COX-2 was immunoprecipitated by COX-2–specific antibody and analyzed by Western blot with antibodies against COX-2 and iNOS. Control indicates untreated cells. (**B** and **C**) RAW264.7 cells were treated with LPS–IFN-γ with or without an iNOS inhibitor 1400W (100 μM) or COX-2 inhibitor SC58125 (100 μM). Cell lysates were subjected to immunoprecipitation (IP) and Western blot analysis with antibodies against COX-2 and iNOS. (**D**) The fragments of iNOS denoted in red bind to full-length COX-2, whereas fragments labeled purple do not, as determined by coimmunoprecipitation of full-length COX-2 by iNOS fragment fused to glutathione *S*-transferase (GST). The numbers represent the number of the amino acid sequence. (**E**) Transfected HEK293T cells expressing COX-2 and iNOS fragments expressed as fusion proteins with GST were precipitated with glutathione-conjugated beads. Proteins were detected by Western blot with antibodies against GST or COX-2. (**F**) Transfected HEK293T cells expressing COX-2 and epitope-tagged (Myc) iNOS fragments were immunoprecipitated with Myc-specific antibody and then analyzed by Western blot. (mock: The cells were treated with transfection reagent without the plasmid.) (**G**) Generated fragments of COX-2 that bind to full-length iNOS are labeled in red; those that do not bind are labeled in yellow. (MBD, membrane-binding domain). (**H**) Transfected HEK293T cells expressing iNOS and Myc-tagged COX-2 fragments were immunoprecipitated with Myc-specific antibody and analyzed by Western blot. (mock: The cells were treated with transfection reagent without the plasmid.)

precipitated from peritoneal macrophages obtained from mice injected with thioglycollate, an inflammatory stimulus that induces peritonitis or pleuritis (fig. S1B). To determine whether catalytic activity of the enzymes influences their interactions, cells that were induced by LPS–IFN-γ were also treated with the iNOS-selective inhibitor 1400W (Fig. 1B) or the COX-2–selective inhibitor SC58125 (Fig. 1C). Coimmunoprecipitation of iNOS and COX-2 by antibodies specific to either protein was unaffected by either inhibitor. The binding of iNOS and COX-2 was selective, because COX-1 did not immunoprecipitate with iNOS. To map the binding sites on both proteins, we generated selective deletions of iNOS (Fig. 1, D to F) and COX-2 (Fig. 1, G and H) sequences. The amino acid segment 1 to 144 of iNOS, which is within the oxygenase domain, is required, whereas the C terminus of COX-2 mediates binding and includes amino acids 484 to 604, which do not exist in COX-1.

The two major mechanisms whereby NO influences its intracellular targets are stimulation of guanylyl cyclase by direct binding of NO to iron in heme at the active site of guanylyl cyclase (*10*) or S-nitrosylation of protein targets on appropriate cysteines (*11*, *12*). Because COX-2 has heme at its active site (*13*), this would be a potential target. However, NO binding to heme in COX-1 does not alter its activity (*14*). COX-2 also contains 13 cysteines whose roles are not fully understood (*15*). To explore the possibility of S-nitrosylation of COX-2 by NO, we examined multiple NO donors including nitroso-*S*-glutathione (GSNO) (Fig. 2A), sodium nitroprusside (SNP), spermine-NO, and (*Z*)-1-[*N*-(2-aminoethyl)-*N*-(2-ammonioethyl) amino]diazen-1-ium-1,2-diolate (DETA-NONOate) (fig. S3A). Using the biotin switch method in which all the S-nitrosylated cysteines are selectively biotinylated (*16*), we observed that all four NO donors elicited S-nitrosylation of COX-2 in transfected HEK293T cells expressing COX-2–Myc (Fig. 2A). S-Nitrosylation of COX-2 was also observed in RAW264.7 cells treated with LPS–IFN-γ. This was prevented when cells were treated with iNOS inhibitor 1400W (Fig. 2B and fig. S3B). The biotin switch method was specific, as H_2O_2 did not elicit S-nitrosylation (fig. S4). We also ruled out the possibility that sulfenic acid modification was detected by the biotin switch assay by demonstrating that arsenite, which reverses sulfenic acid modifications but not S-nitrosylation, failed to provide the biotin switch signal afforded by ascorbate using GSNO with purified COX-2 or LPS–IFN-γ treatment of RAW 264.7 cells (fig. S4B). In some instances there may be no need to deliver NO directly to targets, as some actions of NO are prevented by hemoglobin, which sequesters freely diffusible NO (*17*). We examined the effects of hemoglobin on S-nitrosylation of COX-2 under varying conditions. In transfected HEK293T cells expressing COX-2, hemoglobin prevented the S-nitrosylation elicited by GSNO (fig. S5A), whereas it failed to alter S-nitrosylation of COX-2 in RAW264.7 cells activated by LPS–IFN-γ (fig. S5B). Thus, in the more physiologic macrophage cell line, the S-nitrosylation of COX-2 induced by an inflammatory stimulus does not appear to be elicited by freely diffusible NO.

To determine whether S-nitrosylation of COX-2 alters enzyme activity, we examined transfected HEK293T cells expressing COX-2–Myc. The NO donor SNP, added to cell lysates, elicited a twofold increase in COX-2 activity, reflecting S-nitrosylation. Ascorbic acid reversed S-nitrosylation (*16*, *18*) and prevented the increase (Fig. 2, C and D). The reversal by ascorbate of COX-2 activation by NO donors is not merely a reflection of ascorbate influences on enzyme substrates or intermediate products, as ascorbate failed to affect COX-2 activity in preparations not treated with SNP. Further evidence that S-nitrosylation and COX-2 activation are related is the closely similar concentration-response relation between the effects of the NO donor GSNO on S-nitrosylation and on COX-2 activity (Fig. 2E).

NO activates COX-2 by increasing its apparent V_{max} without changing its K_m (Fig. 2F). The higher concentration of SNP required to activate COX-2 in vitro compared with intact cells accords with earlier studies showing greater potency of NO donors in intact cells (*19*). To ascertain the kinetic basis for NO activation of COX-2, we conducted enzyme assays with increasing concentrations of sucrose to augment viscosity and slow down enzyme kinetics (Fig. 2G). As expected, with increasing viscosity, the ratio of control enzyme activity to the activity in more viscous solutions increased. This increase was diminished in SNP samples, consistent with SNP's accelerating the release of product from the enzyme.

To determine which of the 13 cysteines of COX-2 are critical for the augmentation of COX-2 activity elicited by S-nitrosylation,

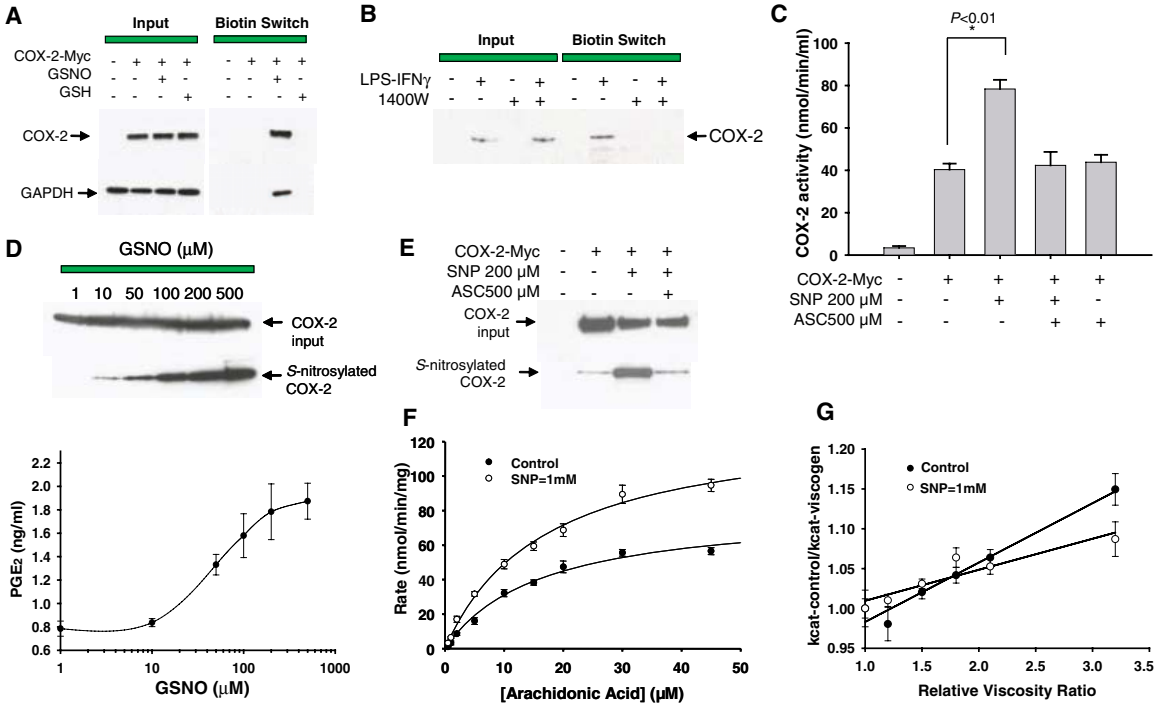

Fig. 2. S-Nitrosylation of COX-2 enhances enzyme activity. (**A**) COX-2 expressed in transfected HEK293T cells is S-nitrosylated in the presence of GSNO (100 μM) or glutathione (reduced form) (100 μM) as determined by biotin-switch assay. All the S-nitrosylated proteins were precipitated and COX-2 was detected by Western blot with COX-2–specific antibody. COX-2 was selectively S-nitrosylated by GSNO. (**B**) LPS–IFN-γ treatment of RAW264.7 cells elicits S-nitrosylation of COX-2, which is prevented by the iNOS inhibitor 1400W (100 μM). COX-2 was selectively S-nitrosylated by endogenously generated NO. (**C**) COX-2 enzyme activity was measured from the cell lysate of transfected HEK293T cells expressing COX-2–Myc in the presence or absence of SNP and ascorbate. Bars represent the mean ± SEM of three independent cell cultures performed in triplicate (*statistically significant by Student's *t* test). (**D**) COX-2–Myc expressed in transfected HEK293T cells is S-nitrosylated by various concentrations of GSNO. The dose-dependence of GSNO-mediated activation of PGE_2 was measured. Data were pooled from at least three independent determinations, each in triplicate. (**E**) COX-2–Myc expressed in transfected HEK293T cells is S-nitrosylated in the presence of SNP and reversed by the addition of ASC. All the S-nitrosylated proteins were precipitated, and COX-2 was detected by Western blot with COX-2–specific antibody. (**F**) Recombinant human COX-2 was treated with SNP, and COX-2 activity was measured (n = 3, control: V_{max} = 81.3 ± 4.8 nmol/min per mg, K_m = 16.2 ± 2.2 μM; SNP: V_{max} = 132 ± 6.5 nmol/min per mg, K_m = 17.0 ± 2.0 μM). (**G**) Recombinant human COX-2 was treated with SNP, and its turnover rate (k_{cat}) was measured in the presence of various concentrations of sucrose. Data were expressed as k_{cat}-control over k_{cat} in each viscosity versus viscosity ratio.

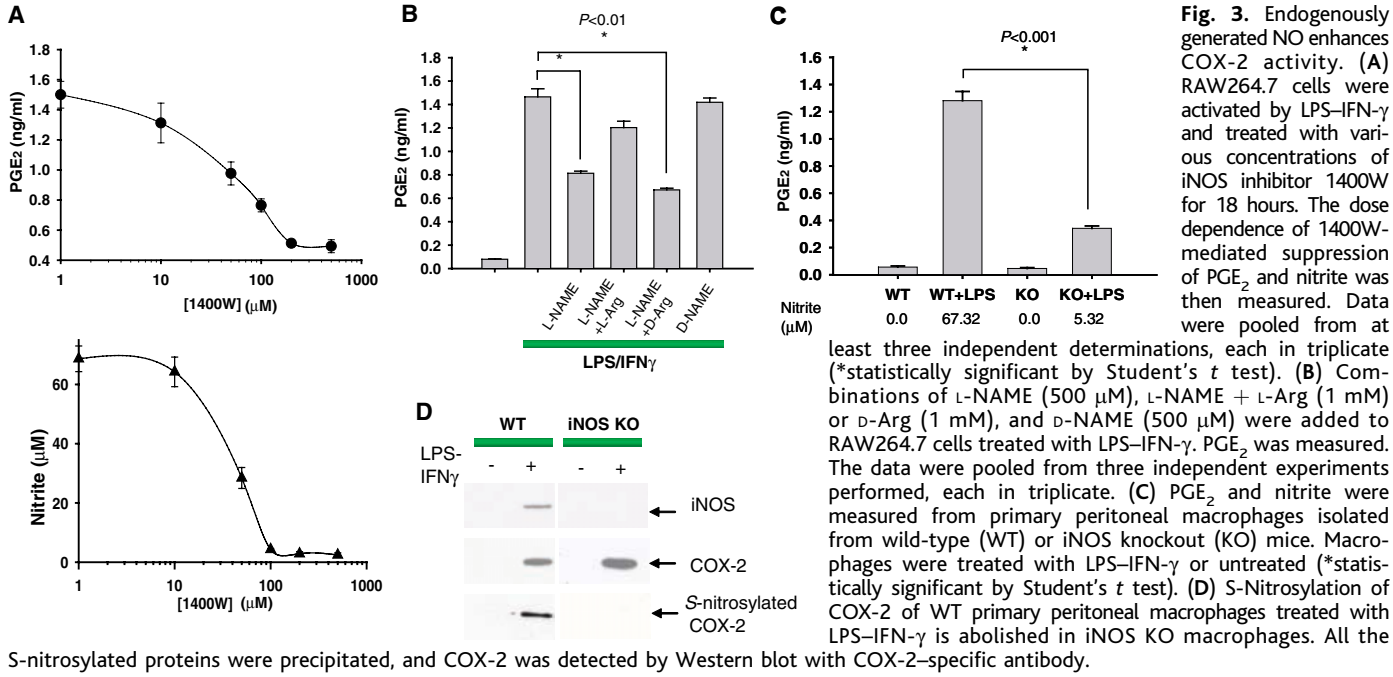

Fig. 3. Endogenously generated NO enhances COX-2 activity. (**A**) RAW264.7 cells were activated by LPS–IFN-γ and treated with various concentrations of iNOS inhibitor 1400W for 18 hours. The dose dependence of 1400W-mediated suppression of PGE_2 and nitrite was then measured. Data were pooled from at least three independent determinations, each in triplicate (*statistically significant by Student's *t* test). (**B**) Combinations of L-NAME (500 μM), L-NAME + L-Arg (1 mM) or D-Arg (1 mM), and D-NAME (500 μM) were added to RAW264.7 cells treated with LPS–IFN-γ. PGE_2 was measured. The data were pooled from three independent experiments performed, each in triplicate. (**C**) PGE_2 and nitrite were measured from primary peritoneal macrophages isolated from wild-type (WT) or iNOS knockout (KO) mice. Macrophages were treated with LPS–IFN-γ or untreated (*statistically significant by Student's *t* test). (**D**) S-Nitrosylation of COX-2 of WT primary peritoneal macrophages treated with LPS–IFN-γ is abolished in iNOS KO macrophages. All the S-nitrosylated proteins were precipitated, and COX-2 was detected by Western blot with COX-2–specific antibody.

RAW 264.7 cells were transfected to express the N-terminal 483 amino acids or the C-terminal 120 amino acids of COX-2. LPS–IFN-γ treatment induced S-nitrosylation of the C-terminal fragment (which contains three cysteines) but not the N-terminal fragment (fig. S6). To ascertain which of these three cysteines is responsible for augmented COX-2 activity, each was mutated to serine. The mutation in which Ser is substituted for Cys^{526} (C526S) prevented activation of COX-2 by the NO donor SNP, whereas the C561S mutation did not (fig. S6).

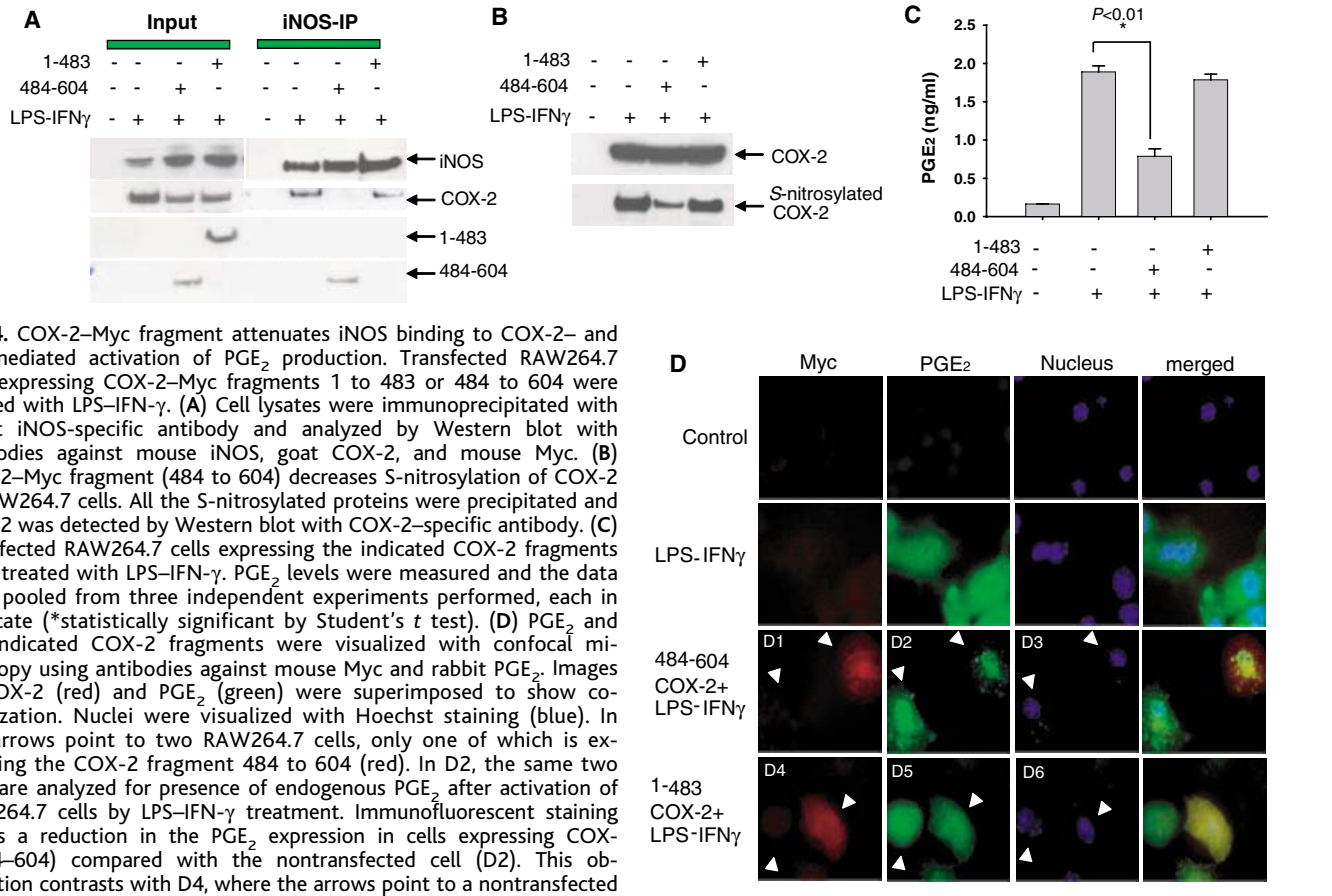

Fig. 4. COX-2–Myc fragment attenuates iNOS binding to COX-2– and NO-mediated activation of PGE_2 production. Transfected RAW264.7 cells expressing COX-2–Myc fragments 1 to 483 or 484 to 604 were treated with LPS–IFN-γ. (**A**) Cell lysates were immunoprecipitated with rabbit iNOS-specific antibody and analyzed by Western blot with antibodies against mouse iNOS, goat COX-2, and mouse Myc. (**B**) COX-2–Myc fragment (484 to 604) decreases S-nitrosylation of COX-2 in RAW264.7 cells. All the S-nitrosylated proteins were precipitated and COX-2 was detected by Western blot with COX-2–specific antibody. (**C**) Transfected RAW264.7 cells expressing the indicated COX-2 fragments were treated with LPS–IFN-γ. PGE_2 levels were measured and the data were pooled from three independent experiments performed, each in triplicate (*statistically significant by Student's *t* test). (**D**) PGE_2 and the indicated COX-2 fragments were visualized with confocal microscopy using antibodies against mouse Myc and rabbit PGE_2. Images of COX-2 (red) and PGE_2 (green) were superimposed to show colocalization. Nuclei were visualized with Hoechst staining (blue). In D1, arrows point to two RAW264.7 cells, only one of which is expressing the COX-2 fragment 484 to 604 (red). In D2, the same two cells are analyzed for presence of endogenous PGE_2 after activation of RAW264.7 cells by LPS–IFN-γ treatment. Immunofluorescent staining shows a reduction in the PGE_2 expression in cells expressing COX-2(484–604) compared with the nontransfected cell (D2). This observation contrasts with D4, where the arrows point to a nontransfected cell and a transfected cell expressing COX-2(1–483). D5 does not show a reduction of PGE_2 in the transfected cell as compared with the nontransfected cell.

The C555S mutation abolished enzyme activity, so the effects of NO stimulation could not be assessed. Individual mutation of the 13 cysteines in COX-2 did not detectably diminish total S-nitrosylation of the enzyme, which suggests that multiple cysteines can be S-nitrosylated, but only C526 is responsible for enzyme activation by NO.

To clarify the influence of NO on prostaglandin E_2 (PGE_2), a prostaglandin synthesized by COX-2 formation in a physiologic context, we examined RAW264.7 cells. The formation of PGE_2 in response to LPS–IFN-γ was inhibited by the iNOS inhibitor 1400W, with 50% reduction of PGE_2 formation at drug concentrations that provide 50% inhibition of iNOS activity (Fig. 3A). Specificity of the NO association was evident by inhibition of PGE_2 formation with the active L-isomer of the NOS inhibitor *N*-nitro-L-arginine methyl ester (L-NAME) but not by D-NAME; the effects of L-NAME were reversed by added L-arginine (Fig. 3B). Thus, about 50% of induced COX-2 activity is determined by S-nitrosylation.

As RAW264.7 cells are a continuous macrophage cell line that may not behave the same as macrophages in intact organisms, we used peritoneal macrophages from mice lacking iNOS. PGE_2 formation from macrophages of mice treated with LPS–IFN-γ was reduced in the iNOS knockout mice by ~70%, in parallel with a similar reduction in nitrite formation by the macrophages (Fig. 3C) and a decrease in S-nitrosylated COX-2 (Fig. 3D). These observations concur with findings of decreased urinary PGE_2 in iNOS knockout mice (*20*).

We hypothesized that the increase in PGE_2 formation by iNOS activation reflects binding of iNOS to COX-2 to deliver NO in appropriate proximity for S-nitrosylation. To explore this possibility we blocked iNOS–COX-2 binding with the fragment of COX-2 (amino acids 484 to 604), which binds iNOS (Fig. 4A). Expression of COX-2(484–604) in transfected RAW264.7 cells abolished the coprecipitation of iNOS and COX-2. Instead, COX-2(484–604) associated with iNOS (Fig. 4A). Moreover, this interference of binding between COX-2 and iNOS by COX-2(484–604) decreased S-nitrosylation of COX-2 in RAW264.7 cells (Fig. 4B). The dominant-negative effect of COX-2(484–604) reduced PGE_2 formation by more than 50%, whereas expression of a COX-2 fragment of amino acids 1 to 483, which does not bind iNOS, failed to influence PGE_2 formation (Fig. 4, C and D).

In summary, our study establishes a physiologic binding interaction of iNOS and COX-2 bringing NO in proximity to COX-2, facilitating its S-nitrosylation and activation, and fitting with earlier findings that NOS inhibition decreases prostaglandin formation (*9*, *21*). Our findings accord with recent evidence that many physiologic actions of NO require its delivery to molecular targets (*12*, *22*, *23*). Whereas scaffolding proteins such as CAPON (*22*) or PSD95 (*23*) link neuronal NOS, respectively, to Dexras1 (*22*) and *N*-methyl-D-aspartate receptors (*23*), iNOS and COX-2 bind directly. The molecular synergism between iNOS and COX-2 may represent a major mechanism of inflammatory responses. Drugs that block the iNOS–COX-2 interaction may be anti-inflammatory, synergizing with COX-2 inhibitors and permitting lower doses. As the binding site on iNOS is in the catalytic domain, derivatives of iNOS inhibitors that also prevent binding to COX-2 may decrease both NO and prostaglandin formation.

References and Notes

1. M. E. Turini, R. N. DuBois, *Annu. Rev. Med.* **53**, 35 (2002).
2. S. Moncada, *J. R. Soc. Med.* **92**, 164 (1999).
3. R. J. Flower, *Nat. Rev. Drug Discov.* **2**, 179 (2003).
4. E. J. Topol, *JAMA* **293**, 366 (2005).
5. T. P. Misko, J. L. Trotter, A. H. Cross, *J. Neuroimmunol.* **61**, 195 (1995).

6. I. Appleton, A. Tomlinson, D. A. Willoughby, *Adv. Pharmacol.* **35**, 27 (1996).
7. D. Salvemini *et al.*, *J. Clin. Invest.* **93**, 1940 (1994).
8. J. R. Vane, Y. S. Bakhle, R. M. Botting, *Annu. Rev. Pharmacol. Toxicol.* **38**, 97 (1998).
9. D. Salvemini *et al.*, *Proc. Natl. Acad. Sci. U.S.A.* **90**, 7240 (1993).
10. J. M. Braughler, C. K. Mittal, F. Murad, *J. Biol. Chem.* **254**, 12450 (1979).
11. S. R. Jaffrey, H. Erdjument-Bromage, C. D. Ferris, P. Tempst, S. H. Snyder, *Nat. Cell Biol.* **3**, 193 (2001).
12. D. T. Hess, A. Matsumoto, S. O. Kim, H. E. Marshall, J. S. Stamler, *Nat. Rev. Mol. Cell Biol.* **6**, 150 (2005).
13. R. M. Garavito, A. M. Mulichak, *Annu. Rev. Biophys. Biomol. Struct.* **32**, 183 (2003).
14. A. L. Tsai, C. Wei, R. J. Kulmacz, *Arch. Biochem. Biophys.* **313**, 367 (1994).
15. T. A. Kennedy, C. J. Smith, L. J. Marnett, *J. Biol. Chem.* **269**, 27357 (1994).
16. S. R. Jaffrey, S. H. Snyder, *Sci. STKE* **2001**, pl1 (2001).
17. F. Murad, C. K. Mittal, W. P. Arnold, S. Katsuki, H. Kimura, *Adv. Cyclic Nucleotide Res.* **9**, 145 (1978).
18. Y. Yang, J. Loscalzo, *Proc. Natl. Acad. Sci. U.S.A.* **102**, 117 (2005).
19. H. M. Lander, J. S. Ogiste, S. F. Pearce, R. Levi, A. Novogrodsky, *J. Biol. Chem.* **270**, 7017 (1995).
20. L. J. Marnett, T. L. Wright, B. C. Crews, S. R. Tannenbaum, J. D. Morrow, *J. Biol. Chem.* **275**, 13427 (2000).
21. D. Salvemini *et al.*, *J. Clin. Invest.* **96**, 301 (1995).
22. M. Fang *et al.*, *Neuron* **28**, 183 (2000).
23. H. C. Kornau, L. T. Schenker, M. B. Kennedy, P. H. Seeburg, *Science* **269**, 1737 (1995).
24. This work was supported by U.S. Public Health Service grant DA000266, Research Scientist Award DA00074 (to S.H.S.), and a Canadian Institute of Health Research fellowship (to S.F.K).

Supporting Online Material
www.sciencemag.org/cgi/content/full/310/5756/1966/DC1
Materials and Methods
Figs. S1 to S6
References

26 August 2005; accepted 11 November 2005
10.1126/science.1119407

Diversity and Function of Adaptive Immune Receptors in a Jawless Vertebrate

Matthew N. Alder,[1] Igor B. Rogozin,[2] Lakshminarayan M. Iyer,[2] Galina V. Glazko,[3] Max D. Cooper,[1] Zeev Pancer[4]*

Instead of the immunoglobulin-type antigen receptors of jawed vertebrates, jawless fish have variable lymphocyte receptors (VLRs), which consist of leucine-rich repeat (LRR) modules. Somatic diversification of the *VLR* gene is shown here to occur through a multistep assembly of LRR modules randomly selected from a large bank of flanking cassettes. The predicted concave surface of the VLR is lined with hypervariable positively selected residues, and computational analysis suggests a repertoire of about 10^{14} unique receptors. Lamprey immunized with anthrax spores responded with the production of soluble antigen-specific VLRs. These findings reveal that two strikingly different modes of antigen recognition through rearranged lymphocyte receptors have evolved in the jawless and jawed vertebrates.

An adaptive immune system based on lymphocytes bearing clonally diverse antigen-specific receptors first appeared at the dawn of vertebrate evolution ~500 million years ago. Within less than 40 million years in the Cambrian, both jawless and jawed vertebrates evolved mechanisms of lymphocyte receptor diversification that were radically different. Thus, jawed vertebrates rearrange immunoglobulin and T cell receptor (TCR) variable, diverse, and joining gene segments (VDJs) to generate highly diverse repertoires of T and B lymphocyte antigen receptors (*1*, *2*). In contrast, lamprey and hagfish, jawless fish representatives of the oldest vertebrate taxon, assemble their VLRs from modular LRR units (*3*, *4*). In the lamprey, a single incomplete germline *VLR* gene generates a diverse repertoire of cell surface receptors through somatic rearrangement of LRR cassettes that flank the gene. Each lymphocyte thus assembles a *VLR* gene of unique sequence. Hagfish have two germline *VLR* genes, called *VLR-A* and *VLR-B*, that can generate equivalently diverse receptor repertoires (*4*). On the basis of the existence of a sizable repertoire of diverse lymphocyte receptors, we hypothesized that VLRs may serve as jawless fish equivalents of the anticipatory antigen receptors of jawed vertebrates.

The potential diversity of lamprey VLRs was estimated by analysis of 517 unique VLR sequences, including 129 previously reported sequences (*3*) and 388 new sequences derived mostly from animals immunized with the *Bacillus anthracis* spore coat (*5*). Analysis of the aligned VLR diversity regions revealed mixed clusters of sequences, with no exclusive clustering of VLRs from animals immunostimulated with particular antigens. The alignment was then converted into a matrix consisting of the individual types of constituent LRR modules (Fig. 1A). This included the 30 to 38 residue N-terminal LRR (LRRNT), 18-residue first LRR (LRR1), 24-residue LRRs (LRRVs), 13-residue connecting peptide (CP), and 48- to 65-residue C-terminal LRR (LRRCT). Noting that the terminal 24-residue LRR module adjacent to the CP had a distinct sequence signature in 98% of the cases (fig. S1) (*5*), we designated this as the LRRV-end (LRRVe).

The data set was screened for repetitive occurrence of each type of LRR module, singly or as recurring pairs (Tables 1 and 2). Most pairs of adjoining LRRVs or LRRVe's were only observed once, but in some cases, repetitious pairs of LRRNT-LRR1 and CP-LRRCT were identified. These may represent VLRs that were assembled from multimodule genomic cassettes, such as one LRR1-LRRV-LRRV triplet previously identified in the *VLR* locus (*3*), or VLRs selected for certain structural conformations. However, 94% of the LRRNT-LRR1 and CP-LRRCT pairs are either unique or consist of the same pair of adjoining modules occurring three times or less in the VLR data set, and the pairing occurrence follows a random Poisson distribution (*6*). Most hagfish VLR-A modules were also found in random combinations (n = 139; tables S1 and S2), whereas the VLR-B sample (n = 70) was too small for reliable analysis. The potential diversity of the VLR repertoire was therefore calculated by considering individual LRR modules as independent recombination units. For the lamprey, we predict a potential repertoire of up to 10^{14} unique VLRs and up to 10^{17} for the hagfish VLR-A (*5*).

The number of LRR cassettes flanking the germline *VLR* gene is unknown. Thus far, 32 unique germline LRR modules have been identified in the partially sequenced lamprey *VLR* locus (*3*), and only 15 of these were identical to one of the 1568 modules from the VLR data set. To estimate the number of LRRV modules in flanking cassettes at the *VLR* locus, we used Monte Carlo simulations to predict at 95% confidence level an upper bound estimate of ~1500 lamprey LRRVs and ~2400 LRRVs for the hagfish *VLR-A* (*5*). These data suggest that the rearrangement process that yields mature *VLR* genes occurs by random selection of each module type from a large pool of genomic LRR modules.

The lamprey germline *VLR* gene of ~13 kb consists of three coding regions separated by two intervening sequences: (i) the signal peptide and 5′ portion of LRRNT, (ii) the 5′ portion of LRRCT, and (iii) the 3′ portion of LRRCT

[1]Howard Hughes Medical Institute, Departments of Medicine, Microbiology, Pediatrics, and Pathology, University of Alabama at Birmingham, Birmingham, AL 35294, USA. [2]National Center for Biotechnology Information, National Library of Medicine, National Institutes of Health, Bethesda, MD 20894, USA. [3]Stowers Institute for Medical Research, 1000 East 50th Street, Kansas City, MO 64110, USA. [4]Center of Marine Biotechnology, University of Maryland Biotechnology Institute, Baltimore, MD 21202, USA.

*To whom correspondence should be addressed. E-mail: pancer@comb.umbi.umd.edu.

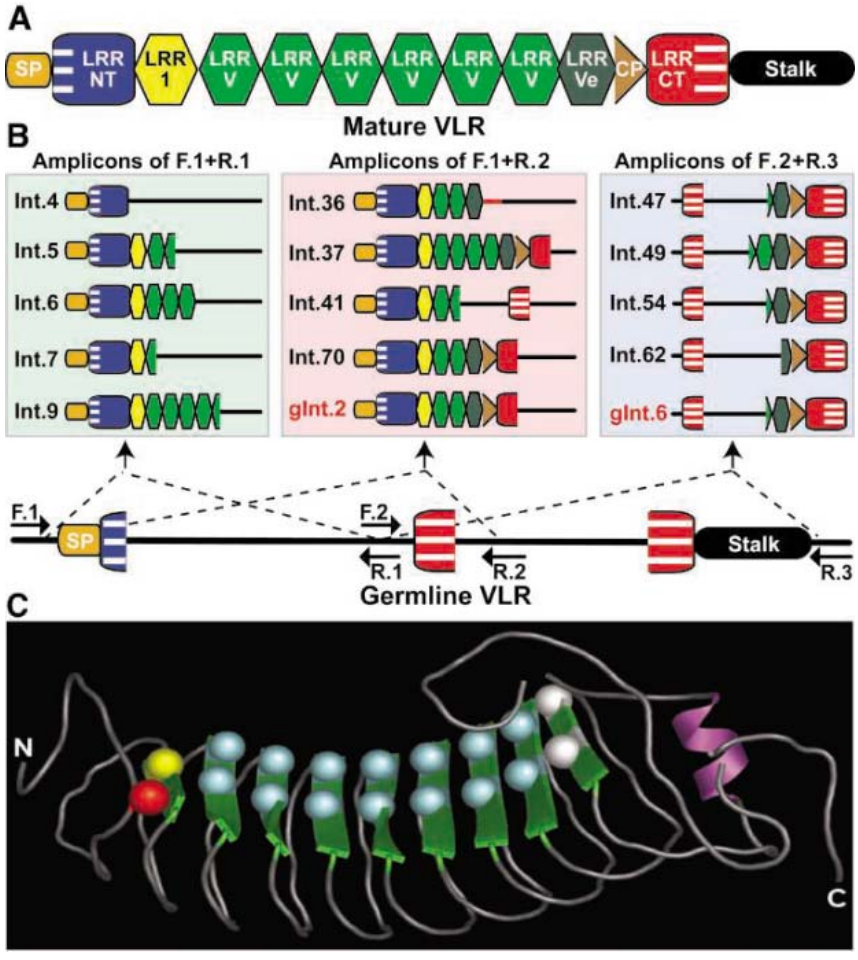

Fig. 1. Lamprey VLR diversity and gene rearrangement intermediates. (**A**) VLR scheme: signal peptide (SP), LRRNT, first LRR1, variable LRRV, end LRRVe, CP, and LRRCT (see text). Germline *VLR*-encoded portions of LRRNT and LRRCT are hatched. (**B**) Germline *VLR* gene rearrangement intermediates. Examples of LRR modules inserted from flanking cassettes into the germline gene: extensions of the *VLR* gene 5′ LRRNT (F.1 + R.1 amplicons); replacements and extensions of the *VLR* gene 5′ LRRCT (F.1 + R.2); and extensions of the *VLR* gene 3′ LRRCT (F.2 + R.3). Most insertions terminate with an incomplete LRR. Position of forward (F) and reverse (R) primers indicated; black, cDNA clones; red, genomic clones; red line in Int.36 indicates a 78-nucleotide noncoding DNA flanking the LRRVe. (**C**) 3D model of VLR diversity region. Positively selected solvent-exposed residues on the concave surface are represented by colored spheres: red, LRRNT; yellow, LRR1; blue, LRRV; white, LRRVe; green, β strands; magenta, α helices.

Table 1. Distribution of unique and repeated adjoining pairs of LRR modules among 517 unique VLR sequences (the modules are shown in Fig. 1A).

Number of pairs	Adjoining pairs of LRR modules					
	LRRNT LRR1	LRR1 LRRV	LRRV LRRV	LRRV LRRVe	LRRVe CP	CP LRRCT
1	287	390	270	388	449	308
2	22	5		3	16	29
3	7	2			3	8
4	4				1	4
5	5					8
6						1
7	2					1
8	2					2
9	2					1
10	2					
11				1		1
13	1					
20					1	
21	1					
22	1					1

and the stalk region (Fig. 1B) (*3*). Previously, we identified germline *VLR* transcripts from lamprey and hagfish lymphocytes, which indicated *VLR* gene transcription before or during the rearrangement process (*4*). We therefore preferentially cloned those rare cDNA amplicons that retained portions of the intervening sequences. For this we used polymerase chain reaction (PCR) primer combinations, wherein one annealed within an intervening region and the other in a coding portion, followed by selection for amplicons shorter than the length expected for germline *VLR* transcripts. Amplicons generated from genomic DNA (gDNA) were also analyzed. Among 37 unique rearrangement intermediates, we identified clones with large DNA deletions at different locations in the intervening regions (nine cDNA clones, two gDNA). In addition to deletions, some clones revealed modular LRR insertions within the germline *VLR* (24 cDNA clones, 2 gDNA). Deletion of coding portions of the germline gene were observed in five cDNA clones, as in no. 36 where the germline 5′ LRRCT is missing. In other cases, the germ line–encoded 5′ LRRCT was replaced with unique 5′ LRRCT from the flanking cassettes (four cDNA clones, two gDNA). The insertions in two clones included noncoding DNA, as shown for the 78-nucleotide insertion flanking the terminal LRR module in no. 36. All of the LRR modules were inserted in-frame with germ line–encoded elements, but in most cases, the insertions terminated with an incomplete LRR module (92%). Insertion of the LRRV modules into the germline *VLR* occurs through multiple independent events as indicated by (i) the variable numbers of LRRVs in the rearrangement intermediates and as many as eight in some of the VLR transcripts, whereas only singlet or doublet LRRV cassettes have been identified in the *VLR* locus; (ii) the rarity of repetitive adjoining LRRV modules (Tables 1 and 2); and (iii) the random Poisson distribution of the number of LRRV modules per transcript (table S5). Among the 32 LRR modules identified in the intermediate clones, only 4 matched any of the 32 known germline modules in the *VLR* locus. Consensus sequences that could mediate rearrangement of the LRR cassettes via recombinase activity were not found. The mechanism for the stepwise *VLR* rearrangement process remains unknown, but the final maturation step into functional *VLR* genes may involve recombination between the ends of the partially rearranged germline gene, thereby eliminating the remaining intervening sequences and any incomplete modules.

A hallmark of genes undergoing positive Darwinian selection is the prevalence of codons with nonsynonymous nucleotide substitutions (Ka), which alter the encoded residue, over codons with synonymous substitutions (Ks). For instance, multiple alleles of the polymorphic major histocompatability complex antigen-

presenting molecules differ by only a few positively selected residues located in the diverse antigen-presentation sites (*7*). In B lymphocytes, however, somatic hypermutation of immunoglobulin genes followed by a selection stage can also result in prevalence of nonsynonymous mutations. We therefore analyzed the distribution of nucleotide substitutions in all the related VLR sequences of identical length that differ by 1 to 21 nucleotides ($n = 20$; two triplets and seven pairs). In most cases, the substitutions clustered discretely in one or more of the LRR modules in a nonrandom distribution ($P < 0.01$) (*8*). Only in one case were "mutations" randomly scattered throughout the VLR diversity region ($P = 0.37$). Hence, the presence of one or more unique LRR modules distinguishes most of the VLR sequences, indicating that somatic hypermutation is not a significant contributing factor in VLR diversification. This conclusion is supported by the finding of recurring identical LRR modules among VLRs collected from different animals (Table 2) and by the observation that scaffold residues in the LRR modules are highly conserved, for example, 10 out of 24 residues are invariant in 90 to 100% of the LRRVe modules (fig. S1).

To identify regions in the VLR that may be undergoing positive selection, we used a three-dimensional (3D) model of the lamprey VLR (Fig. 1C) to predict the position of solvent-exposed and buried residues in the VLR. The residues in each VLR were then divided into three categories: (i) solvent-exposed residues on the concave VLR surface; (ii) solvent-exposed residues elsewhere; and (iii) buried residues. Analysis of nucleotide substitution revealed a rate significantly higher for nonsynonymous substitutions only in the concave VLR surface. A concentration of nonsynonymous substitutions was also found on the concave surface of hagfish VLR-A and VLR-B (Table 3; fig. S2). The invariant scaffold residues within each LRR module are interspersed with hypervariable sites (fig. S1), which indicates that some of these sites may be under positive selection (*7*, *9*, *10*). Positive selection can be distinguished by the ratio of Ka to Ks substitutions: a ratio >1 indicates positive selection, a ratio <1 indicates purifying selection, and a near 1 ratio indicates neutral evolution (*9*).

Using both maximum parsimony (*11*) and maximum likelihood (*12*, *13*) for independent calculations, we identified one to six sites that could be confidently considered as having been under positive selection in all six module types, with the exception of the hagfish VLR-A LRRCT and VLR-B CP (tables S3 and S4). The positively selected sites predicted by both methods were mapped onto lamprey and hagfish VLR models (Fig. 1C; fig. S2). In each LRR module type, except for the CP, one to three of the positively selected residues are solvent exposed on strands of the central β sheet that forms the concave surface of the VLR model, for example, codons 7 and 9 in lamprey LRRV (table S4). Another set of positively selected sites localize at one or both ends of the LRRNT and LRRCT. A conservative estimate of the combinatorial diversity that can be generated by the positively selected solvent-exposed residues on the concave VLR surface is 5×10^7 for the lamprey, 7.1×10^{13} for the hagfish VLR-A, and 1.5×10^6 for VLR-B. Notably, in many LRR-containing proteins, the concave surface is the ligand-binding interface (*14*–*19*).

The remarkable diversity of the VLR repertoire suggested that these may serve as lymphocyte antigen receptors in lamprey immunity. To assess the VLR's role in antigen recognition, we injected animals with anthrax spore coat (exosporium) as a particulate immunogen bearing an immunodominant antigen for mice, the collagen-like BclA glycoprotein (*20*). We then examined cellular and humoral responses after exosporia injections at weekly intervals. Flow cytometric analysis, using a VLR-specific antibody against the conserved stalk, indicated a dramatic increase in large lymphocytes among the VLR-positive cells. Compared with unstimulated animals, the fraction of large VLR-positive lymphocytes increased during the 8-week stimulation period from 4 to 93% in the blood, from 11 to 90% in the kidney, and from 7 to 76% in the typhlosole, the major hematopoietic tissue in larvae. Mitogenic activity of the exosporium may have induced the dramatic activation of VLR-bearing lymphocytes, as in lamprey stimulated with a mixture of antigens and mitogens (*3*). Plasma VLR concentrations in 8-week immunized animals were increased by 8- to 10-fold over preimmunization levels (*5*). An ELISA assay, used to measure levels of soluble anthrax-

Table 2. Different LRR modules and those found only once in adjoining pairs among 517 unique VLR sequences. The distribution of LRRV modules per transcript is shown separately.

Different LRR modules and uniquely paired combinations			Distribution of LRRV modules per transcript	
Module	Different (% total)	Uniquely paired	LRRV modules	Cases
LRRNT	235 (45)	196	0*	109
LRR1	191 (37)	148	1	228
LRRV	530 (78)	518	2	119
LRRVe	353 (68)	335	3	45
CP	71 (14)	54	4	6
LRRCT	188 (36)	160	5	8
			6	1
			7	1
			Average	1.31

*VLR sequences with LRRVe modules but no LRRV.

Table 3. Average Ks and Ka among solvent-exposed and buried residues of the lamprey VLR ($n = 517$), hagfish VLR-A ($n = 139$), and hagfish VLR-B ($n = 70$). A ratio of Ka/Ks >1 indicates positive selection; Ka/Ks < 1 indicates purifying selection; and Ka/Ks ≅ 1 indicates neutral evolution. For Ks and Ka, standard error in parentheses.

Site class	Ks	Ka	Mode of selection
Lamprey VLR			
Exposed residues on concave VLR surface	0.28 (0.03)	0.44 (0.05)	Positive selection ($Z = 2.61$, $P = 0.004$)
Exposed residues elsewhere on VLR surface	0.25 (0.02)	0.21 (0.03)	Neutral evolution ($Z = 1.55$, $P = 0.12$)
Buried residues	0.21 (0.02)	0.12 (0.02)	Purifying selection ($Z = 3.43$, $P = 0.001$)
Hagfish VLR-A			
Exposed residues on concave VLR surface	0.37 (0.05)	0.53 (0.05)	Positive selection ($Z = 3.63$, $P < 0.001$)
Exposed residues elsewhere on VLR surface	0.26 (0.03)	0.29 (0.03)	Neutral evolution ($Z = 0.37$, $P = 0.90$)
Buried residues	0.25 (0.03)	0.10 (0.02)	Purifying selection ($Z = 4.77$, $P < 0.001$)
Hagfish VLR-B			
Exposed residues on concave VLR surface	0.35 (0.04)	0.65 (0.02)	Positive selection ($Z = 8.37$, $P < 0.001$)
Exposed residues elsewhere on VLR surface	0.30 (0.03)	0.17 (0.03)	Purifying selection ($Z = 3.75$, $P < 0.001$)
Buried residues	0.32 (0.03)	0.09 (0.02)	Purifying selection ($Z = 8.72$, $P < 0.001$)

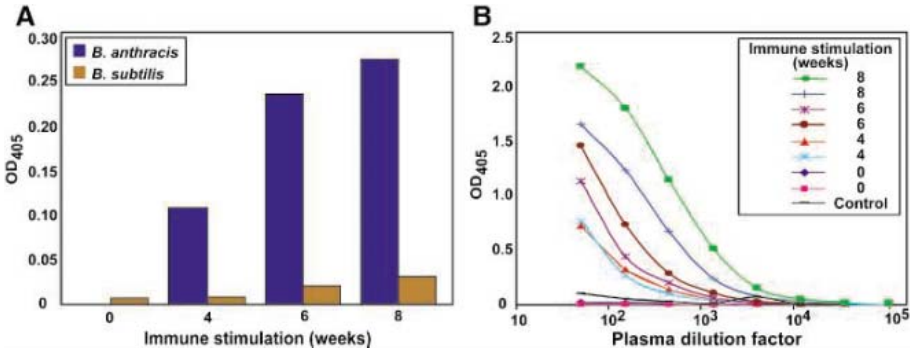

Fig. 2. Antigen recognition by lamprey VLR. Immune responses after weekly injections of anthrax spore coats at 4, 6, and 8 weeks. (**A**) Plasma VLR reactivity with *B. anthracis* spores compared with *B. subtilis* (control); plasma dilution 1:200. (**B**) Plasma VLR recognition of the spore coat protein BclA; two individuals per time point; control, plasma from 8-week stimulated larva reacted with unrelated protein.

reactive VLR, revealed a progressive increase in spore recognition over the immunization period (Fig. 2A). VLR specificity was indicated by selective reactivity with *B. anthracis* versus *B. subtilis* spores, a related bacterium used as a control. BclA antigen–specific VLRs also increased in plasma samples from immunized animals (Fig. 2B), and longer immunization periods led to progressively higher levels of BclA-specific VLRs. These data indicate that lampreys are capable of humoral responses to anthrax exosporium by producing increasing levels of soluble BclA-specific VLRs.

In summary, our data indicate that jawless fish generate a very large repertoire of VLRs, comparable to the predicted diversity of $\sim 10^{14}$ mammalian antibody repertoire (*21*, *22*). These repertoires would clearly be sufficient to recognize a wide range of antigenic determinants, yet this remarkable extent of receptor diversity in both jawless and jawed vertebrates is intriguing given that the available repertoire is limited by the presence of less than 10 million lymphocytes in lamprey larvae and in jawed vertebrate representatives like the zebrafish (*23*). Apart from antibodies, TCRs, and VLRs, such a spectacularly complex repertoire has only been reported for the $\sim 10^{13}$ C-type lectin fold variants in the receptor of the *Bordetella* bacteriophage (*24*).

Analysis of intermediates in the *VLR* gene assembly process indicates a multistep mechanism for insertion of various LRR modules from flanking cassettes into the framework germline gene. These are incorporated precisely in-frame with the coding regions in the incomplete *VLR* and in tandem with previously inserted LRR modules. The molecular machinery used in assembly of mature *VLR* genes is clearly an interesting arena for future investigation, and our prediction that an array of 1500 to 2400 diverse LRR modules in agnathan genomes provides the primary source of VLR diversity will be tested when the sea lamprey genome sequencing project is completed.

Most important, the present studies indicate that lamprey can use their VLRs for specific recognition of particulate and soluble protein antigens in a humoral response. Within 4 weeks of anthrax immunization, soluble anthrax-specific VLRs were abundant in the circulation, and these included VLRs that recognize the exosporium BclA protein. Our data thus strongly suggest convergent evolution of remarkably different strategies for generating anticipatory lymphocyte receptors in jawless and jawed vertebrates.

References and Notes

1. J. P. Cannon, R. N. Haire, J. P. Rast, G. W. Litman, *Immunol. Rev.* **200**, 12 (2004).
2. M. F. Flajnik, L. Du Pasquier, *Trends Immunol.* **25**, 640 (2004).
3. Z. Pancer *et al.*, *Nature* **430**, 174 (2004).
4. Z. Pancer *et al.*, *Proc. Natl. Acad. Sci. U.S.A.* **102**, 9224 (2005).
5. Methods and materials are available as supporting material on *Science* Online.
6. I. B. Rogozin, F. A. Kondrashov, G. V. Glazko, *Hum. Mutat.* **17**, 83 (2001).
7. A. L. Hughes, M. Nei, *Nature* **335**, 167 (1988).
8. H. Tang, R. C. Lewontin, *Genetics* **153**, 485 (1999).
9. M. Kreitman, J. M. Comeron, *Curr. Opin. Genet. Dev.* **9**, 637 (1999).
10. J. Zhang, H. F. Rosenberg, M. Nei, *Proc. Natl. Acad. Sci. U.S.A.* **95**, 3708 (1998).
11. Y. Suzuki, T. Gojobori, *Mol. Biol. Evol.* **16**, 1315 (1999).
12. Z. Yang, R. Nielsen, N. Goldman, A.-M. K. Pedersen, *Genetics* **155**, 431 (2000).
13. R. Nielsen, Z. Yang, *Genetics* **148**, 929 (1998).
14. A. Di Matteo *et al.*, *Proc. Natl. Acad. Sci. U.S.A.* **100**, 10124 (2003).
15. X. L. He *et al.*, *Neuron* **38**, 177 (2003).
16. B. Kobe, J. Deisenhofer, *J. Mol. Biol.* **264**, 1028 (1996).
17. E. G. Huizinga *et al.*, *Science* **297**, 1176 (2002).
18. A. C. Papageorgiou, R. Shapiro, K. R. Acharya, *EMBO J.* **16**, 5162 (1997).
19. W. D. Schubert *et al.*, *Cell* **111**, 825 (2002).
20. C. Steichen, P. Chen, J. F. Kearney, C. L. Turnbough Jr., *J. Bacteriol.* **185**, 1903 (2003).
21. T. Gojobori, M. Nei, *Mol. Biol. Evol.* **3**, 156 (1986).
22. C. A. Janeway Jr., P. Traver, M. Walport, M. J. Shlomchik, *Immunobiology: The Immune System in Health and Disease* (Garland Publishing, New York, 2001).
23. D. Traver *et al.*, *Nat. Immunol.* **4**, 1238 (2003).
24. S. A. McMahon *et al.*, *Nat. Struct. Mol. Biol.* **12**, 886 (2005).

25. We thank C. L. Turnbough and J. F. Kearney labs for advice and anthrax reagents; L. Gartland for the VLR-specific antibody, G. L. Gartland for help with the FACS; L. Aravind, M. F. Flajnik, A. N. Haines, and M. Criscitiello for critical comments. I.B.R. and L.M.I. were supported by the NLM/NIH/DHHS Intramural Research Program; M.D.C. is a HHMI Investigator; Z.P. was funded by NSF-MCB-0317460; contribution 05-122 from COMB. Reported sequences were deposited in GenBank: DQ150997 to DQ151421.

Supporting Online Material

www.sciencemag.org/cgi/content/full/310/5756/1970/DC1
Materials and Methods
Figs. S1 and S2
Tables S1 to S6
References

26 August 2005; accepted 11 November 2005
10.1126/science.1119420

Kinase Assay Kits

TruLight Kinase Assay Kits and the TruLight Universal Kinase/Phosphatase Assay Kit provide new technology for rapid, sensitive detection of enzyme activity. The assays are also convenient for inhibitor screening. Unlike fluorescence resonance energy transfer or traditional fluorescence quenching assays, in which quenching is equimolar between donor and receptor, TruLight assays make use of polymer superquenching, which results in assays that are up to 10 times more sensitive. These kits do not require special equipment, radioactive materials, or secondary (detector) enzymes or antibodies.

EMD Biosciences For information 800-854-3417 www.calbiochem.com/trulight

Gene Regulation Antibody Array

The Panorama Ab Microarray – Gene Regulation I Kit is designed for studying protein expression in cell or tissue extracts and is compatible with human, mouse, and rat proteins. The antibodies in the array represent families of proteins found in the nucleus that are involved in chromatin remodeling and regulation of gene expression. These include transcription factors and histone modifying enzymes, along with antibodies that specifically recognize histone modification.

Sigma-Aldrich For information +44 (0) 1260 296505 www.sigma-aldrich.com

Mass Spectroscopy Silver Stain

FOCUS-FASTsilver is a reliable and economical alternative to current silver staining methods. A 60- to 90-min protocol delivers sensitivity of less than 1 ng with clear backgrounds and sharp, clean bands of proteins or nucleic acid. The kit contains no gluataldehyde and is supplied with silverOUT, which removes inhibitory silver ions for complete trypsin protease digestion.

G-Biosciences/Genotech For information 314-991-6034 www.GBiosciences.com

Recirculating Chiller

A compact, economical recirculating chiller designed to provide reliable heat removal for lasers and other precision laboratory equipment is now available. Capable of maintaining process temperatures from 5° to 35°C, the Durachill 1.5 HP Chiller provides up to 6328 watts of cooling at 20°C ambient and fits conveniently under a standard height laboratory bench. It comes with a wide variety of standard and optional features and is available in both air- and water-cooled models. All models feature a microprocessor-based controller, digital temperature display, one-touch set point display, and digital pressure and flowrate display. These rugged chillers also feature adjustable fluid temperature, pressure, and flow rate alarms as well as a high ambient temperature alarm. Among the options available are remote temperature tracking capability, serial output, audible and visual alarms, and a low liquid level indicator.

PolyScience For information 800-229-7569 www.polyscience.com

Proteomics Software

Dymension 3 is software for rapid, reproducible analysis of proteins run on two-dimensional (2D) multi-stain gels such as cyanine dyes. For proteomics studies, 2D multi-stain gels are considered a more precise method of analysis because each protein spot has its own internal standard, which eliminates the problem of gel-to-gel variation. However, aligning these gels can be a very time-consuming task. By using Dymension 3 software, scientists can automatically overlay images of gels, showing up to three contrasting fluorescently labeled protein samples. Then through its spot-finding algorithm, Dymension 3 can instantly locate and analyze protein spots, assigning statistical confidence to each difference, thus accurately highlighting specific relevant proteins.

Dymension. For information +44 (0) 1223 727123 www.2dymension.com

Fluorescence Measurement

The FluoroMax-P combines time-correlated single-photon counting, the most sensitive technique for obtaining fluorescence lifetimes, with steady-state measurements in an easy-to-use, tabletop instrument. Picosecond light sources from 280 nm and other sources in the ultraviolet through visible to near infrared range let the user tailor the instrument for the latest in fluorescence measurements, whether involving anisotropy, multiple lifetimes, or any other dynamic technique.

Horiba Jobin Yvon

For information 732-494-8660 www.JobinYvon.com

Dual Detector

The Model 270 Dual Detector is an entry-level system for laboratories looking to make detailed characterizations of proteins and other biomolecules. The Model 270 can be configured as a stand-alone low angle light scattering (LALS) detector or as an LALS and viscometry dual detector. The dual detector Model 270 can be added to any commercial gel permeation chromatography/size exclusion chromatography system equipped with a concentration detector, converting it into a powerful triple detector system. The affordable Model 270 allows researchers to make routine direct determination of absolute molecular weight for a wide range of proteins, peptides, and biomolecules. Unlike multi-angle light-scattering techniques that only determine molecular weight by extrapolation, the Model 270 LALS measures molecular weight directly and thus is inherently more accurate. Incorporating patented optical technology that effectively operates at an angle of only 7 degrees, the detector represents a breakthrough in light-scattering technology. Configured with an additional differential viscometer, the Model 270 provides valuable further information including hydrodynamic radius, density, and conformation as well as providing structural data such as branching and aggregation.

Viscotek For information +44 1344 467180 www.viscotek.com

For more information visit GetInfo, *Science*'s new online product index at *http://science.labvelocity.com*

From the pages of GetInfo, you can:
- Quickly find and request free information on products and services found in the pages of *Science*.
- Ask vendors to contact you with more information.
- Link directly to vendors' Web sites.

Newly offered instrumentation, apparatus, and laboratory materials of interest to researchers in all disciplines in academic, industrial, and government organizations are featured in this space. Emphasis is given to purpose, chief characteristics, and availability of products and materials. Endorsement by *Science* or AAAS of any products or materials mentioned is not implied. Additional information may be obtained from the manufacturer or supplier by visiting www.science.labvelocity.com on the Web, where you can request that the information be sent to you by e-mail, fax, mail, or telephone.

ScienceCareers.org

Classified Advertising

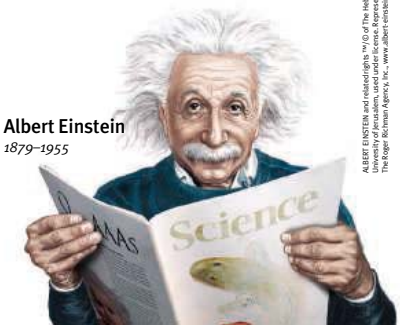

Albert Einstein
1879–1955

For full advertising details, go to **www.sciencecareers.org** and click on **How to Advertise,** or call one of our representatives.

United States & Canada

E-mail: advertise@sciencecareers.org
Fax: 202-289-6742

JILL DOWNING
(CT, DE, DC, FL, GA, MD, ME, MA, NH, NJ, NY, NC, PA, RI, SC, VT, VA)
Phone: 631-580-2445

KRISTINE VON ZEDLITZ
(AK, AZ, CA, CO, HI, ID, IA, KS, MT, NE, NV, NM, ND, OR, SD, TX, UT, WA, WY)
Phone: 415-956-2531

KATHLEEN CLARK
Employment: AR, IL, LA, MN, MO, OK, WI, Canada; Graduate Programs; Meetings & Announcements (U.S., Canada, Caribbean, Central and South America)
Phone: 510-271-8349

EMNET TESFAYE
(Display Ads: AL, IN, KY, MI, MS, OH, TN, WV; Line Ads)
Phone: 202-326-6740

GABRIELLE BOGUSLAWSKI
(U.S. Recruitment Advertising Sales Director)
Phone: 718-491-1607

Europe & International

E-mail: ads@science-int.co.uk
Fax: +44 (0) 1223-326-532

TRACY HOLMES
Phone: +44 (0) 1223-326-525

HELEN MORONEY
Phone: +44 (0) 1223-326-528

CHRISTINA HARRISON
Phone: +44 (0) 1223-326-510

SVITLANA BARNES
Phone: +44 (0) 1223-326-527

JASON HANNAFORD
Phone: +81 (0) 52-789-1860

To subscribe to *Science*:
In U.S./Canada call 202-326-6417 or 1-800-731-4939
In the rest of the world call +44 (0) 1223-326-515

Science makes every effort to screen its ads for offensive and/or discriminatory language in accordance with U.S. and non-U.S. law. Since we are an international journal, you may see ads from non-U.S. countries that request applications from specific demographic groups. Since U.S. law does not apply to other countries we try to accommodate recruiting practices of other countries. However, we encourage our readers to alert us to any ads that they feel are discriminatory or offensive.

POSITIONS OPEN

BIOMEDICAL SCIENCES, TWO FACULTY POSITIONS. As part of an ongoing expansion of biomedical science faculty, Kent State invites applications for two tenure-track positions beginning in August 2006. We seek candidates in neuroscience at the rank of Assistant or Associate Professor who focus on basic or disease related processes at the cell/molecular levels. Candidates with research interests in all areas of the neurosciences will be considered.

We seek a second candidate in cell or molecular biology at the rank of Assistant Professor to support strong interdisciplinary research initiatives in cell or molecular biology. Candidates with research interests in any disciplinary area will be considered, but applicants specializing in the relationship of gene expression and protein function to biomedical endpoints are preferred. Strengths of Kent State include strong interdisciplinary affiliations among the basic science units, The Cleveland Clinic Foundation, Northeastern Ohio Universities College of Medicine and the University of Akron, and superb core research facilities. The successful candidates are expected to establish an extramurally funded research program and exhibit a commitment to excellence in graduate and undergraduate education. Applicants must have a Ph.D. degree and postdoctoral experience. Applicants may apply to one or both positions and should indicate in their cover letter the position(s) for which they are applying.

Applicants should send their curriculum vitae, statement of research and teaching interests, and three letters of recommendation to:

Chair, Neuroscience Search Committee
or
Chair, Cell/Molecular Biology Search Committee
School of Biomedical Sciences
Kent State University
P.O. Box 5190
Kent, Ohio 44242-0001
Fax: 330-672-9391

Review of applications will begin February 2, 2006, and continue until the position is filled.

Kent State University is an Affirmative Action/Equal Opportunity Employer and encourages applications from candidates who would enhance the diversity of the University's faculty.

ASSISTANT PROFESSORSHIP IN MICROBIOLOGY

The Department of Biology **(website: http://www.ecu.edu/biology)** at East Carolina University invites applications for a tenure-track Assistant Professorship in microbiology. Special consideration will be given to applicants who are broadly trained and utilize molecular approaches to resolve problems in microbial ecology or evolution. Applicants should have a Ph.D. and postdoctoral research experience. The successful candidate is expected to teach an undergraduate course in microbiology and a graduate course of choice, and to maintain a strong, externally funded research program. The Department offers B.S. degrees in biology and in biochemistry; M.S. degrees in biology and molecular biology and biotechnology; and participates in two Ph.D. programs: Interdisciplinary Doctoral Program in Biological Sciences and Coastal Resources Management. Departmental facilities include centers for DNA sequencing, electron microscopy and environmental chemistry. Review of applications begins 9 January 2006. Send hard copy of curriculum vitae, a statement of teaching and research interests, and the names and contact information of three current references to: **Robert R. Christian, Department of Biology, East Carolina University, Greenville, NC, 27858-4353, christianr@mail.ecu.edu.** Proper documentation of identity and employability are required at the time of employment. Official transcript required upon employment.

East Carolina University (ECU) is an Equal Opportunity/Affirmative Action Employer that accommodates individuals with disabilities. Individuals requesting a disability accommodation should call the ECU Office Disability Support Services at telephone: 252-737-1016 (Voice/TTY/Relay).

POSITIONS OPEN

ASSISTANT/ASSOCIATE PROFESSOR
Medicinal Chemistry of
Central Nervous System-Targeted Molecules
The University of Montana

Applications are invited for a tenure-track Faculty Position in the Department of Biomedical and Pharmaceutical Sciences to strengthen research and graduate education in the medicinal chemistry of small molecules active in the central nervous system (CNS) as part of an NIH-funded Center for Biomedical Research Excellence (COBRE) in Structural and Functional Neuroscience. Research in the Center focuses on CNS protein structure/function as related to transport, membrane protein dynamics and neuropathology. Much of the progress and growth of the Center has been linked to the successful integration of medicinal chemistry, biochemistry and physiology with the aim of developing small molecules to advance our understanding of neuronal function and CNS disease. We wish to continue this effort by recruiting a new Assistant or Associate Professor. Successful candidates will be expected to establish vigorous externally funded research programs that complement Departmental and Center strengths, supervise graduate students, and be committed to teaching excellence at the graduate and undergraduate levels. Applicants must have a doctoral degree, postdoctoral research experience, and demonstrated ability or potential to secure NIH funding. A competitive startup package is available. The University of Montana is also the recipient of a National Science Foundation Advance Award focused on increasing the presence of women in science. Applications received by February 15, 2006, will receive full consideration; review will continue until the position is filled. More detailed information may be obtained from the **Center Director, R. Bridges (e-mail: richard.bridges@umontana.edu)** or from **website: http://www.umt.edu/csfn.**

The Southwest Oncology Group (SWOG) is seeking a **CHAIR** for our **TRANSLATIONAL MEDICINE COMMITTEE.** We are looking for a candidate who will bring state-of-the-art translational science to this cooperative group. Significant funding has been secured to support this endeavor. The individual should possess the ability to conduct focused research with the potential to translate their research findings into the clinical trial process involving multiple disease oriented committees. In addition, this Chair will recruit and assist other state-of-the-art translational scientists in bringing their research into SWOG. This candidate will interface closely with the leadership of the Southwest Oncology Group and the Disease Committee Chairs.

If you are interested in this opportunity please send your curriculum vitae and a brief two-page letter outlining your research interest and plan for this position.

Submit to:

Southwest Oncology Group
24 Frank Lloyd Wright Drive
Ann Arbor, MI 48106
Attn: Denise Reinke

Deadline for submission is January 30, 2006.

Richard I. Fisher, M.D., Deputy Chair, Southwest Oncology Group, is the Chair of this Search Committee.

For further information, you may call **Denise Reinke, Administrative Director, Southwest Oncology Group, telephone: 734-998-7130** or **e-mail: dreinke@umich.edu.**

POSITION IN BIOLOGY:
MARINE INVERTEBRATES
Department of Biology, Dalhousie University

We invite applications for a full-time probationary tenure-track Assistant Professor position in marine invertebrate biology. Please see **website: http://biology.dal.ca/other/jobs/marine.htm** for more details.

Scientific Director
Division of Intramural Research
National Institute of Mental Health

The National Institute of Mental Health (NIMH)) seeks a Scientific Director to lead its intramural biomedical research programs. The successful candidate will lead a renowned faculty from over 50 basic and clinical research labs (see http://intramural.nimh.nih.gov) and help chart the future of a vibrant, growing neuroscience research community across the NIH (see www.neuroscience.nih.gov). The Scientific Director will manage a $160 million research budget for intramural research and will be responsible for recruiting new faculty and overseeing the expansion of the intramural program into several new, state-of-the-art research facilities on NIH's Bethesda, Maryland campus.

The successful candidate will have a Ph.D. and/or M.D. and an established record of outstanding research accomplishments, scientific leadership and service within the basic or clinical neuroscience community. The successful candidate will need a compelling vision for innovative and translational research relevant to the Institute's mission. The Scientific Director will also supervise his/her own research laboratory, supported by resources commensurate with the size and scope of the program.

Applicants should send a cover letter, curriculum vitae and bibliography and six reference letters to: **Mr. Patrick Shirdon, Deputy Executive Officer, National Institute of Mental Health; 6001 Executive Blvd.; Room 8252, MSC 9653; Bethesda, Maryland 20892-9653; or e-mail to shirdonp@mail.nih.gov.**

Applications will be reviewed beginning **January 20, 2006**. Additional applications will be considered until this position is filled.

Chief, Laboratory of Pathology

The Center for Cancer Research (CCR), National Cancer Institute (NCI), National Institutes of Health (NIH), Department of Health and Human Services (DHHS), is seeking an outstanding physician-scientist to serve as Chief of the Laboratory of Pathology (LP) located on the campus of the NIH in Bethesda, Maryland. The successful candidate will oversee:

- the pathology clinical operations at the Clinical Research Center which serves the entire NIH patient community
- a clinical research program that applies advanced technology to biospecimen research
- an ACGME-accredited 4-year program in anatomic pathology.

This position provides a qualified candidate the opportunity to craft a world-class pathology program in a multidisciplinary translational research environment located in the new NIH Clinical Research Center, the largest clinical research center in the world. Resources available are substantial and include over one hundred staff positions across a full range of clinical research operations including, staff clinicians, principal investigators, staff scientists, medical technologists, technicians, clerical and administrative support, as well as fellowship trainees. These positions are fully funded including salary, awards, and a generous federal government benefits package.

The CCR is the largest component of the intramural biomedical research enterprise at NIH. Areas of emphasis within the CCR that interface seamlessly with the Laboratory of Pathology include molecular targets and oncology, immunology and immunotherapy, advanced imaging and biomarkers, HIV/AIDS, systems biology, genetics and genomics. The clinical pathology program and other CCR areas of focus are supported by a strong foundation in advanced biomedical technologies, enhanced opportunities for collaborations within and between interdisciplinary and multidisciplinary research teams, and an agile infrastructure that promotes a dynamic translational research process.

The Chief of the Laboratory of Pathology will oversee diagnostic anatomic pathology for patients undergoing clinical trials in the NIH Clinical Research Center, for all patients being considered for entry into clinical trials, and for epidemiologic and case studies of disease pathophysiology. Clinical diagnostic services include surgical pathology, cytogenetics, cytopathology, postmortem, hematopathology, pediatric pathology, electron microscopy, flow cytometry, and specialized histology. The Chief will oversee expert consultation in the fields of hematopathology, OB/GYN pathology, cytopathology, and pediatric pathology to the extramural medical community.

The Pathology Chief will guide the establishment of a research program and develop science-based evidence for best practices in procurement and process clinical research specimens in collaboration with the major clinical services and the newly formed Clinical Molecular Targets Core and Biospecimen Procurement and Processing Facility. In addition, CCR will support the successful candidate in the conduct of research in his/her area of interest.

Position Requirements:

Candidates must have an M.D. degree, be board-certified in pathology, have managerial experience overseeing pathology service delivery, have demonstrated an ability to work collaboratively, and have an in-depth knowledge of--and interest in--biospecimen research as it applies to the development of science-based rationale for procurement and processing. Salary is commensurate with experience. All applicants should submit a letter indicating interest in the position, a statement of research interests, a career synopsis and brief bibliography, current curriculum vitae and complete bibliography, and the names and addresses of five references.

Applications should be sent to: Richard Alexander, M.D., c/o Randy Redmond, National Cancer Institute, 31 Center Drive, Suite 3A19, Bethesda, Maryland 20892

WWW.NIH.GOV

Tenured/Tenure-Track/Senior Scientist Positions

The National Eye Institute (NEI) at the National Institutes of Health is seeking outstanding and creative scientists for several Tenured, Tenure-Track and Senior Scientist positions as part of a new multidisciplinary initiative for therapy of retinal genetic neurodegenerations. The program will be located within the Institute's Division of Intramural Research NEI, National Institutes of Health (NIH), Department of Health and Human Services (DHHS). These positions offer an opportunity to participate in an organization dedicated to uncovering new scientific knowledge, both basic and clinical, and ensuring the translation of that knowledge to the treatment of ocular diseases.

Investigators chosen for this Program will have access to clinical resources and research programs of the NEI as well as the intellectual and technical resources of the entire NIH. Investigators are expected to provide scientific leadership and expertise in one or more disciplines that include genetics, gene therapy, molecular biology, cellular biology, physiology, developmental neurobiology, or animal studies as they relate to the design and conduct of pre-clinical and clinical therapeutic retinal genetic disease research. The basic science components will interface with the existing clinical expertise within NEI on ophthalmic genetic diseases.

This will be a comprehensive program to move into human therapy. The following approaches are pertinent to this effort: molecular genetic analysis of fundamental questions in retinal disease; biochemistry of transcriptional regulation; genetic basis of cellular differentiation and pattern formation in a multicellular tissue; molecular and cellular mechanisms of retinal development and their role in the progression and treatment of retinal degenerative diseases; molecular basis of cell-cell interactions that regulate retinal neurogenesis and neuronal specificity during development and regeneration; pre-clinical animal models for retinal degenerative diseases; pharmacogenetics; cell-based therapies; molecular control of stem cell neurobiology and self-renewal; neural remodeling in retinal degenerative diseases.

Salary is commensurate with research experience and accomplishments. A full Federal package of benefits is available (including retirement, health, life and long term care insurance, Thrift Savings Plan etc).

Applicants should submit curriculum vitae, bibliography, copies of three major publications, a summary of research accomplishments, a brief statement of future research goals, and three reference letters to:

Sheila Ayala, Intramural Administrative Specialist, Office of the Scientific Director, National Eye Institute, 31 Center Drive, Building 31, Room 6A22, Bethesda, MD 20892, Tel: 301-451-6763, Email: sayala@nei.nih.gov. This position will be open until filled.

NIAAA
National Institute on Alcohol Abuse and Alcoholism

Oxidative/Nitrosative Stress and Tissue injury
National Institute on Alcohol Abuse and Alcoholism

A postdoctoral fellow position is available to study the mechanisms of oxidative/nitrosative stress and chronic inflammation-induced tissue injury in cardiovascular diseases. Candidates motivated to study cardiovascular pathophysiology and with experience in small animal surgery (ischemia/reperfusion and vascular injury models), molecular biology, and cell biology are encouraged to apply. Skills in oral and written communications are essential. Candidate must have a Ph.D. or M.D. degree and have less than five years of postdoctoral experience. Compensation will be commensurate with relevant work experience.

Interested candidates should submit a C.V., list of publications, and three letters of reference to: **Dr. Pal Pacher, Section on Oxidative Stress Tissue Injury, Laboratory of Physiologic Studies, NIAAA, NIH, 5625 Fishers Lane, Room 2N-17, MSC 9413 Bethesda, MD 20892-9413, or e-mail pacher@mail.nih.gov.**

NIDDK

NIDDK POSTDOCTORAL POSITIONS within the Molecular and Clinical Hematology Branch are available to study hematopoiesis and hemoglobin switching. Current projects include studies of the molecular basis of lineage-specific differentiation of hematopoietic stem cells and the development of therapies for hemoglobinopathies and other genetic blood disorders. A strong background in molecular biology, cell biology and/or signal transduction is required. Opportunities exists to develop relevant clinical or translational projects. Salary and benefits will be commensurate with experience of the applicant. Interested candidates with an M.D. and/or Ph.D., and less than five years of postdoctoral experience should send a CV, bibliography, and names of three references to: **Griffin P. Rodgers, M.D. at (gr5n@nih.gov) or: Molecular and Clinical Hematology Branch, National Institutes of Health, National Institute of Diabetes and Digestive and Kidney Diseases, 10 Center Drive, Building 10, Room 9N-119, Bethesda MD 20814.**

WWW.NIH.GOV
Positions @ NIH
THE NATIONAL INSTITUTES OF HEALTH

Announcement of High Throughput Screening (HTS) Services to Identify Bioactive Small Molecules

Solicitation of Assays for the Molecular Libraries Screening Centers Network (MLSCN) PAR-05-147

The NIH Molecular Libraries and Imaging Roadmap initiative has recently established the Molecular Libraries Screening Centers Network (MLSCN), a new nationwide high-throughput screening (HTS) resource (http://nihroadmap.nih.gov/molecularlibraries/fundedresearch.asp). The MLSCN will use HTS technologies to identify bioactive compounds. Using compounds from the Small Molecule Repository (http://mlsmr.discoverypartners.com/MLSMR_HomePage/) and supported by the informatics capabilities of NIH's PubChem (http://pubchem.ncbi.nlm.nih.gov/), the MLSCN will provide researchers with new chemical tools to explore cellular functions at the molecular level. The ultimate goal of the MLSCN is to empower the research community to use small molecule compounds in their research, as tools to modulate genes and pathways, as imaging probes in basic or clinical applications, or as starting points for the development of new therapeutics for human disease.

The ten MLSCN centers are capable of screening 100-200 assays adaptable to HTS annually. Through Program Announcement PAR-05-147, the MLSCN is soliciting applications three times per year from investigators who have developed innovative assays and are interested in having them used in the MLSCN to screen a large number of compounds and furthermore, interested in expanding the utility of their assay(s) for producing useful in vitro and/or in vivo chemical probes. Investigators do not need to provide funds or personnel to utilize the HTS resource.

Details of the application process, and further information about the MLSCN, can be found in the Program Announcement entitled **Solicitation of Assays for Molecular Libraries Screening Centers Network (MLSCN), PAR-05-147 (http://grants.nih.gov/grants/guide/pa-files/PAR-05-147.html)**. Interested investigators are encouraged to contact **Ingrid Li at 301-443-5288 or via email ili1@mail.nih.gov**. Application receipt dates are **January 18 and May 18, 2006**, with Letters of Intent encouraged 4 weeks prior to these dates. Please refer to the roadmap web site (**http://nihroadmap.nih.gov/molecularlibraries/grants.asp**) for future application receipt dates.

Health Scientist Administrator

The National Institute on Drug Abuse (NIDA), a major research component of the National Institutes of Health (NIH) and the Department of Health and Human Services (DHHS), is recruiting for a Health Scientist Administrator (HSA). The incumbent serves as HSA in the Science Policy Branch of the Office of Science Policy and Communications. The incumbent: (1) Develops position statements on science and science policy issues related to clinical, behavioral and/or social research, which requires expert knowledge of how these research areas relate to drug abuse and addiction; (2) responds to inquiries from all levels of the Department, other federal agencies, the scientific community, and the general public; (3) works with program staff to develop, direct, and implement the science-based strategic planning and evaluation processes for NIDA's research programs in the areas of clinical, behavioral, or social sciences; and (4) represents the Institute before professional, scientific and public interest groups, as well as interagency task forces.

Successful completion of all requirements for an M.D. or a Ph.D. (or equivalent doctoral degree) in an accredited college or university, including (for a Ph.D.) acceptance of the dissertation, in an academic field of the behavioral or health sciences, which has been applied and utilized by the applicant in health or health-related research.

In addition, applicants must have at least one year of specialized experience at the next lower grade level, or equivalent. Specialized experience is experience that is directly related to the position to be filled, and which has equipped the applicant with the particular knowledge, skills, and abilities needed to successfully perform the duties of the position. Annual salary range is $74,782 - $114, 882. A full Civil Service benefits package is available. Physicians may also be eligible for a Physicians' Comparability Allowance of up to $30,000 per year. The position is located in Rockville, Maryland.

APPLICATIONS (RESUME AND APPLICATION QUESTIONS) MUST BE RECEIVED ON-LINE VIA THE HHS CAREERS WEB SITE BEFORE MIDNIGHT EASTERN STANDARD TIME ON THE CLOSING DATE OF THIS ANNOUNCEMENT. PLEASE SEE BELOW FOR DETAILS ON USING THE HHS CAREERS SYSTEM.

For additional information on this position, and for instructions on submitting your application, please see our website, at: http://www.nida.nih.gov/ or https://jobs.quickhire.com. Detailed information is provided under vacancy announcement number: **NIDA-05-102882-DE** Supplemental documentation must be submitted to: **Nancy Delgais, National Institutes of Health, 111 Alexander Drive, Maildrop NH-01, Research Triangle Park, NC 27709 or faxed to 919-541-3659.**


CHALLENGE THE FUTURE
www.becomeaprofessorindelft.nl
Delft University of Technology in the Netherlands has a long history of excellence in Chemical Engineering. Building on this expertise, TU Delft is taking on a new challenge: **nanochemical engineering**, the next stage in the nano-revolution. A revolution in which TU Delft has been a pioneer.
To help us achieve our goals in the nano-domain, we are seeking to create **three new chairs**.
Do you share our ambition to challenge the future? Are you ready to enter an exciting new era with us?
www.becomeaprofessorindelft.nl
TU Delft
Delft University of Technology

ST. THOMAS UNIVERSITY

FACULTY – BIOLOGY

St. Thomas University invites applications for a continuing track position in biology at the Assistant or Associate Professor level, depending on experience, starting August 2006. A PhD and three years postdoctoral laboratory research experience required. Applicants at the Associate level must have an established and funded research program.

We are searching for an individual who will thrive in a liberal arts environment that combines a strong commitment to teaching and research. Mentoring of undergraduate research students is expected. Candidates with research interests that complement the developing cell science program are particularly encouraged to apply. Specifically, research involving microbial physiology and developmental genetic models will be given preference. The successful candidates will be expected to teach at all levels of the curriculum and establish an externally funded research program that provides rigorous collaborative research projects for undergraduates. Opportunities exist for research collaboration within the developing biomedical research community spawned by the newly forming Scripps Research Institute in South Florida.

Research laboratory space and infrastructure will be provided in our current building and in our new building, the Carnival Cruise Lines Science and Technology Building.

The department is a multi-discipline unit consisting of 20 full-time and adjunct faculty members. We offer Bachelor of Arts degrees in biology, computer science, and computer information systems in addition to our pre-nursing and pre-engineering programs.

Located in Miami Gardens, Florida, St. Thomas University is a Catholic university with rich cultural and international diversity. Our community includes more than 2600 students and 105 full-time faculty members. Further information is available at **http://www.stu.edu/**.

Completed applications received by **February 17, 2006** will receive full consideration with later applications as needed until position is filled. Send letter of application, curriculum vitae, undergraduate and graduate transcripts (unofficial copies are acceptable initially), statement of research interests, statement of teaching philosophy, and a list of at least three references to: **Lenore Prado, Associate Director of Human Resources (Req. #S217-06), St. Thomas University, 16401 NW 37 Ave., Miami Gardens, FL 33054; Email: facsearch@stu.edu; Fax: (305) 628-6510**.

St. Thomas University is an Equal Opportunity Employer.

FRESHWATER ECOLOGY ASSISTANT PROFESSOR

The Ecology and Evolutionary Biology Department of the University of California, Santa Cruz, expects to have a tenure track position available in freshwater ecology, subject to the availability of funding. Individuals using any combination of population-level, community-level, and/or evolutionary approaches to major ecological questions are encouraged to apply, with particular interest in individuals whose research addresses issues related to the land-sea interface, thereby complementing our programs in Terrestrial and Marine Ecology. The successful candidate will have opportunities to collaborate with the Santa Cruz Laboratory of the National Marine Fisheries Service (NMFS, **http://santacruz.nmfs.noaa.gov**).

Candidates should send a curriculum vitae and statements of research and teaching, and arrange for three letters of reference evaluating the candidate's scholarly contributions, teaching, and other professional accomplishments, to **susan@biology.ucsc.edu** or to: **Susan Thuringer, Department of Ecology and Evolutionary Biology, University of California, Santa Cruz, 1156 High Street, Santa Cruz, California 95064**. Review of applications will begin **February 7, 2006**. Please refer to position **#737** in all correspondence. The full ad is available at **http://www.biology.ucsc.edu/eeb/recruitment0506.html**.

UCSC IS AN AFFIRMATIVE ACTION/ EQUAL EMPLOYMENT OPPORTUNITY EMPLOYER.

GRADUATE PROGRAM

University of Nebraska Medical Center

Graduate Studies in the Life Sciences

NEBRASKA'S HEALTH SCIENCE CENTER

Graduate programs in the life sciences are offered at the University of Nebraska Medical Center (UNMC) in Omaha, Nebraska. Studies leading to the Ph.D. are available in eight basic science programs and one integrated, interdepartmental training program (MSIA). In addition, the BRTP may be used as a common entry path for most of the basic science programs. Numerous training and research grants as well as significant internal funding sources support students in these degree programs. In the 2005-2006 academic year, most full-time Ph.D. students are being supported by a stipend of $21,000 or more with remission of all tuition. Most students begin their research rotations and orientation program in July or mid-August.

The Ph.D. life science programs currently available at UNMC include:

Biomedical Research Training Program (BRTP; common entry program)
Biochemistry and Molecular Biology
Cancer Research
Cellular and Integrative Physiology
Genetics, Cell Biology and Anatomy
Medical Sciences Interdepartmental Area (MSIA)
Pathology and Microbiology
Pharmaceutical Sciences
Pharmacology and Experimental Neuroscience
Toxicology

Interested students should visit UNMC at **http://app1.unmc.edu/gradstudies/**. Apply online!

UNMC has experienced a rapid growth in the past five years with new research buildings and laboratories added to support the increase in research activity. The campus is a modern, academic health center consisting of four professional colleges (Medicine, Dentistry, Nursing and Pharmacy), the Munroe-Meyer Institute, the Eppley Institute for Research in Cancer and Allied Diseases, and the Graduate Studies program. Our partner, the Nebraska Medical Center is the primary clinical teaching site for UNMC. Our location in metropolitan Omaha allows convenient travel connections and a modest cost of living.

Information regarding all programs, as well as an online application can be accessed through the website at **http://app1.unmc.edu/gradstudies/**. Questions about UNMC Graduate Programs may be addressed to: **David Crouse, PhD, Executive Associate Dean for Graduate Studies, 987810 Nebraska Medical Center, Omaha, NE 68198-7810; phone: 402-559-6531; facsimile: 402-559-7845; e-mail: UNMCGraduateStudies@unmc.edu**.

University of Nebraska Medical Center is an Equal Opportunity, Affirmative Action Employer. Minorities and Women are Encouraged to Apply.

THE OHIO STATE UNIVERSITY

FACULTY POSITION IN MOLECULAR NEURO-ONCOLOGY

Applications are invited for a tenure track faculty position at the Assistant or Associate Professor level. The successful candidate will join thirteen current faculty in the Center for Molecular Neurobiology and hold a joint appointment in the Department of Neurological Surgery. The position requires a Ph.D. and/or M.D. with postdoctoral experience. The successful candidate will be expected to develop a program using molecular tools to address problems of relevance to neuro-oncology.

Applicants should submit a curriculum vitae, statement of research plans, and arrange to have three letters of reference sent to: **Dr. Harald Vaessin, Chairperson of the Molecular Neuro-Oncology Search Committee, 206 Rightmire Hall, 1060 Carmack Rd., Columbus, OH 43210**. Alternatively, applications may be submitted electronically to **bantz.7@osu.edu**. Review of applications will begin **March 1, 2006**. Please visit our websites: **http://cmn.osu.edu**; **http://neurosurgery.osu.edu**.

The Ohio State University is an Equal Opportunity/Affirmative Action Employer. Women, minorities, veterans, and individuals with disabilities are encouraged to apply.

Others call it biotech.

We call it improving and extending people's lives.




For over 29 years, Genentech has been at the forefront of the biotechnology industry, using human genetic information to discover, develop, commercialize and manufacture biotherapeutics that address significant unmet medical needs. Today, Genentech manufactures and commercializes multiple biotechnology products that have helped patients suffering from serious diseases and conditions, including breast cancer, colon cancer, lung cancer, non-Hodgkin's lymphoma, cystic fibrosis, heart attack, stroke, growth hormone deficiency, psoriasis and asthma. The company is the leading provider of anti-tumor therapeutics in the United States.

Genentech's research organization features world-renowned scientists who are some of the most prolific in their fields and in the industry. Genentech researchers have consistently published at a rate of 150+ papers per year and have secured more than 4,600 patents worldwide (with 5,000 more pending). Genentech's research organization combines the best of the academic and corporate worlds, allowing researchers not only to pursue important scientific questions but also to watch an idea move from the laboratory into development and out into the clinic. We are proud of our long history of groundbreaking science leading to first-in-class therapies, and we hope you'll consider joining us as we continue the tradition.

We are seeking:

Postdoctoral Fellows • Research Associates • Scientists

In the areas of:

• Cell Biology • Immunology • Medicinal Chemistry • Molecular Biology
• Molecular Diagnostics • Molecular Oncology • Angiogenesis • Antibody Engineering
• Assay Technology • Bioinformatics • Biomedical Imaging • Cancer Genomics
• Pathology • Protein Chemistry • Protein Engineering
• Translational Oncology • Tumor Biology

Genentech offers one of the most comprehensive benefits packages in the industry. Our culture emphasizes working hard, collaborating and sharing rewards. Our employees enjoy an environment that supports busy people with busy lives through benefits and programs that include sabbaticals, flexible work arrangements and concierge services. Join a company that attracts, retains and rewards talented and committed employees. For immediate consideration, please visit www.gene.com/careers. Please use "Ad-Science" when a "source" is requested. Genentech is an equal opportunity employer.

Genentech
IN BUSINESS FOR LIFE

www.gene.com

Boehringer Ingelheim ranks among the world's 20 leading pharmaceutical corporations. With nearly 36,000 employees in 45 countries we are a global team sharing knowledge and ambition to foster a healthier life.

Boehringer Ingelheim Pharma GmbH & Co. KG in Biberach is the most important research and development site of the worldwide Boehringer Ingelheim Corporation and the company's centre for biotechnological development and manufacture.

Boehringer Ingelheim

Value Through Innovation

Principal Scientist / Laboratory Head Clinical Biomarker Analysis

In the Department of Drug Metabolism & Pharmacokinetics, Group Bioanalytics we are seeking to fill an immediate position.

You will be working in the field of Biomarker Analysis within clinical development of new drug candidates. Specifically, you will

- set-up and lead an ELISA-biomarker laboratory in a GCP-environment with three technicians
- develop and validate methods for the quantitative analysis of relevant biomarkers mainly in biological fluids from clinical studies, initially with ELISA later to include additional methods
- plan, conduct and report biomarker data in clinical trials under GCP-conditions in cooperation with the medical development team
- interact closely with functions in Research, Development & Medicine as part of Boehringer Ingelheim's global Biomarker & Pharmaco-genomics Initiative
- work together with contract research organisations (CROs) and develop an outsourcing strategy, i.e. selection of appropriate CROs and definition of processes

The position requires a doctoral degree (Ph.D., M.D.) in a suitable biomedical science. Several years experience in clinical drug development involving biomarker analysis, clinical chemistry, or similar is indispensable.

A sound knowledge and practical experience in analytical techniques - ELISA, but also other relevant techniques - as well as biochemical processes in the body is required.

In addition practical experience with GLP/GCP as well as bioassays, especially cell based assays, is strongly preferred. Excellent inter-personal and communication skills and the ability to work effectively in a team environment are essential.

Knowledge of the English language as well as a willingness to acquire a basic knowledge of the German language is a prerequisite.

We offer a competitive salary accompanied by a full range of benefits.

Biberach is situated in an attractive area of southern Germany between Ulm and Lake Constance.

For further information please contact Dr. Barbara Withopf, phone +49 (0) 73 51 / 54 78 56.

If you feel qualified please send your application including a detailed CV and a description of previous work experience.

As a company without barriers, we also welcome applications from the severely disabled if they have the relevant qualifications.

Please submit your application preferably online.

Boehringer Ingelheim
Pharma GmbH & Co. KG
A Personal GFB
Annette Späth
88397 Biberach an der Riss
Germany

www.boehringer-ingelheim.com

MICHIGAN STATE UNIVERSITY

Center for Advancing Microbial Risk Assessment (CAMRA) Post-doctoral and Doctoral Fellowship Announcement

The Center for Advancing Microbial Risk Assessment (CAMRA; a $10 million Cooperative Center recently funded by the U.S. Environmental Protection Agency and Department of Homeland Security) at Michigan State University invites applications for post-doctoral and doctoral fellowships working in microbial risk-related sciences. Center's mission is to fill critical gaps in microbial risk assessment framework needed to support the security objectives of EPA and DHS. More specifically it aims to: i) improve our ability to measure exposure to biological agents of concerns in drinking water and indoor air, ii) develop a methodology that links models of environmental exposure and models of disease process to help with early detection outbreaks and control efforts, iii) produce a reference set of information on the dose and subsequent response for specific bioterrorist agents, iv) identify research strategies and risk communication priorities that can improve how society manages bioterrorism risk, and v) develop educational programs, online learning tools, and workshops to increase knowledge about microbial risk assessment.

Post-doctoral fellows will be supported for two years minimum plus benefits and will be matched with CAMRA host faculty working on projects related to priority research areas. Post-doctoral applicants should have a PhD in a relevant field. Doctoral applicants will be recruited through the appropriate departments with doctoral assistantships stipends provided per month plus tuition and fringe benefits. Applicants should have undergraduate and/or MS, PhD degrees in a field that provides the basic foundations to work in the area of microbiology, risk assessment, microbial environmental transport, epidemiology or related fields. Applications will be accepted until positions are filled; review of applications begin January 2006. Applicants who are not US citizens or permanent residents must provide documentation evidencing employment authorization in the US. Interested individuals should prepare (1) a letter of application, (2) curriculum vitae, (3) names and contact information of three references, and (4) a statement describing your research interests and goals, professional experience, and how they relate to the mission and priority research area(s) of CAMRA. Send application materials to: **Dr. Joan B. Rose, CAMRA Co-Director and Homer Nowlin Chair of Water, Department of Fisheries and Wildlife, 13 Natural Resources, Michigan State University, East Lansing, MI 48824. Phone: 517-432-4412, rosejo@msu.edu; and Dr. Charles N. Haas, CAMRA Co-Director, LD Betz Professor of Environmental Engineering, Interim Head-Dept. of Civil, Architectural & Environmental Engineering, Drexel University, Philadelphia, PA. Phone: 215-895-2283, haascn@drexel.edu**.

For more Information call or email Dr. Joan B. Rose, see above.

MSU IS AN AFFIRMATIVE ACTION, EQUAL OPPORTUNITY INSTITUTION.

The Ohio State University at Mansfield

Assistant Professorship

Environment & Natural Resources

The Ohio State University at Mansfield is seeking to fill a **nine-month tenure, tenure-track Assistant Professorship in Environment and Natural Resources beginning autumn 2006.** The successful applicant will be expected to conduct research and teach general biology, environmental science, and more advanced courses related to a research specialty. The standard teaching load is six courses distributed over three quarters.

We are especially interested in candidates with a background in forestry, soils, and/or watershed management. Candidates should hold a **Ph.D. in forest science, soil science, plant ecology, natural resources, or a related field.** Teaching and service responsibilities are on the Mansfield regional campus, but the successful candidate will hold rank in the School of Environment and Natural Resources (SENR) and will have full access to facilities on the Mansfield campus and those of the SENR in Columbus and the Ohio Agricultural Research and Development Center in Wooster.

Applicants should send a letter of application, curriculum vitae, statements of teaching philosophy and research interests, three letters of reference, and teaching portfolio materials (if available) to: **Dr. Ted Dahlstrand, Associate Dean, The Ohio State University at Mansfield, 1680 University Dr., Mansfield, OH 44906. Review of applications will begin January 20, 2006, and continue until a suitable candidate is identified.**

THE OHIO STATE UNIVERSITY MANSFIELD

To build a diverse workforce, Ohio State encourages applications from individuals with disabilities, minorities, veterans and women. EEO/AA employer.

MICHIGAN STATE UNIVERSITY

Center for Advancing Microbial Risk Assessment (CAMRA) Assistant Professor; Associate Director

Fixed-Term, 12-month basis, 100% time.

SALARY: $50,000 to $60,000 based on qualifications

The new Center for Advancing Microbial Risk Assessment (CAMRA) is seeking a microbiologist with experience in risk assessment or related disciplines with strong organizational skills as an Associate Director of CAMRA (approximately 50% time) with duties including oversight of Center facilities, coordination with collaborators at six participating universities, tracking of budget and schedules and preparation of written reports. Other responsibilities will include involvement in research (35%), teaching (5%), and outreach (10%). The Associate Director will be expected to participate in research, training, and service on specifically funded projects as both leader and member of the collaborative teams and will be expected to work with the Center, Co-directors, and collaborators. Communication of results in writing and orally to professional audiences and stakeholders will be an essential activity.

QUALIFICATIONS: Ph.D. in microbiology or a related field with familiarity with microbial risk assessment or quantitative risk assessment in general. Should also have strong skills in several of the following areas: bioterrorism, pathogen fate and transport, models, database management.

APPLICATIONS: Due February 15. Late submissions will be considered if a suitable candidate pool is not identified by the deadline. Women and minorities are encouraged to apply. Send letter of interest, curriculum vitae, description of relevant experience, expertise, and professional goals, and names and contact information for three references to **Professor Joan Rose, Department of Fisheries and Wildlife, Michigan State University, 13 Natural Resources Building, East Lansing, MI 48824. Email: rosejo@msu.edu.** Include "CAMRA associate director" at the start of the subject line in all email correspondence regarding this position.

The initial appointment period is for two years, with reappointment for up to five years possible. The anticipated start date is April 1, 2006.

MSU IS AN AFFIRMATIVE ACTION, EQUAL OPPORTUNITY INSTITUTION.

COLUMBIA UNIVERSITY

Motor Neuron Center Faculty Recruitment

Columbia University Center for Motor Neuron Biology and Disease is recruiting faculty with interests in motor neuron biology, ALS or SMA to join a translational program involving basic and clinical research. We are particularly keen to attract individuals using molecular, genetic, chemical, cellular, electrophysiological and/or imaging approaches to the following areas: cellular, axonal and synaptic aspects of neurodegeneration; CNS gene therapy; motor control circuits; functional imaging of the spinal cord; genetics of ALS; SMN biology; preclinical testing of therapeutic strategies; and locomotion. We encourage applications for positions at the Assistant Professor level, but will also consider applications from more senior investigators for positions at the level of Associate or full Professor.

Columbia University currently has a world-renowned program in neurobiology and behavior and in medical and surgical neurology. The new Motor Neuron Center aims to enhance interactions between basic and clinical researchers in the field; Center members will have access to core facilities including high-throughput screening. Faculty will have opportunities for strong ties and academic appointments with the Center for Neurobiology and Behavior, scientific departments and programs on Columbia campuses.

Applications for this round of recruitment are requested by January 20, 2006. A C.V., cover letter including statement of interests, and three letters of reference under separate cover should be e-mailed care of **Dr. Serge Przedborski, sp30@columbia.edu.** In addition, please mail a hard copy of these documents to:

Motor Neuron Center Search Committee
c/o: Dr. Serge Przedborski
Columbia University Medical Center
William Black Building
Room 302
650 West 168th Street
New York NY 10032

Columbia University takes affirmative action to ensure equal employment opportunity.

BIOMEDICAL SCIENCES
Two Faculty Positions

As part of an ongoing expansion of biomedical science faculty, Kent State invites applications for two tenure track positions beginning in August 2006. We seek candidates in **NEUROSCIENCE** at the rank of Assistant or Associate Professor who focus on basic or disease related processes at the cell/molecular levels. Candidates with research interests in all areas of the neurosciences will be considered.

We seek a second candidate in **CELL OR MOLECULAR BIOLOGY** at the rank of Assistant Professor to support strong interdisciplinary research initiatives in cell or molecular biology. Candidates with research interests in any disciplinary area will be considered, but applicants specializing in the relationship of gene expression and protein function to biomedical endpoints are preferred. Strengths of Kent State include strong interdisciplinary affiliations among the basic science units, The Cleveland Clinic Foundation, Northeastern Ohio Universities College of Medicine and the University of Akron, and superb core research facilities. The successful candidates are expected to establish an extramurally funded research program and exhibit a commitment to excellence in graduate and undergraduate education. Applicants must have a Ph.D. degree and postdoctoral experience. Applicants may apply to one or both positions and should indicate in their cover letter the position(s) for which they are applying.

Applicants should send their curriculum vitae, statement of research and teaching interests, and three letters of recommendation to: **Chair, Neuroscience Search Committee or Chair, Cell/Molecular Biology Search Committee, School of Biomedical Sciences, Kent State University, P.O. Box 5190, Kent, Ohio 44242-0001; Fax: 330-672-9391.**

Review of applications will begin **February 2, 2006**, and continue until the position is filled.

Kent State University is an Affirmative Action/Equal Opportunity Employer and encourages applications from candidates who would enhance the diversity of the University's faculty.

UNIVERSITY OF CALIFORNIA
UCMERCED

Assistant Professor of Life Sciences

UC Merced is the 10th UC campus and the first new US research university of the 21st century. UC Merced is located at the base of the Sierra Nevada foothills, near Yosemite and the San Francisco Bay Area. The Schools of Natural Sciences and Engineering at UC Merced seek applicants for three tenure-track faculty positions in the biological sciences at the assistant professor level. Candidates must have a Ph.D. or equivalent, a **record of research, publication, and teaching commensurate with a faculty** appointment at the UC, and a strong interest in creating a curriculum characterized by strong cross-disciplinary links. Applicants are sought in the following areas (more detailed descriptions provided at the web links listed):

1. **Mechanisms of Complex Disease,** including, but not limited to, cardiovascular, metabolic, neurodegenerative or pulmonary diseases. Preference will be given to candidates with demonstrated multidisciplinary research experience or experience in translational research linking basic science to novel therapies, such as regenerative medicine. **http://jobs.ucmerced.edu/view_academic_position.faces?positionId=335**.
2. **Evolutionary Biology,** including, but not limited to: mechanisms of biodiversity, molecular basis of fitness, population genetics, evolution and ecosystems, speciation, evolution of development, physical constraints on evolution, molecular evolution or studying the evolutionary mechanisms creating behaviors and higher cognitive function. **http://jobs.ucmerced.edu/view_academic_position.faces?positionId=339**.
3. **Systems Biology,** including experimental or computational approaches that use comprehensive datasets and multiple types of analysis to relate the overall function of an organism, organelle, or regulatory pathway to the underlying biochemical or biophysical processes. **http://jobs.ucmerced.edu/view_academic_position.faces?positionId=361**.

Interested applicants should apply online via the appropriate web link provided above. For further information please contact **Prof. Sam Traina, Chair of Academic Personnel Committee, School of Natural Sciences** at: **straina@ucmerced.edu**.

AA/EOE.

The Ohio State University
Department of Horticulture & Crop Science

Chair and Professor

The Department of Horticulture and Crop Science, encompassing a diverse array of programs, 38 faculty, 86 staff, and 48 graduate and 245 undergraduate students, seeks a department chair to foster continued growth in excellence.

Responsibilities: Leads and administers a comprehensive and diverse program of research, teaching, and extension in horticulture and crop science, in accordance with principles of faculty governance; fosters collegiality within the department; fosters interdisciplinary scholarship; provides leadership for the professional development of faculty, staff, post-doctoral researchers, and graduate and undergraduate students; reports to the Vice President for Agricultural Administration and serves as liaison between the Vice President and the department; fosters interactions with industry groups and other external partners; provides financial leadership, including preparation of annual budget recommendation in consultation with department, oversight of budget, and allocation of resources to departmental members; evaluates programs and personnel of department.

Qualifications: Ph.D. in a field related to plant science; distinguished record of research, teaching, or extension, consistent with an appointment as a tenured full professor in the Department of Horticulture and Crop Science; proven ability in leadership and administration, including fiscal and human resource management; proven ability to communicate effectively with University and College administration, faculty, staff, students, and industry groups.

Closing date: February 15, 2006, or until a suitable candidate is identified.

Further information: See the departmental web site, hcs.osu.edu/positions.

Contact: Applications should include a letter addressing interest, qualifications, and administrative philosophy, a complete vita, and names, addresses, and telephone numbers of four references. Nominations, inquiries, and applications can be directed to the chair of the Search Committee:

Dr. Steven K. St. Martin, Dept. of Horticulture and Crop Science, Ohio State University, 202 Kottman Hall, 2021 Coffey Road, Columbus, OH 43210-1086, Phone: 614-292-8499, FAX: 614-292-7162, e-mail: st-martin.1@osu.edu

THE OHIO STATE UNIVERSITY

To build a diverse workforce Ohio State encourages applications from individuals with disabilities, minorities, veterans, and women. EEO/AA employer.

Virginia Tech
VIRGINIA POLYTECHNIC INSTITUTE AND STATE UNIVERSITY

Cluster Hires
College of Science

The College of Science at Virginia Tech is now in its third year of cluster hiring to enhance and strengthen research in strategic areas. Four broad areas remain the foci: **nanoscale science, computational science, infectious diseases** and **developmental science** across the life span.

Cluster hiring is coordinated with similar activities with the College of Agriculture and Life Sciences and the College of Liberal Arts and Human Sciences. Twenty-one faculty members were appointed in the college under the cluster approach in the first two years and similar results are expected this year.

Appointments are possible within the disciplines of biology, chemistry, economics, geosciences, mathematics, physics, psychology, and statistics. See specific position descriptions and instructions at **www.cos.vt.edu/jobs**.

Both junior- and senior-level candidates are encouraged to apply, as well as experimental and theoretical scientists.

Virginia Tech is an AA/EEO employer and an NSF Advanced institution; applications from members of underrepresented groups are especially encouraged.

University of Saskatchewan, Department of Microbiology and Immunology, Tenure-Track Faculty Position in Virology/Viral-Host Interactions

The Department of Microbiology and Immunology of the College of Medicine, University of Saskatchewan, invites applications for a full-time, tenure track position at the level of Assistant Professor. The individual appointed is expected to develop a nationally funded research program investigating virus-host cell and/or viral-host interactions, or viral structure and function. This appointment is part of an initiative to develop a research intensity at the university in Infectious Diseases and Host Resistance.

The department has vigorous research and undergraduate and graduate programs in the disciplines of microbiology and immunology. The successful applicant will contribute to these. Collaboration in research is fostered through the existence of across-campus research groups. Information on the department's undergraduate and graduate programs and faculty research interests is available from **www.usask.ca/medicine/microbio/**.

Applicants must have a Ph.D. or equivalent, postdoctoral experience, demonstrated research potential and an interest in undergraduate/graduate teaching.

The university has Colleges of both Medicine and Veterinary Medicine, as well as other related institutions, such as the Vaccine and Infectious Disease Organization and the Canadian Light Source. The campus of the University of Saskatchewan is situated along the Saskatchewan River in the city of Saskatoon. Saskatoon is a beautiful river city and has a vibrant art community.

Applicants should provide a *curriculum vitae*, a statement of research interests and plans, and the names of three referees to: **Dr. Wei Xiao, Head, Department of Microbiology and Immunology, 107 Wiggins Road, Saskatoon, Saskatchewan S7N 5E5, Canada**. Review of applications will begin on **March 1, 2006**.

Applications are invited from qualified individuals regardless of their immigration status; however, Canadians or permanent residents will be given priority. The University of Saskatchewan is committed to Employment Equity. Members of Designated Groups (women, aboriginal people, people with disabilities and visible minorities) are encouraged to apply and identify themselves as belonging to a designated group.

Chair • Department of Neurobiology and Behavior

Stony Brook University's Department of Neurobiology and Behavior is an internationally recognized interdisciplinary research and education department and ranks 10th in NIH-sponsored funding. We are seeking an outstanding scientific leader in cellular, molecular, and/or behavioral neurobiology with a vigorous research program to direct the future growth of this Department. Currently the Department has 16 tenured or tenure-track faculty whose research interests integrate molecular cellular and systems neurobiology. The new Chair will be expected to recruit new faculty to enhance the Department's research and academic missions and to continue development of close relationships with the Stony Brook Health Sciences Center, the new Stony Brook Center for Computational Neuroscience, and collaborating institutions (Brookhaven National Laboratory and Cold Spring Harbor Laboratory). Substantial resources and laboratory space for the Chair and for the expansion of the Department will be provided through the School of Medicine and the College of Arts and Sciences.

Required: M.D., Ph.D., or equivalent degree; the academic rank of Associate or Full Professor; extramural funding at a national/international level, publications in peer-reviewed journals, book chapters, and reviews; and symposium participation at the national/international level. The candidate will also have a proven record of success in graduate student and/or post-doc training.

The review of applications will begin January 1, 2006, and will continue until the position is filled.

Applicants should forward a curriculum vitae to:
Neurobiology Chair Search Committee, c/o Maria Doelger
407 Administration Building, Stony Brook University, SUNY
Stony Brook, NY 11794-1401
or e-mail *NeuroChairSearch@notes.cc.sunysb.edu*

AA/EOE. Visit *www.stonybrook.edu/cjo* for complete job descriptionand other employment opportunities.

STONY BROOK

Hsinchu Biomedical Science Park 新竹生物醫學園區

Biotechnology Gateway of Asia
Seeking Medical College Professors

The goal of Hsinchu Biomedical Science Park is to establish Taiwan as a crucial link in the international biomedical research and business sectors. We aim at developing HBSP into a world-class biotechnology park, which also plays the role of Asia medical science education and research center, incubation and innovation center, and offer high quality medical services to Southeast Asia, making Taiwan a magnet that attracts elites in related fields.

Six Graduate Biomedical Institutes

- Graduate Institute of Oncology
- Graduate Institute of Clinical Photonics
- Graduate Institute of Clinical Genomics
- Graduate Institute of Cardioangiology
- Graduate Institute of Clinical Tissue Engineering
- Graduate Institute of Biomedical Imaging

Qualifications : M.D. & Ph.D. or Ph.D. degree. Require postdoctoral thesis or equivalent achievements. Teaching experience in medicine or natural sciences is also mandatory.

Applications should be sent to the Division of Biomedical Research and Development, Hsinchu Biomedical Science Park To obtain the application form, please contact us by E-mail **scho@mems.iam.ntu.edu.tw** or download from the website at **http://www.hbmsp.com/index.htm**

National Taiwan University College of Medicine

UCLA

INSTRUCTOR POSITION AVAILABLE
MOLECULAR, CELL, AND DEVELOPMENTAL BIOLOGY

Deadline: March 15, 2006

Position: Full time position. Provide instruction and general education curriculum development in the Department of Molecular, Cell, and Developmental Biology at UCLA (Fall, Winter and Spring Quarters and Summer Sessions). Percentage of employment will vary according to number of courses taught.

Duties: Teach science general education lecture courses in the areas of Stem Cells, Biology of Cancer, and AIDS; plan and coordinate course activity, outside speakers, and service learning components for multiple courses; supervise course reader staff; manage the development and maintenance of course materials; develop computer applications for the classroom; and maintain office hours.

Qualifications: Ph.D. degree in the biological sciences; substantial familiarity with biology concepts related to stem cells, cancer biology, and AIDS. Demonstrated experience in undergraduate teaching at the university level; demonstrated knowledge of pedagogy as related to instruction in biological sciences. Level of appointment and salary commensurate with qualifications, experience and duties.

Application: Please send curriculum vitae, written statement of teaching interests and background, and the names, addresses, and telephone numbers of three references. Applications should be mailed to: **UCLA MCDB Lecturer Search, ATTN: Ms. Grace Angus, 621 Charles E. Young Dr. South, Box 951606, Los Angeles, CA 90095-1606.**

The University of California is an Equal Opportunity Employer committed to excellence through diversity.

Director, Center for Diabetes and Obesity Research
Robert C. Byrd Health Sciences Center
and
West Virginia University School of Medicine

West Virginia University is seeking an established investigator for **Professor and Director, Center for Diabetes and Obesity Research**. The Director will participate in the implementation of a new **Strategic Research Initiative** (*Science* 3/12/04) that includes extensive faculty recruitment into interdisciplinary focus areas of research. The **goal** of this position is to establish a core group of investigators leading to development of program project and pre-/post-doctoral training grants in the areas of diabetes and obesity. The Director will coordinate the recruitment of new investigators and facilitate collaboration between newly recruited investigators and current faculty interested in carbohydrate and lipid metabolism, gene expression, signal transduction, cardiovascular disease, and neuroendocrinology. Excellent opportunities also exist for collaboration with basic and clinical faculty involved in population-based and prevention research as related to diabetes, obesity and cardiovascular disease. Investigators in this center will have access to existing core facilities for protein sequencing and proteomics, transgenics, and molecular imaging including PET scanning.

The desired candidate will have a basic research program that asks questions regarding fundamental cellular mechanisms controlling energy metabolism and glucose homeostasis. Candidates must have credentials for appointment as a tenured Professor in either a basic science or clinical department in the School of Medicine. The candidate must excel at fostering collaboration between basic and clinical researchers. Priority will be given to candidates with experience in multidisciplinary research initiatives such as NIH Program Project or NIH Center Grants. Position includes a competitive salary, laboratory space, start-up package, administrative support and resources to recruit additional faculty to the Center who will also have academic tenure-track departmental appointments. The position of Chair of Biochemistry and Molecular Pharmacology is yet to be filled and could couple with the center director position for applicants with appropriate scientific backgrounds.

West Virginia University is a land grant Carnegie-designated Doctoral Research/ Extensive institution, with approximately 25,000 undergraduate and 5,500 graduate/professional students. The WVU Health Sciences Center includes the Schools of Medicine, Pharmacy, Dentistry, and Nursing, each with health professional and graduate programs. Morgantown has 55,000 residents and is rated as one of the best small towns in the U.S., with affordable housing, excellent schools, a picturesque countryside and many outdoor activities.

Qualifications: Ph.D. or M.D. with outstanding research credentials and excellent leadership skills. Submit curriculum vitae and three references, in confidence to: **Diabetes and Obesity Search Committee, WVU Health Sciences, PO Box 9000, Morgantown, WV 26506**. Review of applicants will continue until the position is filled. CV's submitted by e-mail should be sent to **cbsmith@hsc.wvu.edu**.

West Virginia University is an Affirmative Action/Equal Opportunity Employer.

Senior Faculty Position in Functional Imaging Approaches to Systems Neuroscience and Neurological Disease Mechanisms

The Albert Einstein College of Medicine (AECOM) is seeking a senior tenure-track faculty member with expertise in fMRI-based neuroscience. The successful applicant will be given academic appointments in the Departments of Neuroscience, Neurology and/or Radiology, depending upon the individual's own areas of interest. The applicant should have an M.D. or Ph.D and a record of federally-funded research. Start-up package and salary are highly competitive.

The candidate should have demonstrated expertise in state-of-the-art functional MR imaging research in an area of neuroscience and/or neurological disorders. In addition to continuing an independent research program, the successful applicant will be expected to facilitate the imaging research of faculty members within the neuroscience community of AECOM.

The Albert Einstein College of Medicine has a long-standing tradition of excellence and innovation in neuroscience and neurogenic research and rapidly evolving multidisciplinary program in functional imaging. An unusually vibrant and interactive basic science and clinical research environment is complemented by a number of highly regarded research centers and institutes in the areas of neuroscience, diabetes and metabolism, liver diseases, cardiovascular diseases, cancer biology and gerontology. This academic environment will create exciting opportunities to develop productive collaborations.

The AECOM Gruss MRRC is located in the center of the College campus and has approximately 10,000 square feet of contiguous space, including MR suites, patient support facilities, engineering labs, offices and common work areas. The available MR systems include a 4T whole body Varion INOVA system with a high performance gradient insert and a 9.4T 20cm Varion INOVA animal system. In addition, 6 Phillips and General Electric 1.5 and 3T systems, housed in Radiology at Montefiore Medical Center are available for functional imaging of patient populations and for clinical research.

The Albert Einstein College of Medicine is located in a pleasant residential community in the Morris Park section of the Northeast Bronx in close proximity to a wide variety of attractive and affordable housing opportunities in southern Westchester, northern New Jersey, Long Island, Riverdale and Manhattan. To apply, please send a CV, description of research accomplishments and plans, and the names of three references to: **Ms. Ana Cioffi, Kennedy Center Room 220, Albert Einstein College of Medicine, Jack and Pearl Resnick Campus, 1300 Morris Park Avenue, Bronx, NY 10461; Ph: (718) 430-3164; Email: cioffi@aecom.yu.edu.** EOE

ALBERT EINSTEIN COLLEGE OF MEDICINE
Advancing science, building careers

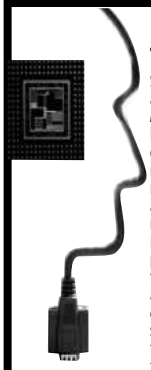

Los Alamos National Laboratory
Title: Group Leader, T-12

Summary: Los Alamos National Laboratory is accepting applications for the position of Theoretical Chemistry and Molecular Physics (T-12) Group Leader. The T-12 Group Leader provides scientific leadership, project management, capability development, and line management. The members of the T-12 group seek to understand the behavior of materials by describing how basic forces operating at the atomic and molecular level manifest themselves in the properties of matter at more macroscopic levels. Current activities include research in gas phase and condensed phase phenomena. Research projects include the development and application of techniques for calculating the electronic properties of molecules and solids, atomistic simulations of materials, the dynamics and kinetics of chemical reactions, molecular modeling of catalysts, and the study of solute-solvent interactions. Particular applications of this research are to the properties of actinide materials and transition metals, to the properties of polymers, biological solvation processes, and fuel cell technologies. Work in the group supports applied missions of the Laboratory, including the Advanced Simulation and Computing (ASC) program, Threat Reduction (TR) programs, and the Department of Energy (DoE) Basic Energy Sciences programs. The Group Leader, with the help of the Deputy Group Leader, will develop and manage the Group's human, financial, computing, and other resources; new programs and funding. The Group Leader will also maintain an active research effort, at the half to three-fourths level.

Required Skills: Demonstrated knowledge and research accomplishments in one or more of T-12's technical research focus areas. Ability to provide scientific and project leadership, project management skills, and fiscally responsible business practices. Demonstrated ability to function effectively in an environment of rapidly changing priorities. Excellent communication skills. Attract and establish research programs from sponsors comparable to those such as the DoE, Laboratory LDRD, industrial partners, and other agencies. Ability to obtain a DoE Q clearance, which normally requires U.S. citizenship.
Ph.D. in Chemistry, Physics, Material Sciences, or the equivalent combination of education and relevant experience.
For a complete job description and application information, visit www.lanl.gov/jobs and search for job# 211737.
Los Alamos National Laboratory is operated by the University of California for the National Nuclear Security Administration of the Department of Energy. AA/EOE

Put your brain to good use.

Los Alamos
NATIONAL LABORATORY

www.lanl.gov/jobs

UNIVERSITÉ DE GENÈVE

THE FACULTY OF MEDICINE is seeking applications for three positions of :

FULL OR ASSOCIATE PROFESSOR
in tissue biology, stem cell biology or molecular mechanisms of host-pathogen interactions, in the Section of basic medical sciences

These are full-time positions involving research and pre- and post-graduate teaching in one of the above-mentioned fields. Candidates should have broad experience in their field of expertise and be open to collaborations with other medical and basic science specialties.

Knowledge of the French language is expected, in the medium term.

A Doctorate in médecine (MD), in science (PhD) or an equivalent degree is required.

The position is open from July 1st, 2006.

Job descriptions for application are available at the following address: **Stephane.jouve@medecine.unige.ch**
Tel: +41 22 379 50 05; **Fax:** +41 22 379 50 02

Applications must be sent before the March 17th, 2006, to : The Dean of the Faculty of Medicine, Centre médical universitaire, 1 rue Michel-Servet, CH-1211 Genève 4, Switzerland

WOMEN ARE ENCOURAGED TO APPLY

Virginia Tech
1872

FACULTY POSITION IN CELL BIOLOGY

The College of Science at Virginia Tech (**http://www.cos.vt.edu**), in cooperation with the Institute for Critical Technology and Applied Science (ICTAS, **http://www.eng.vt.edu/ictas/**) and the Institute for Biomedical and Public Health Sciences (IBPHS **http://www.ibphs.vt.edu/**), is seeking to strengthen research in **NANOSCALE SCIENCE** through interdisciplinary faculty hires. As part of this initiative, the **Department of Biological Sciences** is searching to fill one or more tenure-track positions in **Cell Biology** at the junior and/or senior level. The Department is seeking individuals with interest in working as part of an interdisciplinary team to address cellular questions and/or develop nanoscale technologies to study and treat cancer, infectious disease or nutritional disorders. The successful applicant will be encouraged to developed active interdisciplinary collaborations within the Cell Regulation Group, which includes chemists, physicists, computational biologists, and structural biologists. Applicants must have earned a doctorate in an appropriate discipline (e.g. Biology, Cell Biology, or Molecular Biology), and demonstrated expertise in addressing fundamental or applied biomedical questions in molecular cell biology with preference given to those using mammalian or fungal model organisms.

Applications must be submitted online at **https://jobs.vt.edu/**. The application package should include a cover letter, resume, and a statement of research and teaching interests. Applicants should arrange for at least three letters of recommendation to be submitted by email to **Debbie Cruise** at **debbiec@vt.edu**. Inquires about the position should be directed to **Joe Cowles**, chair of search committee (**cowlesjr@vt.edu**; **540-231-8928**). Review of applications will begin on **January 15, 2006**, and continue until positions are filled.

Virginia Tech is an EO/AA university. Individuals with disabilities desiring accommodations in the application process should notify Melissa Simpkins, (540) 231-4033, or call TTY 1-800-828-1120.

MICHIGAN STATE
UNIVERSITY

Faculty Positions
Coupled Human and Natural Systems

Michigan State University seeks three faculty members in the area of coupled human and natural systems. We are interested in researchers who apply computational methods, such as agent based modeling, to understand human-environment interactions. We have a special interest in population, environment and land use for at least one of these positions. We have a special interest in environmental policy for at least one of these positions. Appointments will be joint between the Environmental Science and Policy Program and a tenure-granting home department. The tenure home may be in Geography, Political Science, Sociology or another appropriate department. We anticipate appointments will be made at the level of Assistant Professor. The positions are academic year appointments. Ph.D. or equivalent is required at the time of the appointment. International experience or demonstrated interest in international issues is an advantage.

The positions will be structured to allow development of internationally renowned research programs with extramural support. We also expect these faculty to engage in an initiative to introduce computational modeling into the undergraduate social science curriculum.

Letters of application should be accompanied by a curriculum vitae, short statement of professional goals, a list of references we can contact and examples of published work.

Applications will be reviewed starting on January 30, 2006, and will be accepted until the positions are filled. Applications and letters of reference can be mailed to: **Dr. Thomas Dietz, ESPP Search Committee, Environmental Science & Policy Program, Michigan State University, 274 Giltner Hall, East Lansing, MI 48824-1011.**

MSU IS AN AFFIRMATIVE ACTION, EQUAL OPPORTUNITY INSTITUTION.

POSITIONS OPEN

VISITING NEUROBIOLOGIST for a one-year appointment at the Assistant Professor level. Ph.D. required. Responsibilities include introductory biology course and an upper-level neurobiology course with labs, and maintaining a research program that involves undergraduates.

Mount Holyoke is an undergraduate liberal arts college for women with 2,000 students and 200 faculty. The college is located about 80 miles west of Boston in the Connecticut River Valley and is a member of the Five College Consortium consisting of Amherst, Hampshire, Mount Holyoke and Smith Colleges, and the University of Massachusetts. Send statements of teaching and research interests, curriculum vitae, copies of publications, list of any relevant courses taught, transcripts, and three letters of recommendation to: **Search Committee, Department of Biological Sciences, Mount Holyoke College, South Hadley, MA 01075-6418. E-mail: biology@mtholyoke.edu.** Applications received by January 18, 2006, are assured full consideration.

Mount Holyoke is committed to fostering multicultural diversity and awareness in its faculty, staff, and student body and is an Affirmative Action, Equal Opportunity Employer. Women and persons of color are especially encouraged to apply.

ASSISTANT PROFESSOR OF BIOLOGY
Grand View College

The Department seeks an Educator who is laboratory oriented, student focused and a team player to teach plant science, general biology and additional course(s) as needed. While teaching is the major component of the position, research involving undergraduates is desirable. A Ph.D. in biology is required.

Application materials: Current curriculum vitae, transcripts, three letters of recommendation, and a letter of interest should be mailed to: **Grand View College, Attn: Human Resources, 1200 Grandview Avenue, Des Moines, IA 50316-1599.** Letters should address the candidate's interest/willingness to participate in a college that engages, equips, and empowers students throughout the entire educational process as well as a statement about one's teaching philosophy and style. Review of applications will begin immediately and will continue until positions are filled. Please view our Website at **website: http://website: http://www.gvc.edu** to ensure position is still open if submitting materials after January 20, 2006.

Grand View College is an Equal Opportunity Employer committed to diversity.

ASSISTANT/ASSOCIATE PROFESSOR
Department of Pharmaceutical Sciences
The Feik School of Pharmacy
University of the Incarnate Word
San Antonio, Texas

A 12-month tenure-track microbiology/immunology Faculty Position in the Department of Pharmaceutical Sciences; preferred start date is June 2006. Candidate for this position should have a Ph.D. in microbiology, immunology, or pharmaceutical sciences with experience teaching microbiology and/immunology. The candidate will be expected to develop and teach courses in microbiology, immunology, and other pharmaceutical or clinical sciences in the Pharm.D. program.

See our **website: http://www.uiw.edu/hr** for further information.

POSTDOCTORAL ASSOCIATE position available in our molecular diagnostics laboratory. Candidates are expected to have experience in diagnostic molecular methods. A Ph.D. in molecular biology and a working knowledge of PCR, TR-PCR, multi locus sequence typing (MLST) and pulse field gel electrophoresis (PFGE) is expected. Submit a resume with names of three references to: **Dr. Ruth Zadoks, e-mail: rz26@cornell.edu, www.qmps.vet.cornell.edu.**

Cornell University is an Affirmative Action/Equal Opportunity Employer and Educator.

The Department of Chemistry at the University of Louisville announces a tenure-track faculty position at the **ASSISTANT PROFESSOR LEVEL IN THE AREA OF BIOCHEMO-INFORMATICS.** Requirements for the position include: Ph.D. and postdoctoral training in chemistry or related fields, commitment to teaching at the undergraduate and/or graduate level on topics related to biochemistry, bioanalytical, biophysical and/or computational chemistry, potential to develop a strong independent research program and willingness to participate in collaborative projects. Candidates with expertise in the following research topics are highly desired: (1) Development of 2-D nuclear magnetic resonance (NMR) and tandem mass spectrometry data transformations for the topics below. (2) Database development of atom-based metabolic networks; (3) Metabolic network flux modeling; and (4) Integration of metabolic and gene regulatory networks. The Department of Chemistry has recently established a Center for Regulatory and Environmental Analytical Metabolomics (CREAM) with a state-of-the-art infrastructure for metabolomic and systems biochemical research that includes state-of-the-art NMR and mass spec instrumentation as well as human resources for collaboration and support. Review of applications will begin January 23, 2006. Please send curriculum vitae, teaching themes and philosophy, and research plan, and arrange for three letters of references to be sent to: **Biochemo-informatics Search Committee, Department of Chemistry, University of Louisville, Louisville, KY 40292.** *African-Americans, women and other minorities are encouraged to apply. Affirmative Action/Equal Opportunity Employer.*

VISITING ASSISTANT PROFESSOR OF BIOLOGY

Centre College seeks applicants for a one-year visiting position for academic year 2006-2007. Successful applicant will hold a Ph.D. in the life sciences or be in the final stages of completion of the degree. Teaching duties include introductory biology, ecology, and a course in area of specialty. Participation in the College's freshman studies program is also expected. Application materials should include a statement of teaching philosophy, curriculum vitae, transcripts, and three letters of recommendation. Send applications to:

Dean John Ward
Vice President for Academic Affairs
Centre College
600 West Walnut Street
Danville, KY 40422

Review of applicants will begin February 1, 2006, and continue until position is filled. *Centre College is committed to promoting diversity among its students and faculty. Women and minorities are especially encouraged to apply.*

BIOLOGY FACULTY

The Department of Chemistry and Chemical Biology of Stevens Institute of Technology is seeking Faculty for teaching and research in molecular biology and biochemistry. We are particularly interested in the areas of functional genomics, molecular genetics, and proteomics. Ph.D. and relevant postdoctoral experience required; successful grantsmanship will be an asset. Stevens created the first educational program in chemical biology in 1979, and this program, retaining its close affiliation with chemistry, is undergoing rapid expansion. Department has excellent mass spectrometry facilities, nuclear magnetic resonance, confocal microscope, small animal facility, et cetera. Stevens is centrally located in the New York metro region and offers easy access to surrounding research and cultural facilities. Review of applications will begin January 31, 2006. Send resume and research plan, and have three letters of recommendation sent to: **Biology Faculty Search, Department of Chemistry and Chemical Biology, Stevens Institute of Technology, Castle Point-on-the-Hudson, Hoboken, NJ 07030.** *An Equal Employment Opportunity/Affirmative Action Employer.*

TENURE-TRACK ASSISTANT PROFESSOR POSITION IN DEVELOPMENTAL GENETICS

The University of Wisconsin, Stevens Point (UWSP) Biology Department, offers a tenure-track, nine-month Faculty Position in developmental genetics beginning August 2005, pending final budget approval. The position requires teaching courses in introductory biology, genetics, and developmental biology; and research involving undergraduates, student advising, and Department service. Commitment to undergraduate education required; teaching and research experience preferred. Ph.D. (coursework, training, research) in animal developmental biology and genetics is required; as is a breadth of training commensurate with teaching in a quality undergraduate program committed to enhancing faculty, student, and curricular diversity. Research and other teaching specialty areas open. Postdoctoral research, publications, grant history, and educational creativity are viewed favorably.

Appointment at Assistant Professor. Applications must include curriculum vitae, statements of teaching philosophy and research interests, three recommendation letters, and undergraduate and graduate transcripts. Address materials to: **Dr. Robert Bell, Chair, Biology Department, University of Wisconsin, Stevens Point, Stevens Point, WI 54481-3897.** Review of applications begins 24 January 2006, until filled. For more information, **telephone: 715-346-2074; fax: 715-346-3624; e-mail: rbell@uwsp.edu.**

UWSP is an Affirmative Action/Equal Opportunity Employer.

HUMAN ANATOMY AND PHYSIOLOGY
Husson College

Husson College in Bangor, Maine is seeking applicants for a full-time **ASSISTANT PROFESSOR POSITION IN HUMAN BIOLOGY** with expertise in human anatomy and physiology. Applicants must possess a Ph.D. in biology or an appropriate biological specialty. Candidates possessing neuromusculoskeletal or histological expertise are particularly encouraged to apply. Successful candidates will be expected to design and teach human anatomy and physiology and pathophysiology courses and the corresponding labs that support the undergraduate nursing, physical therapy, occupational therapy, biology, psychology, and physical education programs at the college. The successful candidate will also advise students, guide undergraduate research in biology, and serve on institutional committees. Husson College has expectations for scholarly activity from its faculty as well as other duties outlined in the Husson College Faculty Handbook.

Salary: Commensurate with experience

Starting Date: September 1, 2006

Send letter of application, curriculum vitae, philosophy of teaching statement, and a list of three references to:

Office of Human Resources, Husson College
One College Circle
Bangor, ME 04401

PROFESSOR AND HEAD, Department of Veterinary Pathobiology, College of Veterinary Medicine and Biomedical Sciences, Texas A&M University, College Station. A description of the Department and a complete position description are available at **website: http://vtpb-www.cvm.tamu.edu.** Candidates must have an earned doctoral degree in a relevant scientific field and have demonstrated understanding of veterinary medicine. Applications should include curriculum vitae and a letter describing the candidate's qualifications and administrative philosophy, along with the names, addresses, telephone numbers, and e-mail addresses of four references. Send applications electronically to: **Dr. Deborah Kochevar, Chair, Search Committee** at **e-mail: dkochevar@cvm.tamu.edu.** Application review will begin February 15, 2006, and will continue until the position is filled. For questions, e-mail aforementioned address, or call **telephone: 979-845-3878.** *Affirmative Action/Equal Employment Opportunity Employer.*

Science Careers Forum

- How long should it take to get my Ph.D.?
- Academia or industry?
- What will make my resume/cv stand out?
- How do I negotiate a raise?

Connect with Experts

Moderator Dave Jensen
Industry Recruiter

Mr. Jensen has over 20 years of experience in human resource consulting and staffing for the biotechnology and pharmaceuticals industry.

Adviser Bill Lindstaedt
Director,
UCSF Career Center

Mr. Lindstaedt has been providing career related advice to scientists and engineers for nearly 15 years, with a particular emphasis on working with graduate-level trainees in the life sciences.

Adviser Naledi Saul
Assistant Director,
UCSF Career Center

Ms. Saul has 7 years of career counseling with 4 years focused on counseling graduate students and postdocs in the biomedical and health sciences. Her forte is working with scientists pursuing careers in the public health arena.

Adviser Jim Austin
Editor, Science's
Next Wave

Dr. Austin has a Ph.D. in physics and worked in academia before coming on board to write about traditional and nontraditional career paths for scientists.

Visit www.sciencecareers.org and click on Career Forum

ScienceCareers.org
We know science AAAS

POSITIONS OPEN

DIRECTOR, NATIONAL CENTER FOR WATER QUALITY RESEARCH

Heidelberg College, Tiffin, Ohio, invites applications for the position of Director of its National Center for Water Quality Research (NCWQR), formerly the Water Quality Laboratory. The NCWQR's research programs emphasize quantifying nutrient, sediment and pesticide export from large agricultural and mixed land-use watersheds into Lake Erie and the Ohio River, aiding in the development of tributary load reduction programs, and assessing the effectiveness of those programs. The NCWQR's tributary loading data bases date from 1974 and are the most detailed and long-term of their type in the United States **(website: http://wql-data.heidelberg.edu/).** In 2005, the NCWQR moved into the newly constructed Gillmor Science Hall. We seek a Director who can guide the continued operation and expansion of NCWQR programs. Applicants must possess a doctoral degree with experience in water resources or a related environmental or agricultural discipline. Depending upon qualifications, the position may be tenured upon appointment. The Director reports directly to the Vice-President for Academic Affairs. More information about this position and NCWQR programs and staff can be found at **website: http://www.heidelberg.edu/wql.**

To apply, submit by mail (1) a letter of application, (2) a full curriculum vitae, (3) a one-to-two page narrative envisioning how you would lead the NCWQR in implementing its mission, and (4) names and contact information for three references. Submit these materials to:

Dr. David Baker
National Center for Water Quality Research
Heidelberg College
310 E. Market Street
Tiffin, Ohio 44883

Screening of applications will begin February 10, 2006, and will continue until the position is filled. *Heidelberg College is an Affirmative Action, Equal Opportunity Employer.*

BIOLOGICAL SCIENCES

The University of Windsor invites applications for three tenure-track **FACULTY POSITIONS** in the Department of Biological Sciences at the rank of Assistant Professor in the areas of ecology, neurobiology, and cell/molecular biology commencing July 1, 2006. The application deadline date for these positions is January 31, 2006. For a detailed position description, visit our **website: http:// www.uwindsor.ca/facultypositions.** Contact: **Dr. William Crosby, Head, Biological Sciences, Biology Building - 119, University of Windsor, Windsor, Ontario N9B 3P4. Telephone: 519-253-3000, extension 2697. Fax: 519-971-3609. E-mail: bcrosby@uwindsor.ca.** For information on the University of Windsor or the City of Windsor, contact: **Professor Brian M Mazer, Director, Faculty Recruitment, telephone: 877-665-6608 (toll free)** within North America. Call collect outside of North America, **telephone: 519-561-1432.** Or **e-mail: recruit@uwindsor.ca.**

SESQUI SENIOR LECTURESHIP (TOTIPOTENT STEM CELL BIOLOGY)
School of Medical Sciences
Reference No. C47/006550

Applications are invited for a Senior Lectureship in the field of totipotent stem cell biology. Embryonic stem cell biology, mammalian development, and cell physiology are major research interests within the School of Medical Sciences, which includes the disciplines of physiology, pathology, anatomy, and histology and pharmacology.

For full advertisement, please refer to the University's **website: http://www.bull.usyd.edu.au/personnel/,** or for further information contact: **Associate Professor Chris O'Neill, telephone: (+61 2) 9926 7148, fax: (+61 2) 9926 6343,** or **e-mail: chriso@med.usyd.edu.au** or **Ms. Lali Jacob, telephone: (+61 2) 9351 3247, fax: (+61 2) 9351 5182,** or **e-mail: lalij@physiol.usyd.edu.au.**

Closing 26 January 2006.

POSITIONS OPEN

City of Hope
Where the Power of Knowledge Saves Lives

IMMUNOLOGY FACULTY POSITION

The Division of Immunology, Beckman Research Institute, City of Hope **(website: http://www.cityofhope.org/immunology/)**, invites applications for a full-time tenure-track faculty position at the **ASSISTANT PROFESSOR** level in the general field of immunology to expand and complement existing strengths on campus in immune regulation, autoimmunity, cancer immunology, lymphocyte activation and signaling, and innate immunity. Applicants should possess a Ph.D. (or equivalent) and have postdoctoral experience in basic science in an immunology-related field. The candidates are expected and encouraged to establish an extramurally funded independent research program. The successful candidate will also have the opportunity to participate in teaching activities at the Graduate School for Biological Sciences on campus and mentor Ph.D. and postdoctoral fellows. Very competitive startup package, salary, and benefits will be provided to the selected candidate. The Beckman Research Institute, City of Hope and its affiliated NCI-designated Comprehensive Cancer Center have experienced, in the past five years, a major growth in research capacity and will continue its expansion in both basic and clinical research. The Institute offers a strong interactive environment and various excellent opportunities for collaborative research exist within the Institute and the surrounding area in Southern California near Los Angeles. Applicants should submit curriculum vitae, a research statement of past scientific accomplishment, a research plan describing specific future research interests and goals, and three recommendation letters sent directly from references to: **Dr. John E. Shively, Professor and Chairman, Division of Immunology, Beckman Research Institute, City of Hope, 1450 E. Duarte Road, Duarte, CA 91010. E-mail: jshively@coh.org.** Review of candidates will begin March 1, 2006, and will continue until the position is filled. *Equal Opportunity Employer.*

Two **POSTDOCTORAL FELLOWSHIP** positions are available in the Sarah W. Stedman Nutrition and Metabolism Center at Duke University Medical Center. Applicants with M.D. or Ph.D. degrees are welcome. The available project will use zebrafish as a model organism to study organogenesis and stem cell biology related to the pathophysiology of metabolic disease. A variety of scientific tools will be used to probe regenerating pancreas cells including genetics, stem cell biology, pharmacological intervention and physiological analysis. The laboratory is located within a multidisciplinary metabolism research center where the interactive environment affords a wealth of technical expertise, instrumentation, and resources.

Larry Gene Moss, M.D.
Associate Professor of Medicine
Sarah W. Stedman Nutrition
and Metabolism Center
Duke University Medical Center
4321 Medical Park Drive
Durham, NC 27704
E-mail: larry.moss@duke.edu
Website: http://www.stedman.mc.duke.edu/stedman/competencies/science.aspx.

POSTDOCTORAL POSITIONS are available at Harvard Medical School to study cardiovascular and/or metabolic diseases using murine models. Candidates with at least one of the following fields are encouraged to apply: signal transduction, atherosclerosis, aortic aneurysms, diabetes, and obesity. Successful candidates should have demonstrated molecular and cellular biology background. Experiences in immunohistology and flow cytometry would be advantageous. Please send curriculum vitae and telephone numbers of at least two references to **Dr. Guo-Ping Shi** at **e-mail: gshi@rics.bwh.harvard.edu.**

POSITIONS OPEN

SENIOR SCIENTIFIC EDITOR

Stanford University School of Medicine is seeking to fill a full-time position as Senior Scientific Editor to head an editorial office within the Department of Neurosurgery consisting of approximately 18 clinical faculty, five research faculty, postdoctoral fellows, and residents. We are seeking an experienced Editor or qualified Biomedical Researcher with broad-based interest and expertise preferably in the areas of neurosurgery, neurology or neurobiology. The ideal candidate should have experience with publications in peer-reviewed journals, excellent written and oral communication skills and a commitment to the communication of basic, translational, and clinical science. Candidates should have significant experience in editing peer-reviewed manuscripts, book chapters, and NIH-grants. We are particularly interested in applicants with expertise and background in neuroscience but would welcome applications from outstanding candidates in any area of biomedical research. Please submit a curriculum vitae, a short (500 to 1000 words) article on any exciting and newsworthy recent developments in neuroscience or any area of biomedical research and a cover letter explaining your interest in the position to: **Cheryl Joo, Stanford University School of Medicine, Department of Neurosurgery, 300 Pasteur Drive, Room R283A, Stanford, CA 94305-5327. E-mail: cjoo@stanford.edu. Fax: 650-723-1408.**

Stanford University is committed to increasing representation of women and members of minority groups and particularly encourages applications from such candidates.

AQUATIC ECOLOGIST/GREAT LAKES FIELD STATION DIRECTOR
Illinois Natural History Survey

The Center for Aquatic Ecology and Conservation (CAEC) invites applications for a position at the Assistant level. Scientists within CAEC conduct self-directed research, work closely with state and federal resource managers, have full access to University of Illinois campus facilities and resources, hold adjunct or affiliate positions in University departments, teach courses, and supervise graduate students. We seek a scientist and program leader who can develop a strong, externally funded research program on Lake Michigan ecology. The successful candidate will serve as Director of the Lake Michigan Biological Station in Zion, Illinois. To qualify for this position, candidates must possess a doctorate in aquatic ecology or a related discipline. Candidates with postdoctoral research experience are preferred. Willingness and ability to work on interdisciplinary projects with scientists in the Illinois Natural History Survey (INHS), other state and federal agencies, and the University of Illinois is desirable. For full position announcement and application instructions see **website: http://www.inhs.uiuc.edu/opportunities/index.html.** Direct technical questions to: **Dr. David Wahl, telephone: 217-728-4400. E-mail: d-wahl@uiuc.edu.** Deadline for application is February 10, 2006. *INHS is an Equal Opportunity Employer.*

MEDICAL WRITER

The Prescott Medical Communications Group (PMCG), a marketing communications company serving the pharmaceutical and biotechnology industries, is again expanding and has immediate openings for Scientific Writer/Editors. Candidates must possess an advanced biomedical science degree (M.S., Ph.D., Pharm.D., M.D.) and a minimum of five years of Continuing Medical Education (CME) or agency (or similar) experience. This full-time in-house position will require residing in the Chicago area and occasional domestic/international travel. PMCG offers an unparalleled opportunity for professional development in a fast-paced and intellectually challenging environment. Please send employment history and three writing samples to: **Jim Bachleda, Prescott Medical Communications Group, 205 N. Michigan Avenue, Suite 3400, Chicago IL 60601. Fax: 312-528-3901. E-mail: jbachleda@prescottmed.com.**

Excellence in Teaching Awards

The USDA CSREES Higher Education Programs Office seeks nominations for the FY 2006 National Awards Program for Excellence in College and University Teaching in the Food and Agricultural Sciences.

Teachers from agricultural resources, forestry, veterinary medicine, human sciences/family and consumer sciences, and closely allied fields may apply. National, regional and new teacher award winners receive institutional awards from $2000- $5000.

Deadline for nomination:
March 15 2006

Visit: **http://www.csrees.usda.gov/business/other_links/serdteachaward.html** for nomination guidelines and more information.

Molecular Medicine and Genetics

WAYNE STATE UNIVERSITY
SCHOOL OF MEDICINE

As part of a multi-year hiring plan, the **Center for Molecular Medicine and Genetics (CMMG)** invites applicants for multiple tenure track positions at the Assistant, Associate, or Full Professor level. The Wayne State University School of Medicine has recently initiated a $20 million project to renovate the Center's facilities, and new state-of-the-art laboratory and core research facilities are scheduled to open in 2006. Successful candidates would join an active faculty conducting research in systems biology, comparative genomics, neuroscience, bioinformatics, and medical genetics. The CMMG (**http://www.genetics.wayne.edu**) offers extensive opportunities for collaboration within the Center and throughout the University. As a member of the Michigan Life-Science Corridor, Wayne State scientists have the opportunity to develop translational research with industry, government, and academic research institutions. Successful candidates are expected to have, or establish, vigorous externally funded research programs as appropriate to their rank and experience. Areas of particular emphasis are **mitochondrial molecular genetics and pathophysiology** and **quantitative human genetics**.

Wayne State University is Michigan's only research university located in an urban setting. Detroit is an exciting and culturally diverse city, and Michigan has extensive outdoor space for boating, hiking, and camping.

Applications should include a letter of application, curriculum vitae, and the names and addresses of at least three references. Selection of initial candidates will begin on **January 1, 2006**, and continue on a rolling basis thereafter. **Applications and supporting materials must be submitted online at http://jobs.wayne.edu**.

WSU is a premier institution of higher education offering more than 350 academic programs through 14 schools and colleges to more than 31,000 students in metropolitan Detroit.

WSU is an Equal Opportunity/Affirmative Action Employer.

Universität Karlsruhe (TH)

Forschungsuniversität · gegründet 1825

The **DFG-Research Center for Functional Nanostructures** (CFN) at the Universität Karlsruhe (TH) invites applications for up to two positions of

Junior Research Group Leaders

in the area of **"Nanobiology"**.

The positions will become available in 2006, and the groups will be funded at least until June 2009, with the possibility for an extension up to a maximum duration of 5 years.

The Junior Research Groups are intended to strengthen the CFN (www.cfn.uni-karlsruhe.de) in the interdisciplinary field of biology, chemistry and physics, hence they are expected to contribute to and participate in projects within the research area "**Nanobiology**". Research groups from molecular biology, physics, toxicology as well as organic chemistry and biochemistry collaborate in this research area. Possible research topics of the Junior Research Groups are biophotonics, mechanochemical sensors, artificial membranes, or bio-assembly of nanomaterials.

The applicants are expected to be outstanding young researchers in one or more fields related to the abovementioned topics. Their competence should be firmly established by publications in international scientific journals, and they should hold their doctorate degree for not more than 5 years.

Further information can be obtained from the coordinator of the CFN Research Area Nanobiology, Prof. Anne Ulrich, anne.ulrich@ibg.fzk.de, or from Prof. Martin Wegener.

Universität Karlsruhe (TH) aims to increase the representation of women among the staff and therefore explicitly encourages applications from female scientists. Universität Karlsruhe (TH) is an equal opportunity employer and will give preference to disabled candidates having the same qualifications as their competitors.

Applications including a short project outline (past and future research), CV, copies of degree certificates, a list of publications, and copies of the five most important publications should be submitted by **22.01.2006** to the CFN coordinator, **Prof. Dr. M. Wegener, Universität Karlsruhe (TH), Institut für Angewandte Physik, Wolfgang-Gaede-Straße 1, 76131 Karlsruhe, Germany**.

BCM

Baylor College of Medicine

FACULTY POSITION

The Department of Molecular Physiology and Biophysics at Baylor College of Medicine is seeking to recruit a new faculty member at the Assistant/Associate Professor. We are seeking candidates with a strong record of research contributions, the potential to establish an exciting, independent research program, and a commitment to excellence in graduate and medical student education. Research interests of the applicant must include a physiological or biophysical approach to studying cell or organismal biology and a focus on advanced technologies or the study of disease models is preferred. The department has a strong commitment to both basic and translational biomedical research and has state-of-the-art facilities for confocal microscopy, mouse MRI, multiphoton imaging and a core for the creation and analysis of new mouse models. Baylor College of Medicine is a world-renowned research institution with strengths in many areas including mouse genetics, cardiovascular sciences, and neuroscience. Ample opportunities exist for scientific interaction and collaborations within the department, throughout the College, and within the Texas Medical Center. Located in the heart of the Texas Medical Center, Baylor College of Medicine is in close proximity to the University of Texas Medical School at Houston, the MD Anderson Cancer Center, Rice University and the University of Houston.

Please e-mail your curriculum vitae, the names and contact information for three references and a description of both your research program and career goals to:

Dr. Susan Hamilton, Department Chair
Department of Molecular Physiology and Biophysics
Mail stop: BCM335
Baylor College of Medicine
One Baylor Plaza
Houston, TX 77030

The deadline for receipt of applications is **February 1, 2006**.

POSITIONS OPEN

ECOLOGIST FACULTY POSITION
Fordham University

The Department of Biological Sciences of Fordham University invites applicants for a tenure-track faculty position in animal ecology and conservation biology at the Assistant Professor level for fall 2006. Preference will be given to vertebrate ecologists interested in establishing research collaborations with the Wildlife Conservation Society. There are also research opportunities at Fordham's biological field station, the Louis Calder Center. We seek individuals who will establish a vigorous, extramurally funded research program. The successful candidate must have a Ph.D. and postdoctoral experience and is expected to teach at the undergraduate and graduate levels. Applicants should submit a curriculum vitae and have three letters of recommendation sent by February 1, 2006, to: **Dr. Robert Ross, Chair, Department of Biological Sciences, Fordham University, 441 E. Fordham Road, Larkin Hall 160, Bronx, NY 10458.** Fordham University is an independent, Catholic university in the Jesuit tradition that welcomes applications from men and women of all backgrounds. *Fordham is an Equal Opportunity Employer/Affirmative Action Employer.*

CELL/MOLECULAR BIOLOGIST
Fordham University

Individuals are invited to apply for a tenure-track position at the Associate Professor level. The Department has an active research program and provides excellent physical facilities, state-of-the-art equipment, a stimulating research environment, startup funds and competitive salaries and benefits. Preference will be given to candidates who possess expertise in the area of cell/molecular biology and have an ongoing grant-supported research effort. The appointee will be expected to establish an active research program and teach at the graduate and undergraduate levels. Please submit a curriculum vitae and the names and addresses of three references by February 1, 2006, to: **Dr. Robert Ross, Chair, Department of Biological Sciences, Fordham University, 441 E. Fordham Road, Larkin Hall 160, Bronx, NY 10458.** Fordham is an independent, Catholic university in the Jesuit tradition that welcomes applications from men and women of all backgrounds. *Fordham is an Equal Opportunity Employer/Affirmative Action Employer.*

ASSISTANT OR ASSOCIATE PROFESSOR
University of South Florida College of Medicine

The Department of Internal Medicine, Division of Allergy and Immunology, Tampa, Florida is seeking a M.D. and/or Ph.D. expert in molecular biology and/or immunology for lung disease research. Assistant Professor position requires three years of postdoctoral experience. Associate Professor position requires evidence of continued NIH-funded grant support. Salary negotiable. Submit resume and three reference letters to: **Michelle Grandstaff, e-mail: mgrandst@hsc.usf.edu** or **fax: 813-631-4030.** Applications will be screened starting January 15, 2006, and continue until the position is closed. For disability accommodations, contact **Michelle Grandstaff, telephone: 813-631-4024** at least five working days in advance. *University of South Florida is an Equal Opportunity/Affirmative Action/Equal Access Institution. According to Florida law, applications and meetings regarding them are open to the public.*

Additional job postings not featured in this issue can be viewed online at **website: http://www.sciencecareers.org.** New jobs are added daily!

Manage your job search more effectively by creating an account at **website: http://www.sciencecareers.org.** You can post your resume (open or confidentially) in our database and use it to apply to multiple jobs simultaneously. Track the jobs you have applied to in special tracking folders. Plus, you can create Job Alerts that will e-mail you notification of jobs that match your search criteria.

POSITIONS OPEN

POSTDOCTORAL AND CLINICAL FELLOWSHIPS
at the
National Institutes of Health
U.S. Department of Health and Human Services

Website: http://www.training.nih.gov

NIH is dedicated to building a diverse community in its training and employment programs.

DIRECTOR
Sticht Center on Aging and Rehabilitation
Wake Forest University School of Medicine

Wake Forest University School of Medicine seeks applications for the position of Director of the Sticht Center on Aging and Rehabilitation, which will include a faculty appointment in the Department of Internal Medicine. Candidates should have the M.D. or Ph.D. degree, must have demonstrated excellence in research and possess exceptional leadership qualities. The successful candidate will be charged with building on a solid foundation of aging research that emphasizes excellence in research and teaching. For M.D. candidates, opportunities exist for leadership of the Section on Gerontology and Geriatric Medicine.

The Center currently consists of five physician and five non-physician faculty members with primary appointments in the Section of Gerontology and Geriatric Medicine; however, more than sixty faculty participate in the multidisciplinary research programs of the Center on Aging. The Center offers a large program for clinicians and scientists that provides training in gerontology and geriatrics for medical students, residents, and clinical and research fellows, as well as junior faculty members.

The Sticht Center on Aging has gained national and international recognition for excellence through a high level of NIH funding including a Claude D. Pepper Older Americans Independence Center, and by attracting scientists and trainees from the United States and throughout the world. The Director of the Sticht Center directly reports to **Dr. William Applegate,** Dean of the School of Medicine. The Sticht Center on Aging is a leader in clinical care, providing innovative services to meet the special health care needs of older adults across a full range of geriatric practice settings (inpatient, outpatient, home and long-term care) as well as rehabilitation and psychiatric care.

Wake Forest University is located in Winston-Salem, North Carolina and has an excellent quality of life, moderate four season climate, nearby mountains/ocean with affordable housing in a metropolitan area of approximately 1.3 million people. Applications including a current curriculum vitae or nominations should be sent by mail or e-mail to:

William Sonntag, Ph.D.
Chair, Search Committee for
Director of the Sticht Center
Attn: Adriene Cunningham, Dean's Office
Wake Forest University School of Medicine
Medical Center Boulevard
Winston-Salem, NC 27157
E-mail: wsonntag@wfubmc.edu

Wake Forest University School of Medicine is committed to Equal Opportunity, Affirmative Action and the diversity of its faculty and staff. Women and minorities are strongly encouraged to apply.

POSTDOCTORAL POSITION available to study mechanisms of DNA repair in telomeres and the mechanisms of chromosome instability resulting from telomere loss in mammalian cells. Applicants should have a strong background in molecular biology. Send curriculum vitae to: **Dr. John Murnane, Department of Radiation Oncology, University of California, San Francisco, 1855 Folsom Street, MCB200, San Francisco, CA 94103. E-mail: murnane@radonc17.ucsf.edu.** *University of California, San Francisco is an Equal Opportunity Employer.*

POSITIONS OPEN

POPULATION BIOLOGY POSTDOCTORAL RESEARCH FELLOWSHIP

The University of Nebraska, Lincoln (UNL) is seeking applications for a two-year Postdoctoral Position at the Interdisciplinary Program in Population Biology. Applicants must have a doctoral degree in biology, ecology, genetics, mathematics or related areas and contact a participating faculty sponsor to develop a research proposal. Starting date can be as early as July 2006. The salary range is in line with international standards for postdoctoral positions. We strongly encourage applications from women, and members of minority groups. Information about the program and complete instructions for application can be found at **website: http://popbio.unl.edu.** Applications should be received by 1 March 2006, in order to ensure full consideration. For further information, contact **Alan C. Kamil, telephone: 402-472-6676** for assistance.

UNL is committed to a pluralistic campus community through Affirmative Action and Equal Opportunity, and is responsive to the needs of dual career couples. We assure responsible accommodation under the Americans with Disabilities Act.

POSTDOCTORAL POSITION AT RUTGERS UNIVERSITY funded by the NIH Botanical Center for Metabolic Syndrome and the pharmaceutical industry to study cellular mechanisms of action of plant-derived compounds on neural and hormonal mechanisms of satiety, energy balance, and insulin/growth hormone signaling. Strong record of publications and scientific achievements is required as well as expertise in cell culture and animal work. Please submit curriculum vitae, summary of research interests, and the names of three references to: **Dr. Ilya Raskin, Biotech Center, Cook College, Rutgers University, 59 Dudley Road, New Brunswick, NJ 08901. E-mail: raskin@aesop.rutgers.edu.** Information on **website: http://www.rci.rutgers.edu/~raskin.** *Rutgers University is an Affirmative Action/Equal Opportunity Employer.*

POSTDOCTORAL FELLOWSHIP available in steroid hormone biosynthesis in male aging. Candidate should have Ph.D. and background in cellular and molecular biology, endocrinology, with experience in Leydig cell steroidogenesis. To apply, log on to **website: http://jobs.texastech.edu.** *Texas Tech University Health Sciences Center is an Equal Employment Opportunity/Affirmative Action Employer.*

ANNOUNCEMENTS

JOINT CARNEGIE MELLON- UNIVERSITY of PITTSBURGH PH.D. PROGRAM in COMPUTATIONAL BIOLOGY

Applications are invited for the Ph.D. Program in Computational Biology offered jointly by the University of Pittsburgh and Carnegie Mellon University, which was recently chosen as a Howard Hughes Medical Institute (HHMI) - National Institute of Biomedical Imaging and Bioengineering (NIBIB) Interfaces Initiative Awardee. The goal of this unique doctoral program is to provide intensive interdisciplinary education to enable outstanding students to become leaders in identifying and solving tomorrow's biological problems using computational methods and fundamental principles of life and physical sciences. Students will have the opportunity to participate in research studies in one of five selected areas of specialization: computational genomics, computational structural biology, cellular and systems modeling, bioimage informatics, and computational neurobiology. Applications from students with a variety of backgrounds are encouraged, including those with degrees in biological, physical, mathematical and computational sciences, and engineering. All enrolled students receive a competitive stipend, complete tuition remission, and excellent health benefits. The application deadline for fall 2006 admission is January 15, 2006. Program details and online application material are available at **website: http://www.compbio.cmu.edu.**

MEETINGS

Believe it!

DNA Sequencing for $2.50 per reaction.

- Read length up to 900 bases.
- High quality electropherograms.
- Fast turnaround.
- Plasmid and PCR purification available.

POLYMORPHIC
Polymorphic DNA Technologies, Inc.℠

www.polymorphicdna.com
info@polymorphicdna.com

1125 Atlantic Ave., Ste. 102
Alameda, CA 94501

Polymorphic exclusively uses ABI 3730XL sequencers.
Data delivered via secure FTP, email or CD.
No charge for standard sequencing primers.
384 sample minimum order.
96 well plates only—no tubes.

888.362.0888

For more information please visit
www.polymorphicdna.com

Expanding options for kinase biology

Looking for kinase options to drive your research and discovery projects? We now offer:

- **250+ human kinases and growing**—access the largest collection available
- **14 clinically relevant mutant kinases**—accelerate therapeutic development
- **Z'-LYTE™ Kinase Assay Technology**—screen more than 200 kinases in a single, fluorescent format
- **SelectScreen™ Kinase Profiling Service**—use the fastest growing selectivity profiling service
- **Stealth™ RNAi Human Kinase Collection**—utilize rapid, high-throughput functional screening
- **CellSensor™ cell-based assays**—elucidate signal transduction pathways

Through the integration of BioSource with Invitrogen, we are adding one of the largest collections of signal transduction antibodies, ELISAs, Luminex® reagents, and signaling arrays to our kinase portfolio. No one else offers you more for kinase research and discovery (Table 1).

Table 1—Invitrogen's kinase portfolio offers more choice than the nearest competitor*.

	Invitrogen	Nearest competitor
Distinct, wild type, human protein kinases	237	206
Phospho site-specific antibodies	272	186
Fluorescent assay (FA) platforms	4	2
Protein kinases validated with FA platforms	201	80
Cell lines for pathway analysis	29	0
Protein kinases addressed by RNAi platform	ALL	<100

To learn more about Invitrogen's expanding kinase collection, visit **www.invitrogen.com/drugdiscovery**.

To order BioSource products, visit **www.biosource.com**.

BIOSOURCE™
invitrogen cytokines & signaling

invitrogen™

*All data pulled from competitor's web site as of 11/8/05.